Thermoplastic elastomers based on recycled plastics and waste tires

Thèse

Ali Fazli

Doctorat en génie chimique
Philosophiæ doctor (Ph. D.)

Québec, Canada

Thermoplastic elastomers based on recycled plastics and waste tires

Thèse

Ali Fazli

Sous la direction de:

Denis Rodrigue, directeur de recherche

RÉSUMÉ

Ce travail développe une approche innovante du recyclage des pneus grâce à l'application de déchets de caoutchouc de pneus et de fibres textiles comme renforts pour la production de composés élastomères thermoplastiques (TPE) entièrement recyclés transformant les déchets en matériaux à valeur ajoutée. Une optimisation expérimentale a été réalisée pour développer une morphologie de phase spécifique et obtenir des propriétés physiques, mécaniques et thermiques équilibrées du TPE à base de matériaux recyclés.

Dans la première partie, de la poudrette de pneu usé (GTR) à partir de caoutchouc régénéré (RR) et de caoutchouc non régénéré (NRR) à base de pneus hors-route (OTR) ont été mélangés à l'état fondu (extrusion à double vis) avec des matériaux recyclés comme le polyéthylène haute densité recyclé (rHDPE) pour étudier l'effet de la régénération et de la composition du caoutchouc sur l'aptitude au moulage, la morphologie des phases et les propriétés du TPE hautement chargé contenant jusqu'à 90% en poids de GTR. L'inclusion de RR dans le rHDPE a contribué à une meilleure fluidité et une aptitude au moulage en raison de la mobilité des chaînes et de la déformabilité des particules plus élevées que les particules NR. Malgré la diminution de la résistance à la traction et du module de traction avec la teneur en caoutchouc (points de concentration de contrainte), l'allongement à la rupture et la résistance aux chocs ont augmenté, ce qui a été attribué à la présence d'une teneur en phase plus élastique et d'une absorption d'énergie plus élevée par la déformation des particules caoutchouteuses retardant la rupture.

Dans la deuxième partie, des mélanges de TPE à base de thermoplastique recyclé ont été préparés par mélange à l'état fondu pour étudier l'effet de la taille des particules de GTR (0-250 µm, 250-500 µm et 500-850 µm) et leur contenu (0, 20, 35, 50 et 65% en poids). Les résultats ont révélé que pour une composition de mélange fixe, les particules de GTR plus petites (0-250 µm) ont donné des propriétés de traction et une ténacité plus élevées par rapport aux particules plus grosses en raison d'une surface spécifique plus élevée (valeur plus élevée et meilleur contact) entre les petites particules de GTR et la matrice favorisant l'interaction interfaciale. Cependant, les particules plus petites ont un effet négligeable sur la résistance mécanique à une teneur en GTR plus élevée (au-dessus de 50% en poids) puisque l'incompatibilité et la mauvaise qualité de l'interphase ont joué un rôle plus important.

Dans l'étape suivante, différents types de caoutchoucs recyclés régénérés (RR_1 et RR_2) ont été utilisés pour produire des mélanges de TPE hautement chargés (plus de 70% en poids). Un fort enchevêtrement entre les chaînes libres RR_2 (degré de régénération de 24%) et les macromolécules thermoplastiques a contribué à une forte interaction interfaciale conduisant à des propriétés mécaniques élevées. L'introduction d'un copolymère éthylène-acétate de vinyle recyclé (rEVA) a montré une augmentation de l'allongement à la rupture et de la résistance aux chocs de 27% et 11% respectivement, via l'encapsulation de la phase de caoutchouc par le copolymère élastomère (10% en poids) formant un interphase épaisse/flexible diminuant la concentration de contraintes interfaciales ralentissant la fracture.

Dans la dernière partie, un mélange maître à base de polyéthylène greffé à l'anhydride maléique (MAPE)/RR (70/30) a été utilisé pour la modification d'impact et la compatibilisation de composites TPE recyclés renforcés de fibres de pneu recyclées (RTF). L'ajout de RR recouvert en surface avec l'agent de couplage a retardé l'initiation et la propagation des fissures en formant une interphase épaisse/flexible diminuant la concentration de contraintes interfaciales ralentissant la fracture. L'encapsulation de la phase caoutchouc par MAPE a fourni une méthode efficace pour le recyclage des pneus usés (caoutchouc et fibres) en produisant des composites TPE renforcés avec des propriétés mécaniques acceptables.

Dans l'ensemble, les résultats obtenus dans ce projet ouvrent la porte à un développement ultérieur du recyclage des pneus usagés via la production de composés TPE respectueux de l'environnement, rentables et à valeur ajoutée pour plusieurs applications industrielles telles que l'automobile, l'emballage et le génie civil.

ABSTRACT

This work developed an innovative approach of tire recycling through the application of waste tire rubber and textile fiber as reinforcements for the production of fully recycled thermoplastic elastomer (TPE), compounds turning wastes into added-value materials. An experimental optimization was performed to develop a specific phase morphology and achieve balanced physical, mechanical, and thermal properties of TPE based on recycled materials.

In the first part, ground rubber tire (GTR) from regenerated rubber (RR) and non-regenerated rubber (NRR) based on off-the-road (OTR) tires were melt blended (twin-screw extrusion) with recycled high-density polyethylene (rHDPE) to investigate the effect of rubber regeneration and composition on the processability, phase morphology and properties of highly filled TPE containing up to 90 wt.% GTR. Inclusion of RR into rHDPE contributed to better flowability and processability because of higher chain mobility and particle deformability compared to NR particles. Despite decreasing tensile strength and tensile modulus with rubber content (stress concentration points), the elongation at break and impact strength increased which was attributed to the presence of a more elastic phase content and higher energy absorption through the deformation of rubbery particles retarding fracture.

In the second part, TPE blends based on recycled thermoplastic were prepared via melt blending to study the effect of GRT particle size (0–250 µm, 250–500 µm and 500–850 µm) and content (0, 20, 35, 50 and 65 wt.%). The results revealed that for a fixed blend composition, smaller GTR particles (0–250 µm) gave higher tensile properties and toughness compared to larger particles because of higher specific surface area (higher value and better contact) between small GTR particles and the matrix promoting interfacial interaction. However, smaller particles had a negligible effect on mechanical strength at higher GTR content (above 50 wt.%) since incompatibility and poor interphase quality played a more significant role.

In the next step, different types of regenerated recycled rubbers (RR_1 and RR_2) were used to produce highly filled TPE blends (over 70 wt.%). Strong entanglement between RR_2 (regeneration degree of 24%) free chains and the thermoplastic macromolecules contributed to strong interfacial interaction, leading to high mechanical properties. The introduction of a recycled ethylene-vinyl acetate (rEVA) copolymer improved the elongation at break and impact strength by 27% and 11% respectively, via

encapsulation of the rubber phase by the elastomer copolymer (10 wt.%) forming a thick/soft interphase decreasing interfacial stress concentration slowing down fracture.

In the last part, a masterbatch based on maleic anhydride grafted polyethylene (MAPE)/RR (70/30) was used for impact modification and compatibilization of recycled TPE composites reinforced with recycled tire fiber (RTF). The addition of surface coated RR with the coupling agent delayed crack initiation/propagation by forming a thick/soft interphase decreasing interfacial stress concentration slowing down fracture. Encapsulation of the rubber phase by MAPE provided an efficient method for waste tire recycling (rubber and fibers) by producing toughened TPE composites with acceptable mechanical properties.

Overall, the results obtained in this project open the door for further development of waste tires recycling via the production of environmentally friendly, cost effective and added-value TPE compounds for several industrial applications like automotive, packaging and civil engineering.

TABLE OF CONTENTS

LIST OF TABLES

LIST OF FIGURES

ABBREVIATIONS

3D	Three-dimensional
AA	Acrylic acid
AAm	Acrylamide
ATR-FTIR	Attenuated total reflection Fourier transform infrared
BR	Butadiene rubber
CB	Carbon black
CNT	Carbon nanotube
COPE	Copolyester
CPE	Chlorinated polyethylene
CV	Conventional vulcanization
DADS	Diallyl disulfide
DCP	Dicumyl peroxide
DHBP	2,5-dimethyl-2,5-di-(tert-butylperoxy)-hexane)
DMA	Dynamic mechanical analysis
DPDS	Diphenyl disulfide
DR	Devulcanized rubber
DSC	Differential scanning calorimeter
DTG	Derivative thermogravimetry
EAA	Ethylene-acrylic acid copolymer
EB	Elongation at break
EDA	Energy dispersive spectroscopy
E-GMA	Ethylene-co-glycidyl methacrylate copolymer
ENB	5-ethylidene-2-norborene
eNR	Epoxydized natural rubber
EOF	End-of-life
EPDM	Ethylene–propylene–diene-monomer rubber
EV	Efficient vulcanization
EVA	Ethylene-vinyl acetate
FTIR	Fourier transform infrared

GTR	Ground tire rubber
H_2O_2	Hydrogen peroxide
H_2SO_4	Sulphuric acid
$HClO_4$	Perchloric acid
HDPE	High density polyethylene
HNBR	Hydrogenated nitrile-butadiene rubber
HNO_3	Nitric acid
$KMnO_4$	Potassium permanganate
LDPE	Low-density polyethylene
LLDPE	Linear low-density polyethylene
LTP	Low temperature plasma
MA	Maleic anhydride
MAPE	Maleic anhydride grafted polyethylene
MAPP	Maleic anhydride grafted polypropylene
Me_3SiO	Trimethylsiloxychlorosilanes
MES	Mild extract solvate
MFI	Melt flow index
MMT	Modified montmorillonite
MW	Molecular weight
Na-MMT	Sodium montmorillonite
NBR	Nitrile-butadiene rubber
NP	Nanoparticles
NR	Natural rubber
NRR	Non-regenerated rubber
OTR	Off-the-road
PA6	Polyamide 6
PE	Polyethylene
PEBA	Polyether block amide
PMMA	Poly (methyl methacrylate)
POE	Ethylene-octene copolymer
PP	Polypropylene

PS	Polystyrene
PU	Polyurethane
PVI	Prevulcanization inhibitor
rEVA	Recycled ethylene-vinyl acetate
rHDPE	Recycled high density polyethylene
rLDPE	Recycled low-density polyethylene
rPE	Recycled polyethylene
rPP	Recycled polypropylene
RR	Regenerated rubber
RR_1	Regenerated rubber (~600 μm)
RR_2	Regenerated rubber (~500 μm)
rSBR	Regenerated styrene-butadiene rubber
RTF	Recycled tire fibers
RTR	Regenerated tire rubber
SBC	Styrene block copolymer
SBR	Styrene-butadiene rubber
SBS	Styrene-butadiene-styrene
SEBS	Styrene-ethylene-butylene-styrene
SEM	Scanning electron microscopy
SiO_4	Silicate
SWCNT	Single walled carbon nanotube
TBBS	N-tert-butyl-2-benzothiazolesulfenamide
TDAE	Treated distillate aromatic extract
TGA	Thermogravimetric analysis
THF	Tetrahydrofuran
TMTD	Tetramethyl thiuram disulfide
TPE	Thermoplastic elastomer
TPNR	Thermoplastic natural rubber
TPO	Thermoplastic elastomeric olefins
TPU	Thermoplastic polyurethane

TPV	Thermoplastic vulcanizate
TS	Tensile strength
UV	Ultraviolet
UDR	Undevulcanized rubber
xNBR	Polar carboxylated nitrile rubber
XPS	X-ray photoelectron spectroscopy
WTD	Waste tire dust
ZnO	Zinc oxide

SYMBOLS

d_1	Density of the solvent (g/cm^3)
d_2	Density of the polymer (g/cm^3)
E	Young's modulus (MPa)
E'	Storage modulus (MPa)
E''	Loss modulus (MPa)
f	Functionality of the crosslinks (-)
G'	Shear storage modulus (MPa)
K	Constant associated to rubber/solvent interaction (g/g min^n)
m_0	Initial mass of sample (g)
M_{min}	Minimum torque (dN.m)
m_t	Mass of the swollen sample (g)
M_t	Solvent mass absorbed (g)
M_∞	Solvent mass absorbed at equilibrium state (g)
n	Exponent indicating the diffusion mode (-)
Q	Swelling degree (%)
S_1	Sol fraction before regeneration (%)
S_2	Sol fraction after regeneration (%)
t	Time (s)
T	Temperature (°C)
$T_{5\%}$	Temperature for 5% weight loss (°C)
T_{10}	Temperature for 10% weight loss (°C)
T_{50}	Temperature for 50% weight loss (°C)
t_{90}	Optimum curing time (cure for 90%) (s)
$tan\ \delta$	Damping factor (-)
T_C	Crystallization temperature (°C)
T_g	Glass transition temperature (°C)
T_m	Melting temperature (°C)
T_{max}	Temperature for highest weight loss rate (°C)
T_r	Torque (N·m)

v_1	Crosslinking density before regeneration (mol/cm^3)
v_2	Crosslinking density after regeneration (mol/cm^3)
V_r	Rubber volume fraction in the swollen sample
V_s	Solvent molar volume (cm^3/mol)
W_0	Initial weight of the sample (g)
W_s	Weight fraction of the solvent in the swollen sample (g)
W_r	Weight fraction of the dry rubber sample (g)
X_c	Crystallinity degree (%)
χ	Polymer-solvent interaction parameter
ΔG_{mix}	Free energy of mixing
ΔH_m	Melting enthalpy (J/g)
ΔH_{m0}	Melting enthalpy of pure crystals (100%) (J/g)
ΔH_{mix}	Enthalpy of mixing
ΔS_{mix}	Entropy of mixing
γ^d	Dispersive part of surface energy (mN.m^{-1})
γ^p	Polar part of surface energy (mN.m^{-1})
γ_{xy}	Interfacial energy (mN.m^{-1})
ω	Wetting coefficient (-)
η_{swell}	Crosslink density (mol/cm^3)
ξ_{oxy}	Degree of oxidation (mg/g)
ξ	Crosslink density of RR (mol/cm^3)
ξ_0	Crosslink density of NRR (mol/cm^3)
ω	Screw speed (rpm)
$\dot{m}$	Mass flow rate of the material processed (g/min)
φ	Weight fraction of filler (-)
σ_Y	Tensile strength (MPa)
ε_b	Elongation at break (%)

DEDICATION

To Mona

To my parents

ACKNOWLEDGEMENTS

I would like to express my sincere gratitude to my supervisor, Professor Denis Rodrigue, for his guidance throughout this research and his constant support and encouragement. It has been a great honor to be supervised by him and I appreciate all his contributions of time, idea developments and financial support which make this Ph.D. research more and more productive and fruitful. His accurate, practical, and realistic attitude toward scientific research will certainly hold positive influences on my career and personal life.

I would like to extend my gratitude to the faculty, technical and administrative staff of the Department of Chemical Engineering at Laval University for providing a unique environment for research. Especially Mr. Yann Giroux, our group technician, for his training and help on different equipment. I would like to extend my acknowledge to my friends and colleagues for their friendship and support which made great memories throughout my Ph.D. program.

I recognize that this research would not have been possible without the financial assistance from the Natural Sciences and Engineering Research Council of Canada (NSERC), Research Center for High Performance Polymer and Composite Systems (CREPEC), and Research Center on Advanced Materials (CERMA).

Last in the list, but first in my heart, are my family and my beloved wife. I would like to deeply thank my parents and my dear sister for their unconditional love and support throughout my life. To my wife, Mona, thank you for your understanding and the sacrifices that you have made during the long drawn-out process. There will never be a right word to express my feeling of appreciation for everything you have done.

FOREWORDS

This Ph.D. dissertation is divided into six chapters based on a series of journal papers. To begin with, a brief introduction on the importance and challenges of recycling waste rubber, in particular discarded tires, is presented as well as the general context and objectives along with a brief discussion on the experimental strategies.
Chapters 1 and 2 present critical literature reviews on recycling waste tire rubber into ground tire rubber (GTR) for the reinforcement of thermoplastics and rubber compounds as:

Chapter 1

A. Fazli and D. Rodrigue, *Waste Rubber Recycling: A Review on the Evolution and Properties of Thermoplastic Elastomers*. Materials, 2020. 13(3): p. 782.

This chapter presents a critical literature review to cover the most recent progress on waste rubber recycling focussing on melt blending of waste tire rubbers with thermoplastic matrices. Furthermore, this section presents developments in surface modification and devulcanization of ground tire rubber (GTR) and compatibilization of thermoplastic elastomer (TPE) blends to improve the interfacial adhesion between a crosslinked rubber phase and a thermoplastic. Several types of TPE are extensively discussed and analyzed in terms of morphological, mechanical, thermal and rheological characterizations. Although GTR is the main material reviewed in this work, the latest developments related to the structure, preparation and characterization of TPE filled with regenerated rubber (RR) are also discussed.

Chapter 2

A. Fazli and D. Rodrigue, *Recycling Waste Tires into Ground Tire Rubber (GTR)/Rubber Compounds: A Review*. Journal of Composites Science, 2020. 4(3): p. 103.

This chapter presents the evolution of GTR recycling methods (retreading, incineration, pyrolysis and composite) and downsizing techniques. Since waste tires have high potential of being a source of valuable raw materials, the recent development and opportunity of using GTR in polymers compounds are reviewed. This section also presents a review of the possible physical and chemical surface treatments to improve the GTR adhesion and interaction with different matrices, including rubber

regeneration processes, such as thermomechanical, microwave, ultrasonic and thermochemical producing regenerated tire rubber (RTR). In this part, a focus is made on using GTR as a partial replacement in rubber compounds.

Chapters 3-6 present the experimental results in the form of journal papers as follow:

Chapter 3

A. Fazli and D. Rodrigue, *Morphological and Mechanical Properties of Thermoplastic Elastomers Based on Recycled High-Density Polyethylene and Recycled Natural Rubber*. International Polymer Processing, 2021. 36(2): p. 156.

This chapter, as the first part of the experimental work, is devoted to a complete study on melt blending GTR and recycled high-density polyethylene (rHDPE) with a focus on processability, phase morphology, mechanical (tension, flexion, and impact) and physical (hardness and density) properties. Two types of recycled rubber (regenerated rubber (RR) and non-regenerated rubber (NRR) are used for the production of recycled TPE blends filled with a wide range of GTR from 20 to 90 wt.% to determine a relation between rubber regeneration and blend composition with structure/properties of the blends. Although RR compounds were easier to process because of lower motor torque and die pressure drop during melt extrusion, the mechanical properties in tension of RR blends were lower than for NRR blends, which was attributed to the degradation of the GTR backbone chains lowering the molecular weight (MW) during the regeneration process. The experimental results also show that 80 wt.% GTR is the optimum concentration for the production of TPE showing good elongation at break (127%).

Chapter 4

A. Fazli and D. Rodrigue, *Effect of Ground Tire Rubber (GTR) Particle Size and Content on the Morphological and Mechanical Properties of Recycled High-Density Polyethylene (rHDPE)/GTR Blends.* Recycling, 2021. 6(3): p. 44.

The next chapter aims at providing a detailed study on the effects of recycled rubber particle size and content on the melt processability, crystallinity, morphological and mechanical (quasi-static tensile and flexural tests, combined with impact strength and dynamic mechanical analysis) properties of recycled

TPE blends. In particular, melt blending of rHDPE with different GTR particle sizes (0–250, 250–500 and 500–850 μm) for blend composition between 20 and 65 wt.% was performed to optimize the formulation of a 100% recycled blend with good mechanical performance. Increasing the GTR content up to 65 wt.% led to phase separation (high interfacial tension) and filler agglomeration, resulting in the formation of voids around GTR particles and increasing defects/cracks in the matrix. However, introducing fine GTR particles (0–250 μm) with higher specific surface area produced a more homogenous blend structure and uniform particle dispersion due to improved physical/interfacial interactions. The results also show that for a fixed composition, smaller GTR particles (0–250 μm) give lower melt flow index (MFI), but higher tensile strength/modulus/elongation at break and toughness compared to larger GTR particles (250–500 μm and 500–850 μm).

Chapter 5

A. Fazli and D. Rodrigue, *Thermoplastic Elastomers Based on Recycled HDPE/GTR/EVA: Effect of GTR Regeneration on Morphological and Mechanical Properties*. Journal of Thermoplastic Composite Materials (submitted).

In this chapter, the effect of GTR regeneration (effect of the regeneration degree and crosslink density) and blend composition on the swelling, morphological, mechanical and physical properties of highly filled TPE blends (above 70 wt.% GTR) were studied. NRR and two types of RR (RR_1 and RR_2) in the range of 70, 80 and 90 wt.% were introduced into rHDPE via continuous melt-mixing in a twin-screw extruder and the specimens were compression molded for further analysis. To further improve the adhesion and achieve rubber-like properties, recycled ethylene vinyl acetate (rEVA) was used as a compatibility/interfacial adhesion promoter. It was found that, strong entanglement between rubber and thermoplastic strongly depends on the regeneration degree and sol fraction of rubber particles controlling interfacial interactions and hence the final structure/properties of TPE. Introduction of an elastomer copolymer promoted uniform GTR dispersion by encapsulating the GTR particles and decreasing the surface energy resulting in improved interfacial adhesion leading to improved resistance to crack propagation and failure.

Chapter 6

A. Fazli and D. Rodrigue, *Phase Morphology, Mechanical, and Thermal Properties of Fiber Reinforced Thermoplastic Elastomer: Effects of Blend Composition and Compatibilization. Journal of Reinforced Plastics and Composites* (Accepted).

In chapter 6, a new approach is proposed for impact modification of recycled TPE composites reinforced with recycled tire fiber (RTF) (20 wt.%). The materials (rHDPE, RR, RTF and coupling agent) were compounded by melt extrusion and injection molded before being characterized in terms of morphological, mechanical, physical and thermal properties. The results showed that adding RTF increased the tensile and flexural moduli of rHDPE/RR/RTF blends, while the impact strength decreased. So, a blend of maleic anhydride grafted polyethylene (MAPE)/RR (70/30) was used as a second step instead of neat RR as an impact modifier for the fiber reinforced composites. The tensile properties were improved as the elongation at break increased up to 173% because of better interfacial adhesion. The resulting TPE composites based on rHDPE/(RR/MAPE)/RTF showed highly improved toughness (60%) via encapsulation of the rubber phase by MAPE forming a thick/soft interphase decreasing interfacial stress concentration slowing down fracture.

Finally, a general overview of the work performed followed by some recommendations for future studies are presented.

For all the articles (Chapters 1-6), my contributions were related to performing the experimental works, collecting and analyzing the experimental results, as well as writing the initial draft of the manuscripts, in collaboration with Prof. Rodrigue who performed manuscripts revision.

NTRODUCTION AND OBJECTIVES

Introduction

The growing generation of waste polymers (plastic/rubber) has been a global environmental concern due to the short lifespan and non-biodegradability of polymer waste with very complex structure and composition [1]. A significant amount of the total polymer wastes are comprised of discarded tires with annual generation of 1.5 billion of whole-tires worldwide [2]. According to current statistics, the growth in tonnes of waste tires collected by all stewardship programs in Canada increased from 350 000 to 418 000 tonnes between 2010-2018, which indicates the importance of storage and elimination of used tires as an urgent issue for the environment and society [3]. For example, RECYC-QUÉBEC awarded in 2018 more than $ 1.8 million in grants to 5 processors for modernizing their recycling equipment to process 25 000 more tonnes of scrap tires, indicating the importance of development of environmentally friendly and cost-effective techniques for the recovery and recycling of waste tires [3]. Waste tires are mainly composed of rubber (40–50% of the total mass of the tire) which is vulcanized (crosslinked structure) and reinforced with a wide range of additives (textile fibers, steels, carbon black, stabilizer, antioxidant, antiozonant, etc.) to improve the performance and properties of tires (tensile properties, abrasion resistance, thermal stability and chemical resistance) and to make tires extremely resistant to severe outdoor conditions (chemical reagents, high temperatures, radiations and mechanical stresses) during their lifetime [4,5]. So, tire rubber as thermoset materials are infusible/insoluble (cannot be melted and reprocessed) with very complex structures and compositions contributing to very difficult recovery and recycling [5]. Landfill and incineration cannot address the problem of waste tire generation because of health and environmental risks for contaminating the soils/groundwater and greenhouse gas/toxic gas emission. Over the last decades, several countries started to impose legal regulations supporting the recycling and recovery of used tires to achieve market benefits and environmental needs [4]. Nowadays, common methods and preferred recycling routes for the sustainable management of used tires are based on the development of recycled-based composites reinforced with tire rubber with reasonable economy of manufacturing and balanced properties [1]. Increasingly environmental standards and market demands have attracted industries for manufacturing of novel materials through compounding tire rubber crumbs with thermoplastics, thermosets or rubbers for wide range of applications, such as extruded products (wheels, gasket, shoe sole), artificial sports equipment, automotive sector parts (tires, wiper blades, seals, hoses

seatbelts, gaskets and insulators) and construction industries material (asphalt, concrete and cement) [6-8]. From the environmental and material engineering point of view, the advantages of this approach include substantial virgin materials resource saving by reusing high amounts of waste tires and the production of inexpensive added-value composites from low cost polymer wastes. Compounding tire rubber crumbs as the main product of tire recycling with thermoplastic resins to produce thermoplastic elastomers (TPE) is the most promising method for reprocessing waste tires as a partial solution to this environmental issue [9]. Tire rubber crumbs have been widely incorporated into several thermoplastics, such as polyethylene (PE) [10-12], polypropylene (PP) [13-15], polystyrene (PS) [16,17], polyamide 6 (PA6) [18] and ethylene-vinyl acetate (EVA) [19,20] through melt blending processes for the production of TPE compounds. In this case, discarded tires need to be shredded to smaller particle sizes; ground tire rubber (GTR), via downsizing processes related to rubber grinding (granulation), while the textiles and steels parts (fiber reinforcement) are removed by pneumatic separators and electromagnets, respectively. The GTR particle size/distribution is influenced by the grinding method used, such as cryogenic, ambient, wet and water jet [8,21]. TPE, as a multi-functional material, not only combines several of the attributes and features of both thermoplastic and thermoset, like processability of thermoplastic and the elasticity of rubber, but these materials can be also be processed and recycled like thermoplastic materials [5,12]. The main limiting factor for the incorporation of GTR in thermoplastic matrices is the lack of compatibility between the thermoplastic and the vulcanized tire rubber (crosslinked network), leading to substantial decreases in mechanical properties and durability/stability of the compounds. The GTR crosslinked rubber molecules do not have the freedom to entangle with thermoplastic molecules resulting in low compatibility, high interfacial tension and phase separation [11,12]. Also, environmental stresses, such as heat, radiation, oxygen, or humidity, as well as the reprocessing of recycled materials, cause degradation (chain scission) leading to losses in ductility and changes in mechanical performance. Low mechanical properties of TPE as a physical mixture of two incompatible polymers in industrial applications can lead to lower safety and shorter product life[1,4]. It is well known that the elongation at break and toughness of TPE blends, depending on compatibility, are crucial factors in several engineering applications because a minimum of 100% elongation at break is required to be recognized as a good TPE [22]. This matter sparked interest in researchers around the world to look for solutions to improve compatibility between the thermoplastic and rubber phase to produce TPE from GTR with acceptable properties without sacrificing other engineering properties. To overcome this challenge, different attempts have been carried out to increase the GTR/thermoplastic

interfacial adhesion generating improved blend homogeneity and processability, as well as mechanical strength and long term durability through GTR surface modification[23,24], devulcanization [25,26], dynamic vulcanization [11,27] and compatibilizing agent addition [28,29]. All these techniques aim to make the interface between each phase similar to each other or to provide specific interaction sites increasing interfacial interaction; i.e. compatibilization [1,12]. Although a large body of literature is available on the compatibilization of TPE based on virgin thermoplastics and recycled tire rubber [1,4,5,9], the number of studies on the production and characterization of TPE based on recycled thermoplastics and GTR compatibilized with recycled copolymers is very limited [17,30,31]. Also, very few studies investigated the potential of recycled tire fibers (RTF) for TPE reinforcement [29,32]. Attention should be paid to the compatibilization of 100% recycled-based TPE since it is most economic and eco-friendly use of recycled plastics and to decrease the amount of polymer wastes and the final cost of these compounds.

Objectives

This work investigates the effect of both recycled tire rubber (GTR and/or RR) and fiber contents (RTF) on the properties of TPE composites with a focus on the structure-property relationships. The general objective is to develop recyclable and sustainable blends of post-consumer recycled thermoplastic resins and recycled GTR reinforced with RTF fillers for the recycling and revalorization of different residual materials with advantages for the environment and will create new applications. The main objective of this project can be broken down into several sub-objectives and activities. These objectives can be described as:

The first part is devoted to the melt blending of recycled high-density polyethylene (rHDPE) from packaging material as the thermoplastic phase and recycled/regenerated tire crumb as the elastomer phase, to produce 100% recycled TPE. This part is focused on the manufacture of highly filled TPE (up to 90% rubber) to study the effect of filler weight ratio, particle size and regeneration on the processability, morphological, swelling, mechanical, physical and thermal properties of binary TPE. This requires the independent optimization of the formulations to achieve balanced properties (especially tensile properties) with a focus on the structure-property relationships. To address these issues, an experimental plan is designed to improve bonding and promote stress transfer between the components using recycled ethylene vinyl acetate (rEVA) elastomer copolymer as a compatibility/interfacial adhesion promoter to produce ternary TPE blends of rHDPE/GTR/rEVA.

The second part is devoted to produce TPE composites using both recycled tire rubber and fiber. The effect of reinforcement type and content on the phase morphology, as well as mechanical and thermal properties, especially blend toughening, is thoroughly investigated. In particular, a new approach is proposed for the compatibilization and impact modification of TPE by adding surface coated rubber particles into a fiber reinforced rubberized composite to improve toughness by creating a thick interface to compatibilize the waste rubber particles with a polyolefin matrix. Also, the incorporation of a suitable compatibilizer can improve the thermal stability of the blends. For each type of materials (thermoplastic, GTR, RTF and coupling agent), an optimized formulation with its processing conditions is developed to improve the physical compatibility (higher interfacial adhesion) leading to increased fracture resistance for a fiber-reinforced system combined with improved stiffness and thermal stability.

Finally, it is expected to produce green composite blends from recycled materials with at least 100% elongation at break to be recognized as good TPE. The efficiency of this approach combined with its simplicity provides good economic and environmental opportunity in recycling different types of waste rubbers as fillers, or even modifiers, in thermoplastic resins. As the plastic/tire recycling industry develops, significant environmental and economical benefits for industries and societies contributing to the advancement of knowledge in the flourishing field of waste materials recycling and creating new job opportunities. The results from this project will help industries to improve the TPE processing conditions, as well as reducing the cost of products and processes by using low-cost recycled materials. The results will certainly help developing new lines of products and attracting new clients working on recycled composites, to market new compounds with good mechanical performance similar to current commercial TPE based on virgin polymers. There is also the possibility to reduce the costs via optimized conditions and develop new applications (second life) for complex materials like vulcanized rubbers after their end of life. As a result, higher volumes of waste materials will be processed, helping to solve an environmental issue by the valorization of discarded waste plastics and tires for the production of recycled rubberized reinforced composites.

CHAPTER 1 WASTE RUBBER RECYCLING: A REVIEW ON THE EVOLUTION AND PROPERTIES OF THERMOPLASTIC ELASTOMERS

Résumé

De nos jours, les plastiques et les caoutchoucs sont largement utilisés pour produire une large gamme de produits pour plusieurs applications telles que l'automobile, le bâtiment et la construction, la manutention, l'emballage, les jouets, etc. Cependant, leurs déchets (matériaux après leur fin de vie) ne se dégradent pas et restent pendant une longue période de temps dans l'environnement. L'augmentation de la production de déchets polymères (plastiques et caoutchoucs) dans le monde a conduit à la nécessité de développer des méthodes appropriées pour réutiliser ces déchets et diminuer leurs effets négatifs par simple élimination dans l'environnement. La combustion et la mise en décharge en tant que méthodes traditionnelles d'élimination des déchets polymères présentent plusieurs inconvénients tels que la formation de poussières, de fumées et de gaz toxiques dans l'air, ainsi que la pollution des ressources en eau souterraines. Du point de vue de la consommation d'énergie et des questions environnementales, le recyclage des polymères est le moyen le plus efficace de gérer ces déchets. Dans le cas du recyclage du caoutchouc, les déchets de caoutchouc peuvent subir une réduction de taille et les poudres résultantes peuvent être mélangées à l'état fondu avec des résines thermoplastiques pour produire des composés élastomères thermoplastiques (TPE). Les TPE sont des matériaux polymériques multifonctionnels alliant l'aptitude au traitement des thermoplastiques et l'élasticité des caoutchoucs. Cependant, ces matériaux présentent des performances mécaniques médiocres en raison de l'incompatibilité et de l'immiscibilité de la plupart des mélanges de polymères. Ainsi, le principal problème associé à la production de TPE à partir de matériaux recyclés via le mélange à l'état fondu est la faible affinité et l'interaction entre la matrice thermoplastique et le caoutchouc réticulé. Ceci conduit à une séparation des phases et à une faible adhérence entre les deux phases. Dans cette revue, les derniers développements liés aux caoutchoucs recyclés en TPE sont présentés, ainsi que les différentes méthodes de compatibilisation utilisées pour améliorer l'adhérence entre les déchets de caoutchouc et les résines thermoplastiques. Enfin, une conclusion sur la situation actuelle est fournie avec des ouvertures pour des travaux futurs.

Mots-clés: Caoutchouc, recyclage, déchets polymères, élastomère thermoplastique, compatibilisation

Abstract

Nowadays, plastics and rubbers are broadly being used to produce a wide range of products for several applications like automotive, building and construction, material handling, packaging, toys, etc. However, their waste (materials after their end of life) does not degrade and remain for long period of time in the environment. Increase of polymeric waste materials generation (plastics and rubbers) in the world led to the need of developing suitable methods to reuse these waste materials and decrease their negative effects by simple disposal into the environment. Combustion and landfilling as traditional methods of polymer wastes elimination have several disadvantages such as the formation of dust, fumes, and toxic gases in the air, as well as pollution of underground water resources. From the point of energy consumption and environmental issues, polymer recycling is the most efficient way to manage these waste materials. In the case of rubber recycling, the waste rubber can go through size reduction and the resulting powders can be melt blended with thermoplastic resins to produce thermoplastic elastomer (TPE) compounds. TPE are multi-functional polymeric materials combining the processability of thermoplastics and the elasticity of rubbers. However, these materials show poor mechanical performance as a result of incompatibility and immiscibility of most polymer blends. So, the main problem associated with TPE production from recycled materials via melt blending is the low affinity and interaction between the thermoplastic matrix and the crosslinked rubber. This leads to phase separation and weak adhesion between both phases. In this review, the latest developments related to recycled rubbers in TPE are presented, as well as the different compatibilization methods used to improve the adhesion between waste rubbers and thermoplastic resins. Finally, a conclusion on the current situation is provided with openings for future works.

Keywords: Rubber, recycling, waste polymers, thermoplastic elastomer, compatibilization

1.1 Introduction

Rubber, as an elastomeric material, has the ability of reversible deformation (between 100 up to 1000%) which is significantly influenced by its chemical structure and molecular weight (MW). Ideally, rubber chains should return to their original shape after removing the applied force (stress). The macromolecular chains of rubber are long and oriented without large substituents which makes them capable of moving and rotating around chemical bonds at low temperatures because of their low glass transition temperature (T_g). Increasing irregularities in the polymer chains or the presence of large substituents (styrene-butadiene rubbers, SBR) leads to higher rubber T_g.

The production of high-quality rubber at large scale with low cost substantially increased with the development of efficient vulcanization processes. Vulcanization is defined as the irreversible crosslinking reaction via curing agents (sulfur or peroxide materials) to form a three-dimensional (3D) network between the rubber macromolecules. Several parameters must be controlled in the rubber vulcanization process such as curing time, temperature and fillers having a direct effect on the chemical, mechanical and physical properties of crosslinked rubbers. Incorporation of vulcanizing agents into an unsaturated rubber improves the rubber strength due to the crosslinked structure created. Therefore, vulcanized rubber as an elastic, insoluble and infusible thermoset material cannot be directly reprocessed. This is an important limitation for material recycling, especially after the end of life of a part. Depending on the final application, different rubbers are mixed with different components and additives. For instance, stabilizers, anti-oxidants, and antiozonants are being used in rubber formulation to make tires extremely resistant to severe outdoor conditions (chemical reagents, high temperatures, radiations and shear stress) during their lifetime [1,9,33].

Tires as the main application of rubber industries are complex materials containing several components suitable to operate in a wide range of environment. Rubber is the main component used for tire manufacturing which can be classified into natural rubber (NR), SBR, nitrile-butadiene rubber (NBR) and ethylene–propylene–diene-monomer rubber (EPDM). However, the presence of reinforcing fillers, antioxidants, antiozonants and curating agents in tire formulation makes them resistant to biodegradation, photochemical decomposition, and high temperatures [9,34]. Therefore, waste tires management is an important issue with respect to the global growth of tire industries. This paper reviews progress of waste tire recycling focused on melt blending of ground tire rubber (GTR) with thermoplastic matrix. Also, this review presents developments in surface modification and

devulcanization of GTR and compatibilization of thermoplastic elastomer (TPE) blends to improve the interfacial adhesion of GTR and thermoplastic matrix.

1.1.1 Microstructural Composition

1.1.1.1 Elastomers

NR is extensively used in rubber production as an elastomer component. NR with high MW and long chain branches has the ability to quickly crystallize under stretching leading to high tensile strength and tear growth resistance. Usually, NR is mixed with other synthetic rubbers such as polybutadiene rubber (BR), hydrogenated nitrile-butadiene rubber (HNBR), SBR, NBR, and EPDM to further improve its properties (tensile strength and tear growth resistance) in tire manufacturing [35].

1.1.1.2 Fillers

Different fillers such as carbon black (CB), precipitated silica, and clay have been used in rubber formulation to improve the rubber strength. This is done via the formation of a flexible filler network and strong polymer-filler interactions [36]. Stiffening fillers (CB and silica) improve rubber stiffness, tensile and tear strength, hardness, and rupture modulus as a result of increased chains entanglements and shear strength between the polymer chains. Montmorillonite, synthetic mica and saponite are clay-based fillers used in rubber production due to better mechanical properties improvement compared to CB [37]. For example, Okada [38] reported the positive effect of 10 vol.% of organoclay in NBR to achieve similar tensile strengths as rubber formulations with 40 vol.% CB. However, the rubber microstructure might be affected by the size, shape and molecular structure of the fillers [6].

1.1.1.3 Other Additives

Several materials have been used to increase the durability and accelerate the crosslinking reaction of rubber compounds. For instance, zinc oxide (ZnO) has been used as an activator during vulcanization. Mild extract solvate (MES), naphthenic oil, treated distillate aromatic extract (TDAE), and paraffinic oils are being used to improve the rubber processability [6]. Nevertheless, the type and level of filler addition strongly depends on the rubber matrix being used.

1.1.2 Rubber Types

Rubbers can be categorized into different groups: saturated/unsaturated, natural/synthetic, etc. But according to the application and properties required, there are general rubbers and special rubbers. General rubbers are relatively low-cost materials produced and consumed in large volume, while special rubbers have special properties such as thermal stability, fire resistance, aging resistance, chemical resistance, and swelling resistance in non-polar oils as well as their elastic properties. Some of the most used rubber materials in industries are described to get a better understanding of their properties and applications.

1.1.2.1 NR

NR is a biopolymer based on cis-1,4-polyisoprene with a vegetable origin obtained from Hevea Brasiliensis (Figure 1.1). NR is an unsaturated rubber with long, regular, flexible, and linear macromolecules as well as high elastic properties (T_g ~ -70 °C). Unvulcanized NR can be reversibly elongated under high deformation up to 800-1000% due to its high resilient characteristics. Although several curing agents are available, NR is almost always vulcanized by sulfur-containing curing systems. Despite poor chemical resistance and processability, NR shows good elastic properties, resilience, and damping. The low aging resistance of NR is due to its poor stability towards ozone and oxygen. This rubber is mainly used for the production of tires, gloves, toys, elastic bands, erasers and sport equipment [7,39,40].

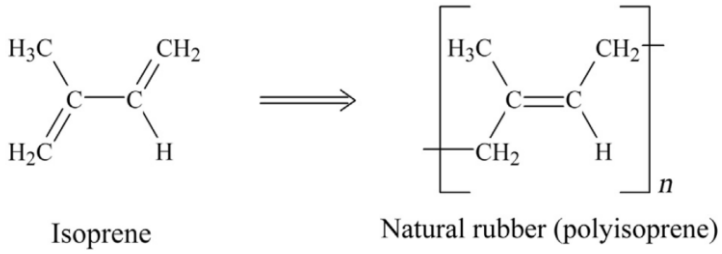

Figure 1.1 Chemical structure of isoprene and NR (polyisoprene). Adapted from reference [7].

1.1.2.2 Synthetic Rubbers

1.1.2.2.1 SBR

SBR is made from the copolymers of styrene and butadiene (Figure 1.2), but its properties are mainly affected by the polymer chain structure and styrene content. SBR cannot crystallize under stress and

is mostly vulcanized by sulfur agents. Currently, free radical copolymerization in emulsion and anionic copolymerization in solution are the main copolymerization methods for SBR preparation. SBR has low mechanical strength making it necessary to add reinforcing fillers into its formulation. SBR has been used in automotive industries, especially for car tires, because of its high abrasion resistance, thermal stability, and resistance against crack formation (better than NR and BR). However, SBR is less chemically reactive with slow curing kinetics which requires more accelerators [7,41].

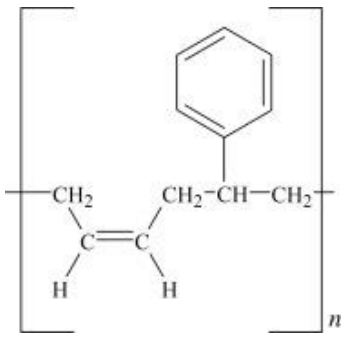

Figure 1.2 Chemical structure of SBR. Adapted from reference [7].

1.1.2.2.2 NBR

As shown in Figure 1.3, NBR is made from the copolymers of acrylonitrile and butadiene via radical copolymerization in emulsion at low temperature (5 to 30 °C). NBR does not crystallize under stress and has low tensile strength, but shows good resistance to non-polar solvents, fats, oils, and motor fuel. Oil resistance is directly dependent on the acrylonitrile content. The NBR structure is determined by its preparation method and changes from linear to highly branched molecules according to the copolymerization temperature. Swelling resistance in non-polar agents and T_g both increase with increasing acrylonitrile content. NBR has been widely used for sealing tubes, oil transport equipment and other devices with oils resistance [7].

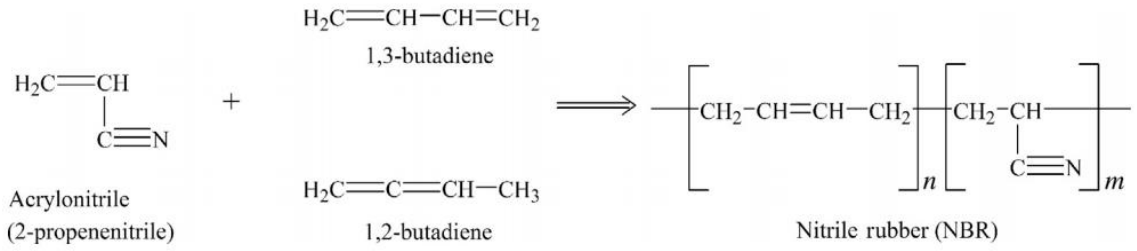

Figure 1.3 Monomers and polymer structure of NBR. Adapted from reference [7].

1.1.2.2.3 EPDM

EPDM is a terpolymer of ethylene, propylene, and a non-conjugated diene with residual unsaturation in the side chain. This synthetic rubber with a non-polar backbone shows better resistance to heat, light and ozone compared to unsaturated rubbers (NR or SBR). One of the most important grades of EPDM is with 5-ethylidene-2-norborene (ENB) as a diene (Figure 1.4). EPDM properties depend on the ethylene and propylene content. The most significant properties of the vulcanized EPDM are the excellent resistance to atmospheric aging, oxygen, and ozone up to 150 °C. EPDM can be cured by peroxide or sulfur systems and these rubbers are extensively used as sealing materials [7,42,43]. Despite peroxidic curing, sulfur vulcanization of EPDM show complex reactions induced by sulfur during crosslinking and a few kinetic numerical models are available on the accelerated sulfur vulcanization of EPDM [44,45].

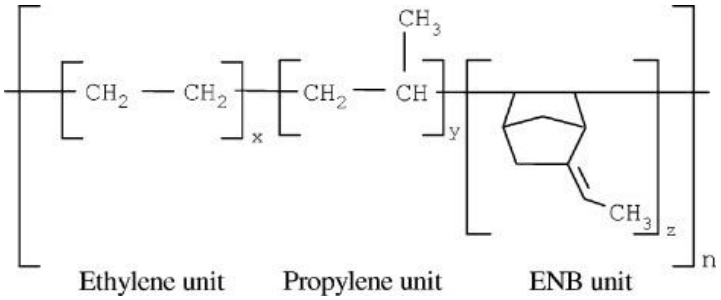

Figure 1.4 Chemical structure of EPDM containing ENB as a diene. Adapted from reference [43].

1.1.2.2.4 Polyurethane (PU)

PU is produced by the polyaddition of diisocyanates and polyols (an alcohol having two or more hydroxyl groups) (Figure 1.5). PU can be obtained in various chemical structures and different properties because of the types of monomers, composition ratios, and reaction conditions. PU has several advantages such as good abrasion and tear resistance, tensile strength, oxygen and ozone resistance, and low friction coefficient. The largest application of PU is in automotive industries as dampers, flexible connections, and electric lines [46].

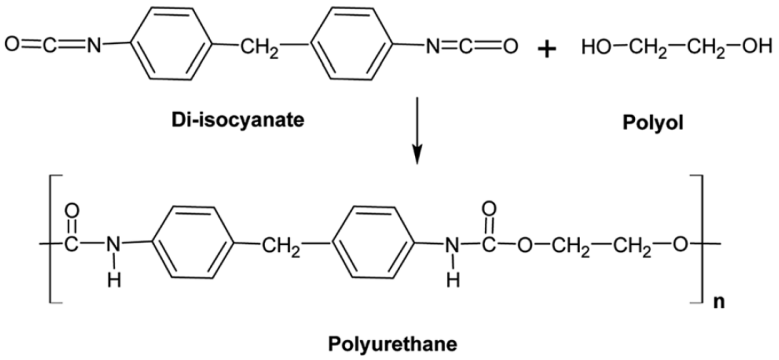

Figure 1.5 Schematic representation of PU and its monomers. Adapted from reference [46].

1.1.2.2.5 Silicone Rubber

Silicon rubber, also known as siloxanes, polyorganosiloxanes or polysiloxanes, is produced by multilevel hydrolysis and subsequent condensation of dimethyldichlorosilane in an acid medium or by ring opening polymerization of cyclotetrasiloxane, catalyzed by strong acids or bases. The polymer backbone is based on chain of silicon and oxygen atoms rather than carbon and hydrogen atoms. Silicone rubbers with very flexible structure show high stability over a wide range of temperatures (-70 to 250 °C) [47]. As shown in Figure 1.6, there are four primary groups identified by letters forming a typical polysiloxane. Silicon rubbers are also resistant to oxygen and ozone aging, so this rubber is mainly used for the manufacture of tubing for ozone transport. Finally, silicon rubbers are highly adhesive, hydrophobic, and biocompatible making this rubber an ideal material for medical implants and other devices biocompatible with human organisms [39,42].

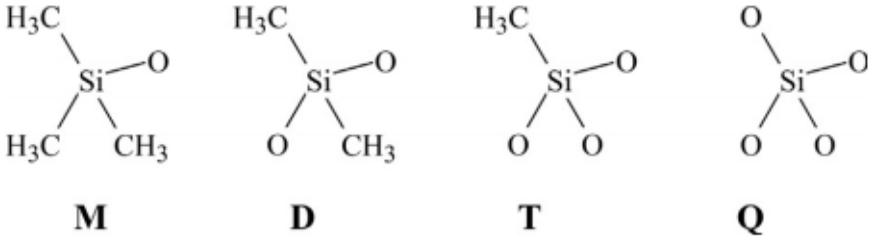

Figure 1.6 The four groups making polysiloxanes (MQ, VMQ, PMQ, PVMQ, PDMS): “M” is trimethylsiloxychlorosilanes (Me_3SiO), “D” is Me_2SiO_2, “T” is $MeSiO_3$ and “Q” is silicate (SiO_4). For “P”, replace Me by phenyl side groups, while for “V” replace Me by vinyl side groups. Adapted from reference [7].

1.2 Recycling

It is well-known that polymer decomposition (biodegradation) takes a long time and causes harmful environmental effects. So, polymer wastes disposal is a serious environmental issue. Tires containing

almost 50% rubber are polymeric materials. The global production of rubber materials in 2017 was about 26.7 million tons divided into 12.31 million tons of NR and 14.46 million tons of synthetic rubber [6]. Discarded rubber pipes, belts and shoes are various types of waste rubber products. However, the tire industries, as the main application of rubbers (65% of the global production), generate the largest amounts of rubber waste materials. Therefore, rubber recycling is often defined as tire recycling. Currently, 1.5 billion tires/year are discarded worldwide containing up to 90% of vulcanized rubber that cannot be easily recycled (reprocessed) due to their complex crosslinked structure [6]. Vulcanized rubbers are being used in tires manufacturing since these thermoset materials can sustain severe mechanical and thermal conditions while their properties do not change with temperature. The chemical composition of tires influences their mechanical behavior and lifespan. As shown in Table 1.1, a typical tire composition for passenger cars (7.5-9 kg) and trucks (50-80 kg) are different based on the rubber type as well as the other components [48].

Table 1.1 Typical compositions of tires [1,2,9,49].

Material	Cars/Passenger (wt.%)	Trucks (wt.%)
Rubber	41-48	41-45
Carbon Black	22-28	20-28
Metal	13-16	20-27
Textile	4-6	0-10
Additives	10-12	7-10

Waste tires are rich materials due to their composition and properties and thus the sources of valuable raw materials. Waste tires can be categorized as worn tires or end of life tires in which some of these worn tires are still suitable for on the road use. However, end of life tires cannot be used for tire manufacture. The incorporation of different additives such as stabilizers, antioxidants and antiozonants into the vulcanized rubber compounds make them resistant to biodegradation, photochemical decomposition, chemical reagents, and thermal degradation. Due to this complex formulation, finding practical methods at a suitable cost for waste tires recycling is a serious dilemma for the tires industries. Landfilling is the easiest approach to get rid of waste tires. However, there are several drawbacks. For instance, impermeable discarded tires might keep water for long periods of time and support sites for mosquito larva breeding, which cause deadly diseases such as dengue and malaria [1]. Several works have been reported on recycling end of life tires for energy recovery [50] and pyrolysis [51]. Waste tires, which contain more than 90% organic materials with a heat value of 32.6 MJ/kg (heat value of coal is 18.6-27.9 MJ/kg), have been used for energy recovery purposes [1]. For example, waste tires are used

as a fuel source in cement kilns which is more environmentally friendly compared to coal combustion. Moreover, waste tires are used as fuel for the production of steam, electrical energy, pulp, paper, lime, and steel. However, burning tires as fuel releases hazardous gases and only recovers 25% of the energy used for the rubber production [52]. Also, the pyrolysis of waste tires decomposes the rubber component to produce carbon black, zinc, sulphur, steel, oils, and gas. However, high operating costs of the pyrolysis plants limit the wide application of this method [53]. Some environmentally friendly recycling techniques have been developed such as triboelectric separation, froth flotation and laser-induced breakdown spectroscopy. However, these methods are expensive and the obtained recycled rubbers vary in cleanliness, size, shape, and surface topography quality [49,54,55]. Although vulcanized waste rubbers are difficult to recycle, they are very durable, strong and flexible materials which can be used as ideal fillers in composite production [6].

So, an interesting option is to blend waste tires with plastics (by the action of heat and pressure) to decrease the final costs of the products due to a lower amount of virgin material being used. Waste tires need to be shredded (grinding) to smaller particles (downsizing) for easier incorporation into plastics matrixes. Usually, pneumatic separators and electromagnets are used for the separation of textiles and steel from waste tires, respectively [1]. Several methods of waste tire downsizing processes are presented in Table 1.2 resulting in different surface characteristics and size of GTR. Cryogenic processes lead to clean granulates without surface oxidation. Shredded tires can be used in virgin/fresh polymers such as rubbers, thermoplastics and thermosets blends for civil engineering, automotive applications, sport equipment, and others. Blends of rubber with thermoplastic are consuming a large amount of waste tires a discussed in the next section [1,56].

Table 1.2 General methods of waste tire downsizing [1,2,9].

Methods	Description	Advantages	Disadvantages
Ambient (0.3 mm rough, irregular)	Repeated grinding following shredder, mills, knife, granulators and rolling mills	High surface area and volume ratio	Temperature could rise up to 130 °C Oxidation on the surface of granulates Cooling needed to prevent combustion
Wet ambient (100 µm rough, irregular)	Grinding suspension of shredded rubber using grindstone Water cools granulates and grindstone	Lower level of degradation on granulates High surface area and volume	Requires drying step and shredding of tires before grinding
Water jet (rough, irregular)	Used for large size tires (trucks and tractors) Water jet of >2000 bar pressure and high velocity used to strip rubber	Environmentally safe, energy saving, low level of noise and no pollutants	Requires high pressure and trained personnel
Berstoff's method (rough, irregular)	Combines a rolling mill with specially designed twin screw extruder in a line.	Small grain size, large specific area and low humidity	Not disclosed
Cryogenic (75 µm sharp edge flat/smooth)	Rubber cooled in liquid nitrogen and shattered using impact type mill	No surface oxidation of granulates and cleaner granulates	High cost of liquid nitrogen High humidity of granulates

1.3 TPE

Thermoplastic resins are being broadly used for melt blending with waste rubber powder to form TPE compounds. TPE is composed of an elastomeric component as a soft fraction and a non-elastomeric material as a hard segment which is a thermodynamically incompatible system. TPE compounds benefit from the processability of thermoplastics and the properties of glassy/semi-crystalline thermoplastics combined with soft elastomers. TPE compounds can be prepared by extrusion through the dissociation of hard domains at high temperature and shear followed by cooling and solidifying the polymer melt. TPE materials are categorized into thermoplastic elastomeric olefin (TPO), thermoplastic natural rubber (TPNR), thermoplastic vulcanizate (TPV), thermoplastic polyurethane (TPU), styrene block copolymer (SBC), polyether block amide (PEBA), and copolyester (COPE) [57].

1.3.1 TPE Structure

TPE compounds can be obtained by three different structures and morphologies as:

• Block copolymers consisting of elastic and non-elastic blocks

• Rubber/thermoplastic blends

• Dynamically vulcanized rubber/thermoplastic blends

1.3.1.1 Block Copolymers

TPE based on block copolymers consist of multi-block copolymers for which the end of these blocks can be crystallized and linked together forming a crosslinked network. The main fraction of block copolymers is the amorphous phase with rubber-like properties. Several copolymers have been used in this category such as TPU, SBC, PEBA and COPE. Figure 1.7 presents a schematic representation of a TPE copolymer illustrating the rigid crystalline segments and rubbery blocks as a continuous domain of soft rubbery chains. Under deformation, the hard blocks remain crystalline and never deform, so TPE deformation is governed by the soft rubber domains. Going through the melt temperature, the copolymer chains start to flow and the material can be processed like all thermoplastic polymers [58,59].

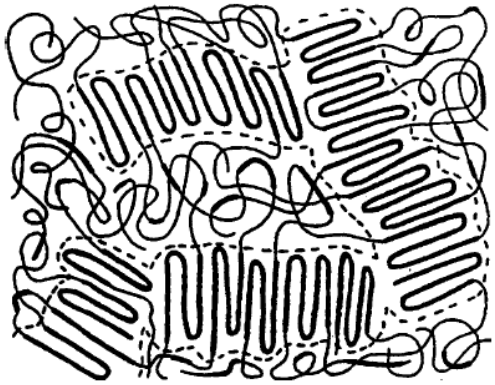

Figure 1.7 Morphology of a block copolymer TPE. Adapted from reference [60].

1.3.1.2 Rubber/Thermoplastic Blends

Typical TPE compounds are prepared by direct melt blending of an elastomer with a thermoplastic by internal mixing (batch) or extrusion (continuous). TPO is a well-known type of TPE based on melt blending of a rubber and a polyolefin such as polypropylene (PP), low-density polyethylene (LDPE), linear low-density polyethylene (LLDPE), and high-density polyethylene (HDPE). As shown in Figure 1.8, the thermoplastic is the continuous phase, but the morphology of TPO is not fixed as the rubber

phase shape and size might change by coalescence or rupture during high shear processing. Since the dispersed rubber phase is not crosslinked with the thermoplastic, TPO can be easily prepared at low cost. TPO have been extensively used in the transportation sector including automotive exterior and interior fascia [58,59].

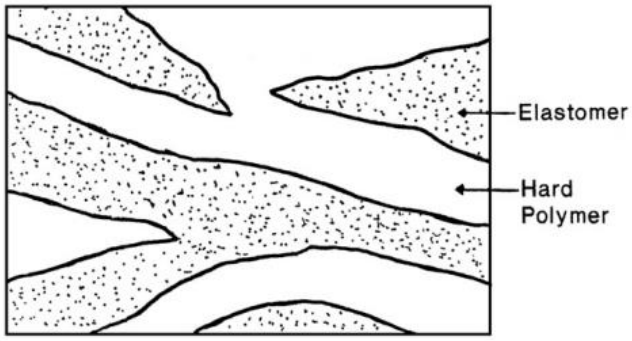

Figure 1.8 Morphology of rubber/plastic TPE blend. Adapted from reference [59].

TPE compounds are mostly prepared from heat resistant rubbers such as EPDM. NR has been introduced in the TPE production especially after the development of dynamic vulcanization through phenolic curatives. TPE containing NR as the elastomer component melt blended with thermoplastics are known as TPNR. Usually, TPNR compounds are melt blended via internal mixer or co-rotating twin-screw extruders. Several thermoplastics such as polystyrene (PS) [61], polyamide 6 (PA6) [62], ethylene-vinyl acetate (EVA) [63] and poly(methyl methacrylate) (PMMA) [64] are reported to be used in TPNR production. Also, different polyolefins (PP, LDPE, HDPE) have been broadly used for TPNR preparation [65]. For example, melt blending of NR and HDPE results in a combination of the excellent processing properties of HDPE and the elastic properties of NR to produce TPNR for automobile components. Since HDPE and NR are nonpolar materials with totally different melt viscosity and MW, they show poor interfacial adhesion. Not only compatibilizers have been reported to enhance interaction between both phases, but also processing oil have been used for their softening ability (plasticizing), processability improvement (lubrication) and elastic recovery [66,67].

1.3.1.3 TPV

TPV compounds are based on melt blending of the elastomer with the thermoplastic at high temperature and shear through dynamic vulcanization or in-situ crosslinking process. The dynamic vulcanization process crosslinks the elastomer component dispersed in the continuous thermoplastic phase, even if its volume fraction is above 50%. The dispersed particles (rubber phase) size directly

affects the physical properties of TPV, with 1 μm being the optimum rubber particles size (Figure 1.9) [59].

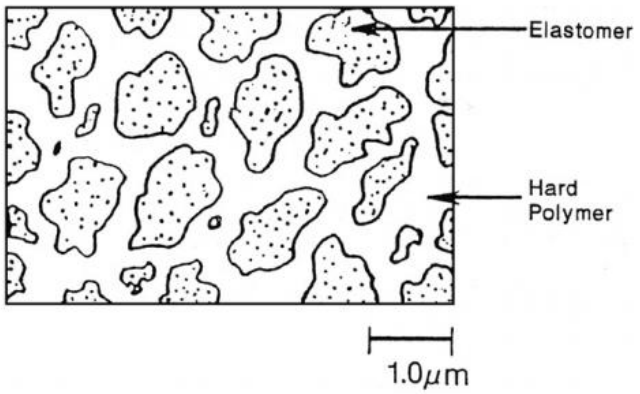

Figure 1.9 TPV morphology with continuous plastic phase and discrete rubber particles. Adapted from reference [59].

The preparation of TPV compounds is expensive and requires complex processing since the dispersed rubber phase needs to be crosslinked during mixing. The high amount of rubber (>50 wt.%) with high crosslinking density leads to high elasticity and rubber being the continuous phase while uniformly dispersed rubber phase is essential for the desired mechanical properties of TPV. On the other hand, a continuous plastic phase is required for appropriate processability. Altogether, the phase inversion of the rubber phase from a continuous phase (in the premix) to a dispersed phase (in the TPV) shows a dominant role in the preparation of TPV compounds. As shown in Figure 1.10, a high amount of rubber (50-80 wt.%) is melt blended with the thermoplastic (20-50 wt.%) at high temperature and shear stress. Dynamic vulcanization is performed after adding the curing agents and other additives into the premixed blends under the same processing conditions to crosslink the rubber phase. Rubber crosslinking and breaking up occur simultaneously, so the phase inversion occurs. Then, intensive mixing is required to achieve uniform dispersion of rubber particles in the thermoplastic matrix. Since the vulcanized rubber domains and thermoplastic matrix show poor interfacial adhesion, compatibilization is required to achieve TPV with good overall properties and mechanical strength. Compatibilizers can improve the interfacial adhesion by decreasing the surface tension of the TPV components [68,69].

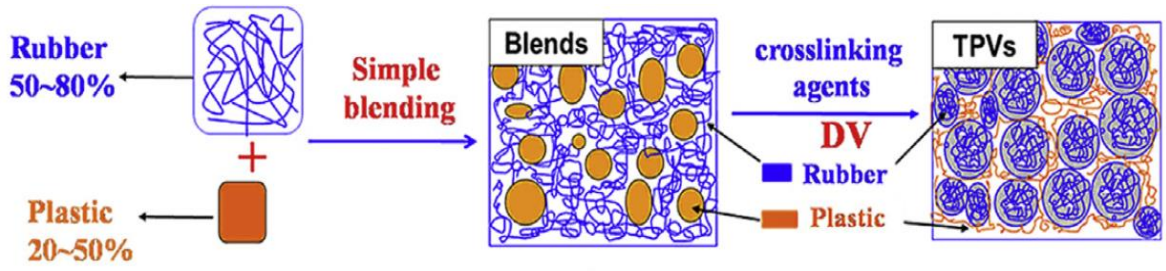

Figure 1.10 Processing steps to produce TPV compounds. Adapted from reference [69].

1.4 Compatibility

Melt blending of waste rubber with a thermoplastic resin is an upcycling process and adequate technique for waste tires recycling. However, interfacial incompatibility between both phases is a critical issue in melt blending processes. Thermodynamically, due to large unfavorable enthalpy, incompatibility of polymer blends leads to phase separation, weak interfacial adhesion, and poor mechanical properties. So, controlling the morphology and interfacial tension play an important role in determining the properties of polymer blends. Miscibility and compatibility in polymer blends are closely related and are often confused since both terms contribute to morphology and properties. Generally, miscibility results in one phase while compatibility creates a disperse phase (interface) for which its size and stability is determined by interfacial interactions [70].

The basic thermodynamic relationship controlling mixtures is:

$$\Delta G_{mix} = \Delta H_{mix} - T\,\Delta S_{mix} \tag{1.1}$$

where ΔG_{mix} is the free energy of mixing, ΔH_{mix} is the enthalpy of mixing and ΔS_{mix} is the entropy of mixing at the temperature T.

The miscibility theory for polymer blends was introduced by Flory and Huggins [71]. Based on this theory, ΔS_{mix} is the entropy factor and corresponds to disorder or randomness value that is always positive; so, it is favorable to mixing or miscibility. In polymer-polymer mixtures, the entropy of mixing has a negligible value, and the enthalpy of mixing (ΔH_{mix}) is the dominant factor to determine miscibility. ΔG_{mix} will be negative if and only if ΔH_{mix} is negative; exothermic mixing requiring specific interactions between the components of the blend.

Incorporation of additives is a common method to improve the miscibility of polymer blends by decreasing their interfacial tension, this is called compatibilization. In fact, the main objectives of compatibilization are:

- Lowering the interfacial tension
- Controlling the morphology by size reduction and stabilization of the dispersed droplets to prevent their coalescence
- Increasing the interfacial adhesion between the phases leading to better stress transfer and mechanical properties [72].

Physical and chemical compatibilization methods are two main strategies for blend compatibilization. For example, Iyer and Schiraldi [73] reported that the functional groups of additives (copolymers or nanoparticles) can interact with one or both of the polymers, thereby improving the compatibility of polymer blends.

Physical compatibilization of polymer blends is based on applying external energy. Generally, the crosslinked structure of the vulcanized rubber is destroyed with energy sources to create physical entanglements and increase the interaction between the thermoplastic and rubber molecules. Physical compatibilization (mechanical or thermo-mechanical stresses assisted by oil), high energy radiation (microwave or γ radiation) and ultrasonics (ultrasonic waves) are conventional physical compatibilization methods.

Chemical compatibilization of polymer blends is conducted through non-reactive and reactive approaches using chemical agents [74]. In non-reactive methods, a block or graft copolymers with chain units similar to the blend components are used. Kumar et al. [75] studied an immiscible blend of GTR/LLDPE and used SBR, NR and EPDM to improve the compatibility of polymer blends. According to their results, the blends containing EPDM showed the highest mechanical properties (almost 60-70% improvement in tensile strength) as a result of improved interaction and compatibility between the components. Recently, inorganic nanoparticles (NP) have been used as compatibilizers since they can bridge immiscible polymers and offer compatibility.

In reactive compatibilization, copolymers are generated in situ during the melt blending process. Copolymers formation might occurs by reaction between the end-groups of the first polymer with the end-groups or pendant groups of a second polymer [72]. Furthermore, dynamic vulcanization involving the immobilization of the dispersed phase via crosslinking can also improve the blend compatibility. Usually, the vulcanized rubber as the dispersed phase is a crosslinked component distributed in the continuous thermoplastic phase [69].

1.4.1 Copolymers

Copolymers are extensively used as compatibilizers in immiscible polymer blends and their efficiency is determined by their composition, chain length and configuration (Figure 1.11). Copolymers need to have segments which can interact with each polymer in the blend [72].

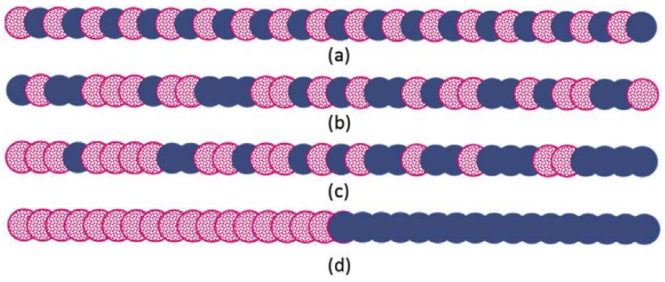

Figure 1.11 Different structures of linear copolymers: (a) alternating, (b) random, (c) gradient and (d) block copolymers. Adapted from reference [72].

For instance, Shanmugharaj et al. [13] used maleic anhydride grafted polypropylene (MAPP) as a compatibilizer in PP/GTR blends by using allylamine grafted GTR and reported 10-20% tensile strength improvement of MAPP containing compound compared with unmodified blends as a result of enhanced compatibility and interaction between all the components. Also, Kim et al. [76] compatibilized acrylamide (AAm) modified GTR/HDPE blends with MAPP and reported impact strength improvements of the AAm-grafted powder-filled composite compared with those of the unmodified powder-filled system and due to the bonding effect between rubber powders and the compatibilizer (Figure 1.12). Similar studies also focused on using copolymers as compatibilizers in TPE blends [77-80].

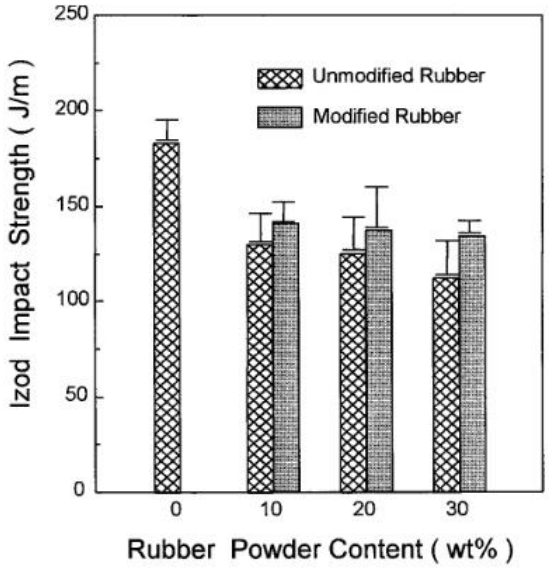

Figure 1.12 Notched Izod impact strength of HDPE/GTR composites as a function of rubber content. Adapted from reference [76].

1.4.2 Nanoparticles (NP)

More recently, inorganic NP with large specific surface area and high aspect ratio such as graphene (specific surface area 2600 m^2/g and aspect ratio 200-1000) [81], single walled carbon nanotube (SWCNT) (specific surface area 1315 m^2/g and aspect ratio >1000) [82] and nanoclay (natural montmorillonite clay specific surface area 750 m^2/g and aspect ratio 200-1000) [83] have been used as compatibilizers in polymer melt blending in addition to their application for improving the mechanical, thermal and barrier properties [84-86]. The Flory-Huggins thermodynamics theory of mixing clarifies the phase separation in a ternary system containing two polymers and NP. However, droplet stabilization against coalescence is not clearly understood. There are different mechanisms for NP compatibilization in polymer blends. Based on thermodynamics compatibility, the large specific surface area and high aspect ratio of inorganic NP adsorb the polymer chains on their surface to increase the stabilizing energy leading to the negative overall free energy of mixing and thermodynamically compatible systems. On the other hand, kinetics compatibility is related to the selective localization of the NP at the polymer interface by decreasing the interfacial tension and preventing droplet coalescence during melt blending. The compatibilization efficiency of NP is affected by their migration and localization in phases during melt blending which can be determined by processing parameters (compounding sequence, melt compounding time and shear rate) [87]. Moreover, blend morphology depends on the viscosity ratio and the interfacial tension between the polymer phases. For instance, finer morphology is achieved in polymer blends as the viscosity ratio between the matrix and dispersed phases is closer

to one [88], as well as when the interfacial tension is low between the blend components [89]. NP are recognized as appropriate compatibilizers to decrease the interfacial tension of polymer blends and stabilize the morphology depending on their localization. If the nanofillers migrate to one phase of the co-continuous blend, they form a percolated particle network in one phase and prevent coarsening related to the increased viscosity [90]. On the other hand, selective localization of NP at the interface of polymer blends can stabilize the co-continuous structure. NP jammed at the interface are more effective than percolated particle networks within one of the two phases by suppressing the coarsening phenomena [91]. NP localization can be predicted by measuring its wetting coefficients (ω) defined as:

$$\omega = \left[\left(\gamma_{NP/x} - \gamma_{NP/y}\right)/\gamma_{x/y}\right] \tag{1.2}$$

where $\gamma_{NP/x}$, $\gamma_{NP/y}$ and $\gamma_{x/y}$ are the interfacial energies (or interfacial tensions) between NP - polymer (x), NP - polymer (y) and polymer (x) - polymer (y), respectively. All these interfacial energies can be theoretically calculated based on the Owens-Wendt equation [92] by measuring the dispersive (γ^d) and polar (γ^p) part of the surface energies:

$$\gamma_{xy} = \gamma_x + \gamma_y - 2\left[\left(\gamma_x^d \gamma_y^d\right)^{1/2} + \left(\gamma_x^p \gamma_y^p\right)^{1/2}\right] \tag{1.3}$$

Based on equation (1.3), if the wetting coefficient is higher than 1 (ω > 1), the NP thermodynamically prefer to stay in the polymer (y) while NP locate in the polymer (x) when ω < − 1. Ideally, NP migrate to the interface between both phases when − 1 < ω < 1 (Figure 1.13 b) and act as smart/functional barriers inhibiting droplets coalescence [84,87].

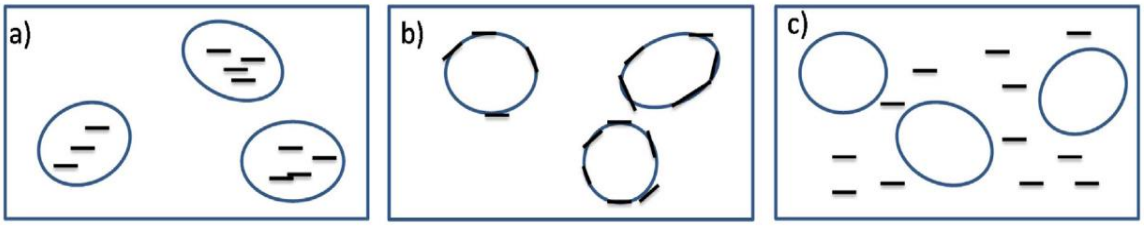

Figure 1.13 The three possible cases for NP localization in an immiscible binary polymer blend: a) in the dispersed phase, b) at the interface (ideal case) or c) in the continuous phase. Adapted from reference [84].

Several inorganic NP have been used for both reinforcing and compatibilization effects in immiscible polymer blends. However, the main challenge in using NP for blend compatibilization is their poor dispersion in the polymer matrix due to particle agglomeration, limiting their efficiency [72].

1.5 Rubber Modification

Several methods, such as graft polymerization, radiation-induced modification, and gas modification have been proposed to modify rubbers. Currently, rubber surface modification techniques have been performed at the laboratory scale. The purpose of rubber modification is to introduce oxygen functional groups (peroxy, hydroperoxy, hydroxyl and carbonyl) on the rubber surface to interact with polar polymers or reactive compatibilizers to improve the interfacial adhesion between the polymer and rubber. Conventional oxidizing agents including potassium permanganate ($KMnO_4$) [24], nitric acid (HNO_3) and hydrogen peroxide (H_2O_2) [93], and sulphuric acid (H_2SO_4) [94] have been used. Moreover, grafting monomers onto rubber particles through free-radical initiation or photo-initiation can prevent particles agglomeration leading to smaller particle size and more homogeneous distribution within the continuous polymer matrix to achieve better blend properties [1,54,95].

1.5.1 Reclamation and Devulcanization

Vulcanized rubbers are infusible and insoluble materials with a 3D crosslinked structure (100% gel content) which are difficult to process and reprocess for further compound production. Therefore, these rubbers need to be partially soluble with lower crosslink density, which can be achieved by partially destroying the initial crosslinked structure giving chains more mobility (molecular freedom). The soluble fraction can interact and bond with the polymer matrix chains. Thermomechanical, thermochemical, ultrasonic and microwave are common techniques for partial breakup of the crosslinked structure of vulcanized rubbers. Regardless of the method used, there are two concepts related to the process of destroying the crosslinked structure of rubber including devulcanization and reclamation. Reclamation is based on the scission of C–C bonds in the rubber backbone to reduce the MW and obtain some plasticity. On the other hand, devulcanization is the specific cleavage of S–S and C–S bonds, partially destroying the 3D network to produce plasticity. In an ideal devulcanization process, the rubber backbone should not be damaged. However, selective breakup of the crosslinked structure inside vulcanized rubber is not possible without damaging some C-C bonds in the backbone. Table 1.3 reports the energy required for breaking the different bonds of crosslinked rubbers. In general, reclamation and devulcanization might occur at the same time making their differentiation difficult in a specific process (Figure 1.14) [1,96].

Table 1.3 Energy required for cleaving typical bonds in vulcanized rubbers [96].

Type of bond	Energy required for cleavage (kJ/mol)
C–C	348
C–S–C	285
C–S–S–C	268
C–S_x–C	251

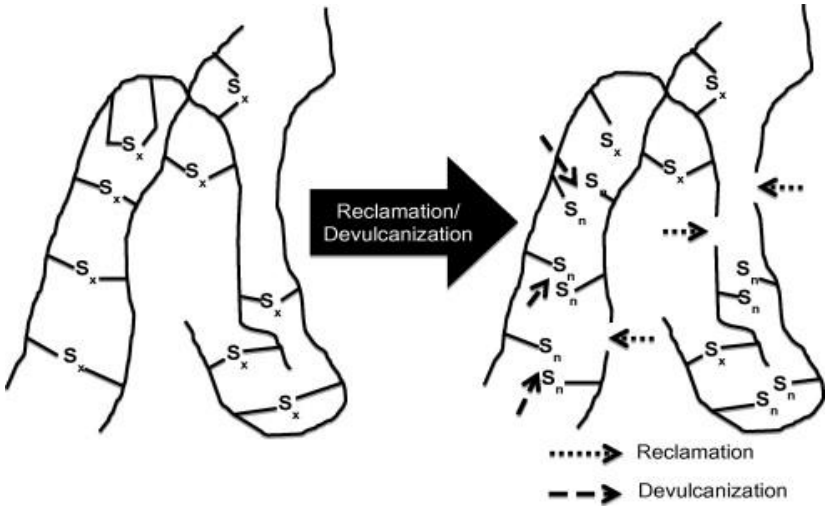

Figure 1.14 Schematic representation of the devulcanization and reclamation. Adapted from reference [1].

1.6 TPE Compatibilization

Vulcanized and reclaimed rubber are being exposed to severe conditions (shear stress, thermal and chemical degradation, radiation) in their lifetime and recycling processes, so the properties of the resulting TPE differ from compounds based on virgin materials. Also, rubbers contain several fillers which might limit possible improvement of blend properties. TPE compounds based on polyolefin (especially PE) have received a great deal of attention because they are easy to process and the materials are easily available at low costs. However, the performance of these blends depends on the nature and concentration of each component, as well as their interaction. The compounds need to show at least 100% elongation at break and compression set lower than 50% to be recognized as good TPE materials [22]. It is known that polymer blend properties significantly depend on the interfacial adhesion between both phases and the size of the dispersed phase inside the continuous matrix. Poor interfacial adhesion between the rubber and thermoplastic phases leads to low mechanical properties. In fact, the vulcanized rubber molecules do not have enough freedom to entangle with the thermoplastic

molecules to create strong bonding. Therefore, the interfacial adhesion and morphological behavior of TPE blends are important parameters to control/optimize the composition and processing conditions for high performance compounds [1,95].

1.6.1 Effect of Rubber Particles Size and Loading

Considering the size of the dispersed phase, small rubber particles usually show better mechanical properties than larger particles due to lower probability of failure/cracks formation. Ismail et al. [14] studied the effect of three different GTR sizes (250-500 µm, 500-710 µm and 710 µm-1 mm) on the mechanical properties of PP/GTR blends. They reported that blends containing smaller GTR particles (250-500 µm) showed higher equilibrium torque due to high friction associated with higher surface area of the smaller GTR particles. As shown in Figure 1.15, the blends containing small GTR particles also showed the highest elongation at break (20%). However, the values were low because of the crosslinked structure of the GTR particles and poor adhesion with the PP matrix resulting in easy crack initiation and rapid crack propagation.

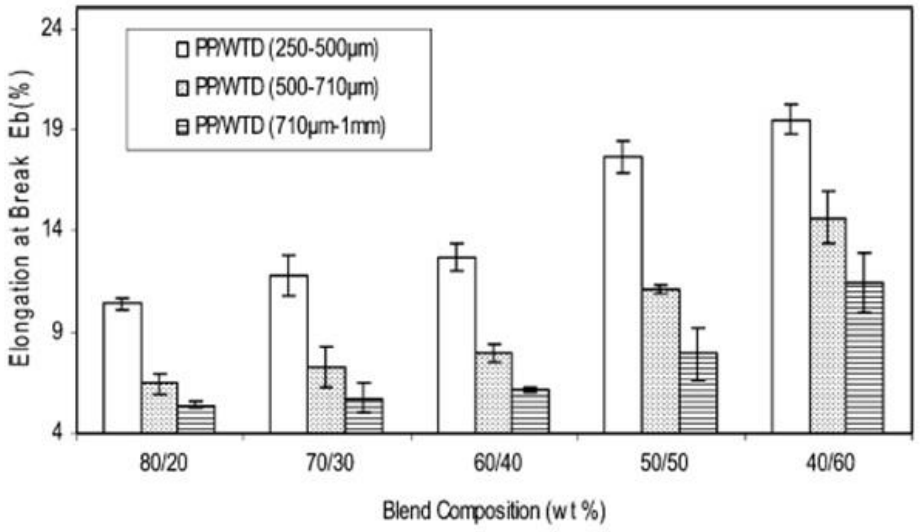

Figure 1.15 Elongation at break of GTR/PP blends. Adapted from reference [14].

Sonnier et al. [10] used three different rubber particle sizes (380-1200 µm) in GTR/LDPE compounds. They did not achieve significant difference in the mechanical properties of GTR/LDPE (50/50 wt.%) blends (impact energy ~ 2.6 kJ/m^2 for all blends with different rubber particle size). So, they suggested that controlling the GTR particles size is not the only parameter to achieve significant mechanical properties improvement. It has been reported that the effective rubber particle size to improve the mechanical properties of TPE is around 500 µm or less (Figure 1.16). However, at high rubber

concentration (above 50 wt.%), the effect of rubber particle size is less important since low interfacial adhesion is the dominant parameter controlling the mechanical properties. In fact, substantial drops in tensile strength and impact strength of TPE compounds filled with vulcanized rubbers are related to low interfacial adhesion, rubber particles agglomeration and void formation at the interface between the rubber and thermoplastic phases. Due to a mismatch in polarity, melt viscosity and MW of both materials, the interfacial adhesion is weak. Poor interface quality leads to high interfacial tension and GTR particle agglomeration facilitating voids formation around the rubber particles. As shown in Figure 1.17, increasing the rubber concentration resulted in the formation of more defects and cracks in GTR/EVA compounds. A clear indication of low interfacial adhesion is confirmed by the clean and easy removal of rubber particles (pull-outs) from the EVA matrix [19].

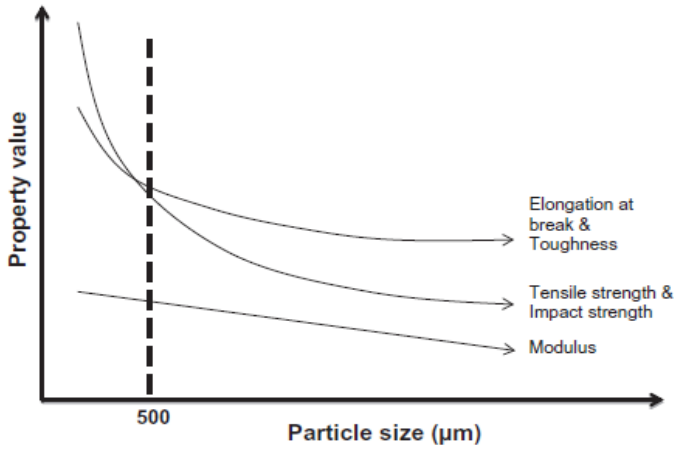

Figure 1.16 Effect of GTR particle size on the mechanical properties of TPE blends. Adapted from reference [1].

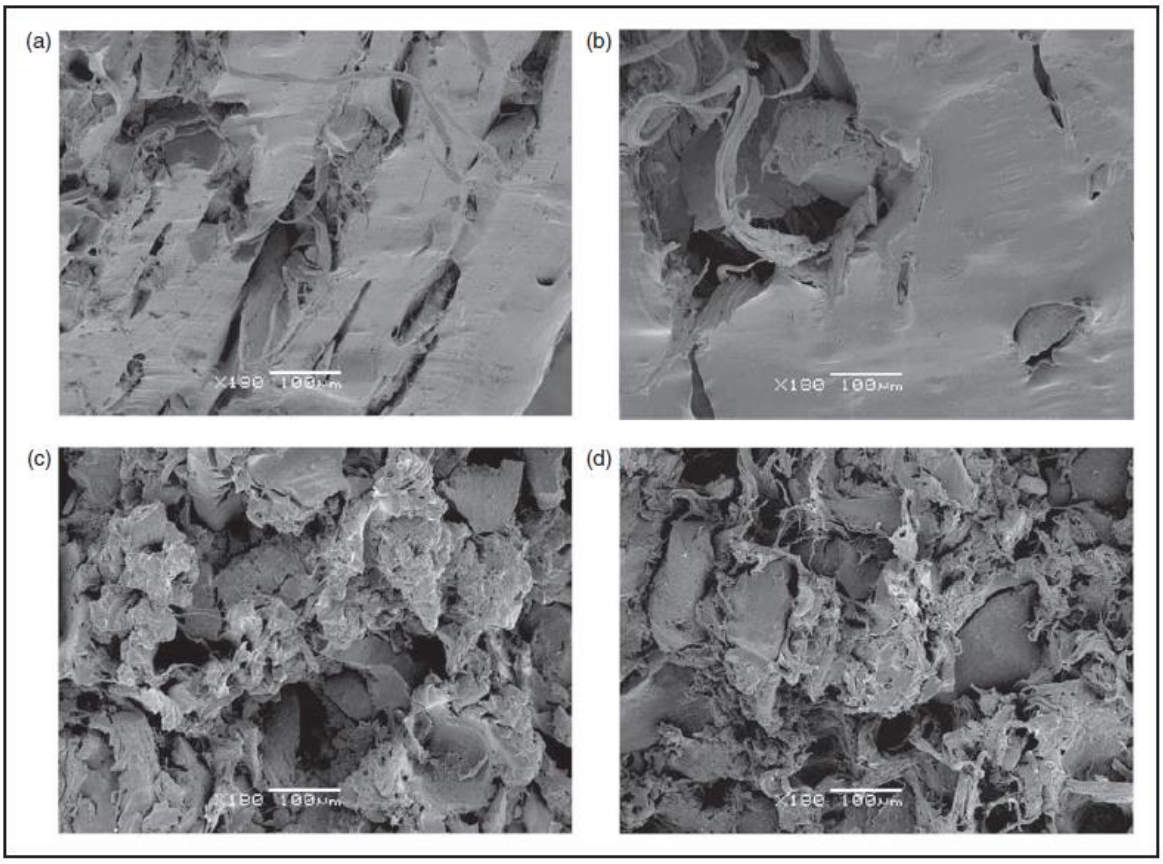

Figure 1.17 SEM micrographs of EVA blends with different GTR contents: (a) 10 wt.%, (b) 20 wt.%, (c) 50 wt.% and (d) 70 wt.%. Adapted from reference [19].

1.6.2 Non-reactive Compatibilization

It is also possible to improve the interfacial adhesion of immiscible polymers blends via compatibilization methods. Addition of compatibilizing aids (copolymers or nanoparticles), surface modification of the materials, as well as a variety of devulcanization methods and processing aids (solvents) are conventional techniques to enhance the compatibility of TPE blends. Incorporation of block or graft copolymers into polymer blends decrease the interfacial tension and promote interaction between polymers. Different compatibilizers such ethylene-acrylic acid copolymer (EAA) [97,98], chlorinated polyethylene (CPE) [99,100], maleic anhydride grafted polyethylene (MAPE) [11,101], ethylene-co-glycidyl methacrylate copolymer (E-GMA) [102,103], epoxydized natural rubber (eNR) [104,105], styrene-butadiene-styrene block copolymer (SBS) [106], and EVA [57] have been used in TPE compounds. For example, MAPE showed good efficiency for improving the mechanical properties of TPO compounds as a result of a reaction between the anhydride groups grafted onto polyethylene (PE) with hydroxyl groups/unsaturated bonds on the GTR particles surface. Therefore, using MAPE as a

compatibilizer can reduce the interfacial tension, improve the dispersed phase uniformity, decrease the domain size and maintain the blends morphology stability [107]. Esmizadeh et al. [11] studied the effect of reactive compatibilization on the mechanical and morphological properties of TPV blends containing HDPE/regenerated rubber (RR). They used MAPE and peroxide as compatibilizer and vulcanizing agent, respectively. Analysis of the torque values showed increasing trends of the plateau region (equilibrium value) with increasing RR content due to the restricted chain mobility and difficult dispersion of crosslinked rubber particles in HDPE. A similar observation was reported by Ismail et al. [14] in which the stabilized torque increased from 4 Nm to 8 Nm with increasing GTR content from 20 wt.% to 60 wt.% due to a good dispersion of hard crosslinked rubber particles in PP (Figure 1.18).

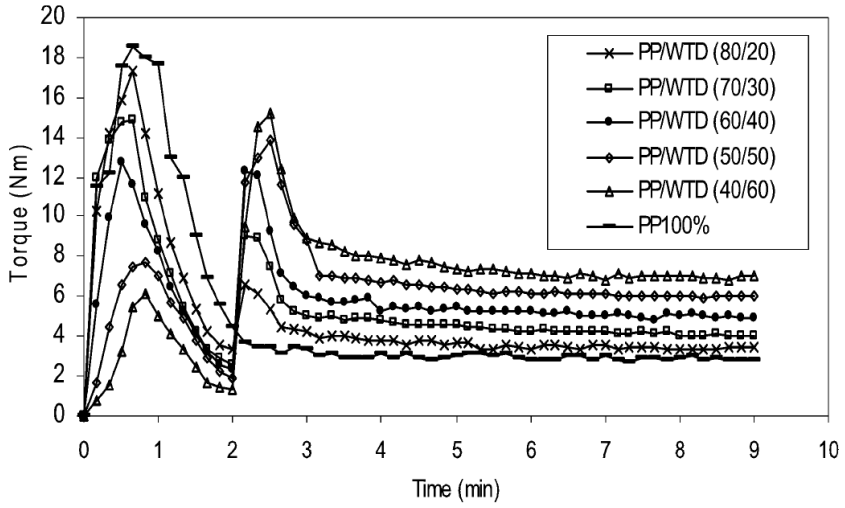

Figure 1.18 Torque evolution for PP/GTR (named as waste tire dust; WTD) blends (250-500 μm). Adapted from reference [14].

Also, reactive compatibilization and dynamic vulcanization can increase the torque plateau due to increased viscosity of the system [11]. Generally, TPE compounds show a shear-thinning (pseudo-plastic) behavior and their viscosity decreases with increasing shear rate. Sae-Oui et al. [108] reported the pseudo-plastic behaviour of NR/HDPE compounds since the complex viscosity decreased with increasing angular frequency (Figure 1.19). Obviously, increasing complex viscosity was directly related to the NR concentration (complex viscosity (NR/HDPE): 90/10 > 80/20 > 70/30 > 60/40) since the fully NR vulcanized structure restricted flowability.

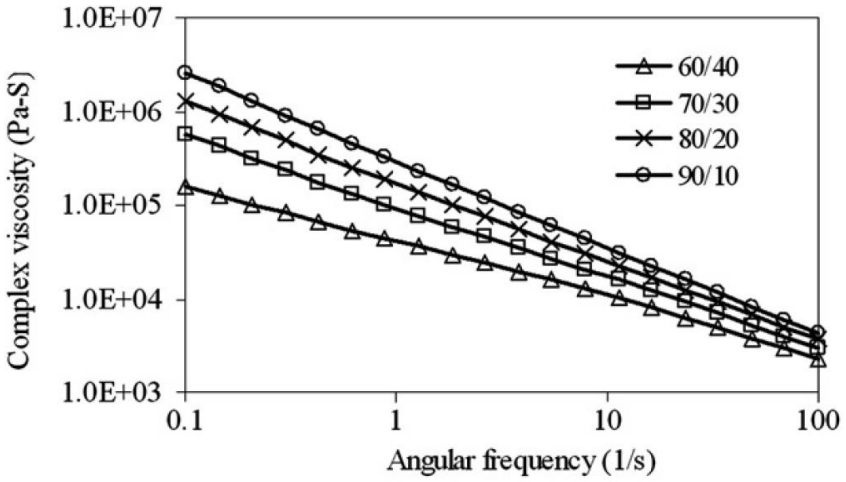

Figure 1.19 Complex viscosity as a function of angular frequency for TPNR based on different NR/HDPE ratios. Adapted from reference [108].

Moreover, the shear storage modulus (G') as a function of angular frequency increased because of less time available for molecular relaxation (Figure 1.20). Also, G' increased more at higher NR content (NR/HDPE = 90/10) because of the crosslinked and highly elastic NR content which gave rise to a stronger elastic response (slope reduction in Figure 1.20).

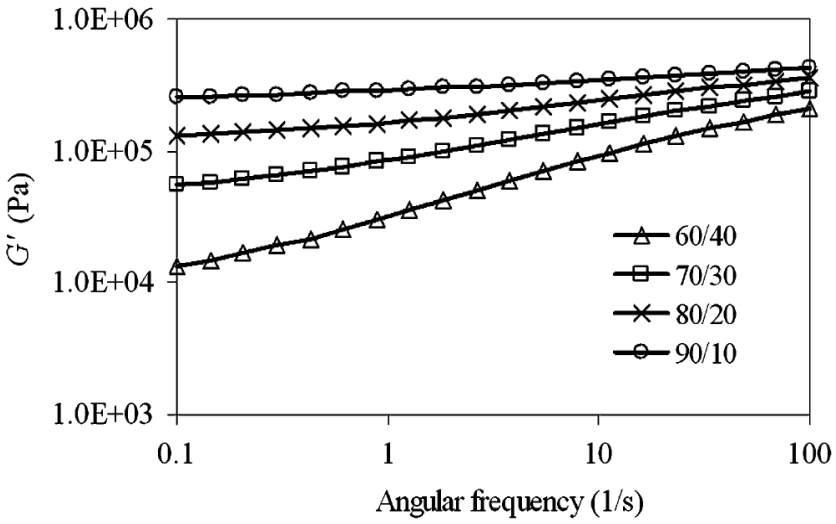

Figure 1.20 Shear storage modulus (G') as a function of angular frequency for TPNR based on different NR/HDPE ratios. Adapted from reference [108].

Table 1.4 compares the mechanical strength of compatibilized compounds showing that compatibilizer addition led to higher interfacial adhesion between RR and HDPE. It is clear that a very small amount of vulcanizing agent (0.2 wt.%) is more effective than compatibilizers to improve the mechanical properties. Figure 1.21 shows that hardness of HDPE decreased with increasing RR content, which

was attributed to the higher concentration of the elastomeric component in the TPE. Also, increased hardness of the compatibilized and dynamically vulcanized blends was related to better interaction between the materials induced by the compatibilizer and the formation of a stronger crosslinked structure (increased rigidity), respectively [11].

Table 1.4 Tensile properties of HDPE/RR blends. Adapted from reference [11].

Sample code	Tensile strength (MPa)	Tensile modulus (MPa)	Elongation at break (%)
H-R30	11.0 ± 0.1	166.7 ± 7.3	31.5 ± 2.7
H-R50	6.0 ± 0.6	101.4 ± 2.8	61.3 ± 5.5
H-R70	2.3 ± 0.1	26.3 ± 5.8	125 ± 6.2
H-R90	0.6 ± 0.2	1.6 ± 0.7	149 ± 4.3
H-R30-C	12.2 ± 4.1	218.4 ± 6.1	45.1 ± 5.7
H-R50-C	7.3 ± 3.2	122.4 ± 3.8	78.9 ± 7.1
H-R70-C	3.0 ± 0.7	29.8 ± 1.8	138.6 ± 2.4
H-R90-C	0.9 ± 0.2	2.1 ± 0.9	183 ± 4.9
H-R30-P	13.5 ± 5.1	346.6 ± 7.4	58 ± 8.2
H-R50-P	9.4 ± 2.6	184.9 ± 5.8	94.1 ± 3.4
H-R70-P	6.0 ± 1.7	36.5 ± 2.7	152.2 ± 1.5
H-R90-P	2.7 ± 0.8	2.8 ± 1.5	213.5 ± 6.1

H: HDPE,
R: Reclaimed rubber,
C: Compatibilizer (MAPE),
P: Peroxide (liquid peroxide with trade name of DHBP (2,5-dimethyl-2,5-di-(tert-butylperoxy)-hexane))

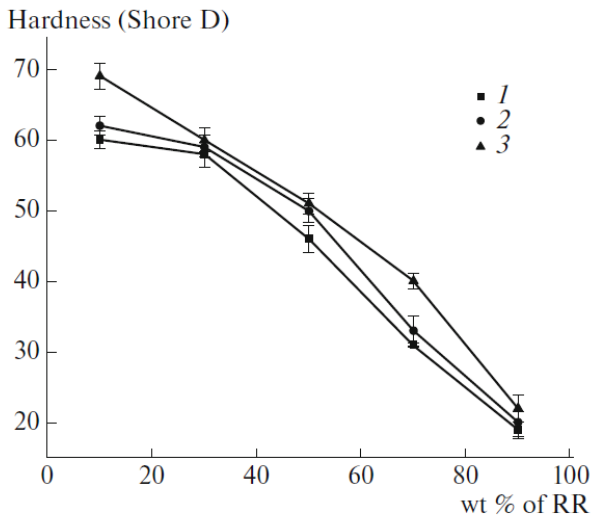

Figure 1.21 Hardness of HDPE as a function of RR content: (1) H-R10, (2) HR10-C, (3) H-R10-P. Adapted from reference [11].

Kakroodi et al. [12] used MAPE as a matrix to produce TPE compounds filled with high GTR contents (50-90 wt.%) and compared their mechanical strength with HDPE/GTR compounds. The results showed that TPE containing 50-70 wt.% of GTR in MAPE had very good elongation at break (ε_b = 465%) and tensile strength (σ_y = 32.7 MPa) at 50 wt.% GTR, while these properties decreased with increasing GTR content to 90 wt.% (ε_b = 219% and σ_y = 4.6 MPa). Also, the tensile properties of HDPE/GTR compounds, with and without MAPE as a coupling agent, were significantly lower than for the blends with MAPE as the matrix. So, MAPE was shown to be a good matrix to produce TPE with high tensile properties.

Wang et al. [30] worked on the production of TPE compounds based on recycled polyethylene (rPE)/GTR and investigated the effect of Engage 8180 and Vestenamer 8012 copolymers on the morphological and mechanical properties. They reported better compatibilizing efficiency of Engage 8180 on rPE/GTR compounds than Vestenamer 8012. This behavior was attributed to the interaction and entanglement of rPE and GTR molecular chains due to the compatibilizing effect of the ethylene-octene copolymer (main component of Engage 8180). In fact, the ethylene part was compatible with rPE while the octene segment showed entanglement with SBR (main part of GTR). Even though they reported improved elongation at break of compounds with 10 wt.% Engage 8180 up to 76%. However, the values were still lower than 100%, which implies the need to do more research on the compatibilization of highly filled TPE compounds, especially when recycled thermoplastic resins are used as the matrix.

1.6.3 Reactive Compatibilization

In general, better interaction between the components leads to the reduction of the dispersed phase particle size and compatibility improvement. In reactive blending, block or graft copolymers as compatibilizers are formed in-situ during mixing. These compatibilizers improve bonding through covalent reactions between the functionalized components in polymers. Grafting through melt blending can be done by two-roll mill, internal mixer, and twin-screw extruder. Kim et al. [76] worked on the surface modification of GTR via grafting of AAm and melt blending of surface modified GTR with HDPE. They used MAPP to induce the reaction between maleic anhydride (MA) and surface modified GTR powders to increase the compatibility between the phases. Both blends containing AAm-grafted GTR and unmodified GTR showed decreasing tensile stress and tensile strain with increasing rubber content. However, the HDPE/AAm-GTR systems showed higher tensile stress and tensile strain. The AAm-GTR filled blends containing 10 wt.% and 20 wt.% rubber did not break and elongated up to 300% and 400%, respectively (Figure 1.22).

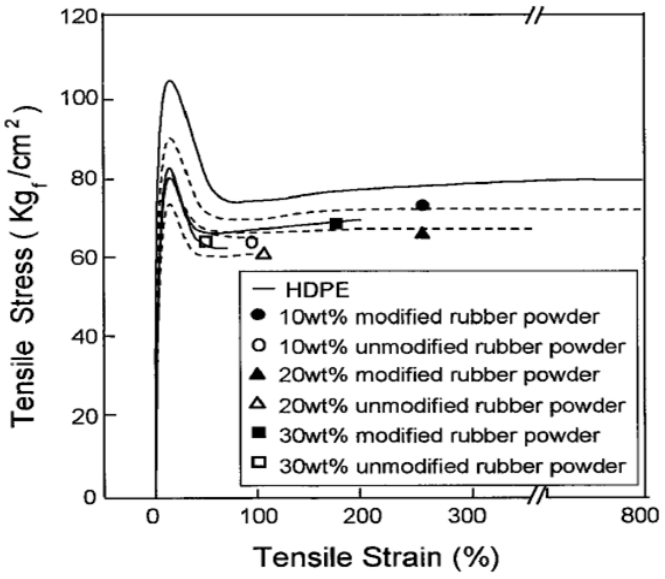

Figure 1.22 Tensile stress-strain curves of HDPE and HDPE/GTR compounds. Adapted from reference [76].

Also, Patel et al. [109] studied the reactive blending of LDPE/NR and LDPE/NBR using acrylic acid (AA) and MA. The reaction mechanism for LDPE/NR modified with MA is presented in Figure 1.23, while similar reactions are expected for AA grafted LDPE/NBR. Dicumyl peroxide (DCP) was used as an initiator to generate the free radical sites on the LDPE chains.

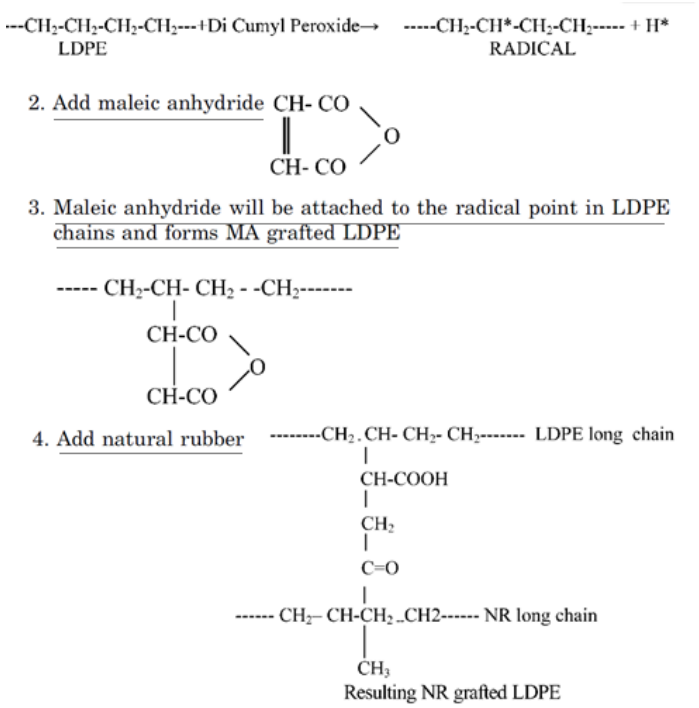

Figure 1.23 Reaction mechanism for LDPE/NR modified with MA. Adapted from reference [109].

The hardness results showed that ungrafted compounds had lower values (Table 1.5). In fact, the grafting method increased the hardness of both NR and NBR compounds up to 98 Shore A for LDPE/NBR (80/20) blends modified with MA grafted particles. Moreover, based on tensile results, the strength decreased after aging (air oven at 70 °C for 16 h) due to the degradation of the elastomer phase. After aging, the ungrafted compounds showed a 20% reduction in tensile strength, while the grafted compounds showed only 1-5% reduction in tensile strength which indicated their higher stability due to grafting [109].

Table 1.5 Hardness (Shore A) of LDPE/NR and LDPE/NBR with and without particle modification. Adapted from reference [109].

LDPE/NBR	LDPE/NR	Ungrafted	AA-grafted	MA-grafted
-	80/20	90	97	95
-	60/40	82	90	85
-	40/60	65	70	69
-	20/80	55	57	58
80/20	-	95	97	98
60/40	-	85	86	87
40/60	-	65	70	72
20/80	-	55	58	56

1.6.4 Effect of NP Incorporation

In recent years, anisotropic nanofillers such as nanoclays, carbon nanotube (CNT) and graphene, with large specific surface area and high aspect ratio, have been used to modify the interfacial adhesion of immiscible polymer blends [84,85]. Incorporation of small amount of NP leads to strong interfacial interaction between the components improving the mechanical strength and thermal stability of TPE nanocomposites.

Mehta et al. [110] studied the effect of nanoclays on the morphology of PP/EPDM (70/30) blends. They showed important size reduced of the dispersed phase by increasing the nanoclays concertation. Generally, the final morphology was influenced by the filler distribution, viscosity ratio between the components and the affinity of the filler toward the polymers. Naderi et al. [111] studied the effect of the matrix viscosity and NP content on the mechanical properties and morphology of PP/EPDM/nanoclays compounds. XRD analysis was used to study clays exfoliation into nanolayers in the polymer blends. As shown in Figure 1.24, the addition of 3 wt.% nanoclays (Cloisite 15A) increased the interlayer spacing from 30.44 Å for PP/EPDM (80/20) to 34.62 Å for TPE nanocomposite (PP/EPDM/nanoclays). This behavior was attributed to the intercalation of polymer chains inside the silicate layers. They used a fixed NP concentration since increasing its concertation led to difficult penetration of the polymer chains through the silicate layers and decreased interlayer spacing of the nanoclays.

Also, they reported the effect of the viscosity ratio on the size of the rubber domain in PP/EPDM (60/40) blends. The results showed that the rubber droplet sizes decreased with increasing the viscosity of the PP phase. As mentioned before, a fine dispersion is achieved when the viscosity ratio of the plastic/rubber is close to one. Also, they showed the effect of nanoclays on breaking up the rubber droplets. Increasing the rubber concertation increased the dispersed rubber phase size in the compounds without nanoclays (Figure 1.25 (a) and (c)) which indicated the effect of NP on preventing coalescence and reducing the dispersed phase sizes. Therefore, the distribution and domain sizes of the dispersed phase were significantly influenced by the presence of NP and the viscosity ratio between both polymers [111].

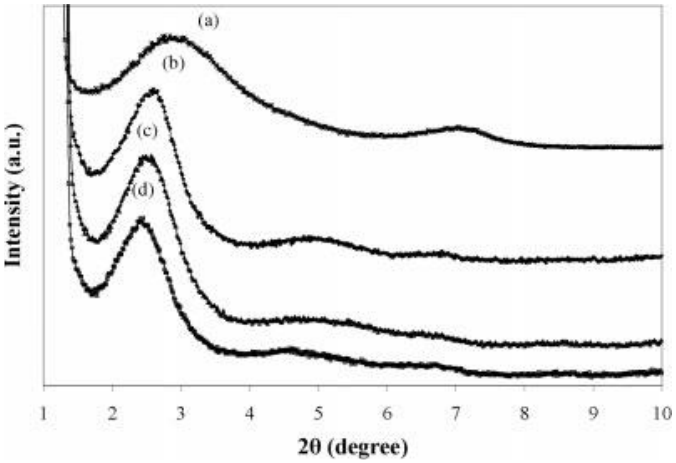

Figure 1.24 X-ray diffraction patterns of: (a) Cloisite 15A and TPE nanocomposites based on PP with: (b) 60%, (c) 40% and (d) 20% EPDM. Adapted from reference [111].

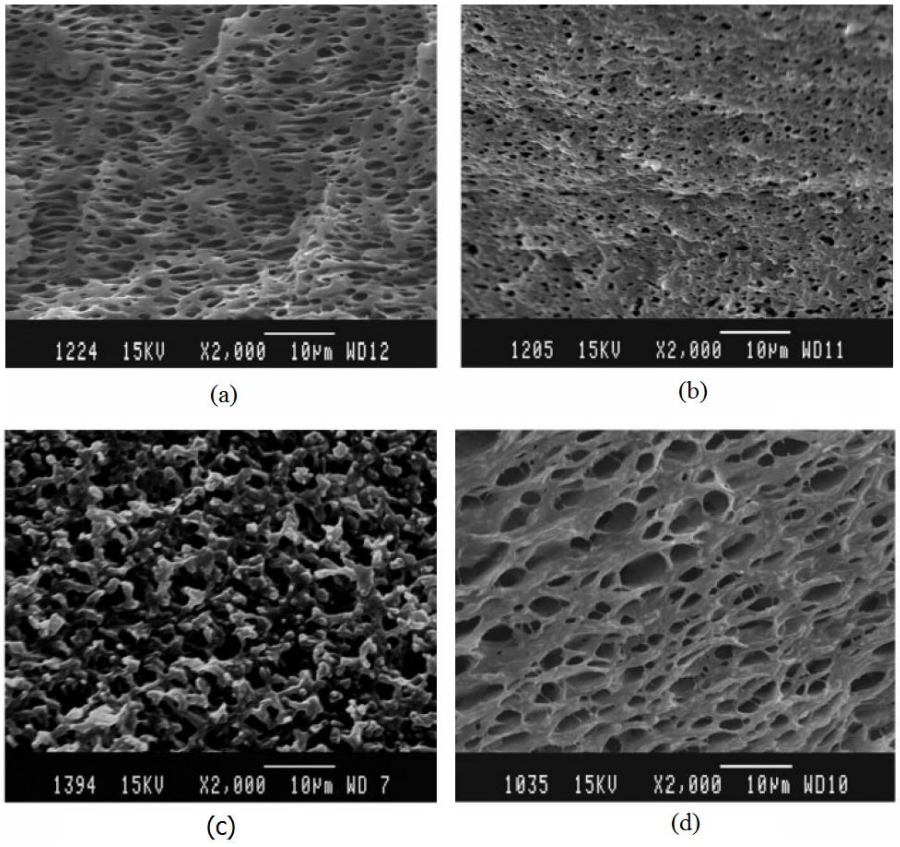

Figure 1.25 SEM micrographs of TPE based on: (a) unfilled PP/EPDM (60/40), (b) nanoclay-filled PP/EPDM (60/40), (c) unfilled PP/EPDM (40/60) and (d) nanoclay-filled PP/EPDM (40/60) blends. Adapted from reference [111].

In another study, Lopattananon et al. [112] investigated the effect of sodium montmorillonite (Na-MMT) concentration on the mechanical and morphological properties of TPV based on NR/PP (60/40). According to the results, the two phase-separated morphology of the blends changed to a droplet-like

structure upon addition of 2-5 phr (parts per hundred resin) nanoclays as a result of a droplet break-up effect.

1.6.5 GTR Surface Modification and Devulcanization

Another compatibilization technique is the surface modification of GTR particles via oxidation to improve the interaction between the components. Colom et al. [113] used various acids such as H_2SO_4, HNO_3 and perchloric acid ($HClO_4$) for the surface treatment of GTR for melt blending with HDPE. They reported improved rubber interaction with HDPE and higher stiffness for the TPE compounds as a result of rubber rigidification after the acid treatment. As shown in Figure 1.26, a smooth surface of $HClO_4$ treated particles (b) is similar to the surface of untreated particles (Figure 1.26) which is an evidence of poor adhesion. However, HNO_3 and H_2SO_4 (Figure 1.26 c and d) provided a rough surface with several micro-pores and cavities that enhanced the interfacial contact area and interaction between the rubber and the thermoplastic matrix. The micro-roughness topography was related to the acid treatment with sulphuric acid which led to decrease the number of double bonds in the tire chemical structure due to the degradation process of BR and other unsaturated hydrocarbon polymer chain (diene) on the GTR surface.

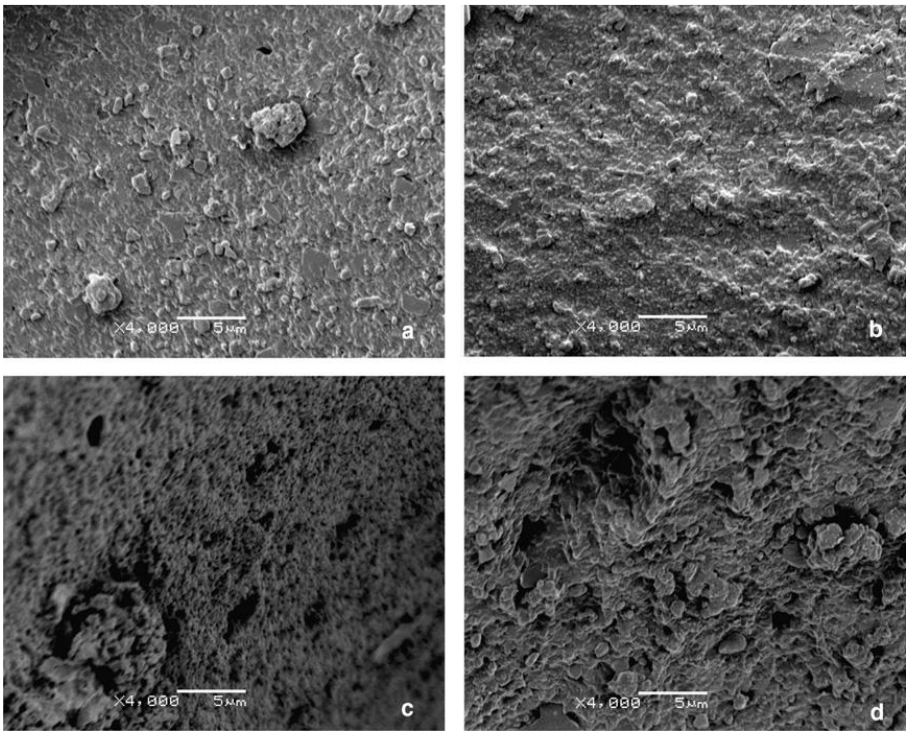

Figure 1.26 SEM of the GTR particles surface: (a) untreated, and treated with: (b) $HClO_4$, (c) HNO_3 and (d) H_2SO_4. Adapted from reference [113].

In another work, Liu et al. [114] investigated the oxidation of EPDM powder by $KMnO_4$ to generate hydroxyl groups by breaking unsaturated C=C bonds in the rubber. The addition of surface modified EPDM into PP containing a small amount of MA grafted chains showed significant elongation at break improvement. It was explained that polar groups on the EPDM surface reacted with MA to form covalent bonds improving the interaction between the rubber and matrix. Several methods are known to improve the polarity (oxygen concentration) of the rubber surface such as high-energy techniques like plasma, corona discharge and electron beam [54]. Sonnier et al. [10] studied the production of compatible GTR/HDPE compounds using surface treated rubber particles. They used $KMnO_4$ as a common oxidizing agent and γ irradiation for which the energy can induce macromolecular chain scission and free radicals formation having the possibility to react with the oxygen in air and create polar groups. However, the surface oxidation of GTR was not efficient enough to improve the mechanical properties of HDPE/MAPE/GTR compounds (elongation at break ~ 24% for all blends with different modified rubber particle size).

It should be mentioned that the polarity of an elastomer can influence the interfacial adhesion between GTR and the thermoplastic matrix. Li et al. [57] studied HDPE/GTR blends using EVA and ethylene-octene copolymer (POE) as polar and non-polar compatibilizers, respectively. According to the results, the impact strength and elongation at break of the HDPE/GTR/POE (60/20/20) compounds were 417 J/m and 129%, both of which being higher than 175 J/m and 82% for the HDPE/GTR/EVA (60/20/20) compounds. After morphological analysis, this behavior was explained by better homogeneity and encapsulation of the GTR particles by non-polar copolymers helping the thermoplastic matrix to deform under applied forces. Also, Formela et al. [106] investigated the effects of non-polar elastomer (partially crosslinked butyl rubber and SBS block copolymers) on the morphological and mechanical properties of LDPE/GTR blends. GTR particles were encapsulated by the elastomer phase which was compatible with the thermoplastic phase improving the interfacial adhesion with the LDPE matrix. As shown in Figure 1.27, small GTR particles showed higher interfacial adhesion as a result of better encapsulation of the GTR particles by the elastomer. Moreover, the compounds containing SBS (branched Kraton 1184) showed up to 125% elongation at break, which is twice the value of LDPE/GTR (50/50), indicating better compatibility with both LDPE and GTR.

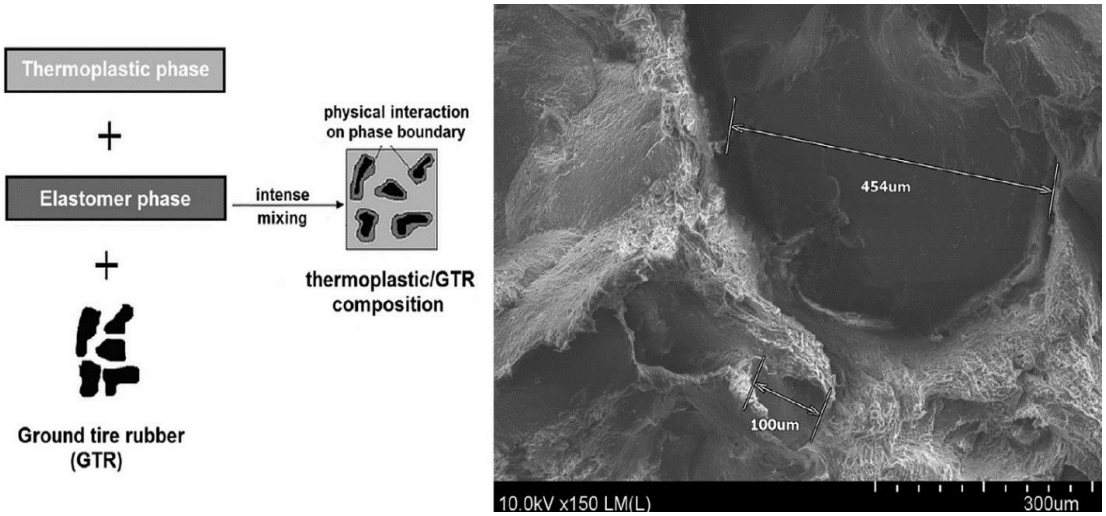

Figure 1.27 Compatibilization mechanism of thermoplastic/GTR blends using an elastomer (SBS) as a modifier. Adapted from reference [106].

Reclamation and devulcanization of rubber have also been used to improve the compatibility and processability of TPE. In fact, destroying the crosslinked rubber structure as well as co-crosslinking at the interface enhanced polymer chains mobility and the mechanical strength of the resulting compounds. Also, the presence of RR short chains and processing oil enhanced the processability and elongation at break of RR containing compounds due to a plasticization effect. The crosslinked gel part of recycled rubber particles act as stress concentration points, so increasing the rubber concentration (gel content) in the blends leads to increased crosslink density producing lower tensile strength and elongation at break [1]. Sripornsawat et al. [115] studied the devulcanization reaction time and temperature through a relation between the soluble fraction (sol) and crosslink density. According to their results, it was required to perform the devulcanization process in a short time to prevent recombination of free radicals to form new covalent bonds. Also, increasing the reaction time leads to the generation of more reactive radicals forming new links and increasing the crosslink density. As shown in Figure 1.28, the optimum devulcanization time is 4 min to obtain the maximum tensile strength (3.7 MPa) and elongation at break (57%) for these samples. The authors also investigated the effect of devulcanization on the mechanical and morphological properties of TPV based on blends of COPE with devulcanized rubber (DR) and undevulcanized rubber (UDR). It is expected that DR had more unsaturated and uncrosslinked chains to participate in dynamic vulcanization. As shown in Figure 1.29, the polar functional groups on the surface of DR domains interacted with the COPE matrix and showed better interfacial adhesion. High interfacial adhesion induced compatibility between the components leading to improved tensile strength and elongation at break of TPV containing DR.

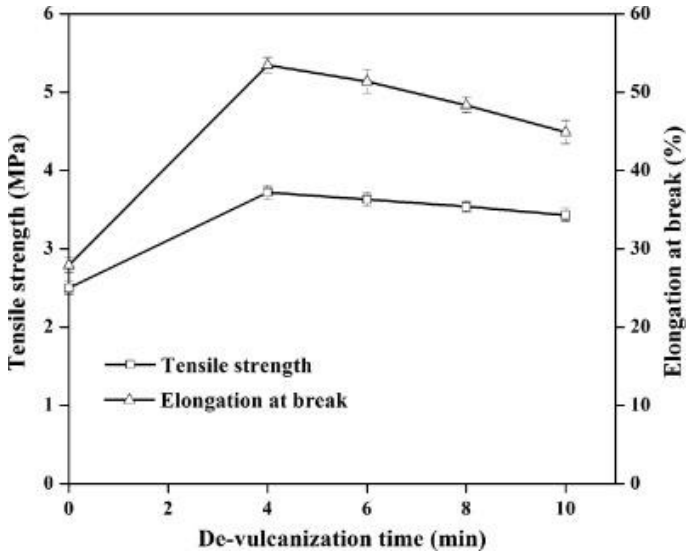

Figure 1.28 Tensile strength and elongation at break of dynamically cured DR/COPE blends as a function of the devulcanization time at 180 °C. Adapted from reference [115].

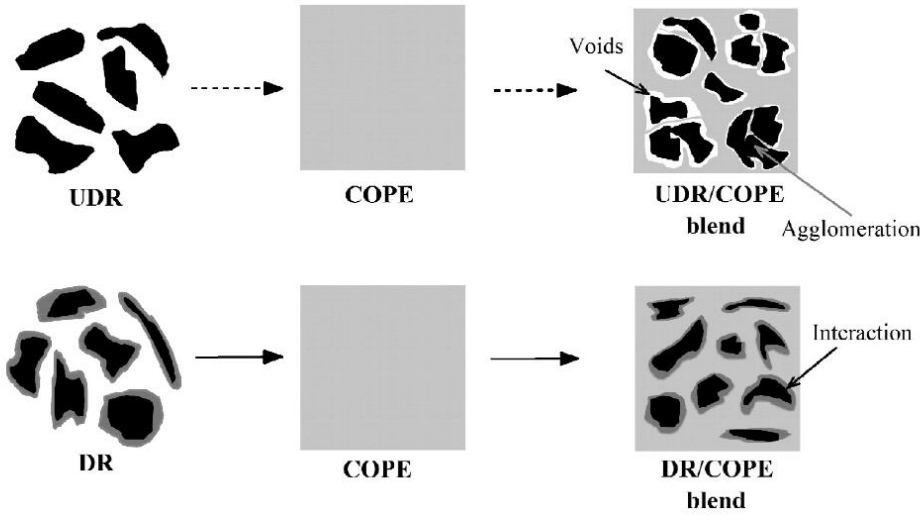

Figure 1.29 Schematic representation of the microstructure differences between TPV based on DR/COPE and UDR/COPE blends. Adapted from reference [115].

Crosslinked polymers do not dissolve in solvents due to their chemically bonded hydrocarbon chains. However, these links do not prevent the swelling of crosslinked polymers. Polymer swelling is defined as a volume increase of the gel fraction by a liquid or a gas [115]. Macsiniuc et al. [16] proposed a pre-treatment of rubber particles in a solvent to improve the compatibility between rubber and plastic for TPE preparation. This method is based on swelling the rubber chains by a solvent improving the penetration of the dissolved thermoplastic matrix molecules into the crosslinked rubber network. Macsiniuc et al. [16] studied the swelling behavior of SBR particles and the penetration of matrix molecules in the crosslinked rubber structure. They reported increased Young's modulus (468 to 652

MPa), tensile strength (5.14 to 9.39 MPa) and impact strength (35.2 to 50.1 J/m). These mechanical properties improvement was attributed to the effect of swelling SBR particles in tetrahydrofuran (THF) which allowed the PS molecules to enter the pores/voids. Consequently, interfacial adhesion of PS/SBR was enhanced by chain entanglement with a PS matrix. However, immersion time and solvent efficiency affected the swelling and penetration. Similarly, Veilleux and Rodrigue [17] investigated the properties of compounds based on virgin PS with recycled SBR powders (0-94% wt.) using a pre-treatment in solution (toluene) to improve the compatibility between the phases. According to the results of extraction tests and thermogravimetric analysis (TGA), the solution treatment allowed to insert about 7.5% wt. of virgin PS inside the SBR particles which was lower than the value obtained in a similar work on recycled PS (10.5% wt.) [116]. This difference was attributed to the lower MW of recycled PS favoring its diffusion into the solvent and the swollen rubber particles. As expected, incorporation of more elastomeric particles (up to 62% SBR) into PS decreased the hardness to 76 Shore A (6 units lower than neat PS). Also, the addition of SBR into the rigid PS matrix decreased both the rigidity (modulus) and strength (stress) of the compounds. Furthermore, the incorporation of 62% SBR into PS led to higher impact strength (up to 38 J/m form 22 J/m) due to the presence of more elastomer in the compounds to absorb the impact energy [116].

1.7 Conclusion

Disposal of waste plastic and rubber is a significant issue from an environmental point of view since the natural degradation of these materials takes several years. Vulcanized rubbers are extensively used in a wide range of applications (mainly the tire industries) because of their mechanical strength, excellent durability, abrasion resistance and low cost.

The recycling of discarded tires as the main fraction of waste rubbers has attracted increasing attention due to the large amounts of waste tires as an environmental issue. However, the complex crosslinked structure and the presence of various additives in the tire composition make their (re)processing difficult. In fact, vulcanized rubber (crosslinked structure) cannot be melted making tire recycling very difficult. Therefore, it is required to develop technologically possible and cost-effective methods for recycling the waste rubber from scrap tires.

The most straightforward and environmentally friendly method is shredding/grinding waste tires into GTR and using the material (different particle sizes) as fillers in thermosets, virgin rubbers or thermoplastics (especially recycled resins) to produce TPE compounds. The most convenient size of

rubber particles for blending with thermoplastic resins are less than 500 μm, since smaller rubber particles are more efficient for improving the TPE mechanical strength. TPE have the combined mechanical properties of thermoplastic/elastomer and easy processability of thermoplastics. SBR, EPDM and NR are the most used recycled rubber particles for melt blending with thermoplastics to prepare TPE materials. Melt blending of waste rubber particles with recycled plastic is an environmentally friendly and sustainable approach not only for higher consumption of waste polymers, but also because of more economical/eco-friendly advantages. However, low compatibility and weak interfacial adhesion between the rubbers and thermoplastics leads to low mechanical properties of TPE. Poor interfacial adhesion between the rubber and thermoplastic is more dominant at higher rubber concentration (above 50 wt.%) which significantly deteriorates the mechanical properties of the blends (especially elongation at break and toughness). Therefore, modification techniques are required to obtain recycled-based TPE compounds with appropriate properties. Several compatibilization methods such as non-reactive and reactive approaches using chemical agents (copolymers), as well as rubber surface modification through oxidizing agents or reclamation/devulcanization process and radiation-induced modification, have been presented here. There is also the possibility of solution treatment using more environmentally friendly (green) solvents. The main objective of these modification techniques is to improve the interfacial adhesion between the rubber particles and thermoplastic matrixes to achieve TPE compounds with appropriate mechanical and morphological properties.

It is expected that, in the near future, industrial and academic research will focus on the development of green and cost-effective TPE compounds based on recycled polymers. The production of TPE from recycled materials reduces the negative effects of these waste materials disposal. It also leads to the production of materials with lower costs. The TPE market is expected to grow significantly in the near future due to increased demand for green and low cost compounds obtained from waste polymers. Even though the incorporation of recycled rubber (NR and SBR) into thermoplastics has been widely studied, more studies should be done using different types of rubber such as EPDM, since this rubber is widely recycled due to its high cost. However, due to variability in the composition of polymer wastes and difficult conditions during their service life, the performance of recycled compounds varies compared to virgin compounds, which needs to be improved. Thermoplastic elastomers seems to be one of the most promising fields of study and several researches have been conducted on the mechanical and morphological properties of TPE compounds. However, the lack of literature about the

thermal, dynamic mechanical and aging behavior of these compounds highlights the need for more research on TPE preparation and their characterization.

Acknowledgements

The authors gratefully acknowledge the financial support of the Natural Sciences and Engineering Research Council of Canada (NSERC).

CHAPTER 2 RECYCLING WASTE TIRES INTO GROUND TIRE RUBBER (GTR)/RUBBER COMPOUNDS: A REVIEW

Résumé

Le recyclage et la récupération des pneus usagés constituent un grave problème environnemental car les caoutchoucs vulcanisés mettent plusieurs années à se dégrader naturellement et restent longtemps dans l'environnement. Ceci est associé à une structure réticulée tridimensionnelle (3D) complexe et à la présence d'un nombre élevé d'additifs différents à l'intérieur d'une formulation de pneumatique. La plupart des pneus en fin de vie sont jetés comme déchets dans des décharges, en prenant de la place, ou incinérés pour la valorisation énergétique, en particulier pour les déchets de caoutchouc très dégradés. Toutes ces options ne sont plus acceptables pour l'environnement et l'économie circulaire. Cependant, de nombreux progrès ont été réalisés sur la durabilité des pneus usagés via le recyclage, car ce matériau a un potentiel élevé pour être une source de matières premières précieuses. Des recherches approfondies ont été menées sur l'utilisation de ces pneus usagés comme charges dans des applications de génie civil (béton et asphalte), ainsi qu'en mélange avec des matrices polymériques (thermoplastiques, thermodurcissables ou caoutchouc vierge). Plusieurs technologies de broyage, telles que les procédés ambiants, humides ou cryogéniques, sont largement utilisées pour réduire la taille des pneus usagés et les convertir en poudrette de caoutchouc (GTR) avec une plus grande surface spécifique. Ici, l'accent est mis sur l'utilisation du GTR comme remplacement partiel dans les composés de caoutchouc vierge. Cet article présente également un examen des traitements de surface physiques et chimiques possibles pour améliorer l'adhérence du GTR et l'interaction avec différentes matrices, y compris les processus de régénération du caoutchouc tels que thermomécanique, micro-ondes, ultrasonique et thermochimique pour produire du caoutchouc de pneu régénéré (RTR). Cette revue comprend également une discussion détaillée sur l'effet de la taille des particules GTR/RTR, de la concentration et du niveau de réticulation sur les propriétés de réticulation, rhéologiques, mécaniques, de vieillissement, thermiques, mécaniques dynamiques et de gonflement des composés de caoutchouc. Enfin, une conclusion sur la situation actuelle est fournie avec des ouvertures pour des travaux futurs.

Mots-clés: Recyclage des pneus, caoutchouc de pneu rectifié, caoutchouc de pneu régénéré, composés

Abstract

Recycling and recovery of waste tires is a serious environmental problem since vulcanized rubbers require several years to degrade naturally and remain for long periods of time in the environment. This is associated to a complex three dimensional (3D) crosslinked structure and the presence of a high number of different additives inside a tire formulation. Most end-of-life tires are discarded as waste in landfills, taking space, or incinerated for energy recovery, especially for highly degraded rubber wastes. All these options are no longer acceptable for the environment and circular economy. However, a great deal of progress has been made on the sustainability of waste tires via recycling as this material has high potential being a source of valuable raw materials. Extensive researches were performed on using these end-of-life tires as fillers in civil engineering applications (concrete and asphalt), as well as blending with polymeric matrixes (thermoplastics, thermosets, or virgin rubber). Several grinding technologies, such as ambient, wet, or cryogenic processes, are widely used for downsizing waste tires and convert them into ground tire rubber (GTR) with larger specific surface area. Here, a focus is made on the use of GTR as partial replacement in virgin rubber compounds. The paper also presents a review on the possible physical and chemical surface treatments to improve the GTR adhesion and interaction with different matrixes, including rubber regeneration processes such as thermomechanical, microwave, ultrasonic and thermochemical producing regenerated tire rubber (RTR). This review also includes a detailed discussion on the effect of GTR/RTR particle size, concentration, and crosslinking level on the curing, rheological, mechanical, aging, thermal, dynamic mechanical, and swelling properties of rubber compounds. Finally, a conclusion on the current situation is provided with openings for future works.

Keywords: Tire recycling, ground tire rubber, regenerated tire rubber, compounds

2.1 Introduction

Vulcanized rubbers, as thermoset materials, show low elasticity and yield strain as well as high Young's modulus. The vulcanization process results in the formation of a crosslinked structure inside the rubber which can resist against intensive shear and temperature applications, as well as environmental agents [117]. Rubbers have been extensively used in various application ranging from household, healthcare, military, automotive and construction [118,119]. Automotive and truck tires are the main application of vulcanized rubber because of their high resistance to severe outdoor conditions (chemical reagents, high temperatures, radiations and shear stress) during their lifetime [120]. Despite the high life expectancy of new tires which is at least 80 000 miles, a large number of scrap tires, about 1.5 billion end-of-life tires per year, are generated annually all around the world due to the increased number of cars on the roads [121]. From an environmental point of view, recycling waste tires with a non-biodegradable structure and a high volume of production raises concern about waste tires management approaches. Landfilling, as the earliest waste management technique, causes health and environmental risks of accidental fires and contamination of the underground water resources [2]. Therefore, regulations for the recovery and disposal of waste tires have been introduced by governments and environmental organizations to adopt more ecofriendly recycling of waste tires. Also, from an economical point of view, discarded tires with low cost can be used in several markets such as tire-derived fuel [122,123], asphalt pavements [124,125], concrete [126,127], plastic composites [12,30], and rubber compounds [128]. Although waste tires have high calorific values to be used as fuel, scrap tires as active or inactive fillers (toughening agents for thermoplastics, thermosets, and rubbers) are more profitable and ecofriendly. In order to melt blend waste tires with polymers, grinding methods are used for downsizing the discarded tires and produce ground tire rubber (GTR) having small particle sizes (granulates in the range of 0.5-15 mm and powders with sizes less than 0.5 mm) [1]. However, poor bonding between GTR and most polymer matrixes leads to low mechanical strength and low durability of the resulting compounds which is a significant challenge limiting the performances of the blends [29,129].

To overcome this challenge, various techniques, such as GTR surface modification [130,131], devulcanization [132], dynamic vulcanization [11], and compatilibizing agent addition [30,133], have been used to increase the GTR-matrix interfacial adhesion generating improved homogeneity and processability, as well as mechanical and long term (durability) properties of the compounds. Recent advances and opportunities on the use of GTR as an inexpensive filler in construction [134,135], energy

storage [136], and polymer blends in general with a focus on thermoplastic matrixes [1,5] have been reviewed. But there is very limited work focusing on the recent advances and evolution of GTR application in virgin rubbers. Therefore, to address this gap in the literature, this paper not only reviews the evolution of GTR recycling methods, downsizing techniques, GTR devulcanization and surface treatments, but also reports on the recent development and opportunity of using GTR into rubber formulations.

2.1.1 Tire composition

Waste automobile and truck tires are the main source of waste rubbers. Figure 2.1 shows a typical structure of a tire with its components. The exterior tread to the interior lining of the tire consist of different materials with specific properties. The tread, which is the part in direct contact with the road, is mainly composed of natural rubber (NR) and synthetic rubbers. Rubber, steel and textiles can be used in the composition of the belts depending on the tire application (car, truck, off-the-road (OTR), etc.). The materials in the sidewalls require good resistance to crack propagation and attack by ozone in air, while abrasive wear resistance is the main requirement of rubber treads. The inner liner, responsible to maintain the air pressure, is made of butyl rubber with a low air permeability and good rolling resistance. The carcass and the beads are composed of twisted metals or textile cords and metal alloys coated steel wires, respectively [137,138].

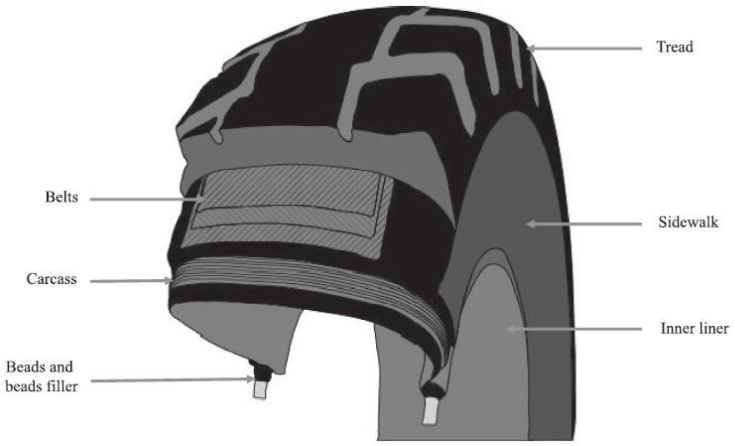

Figure 2.1 Typical tire structure. Adapted from reference [137].

The tire composition depends on different parameters such as long distances, plane braking, road quality and temperature since the tires need to show extremely high resistance to severe outdoor conditions (chemical reagents, high temperatures, radiations, and shear stress) expected during their

lifetime. As presented inTable 2.1, the main components of a tire formulation are natural and synthetic rubbers, carbon black, metal, textile fabrics and other additives with specific concentration depending on the type of tire [139].

Table 2.1 Tire composition depending on the application [137].

Material	Car tire	Truck tire	OTR tire
Rubbers/Elastomers (wt.%)	47	45	47
Carbon black and silica (wt.%)	22.5	21	22
Metals (wt.%)	14	23.5	12
Textiles (wt.%)	5.5	1	10
Vulcanization agents (wt.%)	2.5	3	3
Additives (wt.%)	8.5	6.5	6

The rubber fraction of a tire, mostly in the treads (32.5 wt.%) and the sidewalls (22 wt.%), is a mixture of NR (polyisoprene) and synthetic rubbers such as polybutadiene (BR), styrene-butadiene rubber (SBR) and butyl rubber. The chemical structure of each component is presented in Figure 2.2 [137,139].

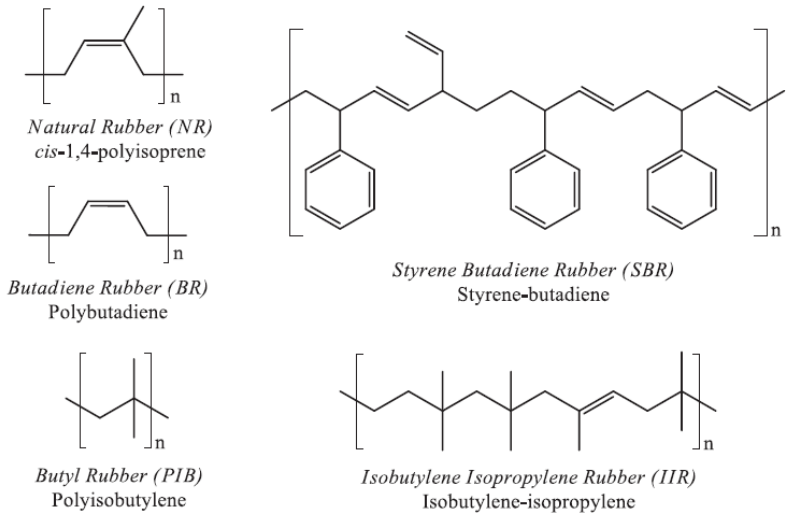

Figure 2.2 Chemical structure of rubbers used in tire composition. Adapted from reference [137].

Carbon black and silica are playing important roles in the mechanical reinforcement and abrasion resistance of a tire depending on their size, structures, and content. Recently, silica compounds gained more attention to replace carbon black to produce more ecofriendly tires. Metals, such as steel and alloys, are used to reinforce the tires. But textiles, such as natural rayon, polyamide and polyester, are mostly used in car tires to replace metals and produce lightweight tires [137,140].

Vulcanization agents (sulfur and sulfur compounds) and different additives (stabilizers, antioxidants, antiozonants, extender oils and waxes) are used in a tire formulation to induce the crosslinked structure

and be resistant to photochemical decomposition, chemical reagents, high temperatures and biodegradability [141]. Other additives containing calcium, magnesium, sodium, potassium, and chloride, can be added to improve the tire properties and durability. Because of their very complex formulation (high number of different components with a wide range of concentration), recycling of waste tires through ecofriendly and inexpensive methods is a serious challenge for the tire industries [142].

2.2 Tire recycling

Recycling of waste tires raises significant environmental concerns due to the highly crosslinked structure of vulcanized rubbers and their chemical composition containing toxic components like leachable heavy metals [135]. About 270 millions of discarded tires are annually generated in the USA alone. This leads to the necessity of finding easy, energy-efficient and cost-effective methods to recycle waste tires [143]. Different solutions have been introduced to reuse discarded tires in order to decrease the amount of disposable scrap tires as poor degradable waste materials in the environment. According to the US Tire Manufacturers Association [144], 16% of waste tires are still landfilled. These do not easily degrade and remain for long periods of time in the environment. But 86% of scrap tires are being recycled in different ways such as retreading, incineration for energy recovery, pyrolysis to obtain gas and carbon black, as well as shredding to produce small particles used as fillers in a wide variety of matrixes such as asphalt, concrete, and polymers. These recycling methods not only help to keep the environment safe, but also contribute to the economic growth of several markets such as artificial reef, erosion control, breakwaters, floatation devices, athletic tracks, playground surface, rubberized composites and many more [5,145].

An ideal solution for waste tires management should not have any adverse effect on the environment and should safeguard natural resources by using less raw materials, as well as creating industrial applications with commercial added-values. So far, several studies were devoted to improve the common recycling methods and introduce novel techniques for the management of waste tires (disposal issues). The main techniques to recycle waste tires can be classified into retreading, incineration, pyrolysis and blending (composites) through downsizing (particle size reduction) for their incorporation into matrixes as explained later [2,9,146].

2.2.1 Retreading

Retreading is a process to increase the lifetime of a used tire by stripping off its tread and applying a new one via cold or hot processes. However, this method is practical only to recycle tires having no damage to the carcass and passing a wear and tear inspection [147,148]. Usually, the tire carcass goes through a recapping system to introduce a new tread to the tire. The retreading process only needs 30% of the energy and 25% of the raw materials required to produce a new tire [149]. Not only is this method cost effective to recycle discarded tires, but it is also an ecofriendly and waste-free method as rubber buffing is the only by-product which can be an appropriate filler for concrete and polymer composites. But the disadvantages of retreading are low quality and safety concerns at high speed, limiting the application of this recycling technique for passenger cars. Nevertheless, end-of-life truck tires can be easily retreaded [147,148,150].

2.2.2 Incineration

Incineration, as a self-supporting and exothermic process occurring above 400 °C, is used for energy recovery due to the high calorific value of waste tires compared to that of coal (18.6-27.9 MJ/kg). Waste tires, with a calorific value of 32.6 MJ/kg, are used as fuels source for the production of steam, electrical energy, pulp, paper, lime and steel [151]. Also, Oriaku et al. [152] reported on the recovery of carbon black (CB) via incineration by burning the tire in a limited air supply. The recovered material can be used in small scale industries for the production of printing inks and paints. The main advantages of incineration are low energy production cost and maximum heat recovery. However, atmospheric contamination by flue gas and particle emission are sources of air pollution needing to be carefully addressed [153].

2.2.3 Pyrolysis

Discarded tires are an excellent source of hydrocarbons that can be reused in the form of gas, oil and residues through pyrolysis. Pyrolysis can be classified into catalytic or non-catalytic reaction which is a thermal decomposition of the waste tires above 400 °C in an oxygen-free environment [83]. Tire pyrolysis oil (40-60 wt.%), gas (5-20 wt.%) and char (30-40 wt.%) are the main products of waste tires pyrolysis. The oil, gas and residues can be used for carbon nanotube (CNT) synthesis, as fuel in the pyrolysis process and the production of porous activated carbon, respectively [154]. The waste tires pyrolysis products and main applications are presented in Figure 2.3. However, this solution for waste

tires management requires large pyrolysis plants which are costly to build and operate (high temperature with low pressure) with limited industrial applications at large scales [136].

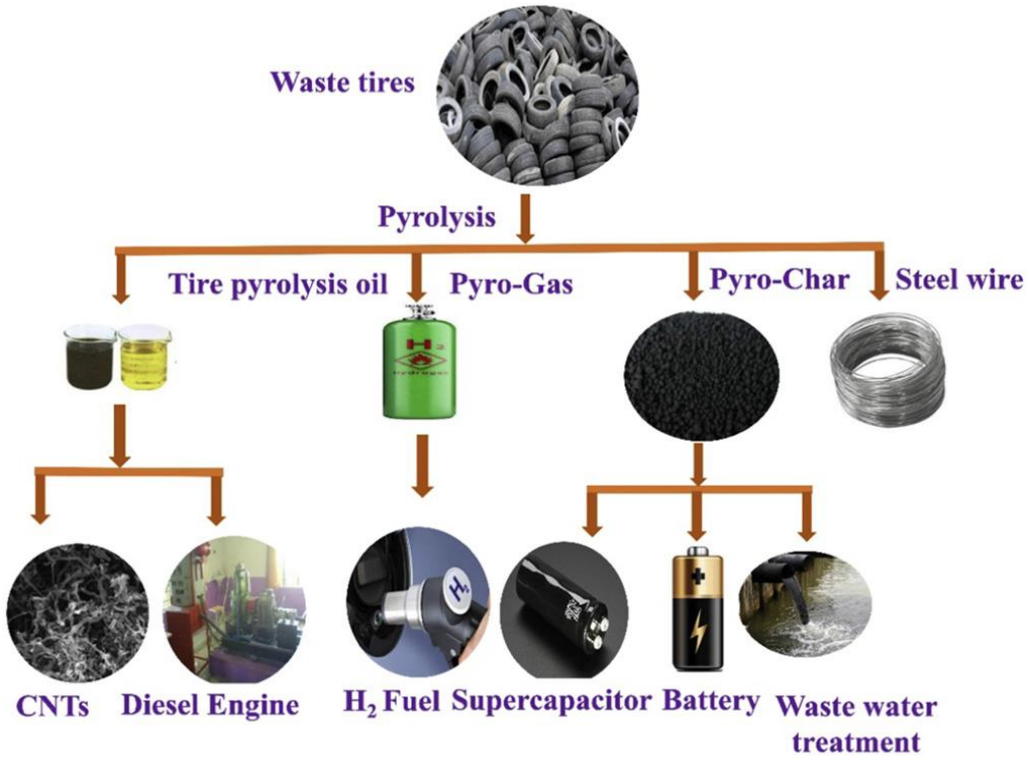

Figure 2.3 Waste tire pyrolysis products and their applications. Adapted from reference [136].

2.2.4 Material Composite

Waste tires contain natural and synthetic rubbers which are appropriate reinforcing materials for composite production. Blending waste tires with virgin matrixes not only decreases the cost of the final products, but also lowers the amount of virgin materials being used [5]. For example, the addition of crumb tire as light fillers in asphalt is used in highways, enhancing the road surfaces quality (lower surface rutting), thermal stability and resistance to ageing [155]. Scrap tires are also being used for construction applications as fillers in cement mortar for the production of concrete compositions more resistant to bending, dynamic loading and cracking [6]. They are also improving the thermal insulation and acoustic properties, as well as decreasing moisture absorption and permeability to chloride ions [156,157]. Blending waste tires with polymer matrixes (thermosets, thermoplastics and rubbers) results in low cost and green composite blends with the possibility of commercialization as substitutes for existing equivalent products. These polymer composites are being used in different applications such as mats, playground surfaces, athletic tracks, automotive parts, etc. [9,158].

Shredding of discarded tires into GTR with small particle sizes and higher specific surface areas improves the filler distribution into matrixes and increases the chance of better bonding with rubber chains. Shredding waste tires, also known as downsizing or down-cycling, requires the removal of the textile and steel reinforcements from the rubber particles by pneumatic separators and electromagnets during grinding, respectively [56]. Figure 2.4 presents typical images of the rubber crumb particles and fibers separated during a grinding process [21]. Different grinding processes have been developed such as cryogenic, ambient, wet and water jet. Each method produces different particle sizes from shred (50-300 mm) to fine powder (<500 µm) with various surface topographies. Both parameters are known to have a direct effect on the final properties of each compound [135,159].

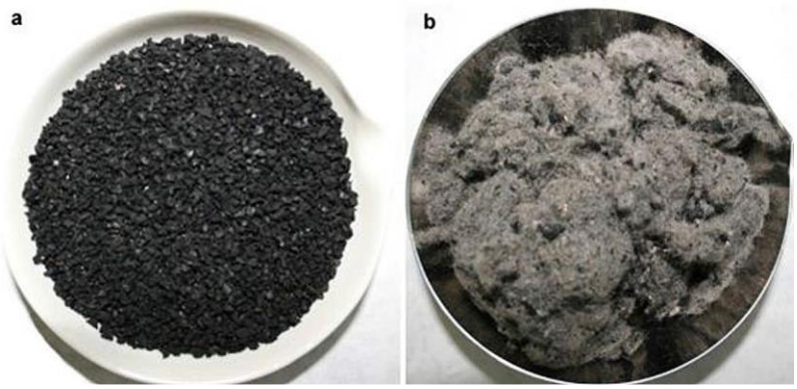

Figure 2.4 General aspects of the waste tire after shredding: (a) crumb rubber particles (1-10 mm) and (b) the reinforcing fibers. Adapted from reference [21].

Ambient grinding (air impact and water jet) is based on passing the waste tires though the nip gap of a two-roll mill to decrease the particle size. During this milling step, the temperature may rise up to 130 °C [9,160]. Increasing the number of passes leads to smaller particles size but increases the processing costs. Metal and polymer fibers can be removed from the tire chips (around 5 cm) from a previous steps and the remaining rubber particles can be used for further size reduction via granulators, cracker mills and micromills [121]. On the other hand, wet grinding is based on circular grinding plates moving concurrently and lubricated by water which is also used to control the temperature, requiring a water jet with pressure above 2 000 psi to strip the rubber. However, different parameters, such as water flow rate and the area over which such pressurized water is applied, can determine the efficiency of this process [161]. Also, solution grinding is widely used by swelling the rubber chips in a solvent such as aromatic or chlorinated hydrocarbons before being fed into the gap of the grinding plates to obtain tire powders (<1 mm) [162]. Finally, cryogenic grinding is using liquified gases to change the elastic rubbery chips into brittle particles to eliminate the rubber degradation due to the heat buildup associated with

shearing at ambient conditions. In general, the rubber chips are immersed in liquid nitrogen to convert them into brittle materials below their glass transition temperature (T_g) followed by grinding through a hammer mill. Cryogenic grinding benefits from higher production rate and lower milling energy consumption compared to ambient grinding and solution processes [163]. Figure 2.5 shows that cryogenic grinding leads to smooth rubber particle surface compared to ambient grinding. Therefore, GTR particles obtained from cryogenic processes have lower surface roughness and lower specific surface area, leading to poor physical bonding with polymer matrixes when blended. Nevertheless, cryogenic grinding operational cost for the production of finer particle sizes (<100 μm) is lower than that of ambient grinding, although the liquid nitrogen consumption is driving the production cost. In all cases, the final particle size is controlled by the number of grinding cycles and the residence time inside the grinding process [9].

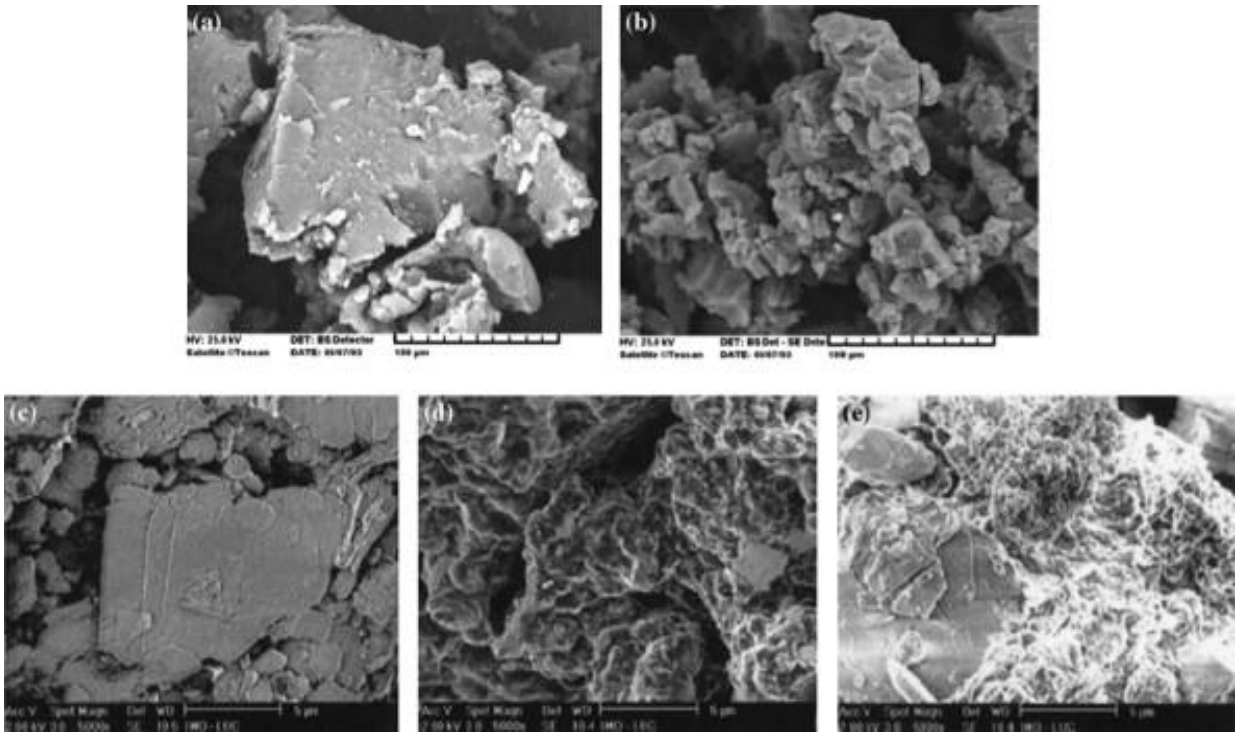

Figure 2.5 Typical particle surface state for GTR produced from different grinding processes: (a) ambient-mechanical, (b) water jet, (c) cryogenic-pin mill, (d) ambient-rotary mill and (e) cryogenic-rotary mill. Adapted from reference [9].

2.3 GTR in Blends

Blending a polymer matrix and GTR (surface modified) with elasticity and impact resistance might result in improved blends properties such as tensile strength and elongation at break depend on the level of interfacial interaction between the GTR and the matrix [11,12,75,129]. The incorporation of even as little

as 10 wt.% GTR into polymer matrixes (thermosets, thermoplastics and rubbers) leads to large consumption of waste tires as a partial replacement of virgin polymers [9]. However, GTR loading in composite materials is limited due to poor interactions between GTR and polymer, resulting in a loss of physical and mechanical properties of the blends [12]. This is why several studies have been conducted to find proper techniques to incorporate higher amounts of GTR (above 50 wt.%) into polymer matrices to decrease the cost and use of fresh/virgin materials. Different approaches, such as compatibilization, surface modification and regeneration, have been introduced to address this challenge and improve the interfacial adhesion between the components [5]. Copolymers with segments similar to blend components can be used to compatibilize GTR-filled blends by acting as (physical/chemical) bridges in immiscible polymers, improving compatibility [1]. For example, maleic anhydride grafted polyethylene (MAPE), as a well-known compatibilizer, is used to decrease the interfacial tension and stabilize the blend morphology of GTR filled polyolefin blends [12,159]. Surface modification leads to the generation of peroxy, hydroperoxy, hydroxyl and carbonyl groups on the GTR surface to promote interaction with polar polymers or reactive compatibilizers. In this method, oxidizing agents, such as potassium permanganate ($KMnO_4$) [10], nitric acid (HNO_3) and hydrogen peroxide (H_2O_2) [93], and sulphuric acid (H_2SO_4) [164], as well as energy radiation (microwave [132], gamma [165], and plasma [130]), and ultrasonic waves [166]) have been used for GTR surface treatment. Also, rubber regeneration is used to partially destroy the crosslinked structure and induce more chain mobility (molecular freedom) for better GTR bonding with the matrix chains [167]. All these techniques will be explained in more details later, including a general discussion on the effect of GTR on the final rubber compounds properties.

2.3.1 Modification of GTR

Insufficient interfacial adhesion and bonding between the crosslinked or partially regenerated GTR and the continuous phase is the main problem associated with GTR introduction into different polymer matrixes, especially at high concentrations (above 50 wt.%). This must be solved to achieve good adhesion and interfacial stress transfer to produce good mechanical strength and long term stability [1]. Therefore, GTR surface modification offers specific interaction sites between the phases, resulting in improved interfacial adhesion (lower interfacial tension), low particle agglomeration and morphology stabilization during processing [168]. Consequently, better compatibility in the blends leads to higher mechanical properties as a result of a strong interface and smooth interfacial stress transfer.

Compatibilization approaches can be classified as physical and chemical methods, in which chemical compatibilization is divided into reactive and non-reactive methods [72]. Physical compatibilization is performed to improve the surface activity and roughness by applying external forces such as mechanical or thermo-mechanical shearing [32], microwave [169], γ radiation [165], ultrasonic waves [166], ultraviolet (UV) light [13], ozone [168], plasma [130], and corona discharge [170] treatment to create a thick interface and improve wetting. On the other hand, reactive compatibilization methods are associated to reactive molecules added during mixing to form a chemically linked interface, while non-reactive methods are based on the introduction of co-polymers (block or graft) and/or nanoparticles (NP) to improve the blend compatibility [30,131,133,171]. It should be mentioned that rubber regeneration also leads to some compatibilizing effect due to possible molecular entanglement with thermoplastic resins and curable rubbers [172].

2.3.1.1 Physical methods

Zhang et al. [32] reported an economical method of waste tires recycling by the preparation of compounds based on GTR and waste tire fibers using mechanical milling. As the pan-mill method exerts strong shear forces, a process similar to pulverization was obtained leading to better dispersion and activation of the materials surface by scission of the vulcanized GTR structure. As shown in Table 2.2, increasing the number of milling cycles generated a large number of oxygen containing groups on the GTR particle surface, attributed to the reaction between the atmospheric oxygen and the free radicals produced during pan milling. Higher oxygen functional groups content implies a higher number of polar groups improving the interfacial interactions (adhesion) between GTR and waste fibers.

Table 2.2 Variation of the elemental concentrations on the GTR surface during pan milling [32].

Sample	Relative concentration (%)		
	C	O	S
Without milling	96.46	3.17	0.37
Milled for 15 cycles	94.82	4.74	0.44
Milled for 25 cycles	94.43	5.10	0.47

Low temperature plasma (LTP) is a promising approach for GTR surface modification at room temperature by applying energies less than 20 eV without significant damage of the bulk materials [173]. Different gases such as air, oxygen, nitrogen, hydrogen or ammonia can be used for hydrophilic modification, while tetramethyl silane, carbon tetrafluoride or glycidyl methacrylate are preferred for hydrophobic modification. The plasma conditions lead to easy cleavage of the surface chemical bonds

and the formation of functional groups, surface roughness, crosslinks, graft polymerization and thin film coating. Figure 2.6 presents the different cases [174].

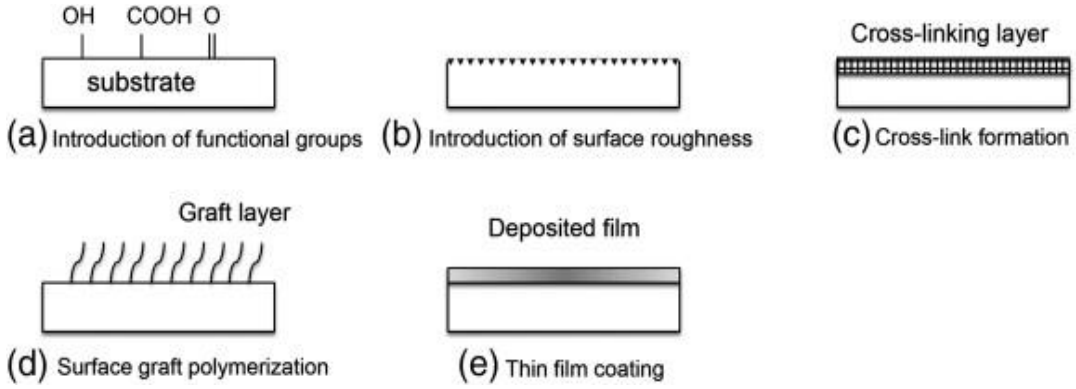

Figure 2.6 Schematic representation of the surface modifications of polymers by plasma treatments: (a) introduction of functional groups, (b) introduction of surface roughness, (c) crosslink formation, (d) surface graft polymerization and (e) thin film coating. Adapted from reference [174].

Xiaowei et al. [175] studied the surface modification of GTR by oxygen plasma and the polymerization of ethanol to introduce surface functional groups. As shown in Figure 2.7, electron bombardment leads to the simultaneous dissociation of oxygen molecules and the rupture of C–X or C=C bonds on the GTR main chains or branched chains. Next, the dissociated ethanol molecules (free radicals) react with the functional groups and are grafted on the GTR hydrocarbon chains. From this process, a substantial increase of the surface roughness was reported as a result of ethanol LTP polymerization and specific surface area of the GTR increased from 0.12 to 0.28 m^2/g after modification. Also, attenuated total reflection Fourier transform infrared (ATR-FTIR) and X-ray photoelectron spectroscopy (XPS) analysis results confirmed the formation of hydrophilic groups such as –COOH, C–OH and –CHO on the GTR surface as the oxygen content increased from 8.1% to 14.5%, and enhanced wetting was confirmed by the decrease of the liquid droplet contact angle on the GTR surface from 122° to 34°.

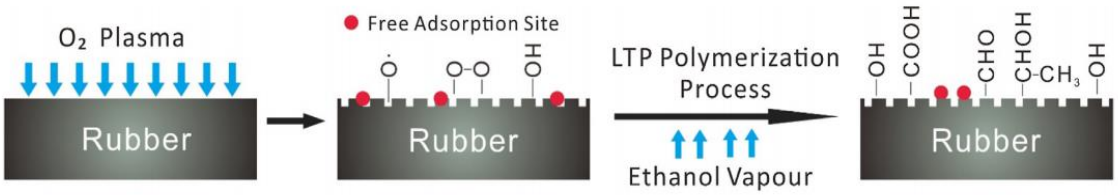

Figure 2.7 Treatment steps related to the LTP process to modify the GTR surface. Adapted from reference [175].

Ozone is widely used for the surface oxidation of materials to increase the polarity, resulting in better interaction between the phases. Also, a combination of UV-ozone treatment is used for the surface

modification of silicon rubber membranes [176], and micro-patterning applications [177]. Cataldo et al. [178] worked on the surface oxidation and functionalization of GTR using ozone as the active agent. To prevent the risk of GTR spontaneous ignition in a fixed bed reactor, the reaction was performed in a fluidized bed reactor. An evacuated large round bottomed flask was filled with an oxygen/ozone mixture and was allowed to reach the desired degree of oxidation (ξ_{oxy}) according to:

$$\xi_{oxy} = mg(ozone)/g\ (rubber) \tag{2.1}$$

Figure 2.8 presents the Fourier transform infrared (FTIR) spectra where the changes in infrared absorption bands related to the degree of oxidation and the formation of functional groups on GTR surface can be seen. Increasing the degree of oxidation up to 26 mg/g led to a more intense absorbance peak of the ketone band at 1710 cm^{-1}, which was also shifted to lower wavenumbers than the normal ketone band (1640 cm^{-1}). Also, split bands related to C-O stretching, together with peroxide and ozonide absorption, are present around 1090 cm^{-1} with increasing level of ozone treatment. The hydroxyl and hydroperoxide stretching bands also appear around 3410 cm^{-1} [178].

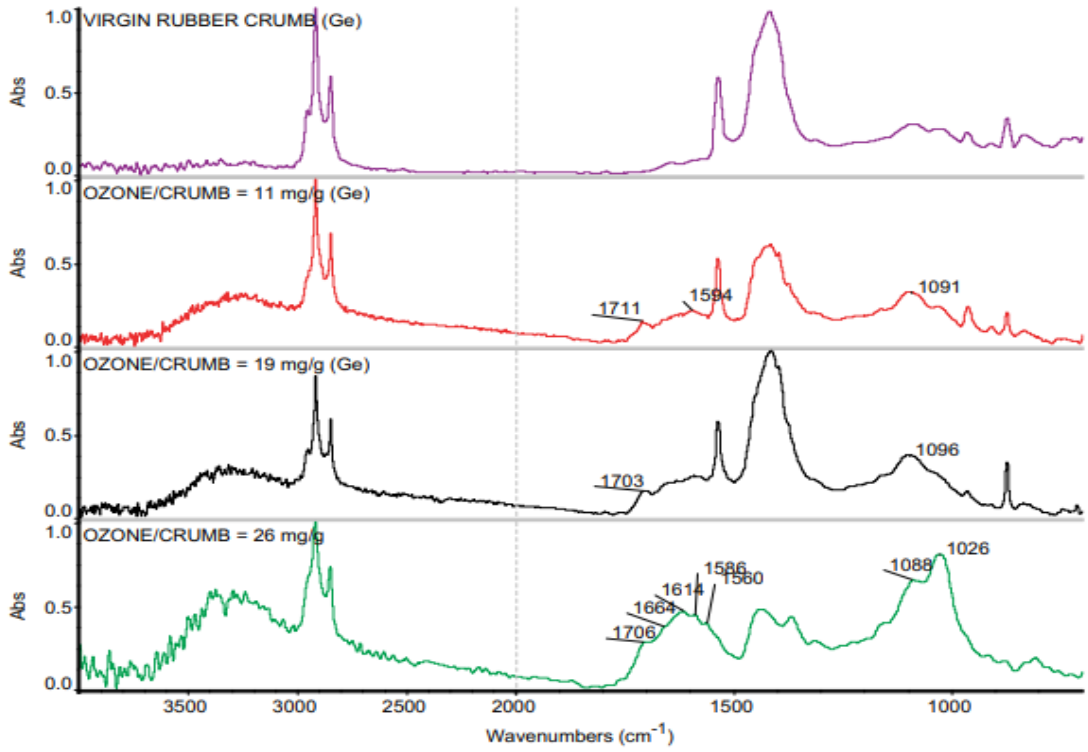

Figure 2.8 FTIR spectra of rubber crumb with different levels of oxidation. From top to bottom, the spectra were taken on pristine GTR for ξ_{oxy} = 11, 19 and 26 mg/g, respectively. Adapted from reference [178].

Martínez-Barrera et al. [165] worked on GTR surface modification by gamma rays at 200, 250 and 300 kGy. SEM images in Figure 2.9 show that the untreated GTR particles have a smooth and grated surface with some small particles. But increasing the gamma radiation energy from 200 kGy to 300 kGy increased the surface roughness with more pronounced cracks and some small cavities. It is expected that the ionizing energy of the gamma rays can form free radicals and chains scissions to produce oxygen functional groups. However, too high intensity leads to the degradation of the rubber chains, indicated by the presence of detached particles, cavities, and cracks.

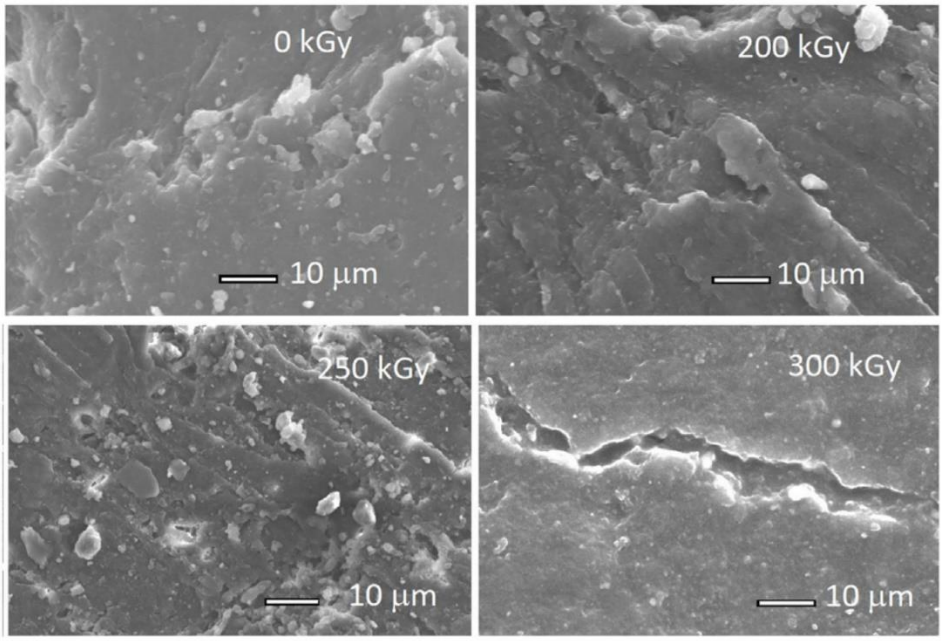

Figure 2.9 SEM images of untreated and irradiated (different energy level) waste tire rubber particles (amplification 1500x). Adapted from reference [165].

2.3.1.2 Chemical methods

As mentioned before, the chemical compatibilization of GTR can be done via non-reactive or reactive methods. Fazli and Rodrigue [5] reviewed the different chemical compatibilization methods to improve the interfacial adhesion between GTR and thermoplastics for the production of thermoplastic elastomer (TPE) compounds. For non-reactive methods, different block or graft copolymers such as MAPE [11], styrene-butadiene-styrene block copolymer (SBS) [106], ethylene-vinyl acetate (EVA) [57], and polyolefin elastomer based on ethylene octene copolymer [30] have been used to increase the compatibility of GTR containing blends.

For example, Wang et al. [133] studied the effects of SBS on the mechanical and morphological properties of high density polyethylene (HDPE)/GTR blends. Figure 2.10 presents typical stress-strain curves of the blends for different SBS loading. The addition of 12 phr SBS significantly improved the tensile strength of HDPE/GTR blends from 11.8 MPa (0 phr SBS) to 15.0 MPa. Also, the elongation at break of the blends increased from 200% to 360% with 12 phr SBS.

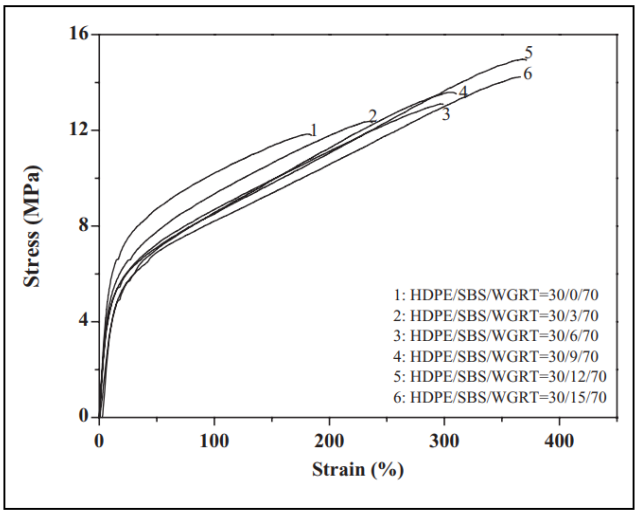

Figure 2.10 Typical stress-strain curves of HDPE/GTR compounds compatibilized by SBS. Adapted from reference [133].

The fractured surface morphology of the uncompatibilized blends (Figure 2.11 (a) and (b)) shows a smooth and clean surface due to easy GTR particles removal (pull-out) from HDPE. However, SBS addition shows no tearing strips, indicating better elastic recovery ability and better interaction between the GTR and HDPE (Figure 2.11 (c) and (d)) [133].

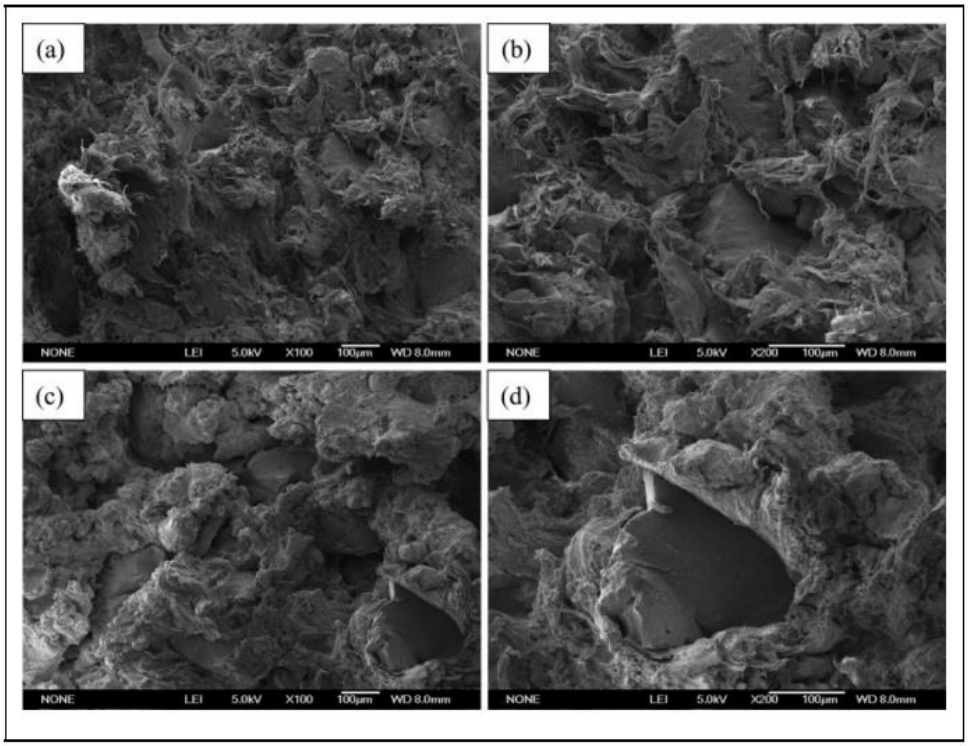

Figure 2.11 Fractured surfaces of HDPE/SBS/GTR compounds prepared by melt compounding (extrusion). The compositions (weight ratio) are: (a) 30/0/70, (b) 30/0/70, (c) 30/12/70 and (d) 30/12/70. Adapted from reference [133].

Also, the addition of NP such as nanoclays with large specific surface area and high aspect ratio (for natural montmorillonite clay, the specific surface area is 750 m^2/g with an aspect ratio of 200-1000, [83]) in rubber compounds have attracted numerous research interests due to the reinforcement potential giving superior mechanical, thermal and barrier properties [86,111]. Moreover, the incorporation of NP (1-10 wt.%) into incompatible blends containing GTR results in a morphological stabilization by selective localisation at the interface, decreasing the interfacial tension and preventing droplet coalescence during melt blending. The filler particle size and specific surface area, as well as its interactions with the matrix and good dispersion state, are controlling the NP efficiency in immiscible polymer blends [179].

Shan et al. [180] reported on the reinforcing effect of exfoliated organoclay (3 phr) in NR/SB as substantial improvement in tensile strength (92%) and tear strength (63%) was observed. The incorporation of 3 phr organoclay also decreased the scorch time and optimum curing time (T_{90}, cure for 90%) of NBR/SBR from 2.48 and 14.08 min to 1.06 and 8.03 respectively, indicating that the organoclay acted as a vulcanization accelerator.

Satyanarayana et al. [171] studied the effect of modified montmorillonite (MMT) on the phase morphology of incompatible polar carboxylated nitrile rubber (xNBR)/nonpolar NR evaluating the solubility parameter and interaction parameter (X). As expected, lower difference in interaction parameter between NR-toluene and Cloisite 15A-toluene ($X_{NR/\ toluene}$-$X_{\ Cloisite\ 15A/toluene}$ = 0.04) compared to that of xNBR-toluene and Cloisite 15A-toluene ($X_{xNBR/toluene}$-$X_{Cloisite\ 15A/toluene}$ = 0.17) was observed as the majority of Cloisite 15A (at 8 phr) migrated to the NR phase, resulting in a morphology stabilization (suppressed NR droplet coalescence), and leading to a better compatibilizing effect on the system.

As mentioned above, reactive chemical compatibilization is performed through the formation of block or graft copolymers in situ acting as bridge through covalent reactions of the functionalized components [5]. The main reactive compatibilizers are based on reactive groups randomly grafted onto the main chain, inducing a linear structure. Graft compatibilizers have segments showing chemical affinity towards the blend components to decrease the interfacial tension, improving the droplet phase dispersion and stabilizing the morphology [181]. Maleic anhydride (MA) is widely used for the surface modification of rubbers to enhance compatibility and interfacial adhesion of immiscible blends [131,182,183]. Yassin et al. [131] worked on the graft polymerization of styrene and MA onto the GTR surface using H_2O_2 as an initiator. The grafting level of styrene increased from 2% at 75 ˚C to 23% at 125 ˚C. Higher temperatures induced better chain mobility inside the GTR and increased the chance of styrene grafting on its active sites. However, temperatures above 125 ^oC led to lower grafting level attributed to the degradation of the grafted monomers. Abou-helal et al. [183] reported on the positive effect of MA grafted on ethylene-propylene-diene monomer (EPDM) rubber to improve the compatibility of EPDM/NR compounds. As expected, the tensile strength and elongation at break of compatibilized EPDM/NR blends increased with higher MA concentration. For example, the tensile strength and elongation at break of EPDM/NR (25/75) increased from 2.4 MPa and 250% to 3 MPa and 290% respectively, by increasing the MA content from 1.5 to 6 phr. This behavior was attributed to a better penetration of compatibilizers segments similar to those in rubbers at the interface with increasing MA content. Thus, better interfacial interaction provided better stress transfer and better overall mechanical properties.

2.3.2 Regeneration of GTR

GTR regeneration is widely used to convert a three dimensional (3D) crosslinked, insoluble and infusible vulcanized rubber (100% gel content) into a partially soluble materials with lower crosslink

density, having more chain mobility. The process leads to a material called regenerated tire rubber (RTR). The soluble fraction of RTR with high molecular weight (MW) results in sufficient bonding with the polymer matrix to improve interfacial adhesion between the phases [54]. Swelling degree estimation combined with the Flory-Rehner equation are used to determine the gel content and to quantify the crosslink density [184]. Devulcanization and reclamation are used interchangeably to the process of destroying the crosslinked structure of thermoset rubbers. But devulcanization aims at S–S and C–S selective bonds scission for partial breakdown of the 3D network of the vulcanized tire to achieve plasticity, while reclamation is associated with the rubber backbone (C–C bonds) degradation to decrease the MW. However, the selective rupture of the crosslinked network is not possible without damage to the backbone chain since the required energies to break the S-S and C-S bonds (227 and 273 kJ/mol, respectively) are very close to the energy required to break the C-C bonds (348 kJ/mol) [167,185]. In this review, both reclaimed and devulcanized processes are associated with regeneration processes to produce RTR particles.

GTR regeneration processes are classified as physical and chemical processes in which thermo-mechanical [186], microwave-assisted [132,187], ultrasonic-based [166,188,189], and thermochemical processes [190] are broadly studied. A detailed description of these methods is reviewed in numerous papers and patent applications [54,137,172,185]. In general, physical regeneration uses external energy sources to breakdown the vulcanized structure, while chemical regeneration is based on organic and inorganic reclaiming agents to react with the crosslinked rubber. Not only sulfide and mercaptan compounds are being used in chemical regeneration processes, but also non-sulfured agents have attracted attention due to ecological and economic benefits [185]. A brief description of the main GTR regeneration processes is presented next.

2.3.2.1 Thermo-mechanical processes

This process is based on the shear (mechanical energy) and heat around 200 ˚C (thermal energy) using mills and twin-screw extruders to decrease the rubber MW. There is also substantial heat generation (friction) generated in these processes. The use of different solvents such as hexane, supercritical fluids or oils are effective for better heat transfer, as well as to swell the rubber impose internal stresses, making the crosslinks easier to break [191]. Although batch processes, like open mills, were used for GTR regeneration, continuous processes using extruders attracted more attention due to better scalability for industrial application. Figure 2.12 presents a typical screw configuration for a

co-rotating twin-screw extruder which is divided into three zones. The first section is composed of conveying and kneading elements, followed by the devulcanization zone in the second part. The last part consists of the discharge zone after a vacuum extraction step to remove the volatiles [167].

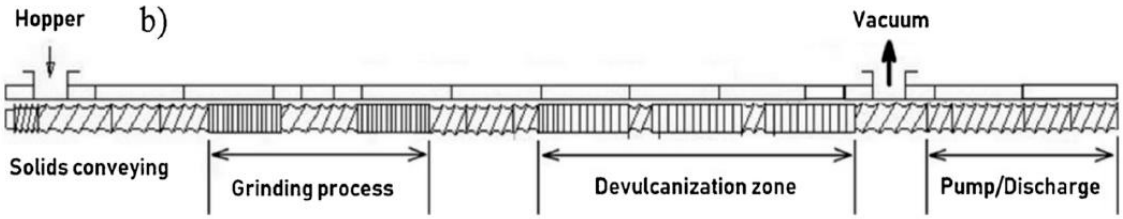

Figure 2.12 A typical screw configuration for GTR regeneration showing the different processing sections. Adapted from reference [167].

Yazdani et al. [192] studied the effect of the barrel temperature and the screw speed of a twin-screw extruder on the GTR regeneration rate. It was found that increasing the temperature from 220 °C to 280 °C at constant screw speed (120 rpm) led to slightly lower regeneration rate from 88% to 85% which might be related to the degradation of the backbone chains instead of the crosslinked network. Similar results were reported by other studies focusing on the effect of processing parameters (compounding sequence, feeding speed, screw speed and temperature profile) on the GTR regeneration rate [25].

Formela et al. [186] studied the effect of the extruder operation by comparing a counter-rotating (screw profile A) and a co-rotating (screw profile B and screw profile C) screw. They reported a decrease of the screw torque and crosslink density, and hence a higher regeneration rate by increasing the speed of the counter-rotating twin-screw extruder. They used the Horikx's theory to quantify the difference between crosslink scission and main chain scission during the regeneration process [193]. Horikx's theory describes the relationship between the sol fraction and changes in the crosslinking density after degradation via:

$$1 - \frac{v_2}{v_1} = 1 - \frac{\left(1 - S_2^{1/2}\right)^2}{\left(1 - S_1^{1/2}\right)^2} \tag{2.2}$$

Where v_1 and v_2 are the crosslinking density before and after regeneration (mol/cm^3) respectively, while S_1 and S_2 represent the sol fraction before and after regeneration (%), respectively. According to the sol fraction curves, results lower than the theoretical values indicated a selective rupture of the crosslinks (S-S and C-S bonds) during regeneration [194]. Although GTR regeneration was achieved

with the counter-rotating twin-screw extruder, the co-rotating design achieved better RTR mechanical properties (closer to virgin rubber).

Most GTR regeneration based on thermo-mechanical processes use reclaiming agents. For example, Shi et al. [195] studied the effect of different regeneration factors, such as temperature, shear force, reaction time, regeneration atmosphere and regeneration agent, on the GTR structure and properties. They used a regeneration activator (RA 420; Henan Jinfeng Chemical Industry) and diphenyl disulfide (DPDS) as reagents and observed that high temperatures (200-240 °C) and strong shear forces in a twin-screw extruder led to lower tensile strength and elongation at break attributed to the degradation of the main polymeric chain and a high sol fraction with low MW. The incorporation of RTR into NR increased the tensile strength and elongation at break of NR/GTR from 15 MPa and 350% to 21 MPa and 550%, respectively. These variations were related to the partial break-up of the crosslink network and good interfacial interactions between RTR and NR.

2.3.2.2 Microwave method

Microwave regeneration can be performed on GTR having polar groups by applying a 915 to 2450 MHz frequency and 41 to 177 Wh/lb energy to destroy the crosslink bonds and produce RTR with properties very close to the original rubber [54]. Garcia et al. [132] reported long microwave exposure (7 min) of GTR (NR, SBR and carbon black) resulting in lower gel content by breaking the sulfur crosslinks (C-S and S-S) and carbon (C-C) bonds leading to higher RTR chain mobility (fluidity).

Figure 2.13 shows SEM micrographs of the GTR sheets surface after microwave exposure for 5, 6, and 7 min. Homogenization of the modified GTR in an open two-roll mill enabled the sol phase to more efficiently wet the gel phase. This is why GTR7 shows a smoother surface with smaller voids due to its higher fluidity and sol fraction as a result of a higher level of regeneration. On the other hand, GTR5 shows larger voids because of weak interaction because the rigid particles (higher crosslink density) were not able to deform under mechanical shearing, leading to low interaction [132].

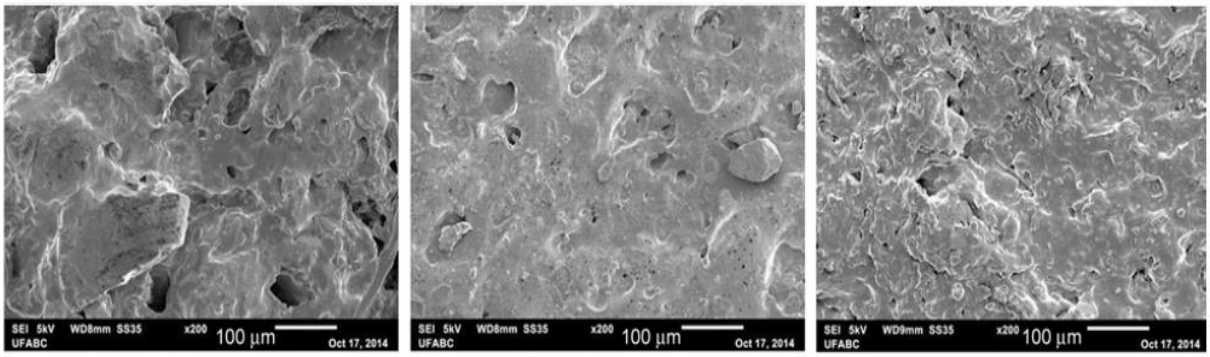

Figure 2.13 SEM images of the surface sheets of different GTR microwave treated for 5 (GTR5), 6 (GTR6) and 7 (GTR7) minutes. Adapted from reference [132].

Zanchet et al. [196] regenerated SBR via microwave exposure for 1, 2 and 3 min and blended the regenerated styrene-butadiene rubbers (rSBR) with virgin SBR (20 phr) for subsequent revulcanization. As presented in Table 2.3, the gel fraction, which is a direct indication of the regeneration level, increased with increasing exposure times and temperature.

Table 2.3 Temperature after microwave treatment and gel content of the rSBR for different exposure time (1 to 3 min) with a power of 900 W). Adapted from reference [196].

Sample	Temperature (°C)	Gel content (%)
SBR-r	–	93 ± 2
rSBR 1 min	45 ± 2	90 ± 1
rSBR 2 min	60 ± 2	43 ± 2
rSBR 3 min	80 ± 4	33 ± 1

2.3.2.3 Ultrasonic method

Continuous ultrasonic regeneration of GTR is a promising method to break-up the crosslinked structure of vulcanized waste tires in a short time using cavitation bubbles induced by mechanical waves at high frequencies. The amplitude of the ultrasonic wave and the treatment time determine the efficiency of this GTR regeneration process [188].

Isayev et al. [189] investigated the effects of GTR particle size (10 and 30 mesh) on the ultrasonic regeneration efficiency. Ultrasonic regeneration at 250 °C with an amplitude of 10 µm revealed that the crosslink density (0.1 kmole/m^3) and gel content (57%) of 30 mesh (600 µm) RTR were lower than the crosslink density (0.2 kmole/m^3) and gel content (67%) of 10 mesh (2 000 µm) RTR particles, indicating that higher regeneration rates can be achieved for smaller particles.

The ultrasonic method can also be combined with an extruder for better efficiency as a continuous process. Feng et al. [166] studied the ultrasonic regeneration of butyl rubber waste tires using a grooved barrel ultrasonic extruder, varying the ultrasonic amplitude (5, 7.5 and 10 μm) and the rubber flow rate (0.63, 1.26 and 2.52 g/s). As shown in Figure 2.14 (a), the complex viscosity of the regenerated particles is lower than that of the untreated rubber particles, attributed to the lower RTR gel content and indicating higher regeneration level. Moreover, increasing the ultrasonic amplitude led to lower RTR complex viscosity. But the damping factor (tan δ; ratio between the loss and storage moduli) of RTR increased after regeneration, indicating a more viscous (less elastic) behavior attributed to a higher sol fraction.

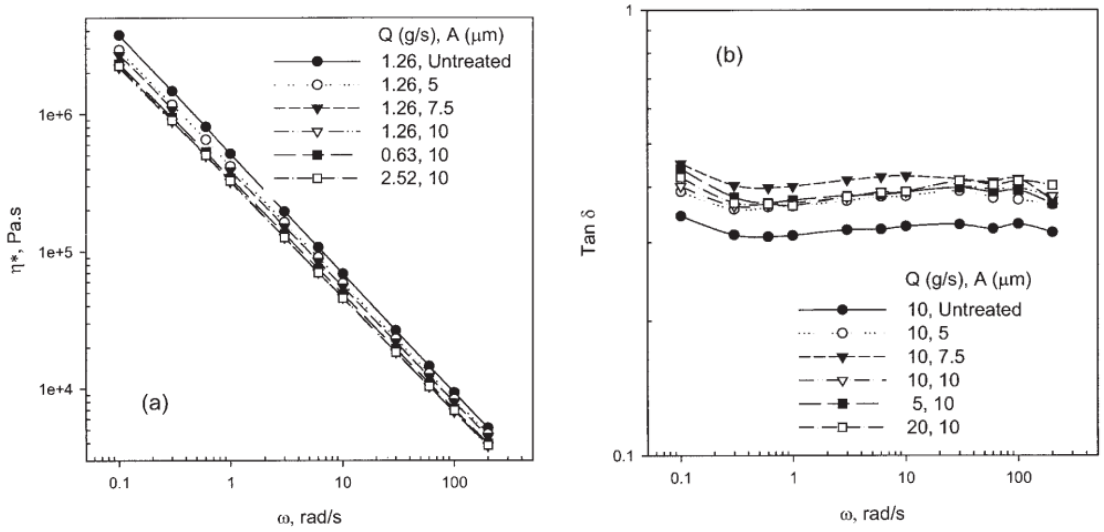

Figure 2.14 (a) Complex dynamic viscosity and (b) damping factor as a function of frequency for untreated and regenerated rubber obtained at various amplitudes and flow rates. Adapted from reference [166].

2.3.2.3 Thermo-chemical processes

Chemical reclaiming agents, such as such as benzoyl peroxide [197], tetrabenzylthiuram disulfide [198], diphenyl disulfide [199], and thiosalicylic acid [200] are extensively used in the range of 0.5-10 wt.% for the chemical regeneration of natural and synthetic rubbers. Figure 2.15 presents the chemical structure of different organic disulfides and mercaptans involved in the chemical regeneration of waste tires [151].

Thermo-chemical regeneration is based on applying thermal energy and mechanical mixing/kneading, as well as adding chemical reclaiming agents to combine the advantages of both regeneration processes. However, elevated temperatures might result in severe degradation of the main chain and a drop in mechanical properties for the regenerated rubber [186,201].

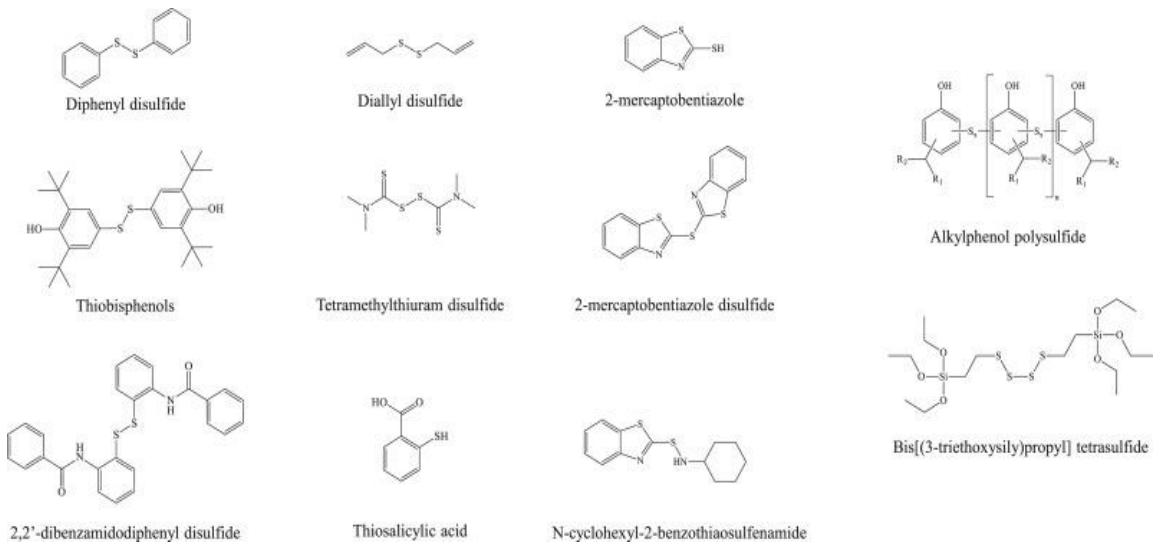

Figure 2.15 Typical sulfides and mercaptans used in tire regeneration. Adapted from reference [137].

Adhikari et al. [54] reviewed the list of inorganic and organic chemical reclaiming agents used in GTR regeneration. Zhang et al. [190] synthesized 4,4'-dithiobis(2,6-di-t-butylphenol) and used it as a novel reclaiming agent in an internal (batch) mixer at 180 °C and 200 °C. As shown in Figure 2.16, the RTR crosslink density decreased with increasing reclaiming agent content and temperature because of the break-up of both crosslink bonds and main backbone chains. They explained the inverse relation between crosslink density and MW between crosslink by the reaction scheme presented in Figure 2.17.

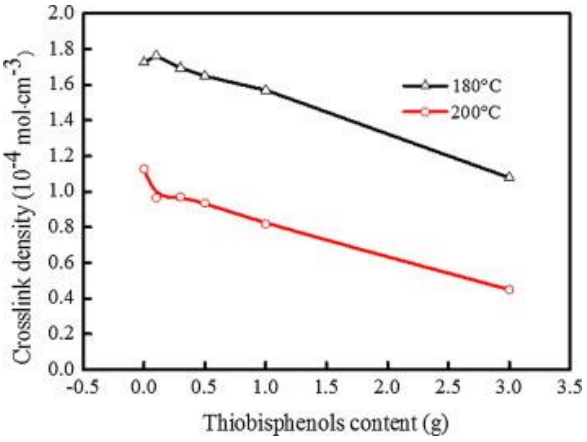

Figure 2.16 Effect of thiobisphenols content and temperature on the crosslink density of reclaimed rubber. Adapted from reference [190].

Figure 2.17 (a, b) show the reaction leading to the simultaneous breakup of both main chains and crosslink bonds by thiobisphenols (Figure 2.17 (c)) to form radicals which can react with polymer radicals. As shown in Figure 2.17 (d, e), thiobisphenols radicals may combine with polymer radicals and different types of chain ends are generated decreasing the crosslink bonds, resulting in lower

crosslink density. However, low thiobisphenols contents led to lower thiobisphenol radical concentration and less chance for reaction with polymer radicals. Therefore, uncapped polymer radicals can combine together, resulting in chain extension, leading to higher RTR MW and higher crosslink density (Figure 2.17) [190].

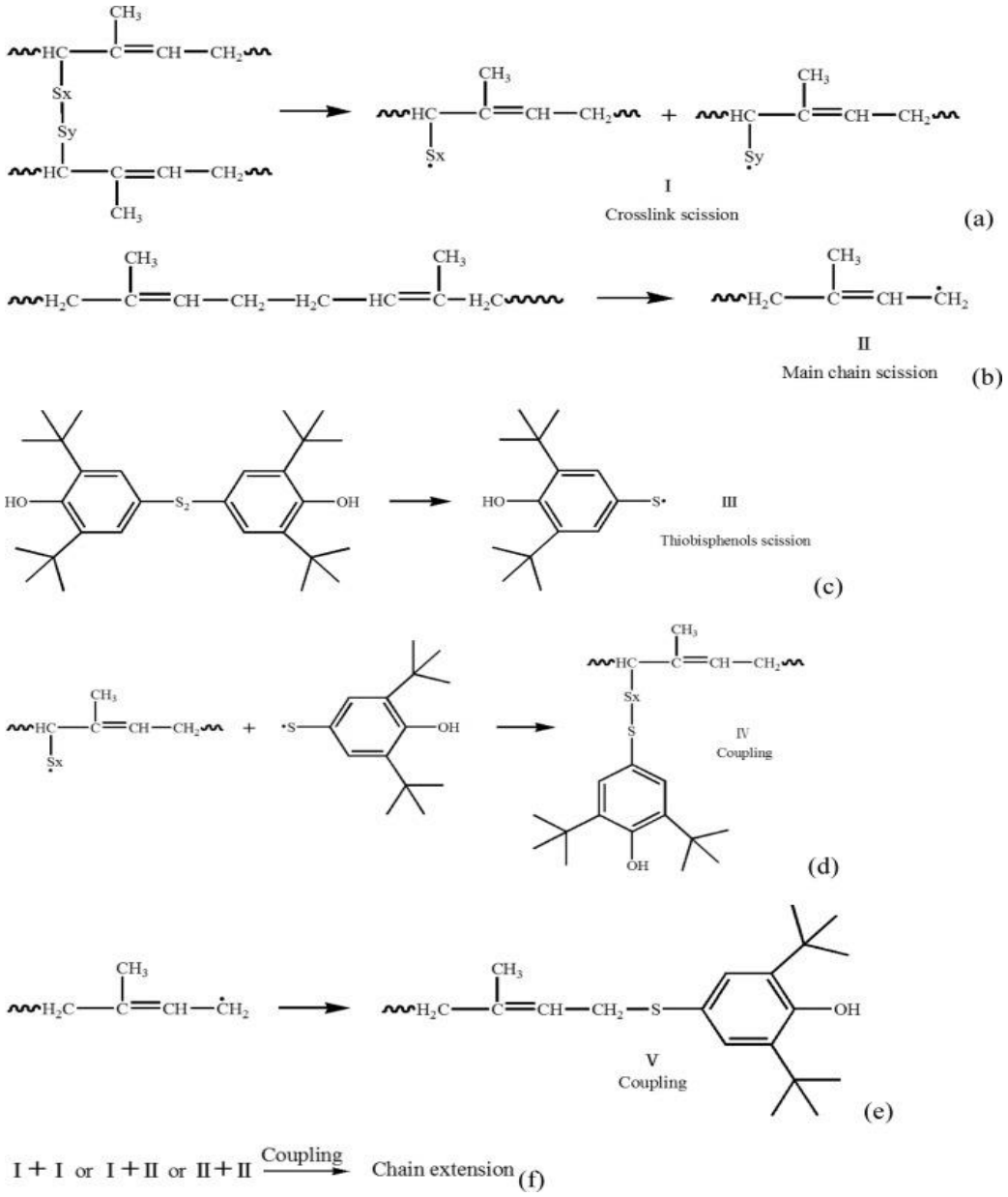

Figure 2.17 Reaction scheme for the regeneration of sulfur vulcanized rubber with thiobisphenols. Adapted from reference [190].

Not only solvents, such as alcohol and ketone, were used during GTR regeneration processes, but supercritical solvents (water, ethanol, carbon dioxide and toluene) were also studied. Li et al. [202] investigated the effect of temperature on the regeneration of waste sidewall rubber from passenger car

tires using supercritical ethanol and diphenyl disulfide (DPDS) as a regeneration agent. As shown in Figure 2.18, increasing the reaction temperature from 240 to 270 °C increased the RTR sol fraction from 25 to 55% since ethanol reached its supercritical state, making it easier to penetrate into the GTR vulcanized structure to facilitate the crosslinked network breakdown.

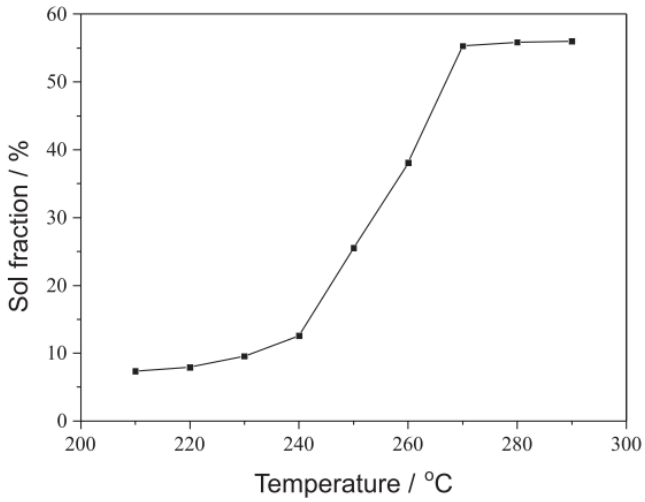

Figure 2.18 Effect of temperature on the sol fraction of regenerated sidewall rubber obtained from a passenger car tire (regeneration reaction conditions are 8 MPa for 60 min). Adapted from reference [202].

2.3.3 GTR in curable rubbers

Ramarad et al. [1] and Karger-Kocsis et al. [9] reviewed the evolution, properties and future of waste tire rubber as a filler/reinforcement in polymer blends. Also, Fazli and Rodrigue presented a review on waste rubber recycling focussing on size reduction and melt blending of GTR/RTR with thermoplastic resins to produce TPE compounds [5]. Even though thermoplastic matrixes containing GTR/RTR are being studied by several researchers, very few publications reviewed the progress of blending GTR/RTR with virgin rubbers.

GTR, with and without regeneration, have been rarely mixed with virgin rubbers such as NR, SBR, BR and acrylonitrile butadiene rubber (NBR) to produce lower cost compounds [9]. The introduction of GTR/RTR into virgin rubbers mainly leads to the sacrifice of some properties in the final compounds.

As expected, particle size and regeneration level of the GTR directly affect the rubber compounds properties. As described later, smaller particle size show less effects on the mechanical properties loss due to better dispersion and higher specific surface area for sufficient interaction with the rubber matrix chains [14]. On the other hand, RTR offers better mechanical strength, thermal stability and curing

behavior compared to GTR. This is attributed to the soluble fraction of RTR responsible for a good interfacial adhesion with rubber molecules and possible co-crosslinking at the interface between RTR and rubber matrix [11,129]. Recently, more research attention was directed to find the optimum GTR/RTR loading in rubber matrixes with less properties loss compared with virgin rubber properties. The next section reports the effect of GTR/RTR addition into rubber matrixes and reviews the literature related to the curing characteristics, rheological, mechanical, aging, thermal, dynamic mechanical, and swelling properties of such compounds.

2.3.3.1 Cure characteristics

Curing properties of rubber compounds can be determined by evaluating the maximum and minimum torque beside scorch time and cure time using a rheometer. GTR incorporation into virgin rubber is expected to modify the cure characteristics since the material already has some formulation/history. In general, GTR introduction leads to lower maximum torque and scorch time, while increasing the minimum torque [203]. On the other hand, RTR particles leads to lower increase in the minimum torque compared with GTR [204]. This is attributed to the partial breakup of the crosslinked RTR structure, which better flows and agglomerates less in the rubber matrix, decreasing the compound viscosity [205]. Not only better chain mobility of the RTR particles changes the minimum torque, but also the presence of 10-15% of processing oil in their formulation induces a lower increase in the minimum torque, which implies better processability of RTR compared to GTR [204,206]. Also, the presence of carbon black in both GTR and RTR leads to higher minimum torque [207]. On the other hand, the maximum torque, as a measure of the elastic modulus, did not decrease much with RTR loading because its shorter chains acted as plasticizers combined with the presence of some processing oil [204,208]. GTR incorporation leads to a reduction of the maximum torque, which stabilizes upon further addition of crosslinked GTR particles [204]. In general, lower torque for RTR containing rubber compounds is related to the break-up of the crosslinked structure and to a lower crosslink density compared to GTR [1].

Rubber compounds crosslinking starts at the scorch time, which decreases upon the addition of GTR/RTR into the rubber matrix. This behavior is more prevailing with RTR, which is attributed to the presence of active crosslinking sites or crosslink precursors and unreacted curatives, facilitating the crosslinking reaction upon heating [209]. For example, accelerators, as crosslink precursors, migrate to the rubber matrix from GTR/RTR particles and decrease the scorch time, which implies an early start of the crosslinking reaction, which is an undesirable property in the industry [204,210]. Several

researches have been done to overcome this challenge and control the cure time of rubber compounds. For example, De et al. [211] reported on the positive effect of 0.25 phr N-cyclohexyl thiophthalimide as a prevulcanization inhibitor (PVI) in NR/RTR (50/50) blends to increase the scorch time by 150% (from 1.5 to 2.25 min) and to cure uniformly in thick products such as tires. Also, Nelson et al. [206] reported longer scorch times and cure time for NBR/RTR blends by grafting MA onto the RTR surface. Incorporation of 20 wt.% modified RTR increased the cure time of NBR/RTR compounds from 4 to 7 min after the addition of modified RTR particles. This was attributed to the presence of anhydride in the MA structure, delaying the curing process (longer onset of the curing process) and decreasing the cure rate, resulting in higher cure times.

The optimum cure time is another parameter for the analysis of the rubber cure characteristics, revealing the required time to achieve optimum physical properties of the rubber compounds. The optimum cure time varies upon the incorporation of GTR/RTR similar to the scorch time, which decreases with filler content [204]. However, further increase of GTR content leads to the stabilization of the optimum cure time due to the crosslinked GTR structure limiting the crosslink ability [207,212]. A summary of all the changes in the cure characteristic of GTR/RTR containing rubber blends is presented in Figure 2.19.

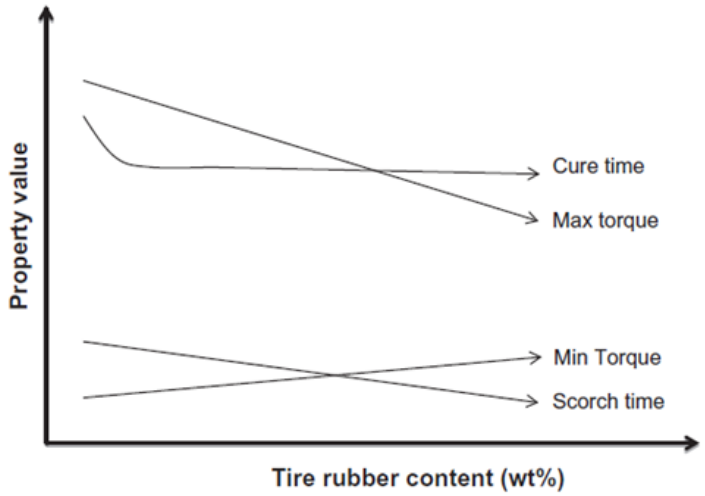

Figure 2.19 Effect of tire rubber content on the cure characteristic of rubber blends. Adapted from reference [1].

2.3.3.2 Rheological properties

The incorporation of waste tires rubber into a rubber matrix increases the Mooney viscosity of the rubber compounds due to the crosslinked gel fraction and the presence of carbon black, which limit

chain mobility. Increasing the GTR loading leads to the presence of a more crosslinked gel content and carbon black content, resulting in a further increase in the rubber compound viscosity [212,213]. Debapriya et al. [212] reported on the increasing Mooney viscosity of NR-polybutadiene rubber (PBR) compounds upon RTR addition, due to the increase in carbon black loading, inducing more stiffness and processing difficulty of the compounds (Figure 2.20).

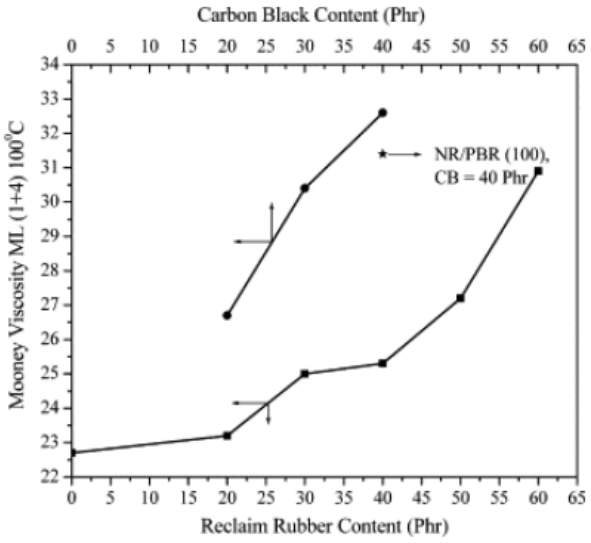

Figure 2.20 Mooney viscosity of NR-PBR/RR blends as a function of carbon black/RTR loading. Adapted from reference [212].

Similar to the Mooney viscosity, the incorporation of waste tires rubber influences the shear viscosity trend and the material shows a pseudoplastic behavior. Extrudate swell, or the Barus effect, is described by the ratio of the extrudate diameter to the capillary die diameter. This phenomenon is attributed to normal stresses released when the material emerges from a capillary die [214]. Sombatsompop et al. [213] studied the effect of RTR incorporation into two NR matrixes (STRVS60 and STR20CV) using a sulfur vulcanization system to analyse the extrudate swell. As shown in Figure 2.21, increasing the RTR loading led to lower extrudate swell due to the higher carbon black content, decreasing the rubber chain mobility and elasticity of the compound. Also, molecular interactions between the rubber molecules and the carbon black might be responsible for lower elasticity (normal stresses).

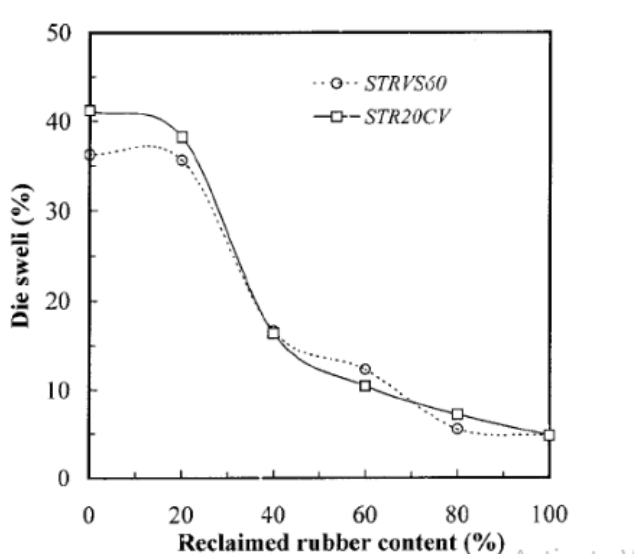

Figure 2.21 Extrudate (die) swell as a function of RTR content for NR (STRVS60 and STR20CV) at a temperature of 80 °C for 10 min of mastication and a shear rate of 3.6 s^{-1}. Adapted from reference [213].

2.3.3.3 Mechanical properties

Different investigations were devoted to the effect of GTR incorporation into rubber matrixes to evaluate the final compound mechanical properties such as tensile strength, hardness, abrasion resistance, resilience and compression set. As presented in Table 2.4, GTR incorporation into NR leads to a drop in tensile strength (TS) and elongation at break (EB), while blending GTR with NBR resulted in an improvement of both properties [206,207]. However, the incorporation of GTR into SBR did not show clear trends in mechanical properties changes since sometimes TS and EB improved [208], while other times they deteriorated [205]. Lower TS and EB of the compounds based on GTR/RTR can be attributed to the low level of blend homogeneity and weak interfacial adhesion between the phases. Increasing the GTR loading implies an increase of the gel fraction with a crosslinked structure that cannot be dispersed as a continuous matrix in the virgin rubber, thus acting as stress concentrating point, resulting in lower TS and EB.

Table 2.4 Common mechanical properties of GTR/RTR rubber blends. Adapted from reference [1].

Blends	GTR/RTR loading	Tensile strength (MPa)	Elongation at break (%)	Tear strength (N/mm)	Abrasion resistance (cc/h)	Compression set (%)	Resilience (%)
NR/RTR [203]	20	15	610	27	10.6	18	58
	40	12.5	580	29	10.7	25	52
	60	12	60	30	10.7	25.2	50
NR/GTR [205]	20	15.9	500				
	40	13.4	417		Not reported		
	60	11.6	260				
NBR/RTR [207]	20	2.5	320	27.9	2.5	18	30
	40	3.0	380	27.5	5	21	29
	60	5.5	500	27.3	8	26.5	28
NBR/GTR [215]	20	4	325	22	4	15.5	30.5
	40	6	310	27	7	17.5	27
SBR/RTR [208]	20	2.5	350	13	14.5	4.5	46
	40	3.8	525	17	19	5.0	45
	60	5.5	600	21	20	6.2	38
SBR/RTR [205]	20	17.5	350				
	40	14.8	317		Not reported		
	60	8.7	260				

Sombatsompop et al. [213] investigated the effect of RTR addition on the properties of two natural rubber compounds (STRVS60 and STR20CV) with respect to the RTR concentration and mastication time. As shown in Figure 2.22, the tensile stress at break and elongation at break of both rubber compounds decreased with increasing RTR content, due to the difficult distribution of the high filler concentration (80 wt.% RTR) and insufficient interaction with the rubber matrix, due to restricted chain mobility of partially regenerated RTR. As shown in Figure 2.23, SEM micrographs of the fractured blend surface (STRVS60/RTR (20/80)) show less homogeneity generating defects at the interphase, leading to lower mechanical properties. Also, the presence of carbon black in the RTR formulation acts as stress concentration points, inhibiting the molecular orientation and chain mobility of the rubber chains, leading to compound failure at lower TS and EB.

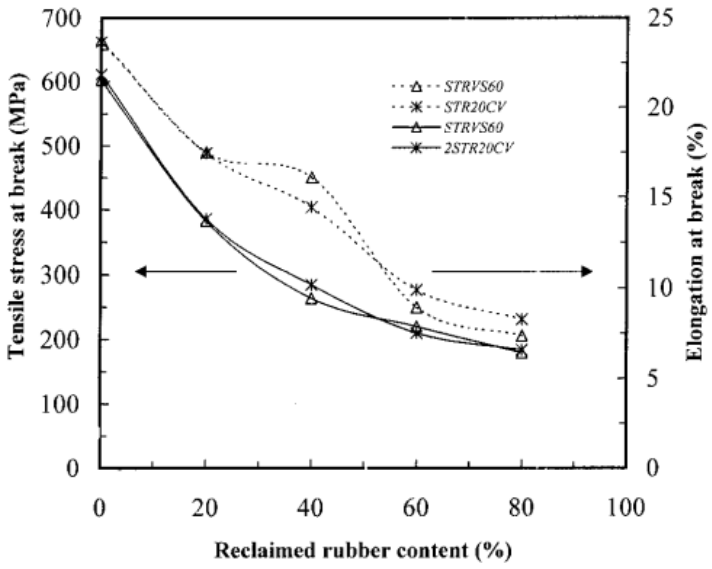

Figure 2.22 Tensile stress at break and elongation at break as a function of RTR content in NR (STRVS60 and STR20CV) compounds. Adapted from reference [213].

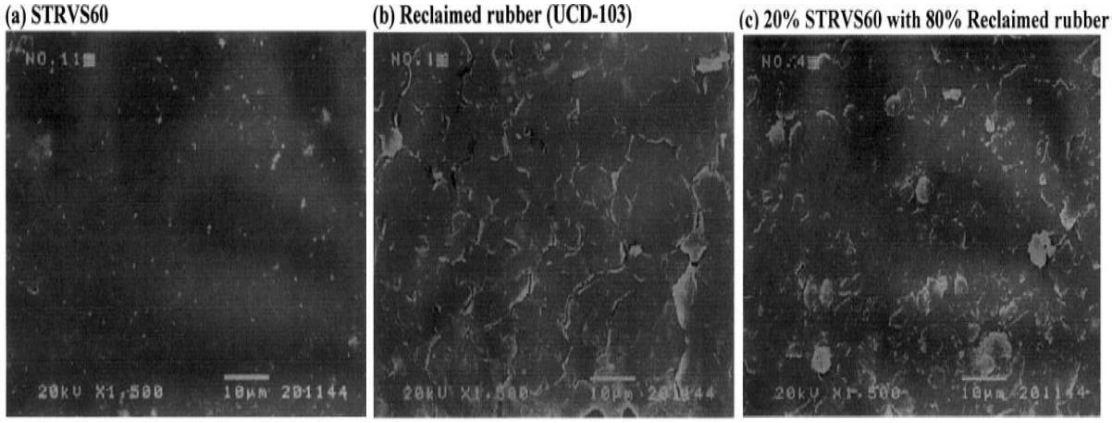

Figure 2.23 SEM micrographs of some rubber compounds related to Figure 2.22: (a) STRVS60, (b) RTR and (c) STRVS60/RTR (20/80). Adapted from reference [213].

Debapriya et al. [212] investigated the cure characteristics and tensile properties of NR-PBR compounds filled with different concentrations of tire rubber powders. They reported a tensile modulus increase with increasing rubber powders content due to the higher gel content and crosslink density of the highly filled (up to 60 wt.%) compounds (Figure 2.24). As reported earlier, increasing the filler content with higher crosslink density restricts the chain mobility, so a higher load is required for elongation increasing the modulus of the blends. Increasing the proportion of rubber powders also increases the presence of carbon black as an effective reinforcing filler, restricting the mobility of the

rubber chains under tension; i.e. a higher modulus results [172]. The incorporation of rubber powders into virgin rubber affects the homogeneity of the rubber compounds, which can be corroborated from SEM micrographs. Increasing the RTR loading increased the number of crack paths and holes, and samples show less homogeneity, making the compounds more vulnerable under mechanical stress. As shown in Figure 2.25, increasing the RTR content from 20 to 60 wt.% decreased the blend homogeneity of NR-PBR/RTR blends, attributed to the poor filler distribution with higher crosslinked fraction (gel content) at 60 wt.% [212].

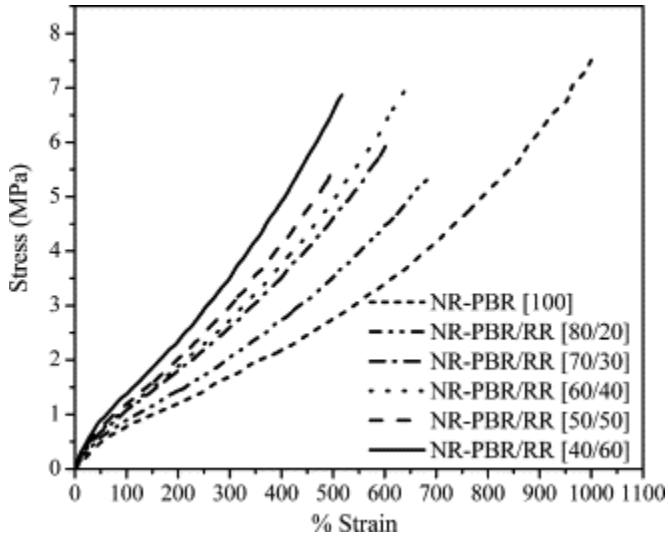

Figure 2.24 Stress-strain behavior of NR-PBR/RR blends. Adapted from reference [212].

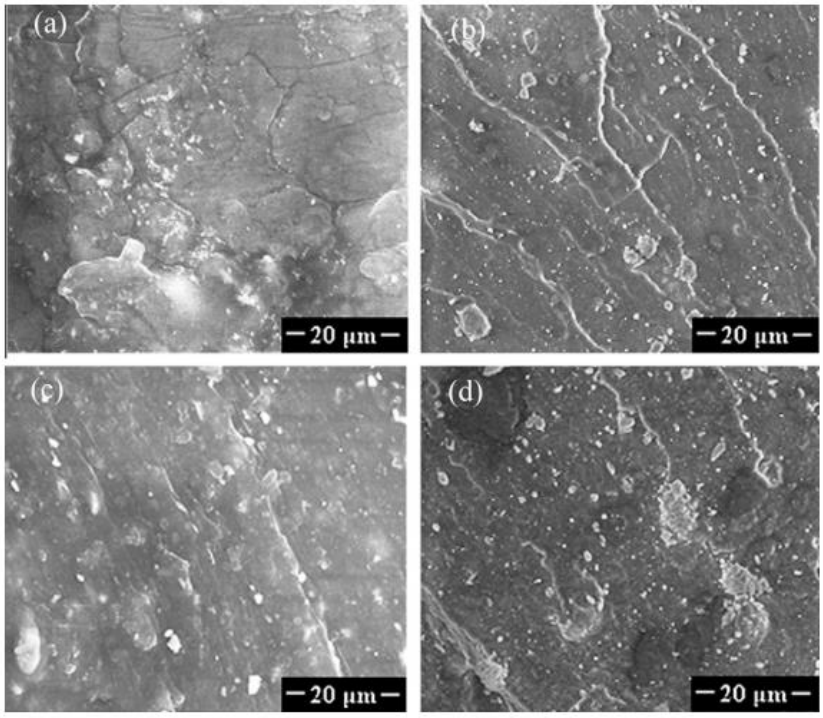

Figure 2.25 Tensile fractured surface of the compounds of Figure 2.24: (a) NR-PBR (100), (b) NR-PBR/RTR (80/20), (c) NR-PBR/RTR (60/40) and (d) NR-PBR/RTR (40/60). Adapted from reference [212].

However, Sreeja et al. [207,208] reported an increasing trend of the tensile strength with RTR incorporation into NBR and SBR matrixes in contrast to the decreasing trend of the tensile strength of NR/RTR compounds [203]. The tensile strength of NBR and SBR samples increased from 1.8 MPa and 1.9 MPa to 6.3 MPa and 5.1 MPa respectively, with the addition of 80 parts RTR [207,208]. But increasing the RTR loading led to a tensile strength drop for NR/RTR compounds, indicating a higher degradation level (scission of rubber chain) of RTR in the regeneration process [203]. Also, the difference between the tensile strength of NBR and SBR compounds compared to NR compounds containing RTR can be attributed to the non-crystallizing nature of the NBR and SBR, leading to poor strength. The tensile strength of NBR and SBR might be related to the presence of reinforcing fillers in the RTR, producing a higher dilution effect of the NR matrix than a reinforcement one. The EB increased with increasing RTR content, which is attributed to a plasticization effect caused by the presence of the processing oil in RTR [207,208]. As shown in Figure 2.26, the elongation at break of NBR/RTR and SBR/RTR compounds increased from 278% and 304% at 0 parts, to 506% and 629% at 80 parts of RTR, respectively [207,208].

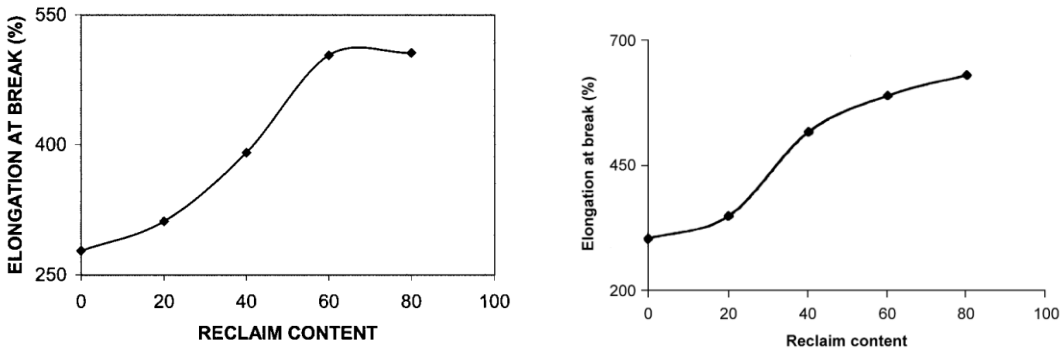

Figure 2.26 Elongation at break as a function of reclaim rubber content for NBR (left) and SBR (right) compounds. Adapted from references [207,208].

The presence of reinforcing filler in GTR enhances the energy dissipation and deviation of tear path, resulting in higher intrinsic strength. The reinforcing fillers can alter the crack path by resisting or delaying the crack growth to stabilize or even improve the tear strength of blends containing GTR. As shown in Figure 2.27, the incorporation of GTR into a SBR matrix led to the deviation of uniform pattern spacing and deflection of unidirectional crack path [210].

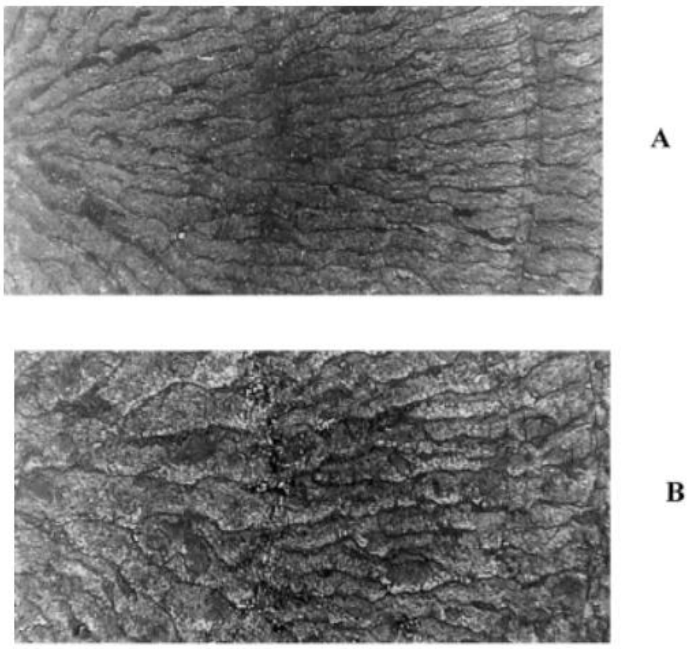

Figure 2.27 Abrasion pattern of SBR samples (normal load = 25 N): (A) without GTR, (B) with GTR (particle size = 420-600 µm; content = 30 phr). Adapted from reference [210].

Han et al. [210] reported on the abrasion resistance improvement of NR/GTR compounds due to the presences of vulcanized GTR particles with higher modulus. However, the incorporation of RTR with a weaker surface and lower MW (shorter fragments and smaller chains) led to the deterioration of the

abrasion resistance [204,216]. Rattanasom et al. [216] studied the effect of conventional vulcanization (CV) and efficient vulcanization (EV) on NR/RTR compound properties using sulfur (S):N-tert-butyl-2-benzothiazolesulfenamide (TBBS) ratios of 1.75:0.75 and 0.75:1.75 for CV and EV systems. The addition of 10 phr RTR resulted in 100 mm^3 and 90 mm^3 volume loss of CV and EV vulcanizates respectively, which are inversely proportional to the abrasion resistance. So higher abrasion resistance of NR/RTR compounds was obtained by CV systems through vulcanization of the RTR surface with the virgin NR matrix. Since the crosslink density, hardness and modulus all influence the abrasion resistance, a CV process increasing the crosslink density should also increase the hardness and modulus, leading to better abrasion resistance. As CV results in the formation of crosslink bridges between shorter fragments from the RTR surface and the NR matrix, longer chain length for effective stress transfer to the continuous matrix is obtained.

The effect of GTR particle size on the mechanical properties of the final compounds has been reviewed in different publications [1,5]. Han et al. [210] studied the effect of four different GTR particle sizes (30-40, 60-80, 100-120 and 170-200 mesh) on the mechanical properties of SBR/GTR compounds. As shown in Figure 2.28, the tensile strength of SBR compounds containing 30 phr GTR decreased from 240 to 160 kg/cm^2 with an increase in GTR particle size from 100 to 500 μm (140 to 35 mesh). The incorporation of smaller GTR particles with higher specific surface area and uniform dispersion resulted in strong bonding and good stress transfer, leading to higher tensile properties.

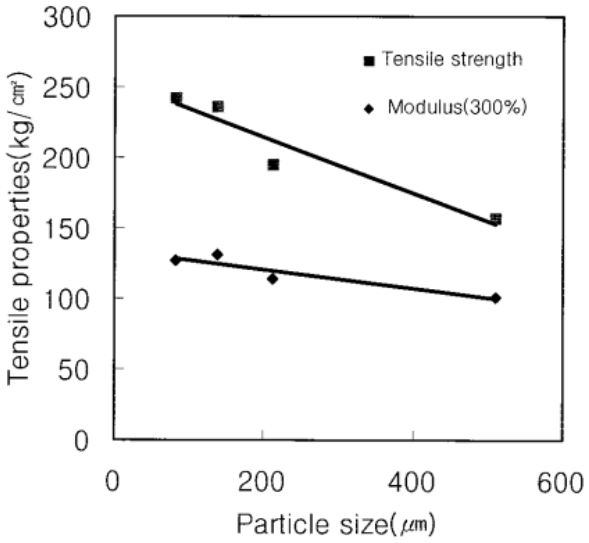

Figure 2.28 Tensile properties of SBR/GTR compounds as a function of GTR particle sizes at 30 phr. Adapted from reference [210].

But the effect of using smaller particles on tensile properties becomes negligible at high GTR/RTR content (above 50 wt.%) since the interfacial adhesion, rubber particles agglomeration and void formation at the interface between GTR/RTR and rubber matrix are controlling the mechanical strength of highly filled compounds [1].

In general, RTR shows higher TS and EB than GTR. Zhang et al. [215] reported a 69% (23.2 MPa from 13.7 MPa) and 47% (612% from 416%) improvement of TS and EB respectively, in NR/RTR compounds compared to NR/GTR compounds (10 wt.%). Partial regeneration of the RTR led to better tensile properties as a result of improved interfacial bonding between the RTR and the NR matrix. As schematically shown in Figure 2.29, the sol fraction of RTR is responsible for co-crosslinking with the NR matrix to form a strong interphase, leading to better stress transfer and mechanical properties.

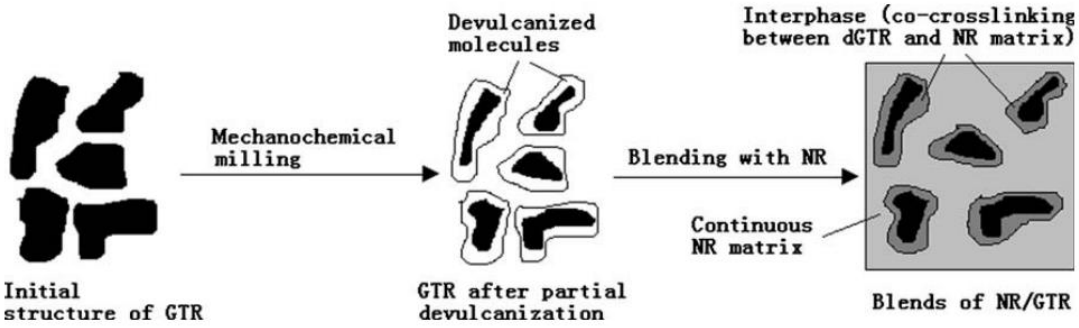

Figure 2.29 Schematic representation of the partial regeneration process and its effect on the morphology of rubber blends. Adapted from reference [215].

In another work, the incorporation of 20 wt.% RTR in SBR led to 10% and 12% improvement of TS and EB respectively, compared to the addition of the same concentration of GTR. SEM micrographs of the tensile fracture surfaces of the blends show poor interfacial adhesion of GTR to the SBR indicated by clear gap between both phases (Figure 2.30 a, b) [217]. On the other hand, no significant void between RTR and SBR can be seen due to better wettability of RTR associated with better compatibility and stronger interface, resulting in improved deformation and strength (Figure 2.30 c, d) [217]. Li et al. [218] reported similar observations about the positive effect of partially regenerated RTR particles on better compatibility and co-crosslinking at the interphase between RTR and virgin NR matrix, leading to improved TS and EB.

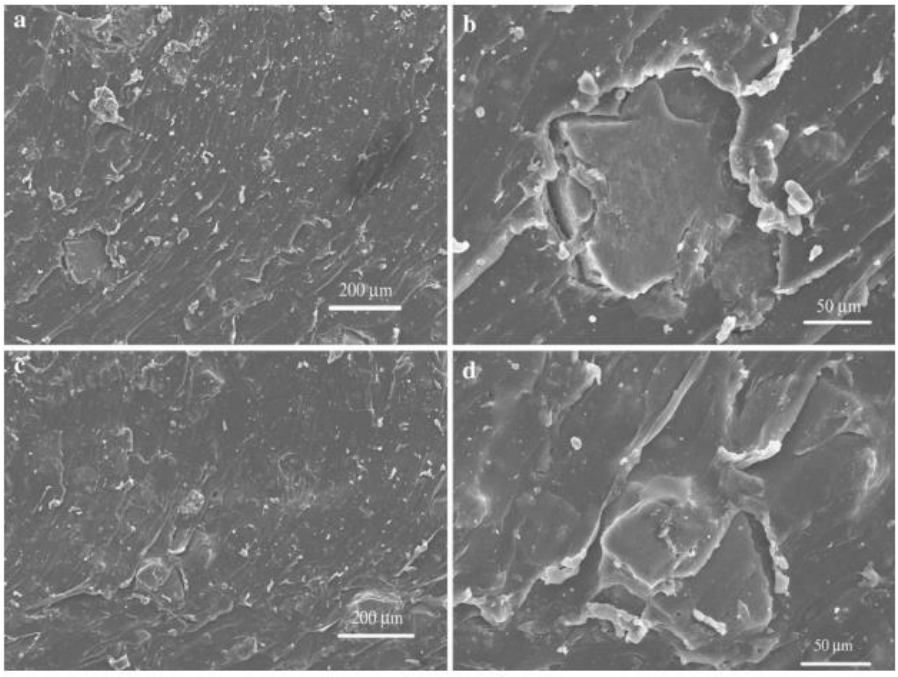

Figure 2.30 SEM micrographs of the tensile fracture surfaces of SBR compounds filled with GTR (a, b) or RTR (c, d) (30 phr). Adapted from reference [217].

In general, GTR is a vulcanized material with restricted chain mobility and weak interaction with polymer matrixes compared to RTR, which is a partially regenerated material that can form a good interphase, as well as allowing for co-crosslinking between RTR and matrix chains. Contrary to a 100% gel fraction for GTR, RTR benefits from the presence of a soluble fraction responsible for the interaction or bonding with the polymer matrix to improve interfacial adhesion, and hence the tensile strength and elongation at break of the final compounds. Also, regeneration results in lower crosslink density of RTR and lower MW (smaller fragments and shorter chains) compared to GTR, which correspond to lower modulus of RTR blends. The effect of GTR/RTR incorporation on the tensile properties of rubber compounds (mainly NR) is summarized in Figure 2.31.

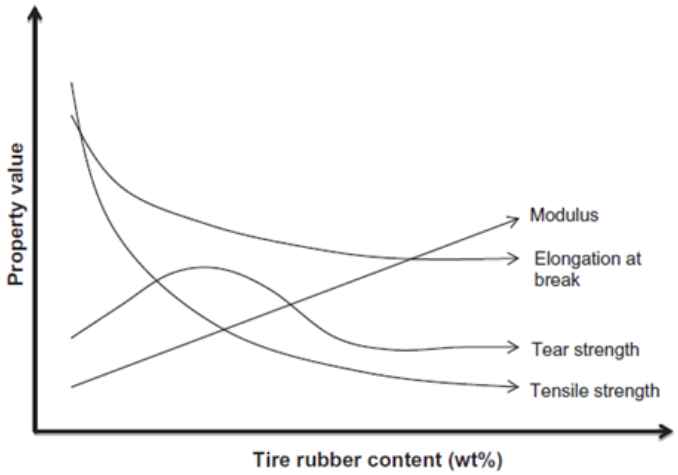

Figure 2.31 The effect of tire rubber content on the mechanical properties of rubber blends. Adapted from reference [1].

In general, the hardness of a rubber compound is influenced by the elastic modulus and crosslink density. This is why a difference is again expected between GTR and RTR. As shown in Figure 2.32, the incorporation of RTR increased the crosslink density (higher gel fraction) of rubber blends with increasing content, resulting in higher chain mobility restriction and blend rigidity. This is why the hardness values (Shore A) of NR/RTR compounds increased with RTR content [213].

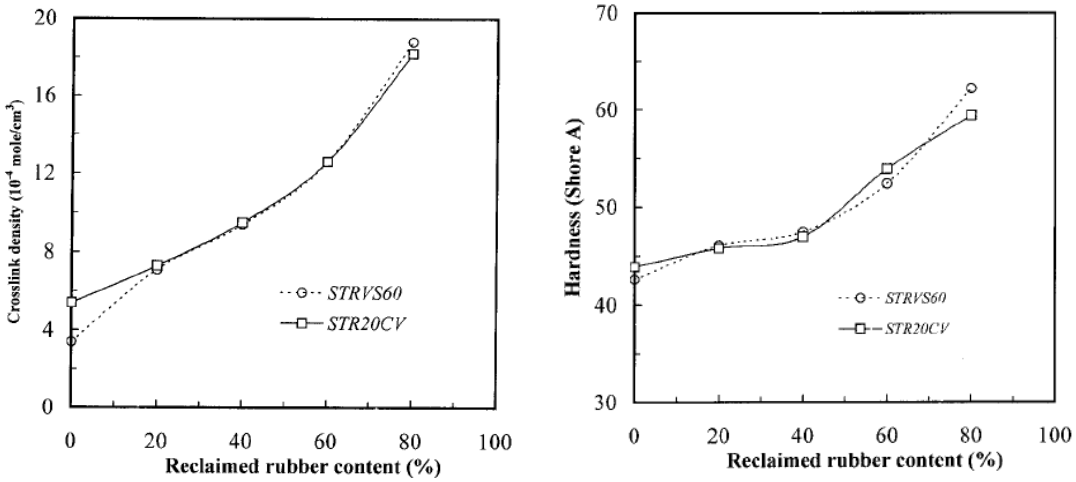

Figure 2.32 Crosslink density (left) and hardness (right) of NR/RTR compounds as a function of RTR content. Adapted from reference [213].

2.3.3.4 Aging properties

Waste tires are aged and degraded materials to different levels. This is why the investigation of the aging properties of GTR/RTR rubber compounds is very important. However, very few studies

investigated the effect of GTR/RTR on the aging behavior of rubber compounds. Debapriya et al. [212] reported an increase of the 200% moduli retention of NR-PBR/RTR with increasing RTR content from 20 to 60 phr after aging at 70 °C for 24, 48 and 72 h. The variation was attributed to increasing crosslink density and the formation of new crosslinks due to the presence of active sites in RTR (Figure 2.33). They also reported better aging resistance of RTR containing compounds compared to that of the virgin rubber. Better thermal aging behaviour of RTR is related to the hydrocarbon chains stabilization induced by the regeneration process through heating and mechanical shearing, as well as residual additives form the original processing. Therefore, anti-oxidant addition is not required for the production of rubber compounds due to the intrinsic aging properties of the RTR [54].

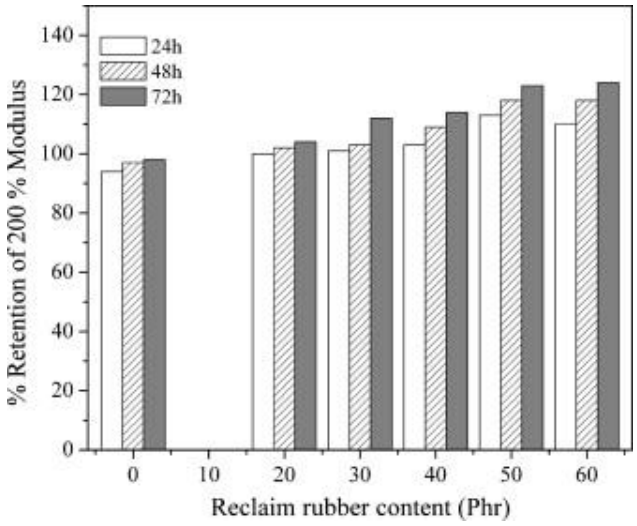

Figure 2.33 Effect of RTR content on the retention of the 200% modulus of NR-PBR/RR blends. Adapted from reference [212].

As shown in Table 2.5, Sreeja et al. [207] reported a 120% retention in tensile strength of NBR compared to that of cured NBR/RTR compounds, indicating that the state of cure (crosslink density) is increasing while ageing. The presence of RTR in the rubber blends led to some degradation since RTR was obtained from a NR source, which was more prone to degradation under elevated temperature and lower tensile strength of the filled compounds.

Table 2.5 Tensile strength of NBR/RTR compounds before and after aging. Adapted from reference [207].

	Tensile strength (MPa)		
Sample	Before aging	After aging	Retention (%)
NBR	1.8	2.2	120
NBR/RTR20	2.6	2.3	89
NBR/RTR40	2.6	2.5	92
NBR/RTR60	5.0	4.7	94
NBR/RTR80	6.3	5.7	91

2.3.3.5 Thermal properties

The thermal stability of rubber compounds is highly important with respect to waste tires addition into rubber formulations since the materials are already degraded, affecting the overall compounds thermal stability. The presence of volatile materials in GTR leads to lower thermal degradation onset temperature. However, increasing the GTR loading results in lower weight loss of the rubber compounds [1].

Debapriya et al. [219] reported improved thermal stability of SBR/RTR compounds with RTR incorporation as the char residue of SBR increased from 5.3% to 22.6% with the addition of 60 wt.% RTR in SBR/RTR (40/60) compounds. As shown in Figure 2.34, the initial weight loss of SBR under a N_2 atmosphere increased from 3.6% to 10% after the addition of 60 wt.% RTR, which was attributed to the volatilization of the processing oil associated with the regeneration process. The presence of RTR in NR produced two distinct peaks in the derivative thermogravimetry (DTG) curve, similar to NR/SBR blends [220].

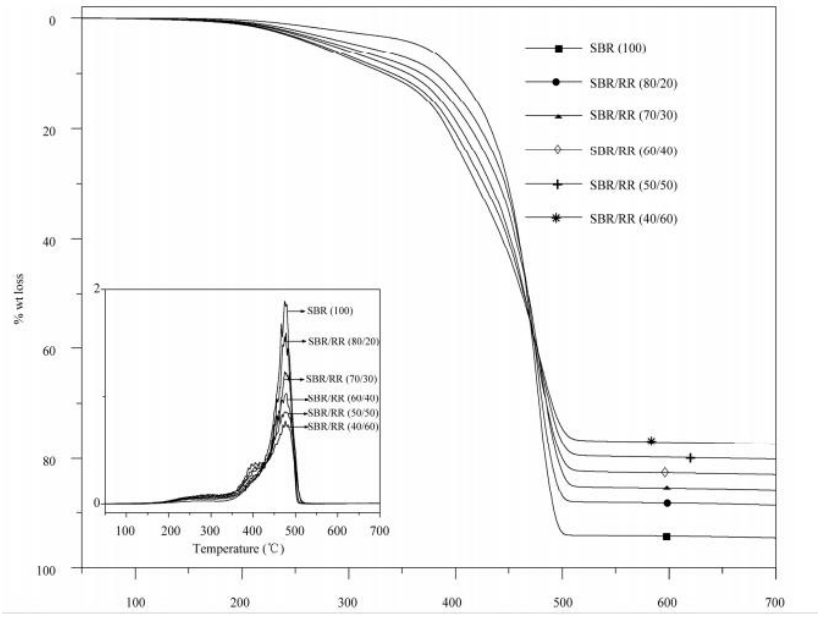

Figure 2.34 Thermogravimetric analysis (TGA/DTG) of SBR/RR compounds. Adapted from reference [219].

Cañavate et al. [169] evaluated the effect of GTR surface treatment on the thermal stability of NBR/NR/GTR compounds. The incorporation of GTR increased the residues at 600 °C of NBR/NR compounds from 15% to 30% with the addition of 50 phr GTR. GTR addition increased the crosslinking degree, resulting in better thermal stability, and also microwaves treatment led to a shift of the initial decomposition temperature ($T_{5\%}$) to higher temperatures, indicating increased thermal stability attributed to the regeneration that improved the crosslinking, in agreement with similar observations in SBR/GTR blends [221]. However, GTR exposure to microwave radiation above 5 min resulted in a thermal stability drop due to excessive treatment degrading the GTR main chains [169].

Xavier et al. [222] determined the stability of NR/GTR compounds using microwave treated GTR_{car} and GTR_{truck} (Figure 2.35). As shown in Table 2.6, truck tires contain more NR and less carbon black than passenger car tires due to their specific requirements. The temperature for 5% weight loss ($T_{5\%}$) of NR/GTR_{car} compounds was higher than that of NR/GTR_{truck} compounds due to higher GTR_{car} thermal stability. In both cases, the incorporation of 50 phr GTR increased the char residues at 550 °C of NR from 26.6% to 30.8% and 29.4% for NR/GTR_{car} and NR/GTR_{truck} respectively, which was related to the presence of carbon black and SiO_2 in GTR. Despite reports on the positive effect of GTR regeneration on improving the thermal stability, negligible effect of the regeneration was reported on the thermal stability of NR/GTR compounds.

Table 2.6 Typical composition of passenger and truck tires. Adapted from reference [222].

Composition	Passenger car tire	Truck tire
Natural rubber	25%	35%
Synthetic rubber	32%	25%
Carbon black	33%	30%
SiO_2	5%	6%
Other additives (curing system, processing aids, etc.)	5%	4%

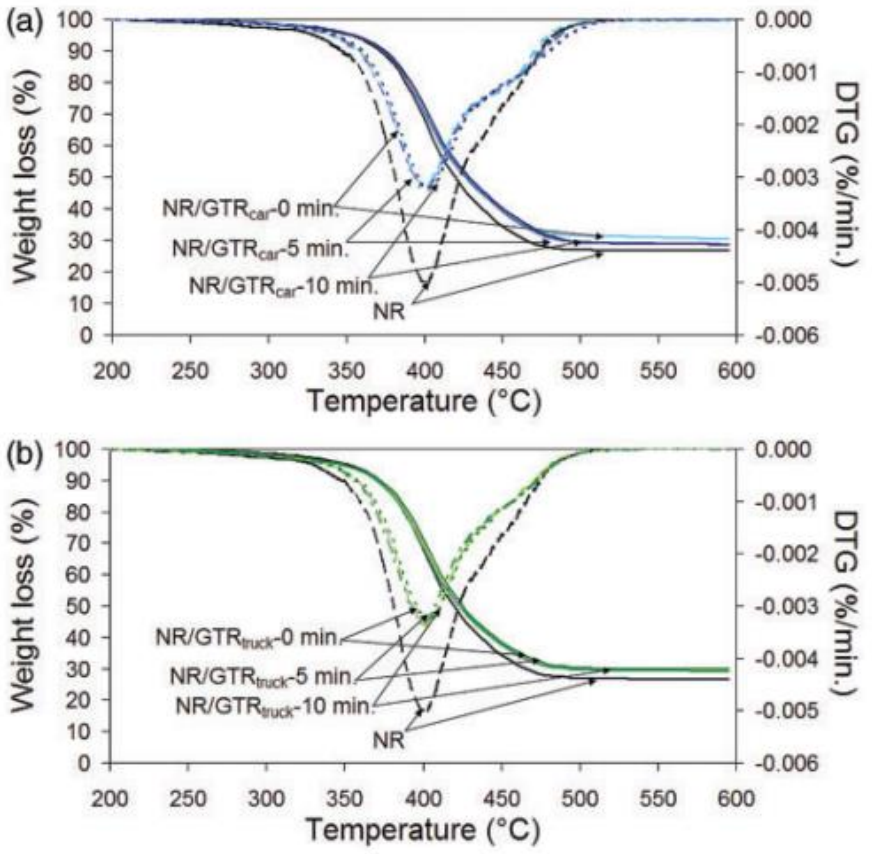

Figure 2.35 TGA and DTG curves of: (a) NR/GTR$_{car}$ and (b) NR/GTR$_{truck}$ samples (N_2 atmosphere and a heating rate of 20 °C/min). Adapted from reference [222].

Garcia et al. [132] reported that the improved thermal stability for RTR compounds can be related to the barrier effect of the carbon black, adsorbing low MW volatile products formed during the thermal degradation, hence improving the thermal stability. However, the preparation of NR/RTR compounds using an internal mixer and compression molding at elevated temperature (160 °C for 12 min) led to some RTR thermal degradation and the evaporation of low molecular weight volatile products. Also, using a compatibilizer such as MA increased the blend compatibility and interfacial bonding between GTR/RTR and virgin rubber matrixes resulting in higher thermal stability of the compounds. Medhat et

al. [159] reported that the addition of 5% MA can substantially increase the initial decomposition temperature of NR from 181 to 237 °C for NR/RTR/MA (30/70/5).

2.3.3.6 Dynamic mechanical properties

Dynamic mechanical analysis (DMA) can provide information about the loss modulus (E''), storage modulus (E') and damping factor (tan δ = E''/E') which are essential to understand the viscoelastic behaviour of rubber compounds. The loss and storage moduli are related to the maximum heat dissipation per unit deformation and the maximum energy that can be stored in a period of time reflecting the degree of elasticity/rigidity (crosslinking density), respectively. The value of tan δ is an indication of the ability of a rubber compounds to absorb and diffuse energy [119].

As reported before, increasing the GTR/RTR content in a rubber matrix leads to higher crosslink density and carbon black content, as well as further chain mobility restriction, leading to increased rigidity and storage modulus of the compounds. Li et al. [217] reported lower storage modulus for RTR/SBR than GTR/SBR, which was attributed to the lower crosslink density of RTR (named DGTR) (Figure 2.36).

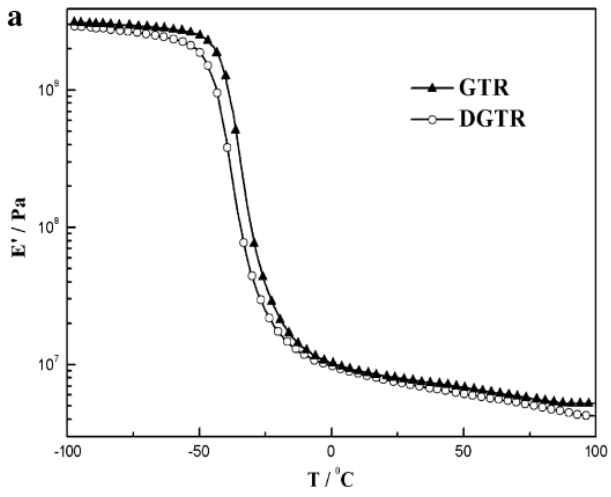

Figure 2.36 Storage modulus as a function of temperature for SBR/GTR and SBR/DGTR at 30 phr. Adapted from reference [217].

Also, the loss modulus of rubber compounds increases with increasing GTR/RTR content, indicating enhanced viscoelasticity of the compounds with higher filler content. The tan δ peak corresponds to the glass transition temperature (T_g), which is related to the mobility of pendant groups and molecular chains in the rubber. Similar to the effect of GTR loading on E' and E", the tan δ peak increases with increasing GTR content because of higher crosslink density and the presence of carbon black limiting

chain mobility. Lower intensity of the tan δ peak with increasing GTR content implies improved compounds elasticity. So, the molecular chain motion needs lower energy as it approaches the transition from a glassy to a rubbery state. Li et al. [217] reported higher elasticity of RTR compounds compared to GTR ones as determined by the lower peak height of the former.

2.3.3.7 Swelling properties

The swelling degree of rubber compounds represents the sorption and desorption behavior of a solvent, such as toluene or cyclohexane, to determine the crosslink density of the sample. The swelling degree (*Q*) of rubber compounds is measured at equilibrium in a solvent as:

$$Q = \frac{m_t - m_0}{m_0} \times 100\% \tag{2.3}$$

where m_t and m_0 are the mass of the swollen sample (g) and its initial mass (g), respectively. Also, the Flory-Rehner equation is used to evaluate the crosslink density as [184]:

$$-ln(1 - V_r) - V_r - \chi V_r^2 = 2V_s\eta_{swell}\left(V_r^{\frac{1}{3}} - \frac{2V_r}{f}\right) \tag{2.4}$$

where V_r and V_s are the rubber volume fraction in the swollen sample and the molar volume of the toluene (106.2 cm^3/mol), respectively. χ is the rubber-solvent interaction parameter, while η_{swell} is the crosslink density of the rubber (mol/cm^3) and f is the functionality of the crosslinks (f = 4 in sulphur curing systems). Equation (2.5) is used to determine the gel volume in the swollen phase:

$$V_r = \frac{\left(\frac{W_r}{d_r}\right)}{\left(\frac{W_s}{d_s}\right) + \left(\frac{W_r}{d_r}\right)} \tag{2.5}$$

where W_r and W_s are the weight of the dry rubber sample (g) and weight of the solvent absorbed by the sample (g), respectively, while d_s and d_r are the density of the solvent (g/cm^3) and the polymer (g/cm^3), respectively.

GTR is composed of the sol and gel fractions formed by free chains (uncrosslinked) and crosslinked chains, respectively. The swelling degree of a rubber compound indicates its state of cure [223]. So, the incorporation of GTR results in increased crosslink density of the compounds due to the presence of active crosslinking sites in the GTR to form further crosslinking during mixing. Kumnuantipa et al. [224] reported a fast increase of the toluene uptake in NR/RTR before reaching a plateau (equilibrium state).

Figure 2.37 shows that compounds filled with 80 wt.% RTR reached an equilibrium faster than less filled samples because they have the lowest toluene uptake. Other works reported similar results of higher GTR content needing less time for the rubber compounds to reach an equilibrium state while having lower swelling degree [225]. So, an inverse relation between the swelling degree and the crosslink density exists, as lower swelling degree implies higher crosslink density.

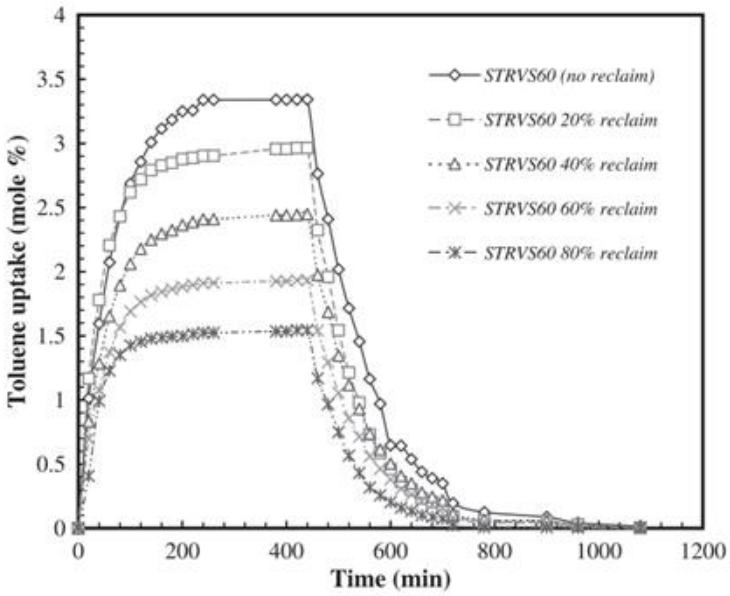

Figure 2.37 Effect of RTR content on the toluene sorption (25 °C) and desorption (70 °C) curves of RTR/NR(STRVS60) compounds. Adapted from reference [224].

Solvent penetration through vulcanized rubbers with high crosslink density and restricted chain mobility is very difficult. But swelling experiments must be performed until an equilibrium state is reached. Therefore, the swelling ratio does not depend on the kinetics of solvent molecules penetration, but on the length of chain segments between crosslink points; i.e. the amount of crosslink points per unit volume (crosslink density) and the polymer-solvent interaction parameter. Figure 2.38 presents a comparison between GTR and RTR on the swelling degree of NR compounds. It can be seen that RTR induces a higher swelling degree compared to GTR which is attributed to the lower crosslink density of the partially regenerated RTR [215].

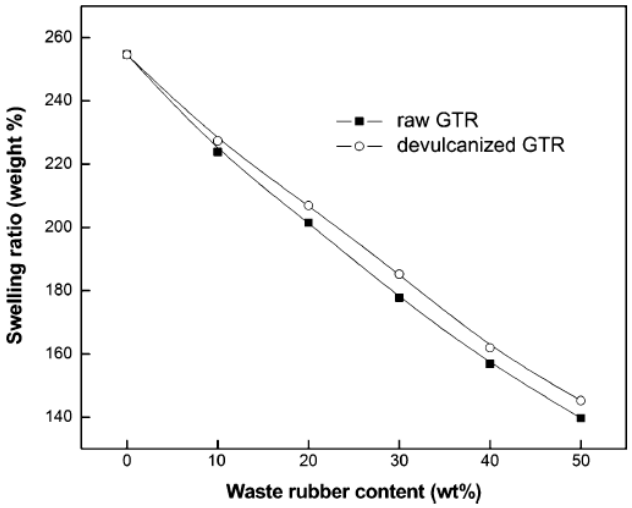

Figure 2.38 Effect of GTR and RTR content on the swelling ratio of NR compounds soaked in toluene at room temperature for 72 h. Adapted from reference [215].

Data analysis of the swelling curves can be used to determine the transport mechanism inside the rubber compounds. For example, the solvent mass absorbed (M_t) as a function of time (t) and the value at equilibrium (M_∞) can be related via [226]:

$$\frac{M_t}{M_\infty} = Kt^n \tag{2.6}$$

or

$$\log\left(\frac{M_t}{M_\infty}\right) = \log K + n\log t \tag{2.7}$$

where the slope (n) and intercept (K) are obtained by linear regression. The value of K is a constant associated to rubber/solvent interaction, while the value of n is an indication of the solvent diffusion mode through the rubber blends, which is normally between 0.5 and 1 [226]. A value of n = 0.5 indicates a Fickian mode of transport where the diffusion coefficients are functions of concentration alone. When n = 1, the mechanism is non-Fickian, Case II (relaxation controlled) transport, while a value between 0.5 and 1 represents an anomalous transport behaviour. The values of n and K for rubber vulcanizates can be obtained from a plot of $\log(Q_t/Q_\infty)$ against $\log(t)$ [227].

Kumnuantip et al. [224] reported that K increases with increasing RTR content in NR/RTR compounds because of higher rubber/solvent interaction associated to the increased crosslink density with RTR addition (Table 2.7). But increased interaction can lead to more contacts between the rubber and solvent and faster time to equilibrium. So, less possibilities are provided for the solvent molecules to

penetrate the rubber structure decreasing its swelling. The *n* values slightly decreased with increasing RTR content, attributed to a more restricted diffusion of the solvent into the rubber matrix, resulting in a lower degree of swelling.

Table 2.7 Values of n and K (Equation 2.6) for RTR/NR blends (compounding by a two-roll mill at 25 °C). Adapted from reference [224].

RTR content (%)	STRVS60		STR20CV	
	n	***K*×10^2 (g/g min^n)**	***n***	***K*×10^2 (g/g min^n)**
0	0.40	1.44	0.39	1.39
20	0.34	1.58	0.38	1.47
40	0.35	1.65	0.34	1.52
60	0.32	1.81	0.32	1.63
80	0.27	2.07	0.28	1.93

Finally, to provide the reader with a general overview of the current literature, Table 2.8 presents a list of the works performed on GTR/RTR containing rubber compounds. Based on the results summarized in Table 2.8, the development of GTR/RTR containing rubber compounds is a promising approach for waste tires recycling at a low cost and negligible environmental impact, as well for achieving good (comparable) properties with virgin rubber compounds.

Table 2.8 Effects of GTR/RTR treatment, composition, regeneration, and compounding on the properties of rubber compounds.

Compound	GTR/RTR content	Mixing	Results	Ref.
NR/RTR	RTR (25, 40, 50 and 60 phr)	NR regeneration by diallyl disulfide (DADS) at 60 °C for 35 min on an open two-roll mixing mill. Compounding in a laboratory size two-roll mill based on ASTM D 15-54T (1954).	Increasing RTR content resulted in decreased scorch time and optimum cure time. Addition of N-cyclohexylthiophthalimide as PVI increased the scorch time of NR/RTR (50/50) blend.	[211]
NBR/RTR	RTR (20, 40, 60 and 80 phr)	MA grafting on RTR at 150 °C in a Brabender Plasticorder at 30 rpm for 3 min. Blends preparation on a laboratory size two-roll mill based on ASTM D 3182.	MA modification of RTR led to longer cure time, scorch time and lower cure rate in all blends since anhydrides grafted on the RTR surface as cure retarders delay the onset of cure reaction resulting in higher cure times.	[206]
NR/PBR/RTR	RTR (20, 30, 40, 50 and 60 phr)	Regeneration of GRT by tetramethyl thiuram disulfide (TMTD) in the presence of spindle oil. Mixing of NR/PBR/RTR compounds for 15 min via laboratory size two-roll mill at room temperature.	Increase in minimum torque and Mooney viscosity of the compounds by RTR addition due to higher carbon black content resulting in higher stiffness and chain mobility restriction, as well as lower optimum cure time related to the presence of active crosslinking sites in RTR. Increase in tensile modulus with increasing RTR content attributed to the higher gel fraction and crosslink density of the compounds. Also, increase in 200% moduli retention of NR/PBR/RTR with increasing RTR loading after aging attributed to higher crosslink density and the formation of new crosslinks due to the presence of active sites in RTR.	[212]

NR/RTR	RTR (20, 40, 60 and 80 phr)	NR mastication on a laboratory two-roll mill for 10, 20 or 30 min followed by blending with RTR for 10 min at 25 °C.	Shear viscosity increased with RTR content but decreased with mastication time. Increase in tensile modulus with RTR loading due to the variation of crosslink density and chain mobility of RTR, as well as better blends homogeneity.	[213]
NBR/RTR	RTR (20, 40, 60 and 80 phr)	Compound mixing according to ASTM D 3182 on a two-roll laboratory size mixing mill.	Increasing trend of elongation at break with RTR incorporation attributed to a plasticization effect of the processing oil in RTR. Decrease in ageing resistance of the blends after RTR addition as it contains NR which is more prone to degradation during mixing.	[207]
SBR/GTR and SBR/RTR	GTR and RTR (10, 20, and 30) phr)	SBR mastication on a two-roll mill and blending with various contents of GTR or RTR for 10 min.	Microbial desulfurization of the GTR led to increased GTR sol fraction from 4.69-8.68%. Higher storage modulus and rigidity of SBR/GTR compounds than SBR/RTR compounds attributed to the higher crosslink density, carbon black content and chain mobility restriction of GTR. Higher elasticity of RTR compounds determined by the lower tan δ peak height of RTR. Also, better wettability of RTR due to more compatibility and good interfacial interactions between RTR and SBR.	[217]
NR/RTR NR/GTR	GTR and RTR (10, 30 and 50 phr)	GTR regeneration via a pan-mill type mechano-chemical reactor for 25 cycles. Blending with NR using a two-roll mill.	Lower scorch time and optimum cure time of NR/RTR blends compared to NR/GTR blends due to more unsaturated rubber in the RTR. Higher tensile strength and elongation at break of NR/RTR blends because of better compatibility and homogeneity of the blends. Also, RTR induced a higher degree of swelling compared to GTR attributed to the lower crosslink density of the partially regenerated RTR.	[215]

NR/GTR	GTR (50 phr)	GTR_{car} and GTR_{truck} were exposed to microwave irradiation for 0-10 min. Preparation of NR/GTR blends at 70 °C using an internal batch mixer with rotational speed of 100 rpm.	Better thermal stability of NR/GTR_{car} than NR/GTR_{truck} attributed to the higher content of synthetic rubbers in GTR_{car} and also the evaporation of low MW volatile products formed during the thermal degradation of GTR. Improvement of tensile properties of modified GTR containing blends due to improved interfacial interaction confirmed by SEM images.	[222]
NBR/NR/GTR and NBR/NR/RTR	GTR (50 phr)	GTR regeneration in a microwave reactor for 3, 5 and 10 min with a power of 700 W. Blends preparation at 70 °C using an internal batch mixer with a rotational speed of 100 rpm. The curing system was based on by zinc oxide (ZnO), stearic acid, TBBS, TMTD and sulphur.	Microwave modification of GTR enhanced the tensile properties due to good interaction between the RTR and the matrix. GTR microwaves treatment resulted in an improvement of the crosslinking and hence better thermal stability of the blends after revulcanization, but microwave radiation for more than 5 min led to the degradation of the GTR main chains.	[169]
SBR/RTR	RTR (20, 30, 40, 50 and 60 phr)	GRT regeneration by TMTD in the presence of spindle oil in an open two-roll mill. Mixing of fresh SBR and RTR on an open two-roll mill at room temperature for 15 min.	Increase in minimum torque and Mooney viscosity of the SBR/RTR compounds with increasing RTR content, while the scorch time remained unchanged. RTR addition led to increase in tensile strength by about 19% for 20 parts filler and 115% for 60 parts RTR in compounds. Enhanced thermal stability of SBR/RTR compounds with RTR incorporation as char residue of SBR increased from 5.3% to 22.6% with the addition of 60 parts RTR.	[219]

NBR/GTR	GTR (5, 10, 15 and 20 phr)	The plasma treatment modification of GTR was carried out before mixing with NBR for 2 min with a plasma discharge power in range of 30 to 80 W. NBR/GTR compounding was performed on a two-roll mill for 10 min.	The water contact angle of the modified GTR decreased from 116° to 0° after 10 s of irritation inducing a hydrophilic nature to the modified GTR. The TS and tear strength of NBR/GTR improved by 42% and 21% respectively, due to increased interfacial bonding between the plasma modified GTR (20 wt.%) and NBR matrix.	[130]
SBR/RTR	RTR (20, 40, 60 and 80 phr)	The SBR/RTR blends were prepared in a laboratory size two-roll mill and vulcanization was carried out at 150 °C and 180 kg/cm^2 using an electrically heated hydraulic press.	The tensile strength of SBR/RTR compounds increased from 1.9 MPa to 5.1 MPa with the addition of 80 parts RTR. Also, the elongation at break of SBR increased from 506% to 629% at 80 parts of RTR due to a plasticization effect caused by the presence of the processing oil in RTR.	[208]
NR/RTR	RTR (20, 40, 60 and 80 phr))	NR masticating was performed on a laboratory two-roll mill for 10 min followed by the addition of RTR and further mastication for 2 min. NR compounding with RTR was performed on a two-roll mill for 8 min at 25 °C.	The swelling degree of the compounds at the equilibrium state decreased with RTR content due to the increased crosslink density and the polymer–solvent interaction. Also, increasing the RTR content led to a higher elastic behavior (reduced tan δ_{max}) and T_g attributed to the increase in crosslink density and the presence of carbon black in RTR.	[224]

NR/GTR and NR/RTR	GTR and RTR (0, 10, 20, 30 and 40 phr)	GTR surface regeneration was performed using a biological treatment by *Thiobacillus sp*. NR was masticated on a two-roll mill and then blended with GTR or RTR for 10 min followed by vulcanization in a press at 15 MPa and 150 °C according to ASTM D 2084.	GTR regeneration resulted in 30% increase of oxygen content on the GTR surface and a reduction of the GTR contact angle from 120.5° to 93.5° (RTR) after regeneration. NR/RTR compounds showed better compatibility and co-crosslinking at the interphase between RTR and virgin NR leading to better tensile properties. Addition of 10 phr RTR in the compounds retained 91% and 92% of their original TS and EB, respectively.	[218]

2.4 Conclusion

Based on the current environmental situation and social acceptance, discarded tires should no longer be seen as a pollutant and useless waste material, but rather as a durable and inexpensive raw material for the production of different and innovative parts. The incorporation of even a small fraction of waste tires into polymer matrixes (thermosets, thermoplastics, and rubbers) can lead to a substantial consumption of discarded tires as a partial replacement of virgin raw materials with advantages such cost reduction and sustainable compound production.

Waste tires can be finely shredded to obtain GTR particles with higher specific surface area to improve the interaction with the corresponding matrixes. GTR particle size and surface topography depend on the residence time/number of cycles and temperature of the grinding process, such as ambient, wet, or cryogenic methods. In general, GTR particles obtained from an ambient grinding process have higher surface roughness and higher specific surface area, promoting better bonding with polymer matrixes. But the GTR particles are incompatible with most polymer matrixes due to a lack of sufficient chain mobility and interaction with the corresponding matrix, limiting the use of high GTR concentrations (above 50 wt.%). To address this issue and promote smooth stress transfer between the blend components, GTR surface modification (compatibilization) can be used to decrease the surface tension, suppress droplet coalescence, and obtain uniform GTR dispersion in the polymer matrix. Physical surface treatment was developed to increase the surface roughness and wetting properties by introducing polar (oxygen) functional groups on the GTR surface to better interact with polar polymers. Chemical surface modification can also be applied to improve the blend compatibility

through in situ generation of a compatibilizer during mixing or by the addition of block/graft co-polymers and nanoparticles to modify the interface. Moreover, GTR regeneration is extensively used to partially breakdown the crosslinked structure of vulcanized waste tires to increase the chain mobility (molecular freedom) of GTR for better interaction with the polymer matrix molecules. It can be concluded that a regeneration process can produce a partially vulcanized rubber (RTR) with lower crosslink density and more chain mobility, as well as physico-chemical properties similar to that of a virgin rubber depending on the regeneration process.

The addition of GTR/RTR in rubber matrixes results in changes of the curing, rheological, mechanical, aging, thermal, dynamic mechanical, and swelling properties of rubber compounds. The introduction of RTR into a rubber formulation results in improved flowability and less agglomerates in the rubber matrix compared to GTR addition, hence decreasing the compound viscosity and the minimum torque, leading to better processability. Considering the mechanical properties, increasing the GTR concentration in compounds decreases the tensile strength and elongation at break because of higher gel fractions acting as stress concentrating points. Since waste tires are aged recycled materials exposed to severe conditions (chemical, mechanical, physical, and thermal degradation) during their lifetime and recycling processes, the tensile strength of the compounds changes after ageing. The thermal stability of the compounds filled with GTR/RTR is still an active research area requiring more attention. The addition of GTR/RTR results in enhanced thermal stability of the rubber compounds due to the barrier effect of carbon black in waste tires formulation. Based on dynamic mechanical analysis, the rigidity and storage modulus of the compounds increase with GTR/RTR loading. It should be mentioned that regeneration leads to a lower storage modulus of RTR/rubber compounds compared to that of GTR/rubber ones, attributed to the lower crosslink density of RTR. The swelling behavior of the rubber compounds is directly related to the degree of crosslinking. It is concluded that RTR particles show higher swelling degree compared to that of GTR particles, attributed to the lower crosslink density of partially regenerated RTR particles, and to the presence of less active sites for crosslinking during mixing. Therefore, higher free volume is available for the solvent molecules to enter and diffuse.

It is expected that in the near future, material recycling in general, and waste tires in particular, will attract more attention for research projects and government investments as a promising approach to improve the circular economy and sustainability of rubber tires.

Depletion of natural resources like virgin/natural rubber consumed by the tire industries is expected to accelerate the research efforts and industrial dedication towards waste tires recycling for potential applications in artificial reef, erosion control, breakwaters, floatation devices, mats, playground surfaces and athletic tracks. As stated earlier, waste tires (GTR and RTR) can be used as a source of valuable raw materials in different polymeric matrixes for the manufacture of low-cost products and a cleaner environment. But a complete understanding of the phenomena involved in bond break-up mechanisms and the interaction at the interphase of GTR/RTR and virgin rubber are critical steps to control the processing conditions and optimize the final compounds properties. In the near future, more research should be directed on improving the interfacial interaction between all the components. Also, GTR surface modification and compounding/mixing processes should be more environmentally friendly and cost effective following the concepts of green chemistry. Based on the review performed, there is a clear lack of literature about mixing GTR/RTR with virgin rubber, especially for other matrixes than NR. This should be the focus for more research on the preparation and characterization of such rubber compounds.

Acknowledgement

The authors gratefully acknowledge the financial support of the Natural Sciences and Engineering Research Council of Canada (NSERC).

CHAPTER 3 MORPHOLOGICAL AND MECHANICAL PROPERTIES OF THERMOPLASTIC ELASTOMERS BASED ON RECYCLED HIGH-DENSITY POLYETHYLENE AND RECYCLED NATURAL RUBBER

Résumé

Dans ce travail, des élastomères thermoplastiques (TPE) sont produits en mélangeant à l'état fondu du polyéthylène haute densité recyclé (rHDPE) avec deux types de pneus hors-route (OTR) menant à de la poudrette de pneu (GTR). Le caoutchouc non régénéré (NRR) et le caoutchouc régénéré (RR) sont utilisés pour étudier l'effet de la concentration et de la régénération de GTR sur les propriétés du mélange contenant jusqu'à 90% en poids de GTR. La morphologie du mélange est étudiée par microscopie électronique à balayage (MEB) pour montrer une incompatibilité et une faible adhérence interfaciale entre le rHDPE et le GTR (NRR et RR), en particulier au-dessus de 40% en poids de RR. Ce comportement est attribué au processus de régénération GTR et à l'agglomération de particules RR avec une surface spécifique faible et une affinité inférieure pour le rHDPE par rapport au NRR. Dans tous les composés, les propriétés mécaniques de tension des mélanges RR étaient inférieures à celles des mélanges NRR, ce qui est attribué à la dégradation des chaînes de GTR abaissant le poids moléculaire (MW) pendant le processus de régénération. De plus, le NRR a un effet plus important sur l'amélioration de la résistance aux chocs en raison de sa structure réticulée plus élevée rendant les particules plus déformables/élastiques pour absorber l'énergie mécanique avant l'initiation des fissures. Les résultats expérimentaux montrent également que 80% en poids de GTR est la concentration optimale pour la production de TPE à faible coût et respectueux de l'environnement à base de matériaux recyclés.

Mots-clés: Pneu usé, élastomère thermoplastique, régénération de caoutchouc, polyéthylène haute densité recyclé

Abstract

In this work, thermoplastic elastomers (TPE) are produced by melt mixing of recycled high-density polyethylene (rHDPE) with two types of off-the-road (OTR) ground tire rubber (GTR). Non-regenerated rubber (NRR) and regenerated rubber (RR) are used to investigate the effect of GTR concentration and regeneration on properties of blends containing up to 90 wt.% GTR. The blend morphology is studied by scanning electron microscopy (SEM) to show incompatibility and low interfacial adhesion between rHDPE and GTR (NRR and RR), especially above 40 wt.% RR. This behavior is attributed to the GTR regeneration process and agglomeration of RR particles with lower surface area and affinity toward rHDPE compared with NRR. In all the compounds, the mechanical properties in tension of RR blends were lower than for NRR blends, which is attributed to the degradation of the GTR backbone chains, lowering the molecular weight (MW) during the regeneration process. Also, NRR has a more important effect on impact strength improvement due to its more crosslinked structure, making the particles more deformable/elastic to absorb the mechanical energy before crack initiation. The experimental results also show that 80 wt.% GTR is the optimum concentration for the production of low cost and eco-friendly TPE based on recycled materials.

Keywords: Waste tire, thermoplastic elastomer, rubber regeneration, recycled high-density polyethylene

3.1 Introduction

Vulcanized rubbers are extensively used in the tire industries since these thermoset materials show dimensional stability even under severe mechanical and thermal conditions, without changes in their properties over a wide range of temperature. However, disposal of waste tires is a significant environmental issue, since the crosslinked structure of vulcanized rubber cannot be remelted and reprocessed. Also, the presence of different additives such as stabilizers, antioxidants and antiozonants in tire formulation make them resistant to biodegradation, photochemical decomposition, chemical reagents and thermal degradation [6,54]. According to Sienkiewicz et al. [3], the annual global production of tires is about 1.5 billion units, leading to 17 million tonnes of scrapped tires discarded all around the world every year. To date, various efforts have been made to use end-of-life (EOF) tires by reclamation [228,229], devulcanization [230,231], energy recovery [50,232], pyrolysis [51,233] and recycling [12,30]. Shredding (particle size reduction) waste tires to use in different rubber or plastics applications is categorized as rubber recycling to produce artificial reef, playground equipment, highway crash barrier, asphalt mix and floatation devices [5].

Waste tire rubbers are appropriate fillers to be melt blended with thermoplastics, thermosets, and virgin rubbers. Thermoplastic elastomers (TPE) have gained significant attention due to the low amount of virgin plastics needed to produce inexpensive compounds. TPE are rubber-like materials showing properties similar to vulcanized rubbers, while being processed in a molten state as thermoplastic polymers [9]. Thermoplastic elastomeric olefins (TPO) are blends of olefinic thermoplastics and recycled rubber particles, and benefit from the excellent processing characteristics of polyolefins and the elastic properties of rubbers. Different olefinic thermoplastics have been used in TPO production such as polypropylene (PP) [234,235], low density polyethylene (LDPE) [236], linear low density polyethylene (LLDPE) [237], and high density polyethylene (HDPE) [65]. TPE compounds need to show at least 100% elongation at break [22]. However, poor entanglement between the crosslinked chains of rubber molecules and thermoplastic molecules limit molecular interaction and strong bonding [1]. This is why reclamation, regeneration or devulcanization are widely used for rubber modification to partially break down the crosslinked structure by cleavage of S–S and C–S bonds (devulcanization) and sometimes scission of C–C bonds (reclaiming) of the rubber backbone chains. In general, devulcanized and reclaimed rubber particles are known as regenerated rubber (RR) particles.

Shi et al. [195] studied the effect of the reclaiming process on the rubber properties by changing the temperature, shear stress and atmosphere. According to their results, the reclaimed rubbers consisted of a sol fraction and a crosslinked gel fraction in which good interaction between the soluble fraction and polymer matrix led to strong interfacial adhesion. The soluble fraction needs to have a high molecular weight (MW) to ensure its interaction with the polymer matrix, but it is difficult to get a high MW sol fraction because of the nonselective scission of the main chain and crosslink bonds [208].

Shaker and Rodrigue [129] studied ground tire rubber (GTR) regeneration of mechanical strength of LDPE/GTR blends produced by rotomolding. The mechanical properties (flexural and tensile moduli) of rotomolded samples decreased with increasing GTR (up to 50 wt.%) due to the lower rigidity of GTR particles compared to the LDPE matrix. The crosslinked network of GTR restricts the processability of vulcanized rubber, while break down this network resulting in further processing of RR. Minimum torque (M_{min}) can be used to determine the effect of GTR regeneration on processability or flowability of RR containing compounds. RR particles show better processability than non-regenerated (NRR) GTR, which is attributed to the presence of 10-15% processing oil, decreasing the minimum torque, and producing higher chain mobility in RR particles compared to NRR ones. Li et al. [204] reported higher values of M_{min} for natural rubber (NR) compounds filled with 50 phr GTR (10 dN.m) compared to that of compounds filled with the same loading of regenerated waste tire rubber (6 dN.m), which indicates that the processing of GTR compounds becomes more difficult. The incorporation of GTR (NRR or RR) into thermoplastics changes the tensile strength and elongation at break due the presence of carbon black and gel fraction acting as stress concentration points, as well as restricting the molecular orientation and chain mobility, causing the blend to fail at lower stress and elongation [215,225]. Kakroodi and Rodrigue [12] reported that incorporation of GTR powder inside HDPE led to very low homogeneity and the elongation at break of GTR/HDPE (70/30) was only 64%, whereas increase in GTR reduced that value even more significantly. Also, Punnarak et al. [238] reported a 21% increase in impact strength with increasing RR content (up to 50 wt.%) in HDPE due to the ability of RR particles to absorb the impact energy.

It is more economic and eco-friendly to use recycled plastics in TPE since this decreases the amount of polymer waste and the final cost of the compounds [5]. HDPE has good mechanical properties, excellent processability and low cost, leading to its high availability and use as recycled polyolefins. But there is very limited work focusing on the melt blending of recycled high density polyethylene (rHDPE) with GTR. Wang et al. [30] produced TPE based on recycled polyethylene (rPE)/GTR and

reported a positive effect of adding 10 wt.% Engage 8180 as a compatibilizer to improve the elongation at break (76% increase). Unfortunately, there is no similar work studying the morphological and mechanical properties of TPE based on rHDPE and recycled NR. In particular, the aim of this work is to study the effect of GTR regeneration and concentration by using two different types of off-the-road (OTR) GTR (NRR and RR).

3.2 Experimental

3.2.1 Materials

GTR particles were provided by Phoenix Innovation Technologies (Montreal, QC, Canada) in two forms: NRR (average particle size of ~300 µm) and RR (average particle size of ~600 µm) with a density of 1.169 g/cm^3 and 1.246 g/cm^3, respectively. Post-consumer rHDPE was kindly provided by Gaudreau (Victoriaville, QC, Canada) as the matrix with a melt flow index (MFI) of 1.3 g/10 min (190 °C and 2.16 kg) according to ASTM D1238. The density (ASTM D2856) and melting point (ASTM D3418) of the rHDPE were 0.967 g/cm^3 and 129.5 °C, respectively.

3.2.2 Processing

The rubber particles and thermoplastic matrix were compounded in a Leistritz ZSE-27 twin-screw extruder with a L/D ratio of 40 and 10 heating zones. Figure 3.1 shows the extruder screw configuration design in which the numbers above the elements are used to mention the screw profile orders. Different concentrations of GTR particles were used to produce the compounds according to the formulation presented in Table 3.1. A flat temperature profile of 175 °C was used to prevent degradation since the initial decomposition temperature of the rubber (NRR and RR) is around 180 °C [129]. The screw was set at 100 rpm. The rHDPE pellets were fed to the extruder through the first zone (main feeder), while the GTR particles were fed via a side feeder (zone 4). The overall flow rate was 3 kg/h to prevent high motor torque and die pressure, especially at high rubber content (above 50 wt.%). The compounds were cooled in a water bath and then pelletized. Next, the compounds were dried at 70 °C for 6 h to eliminate any residual water. Finally, the compound were compression molded at 180 °C to prepare the samples. The compounds were preheated for 3 min and pressed for 5 min in molds with dimensions of 115x115x3 mm^3 under a load of 3 tons.

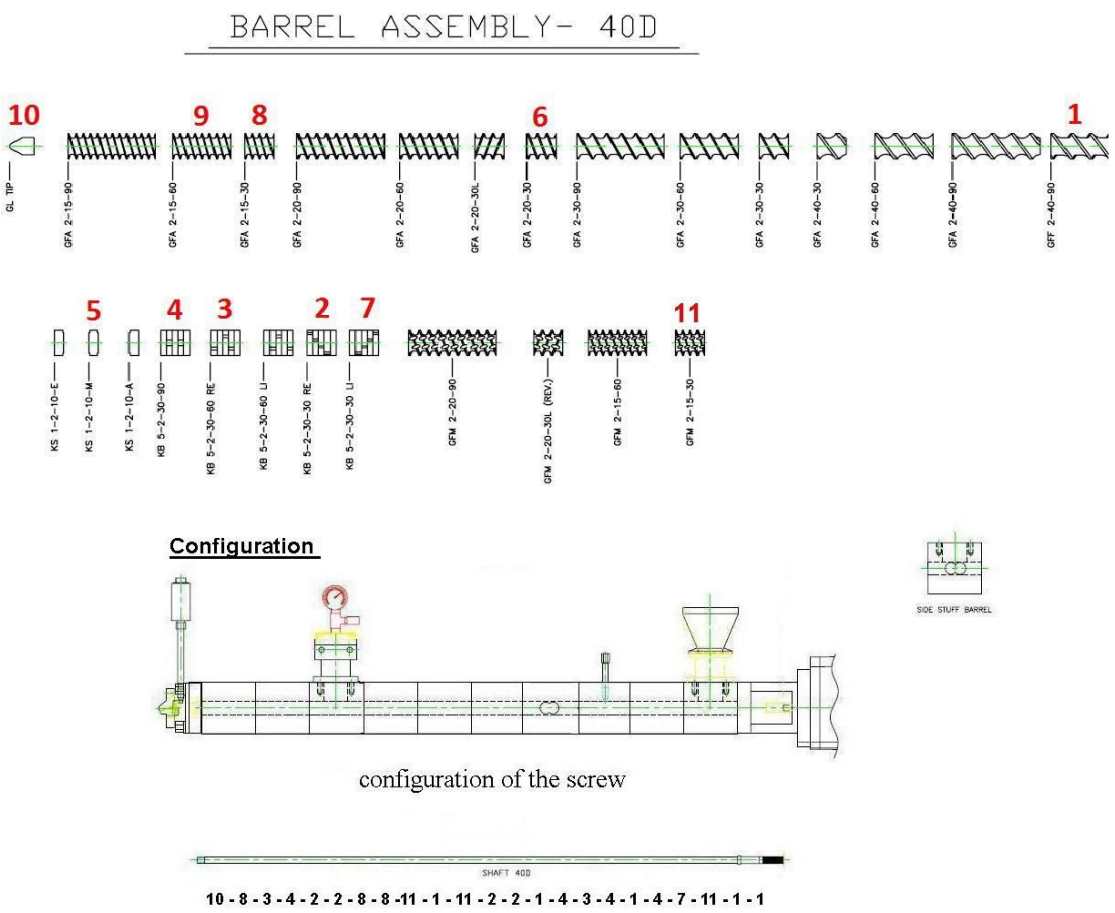

Figure 3.1 Screw configuration designs: ZSE-27 HP

Table 3.1 Coding and formulation of the samples produced.

Sample Code	rHDPE (wt.%)	NRR (wt.%)	RR (wt.%)
RHD	100	-	-
NR20	80	20	-
NR30	70	30	-
NR40	60	40	-
NR50	50	50	-
NR60	40	60	-
NR70	30	70	-
NR80	20	80	-
NR90	10	90	-
RR20	80	-	20
RR30	70	-	30
RR40	60	-	40
RR50	50	-	50
RR60	40	-	60
RR70	30	-	70
RR80	20	-	80
RR90	10	-	90

3.2.3 Characterization

3.2.3.1 MFI measurement

The melt flow index was determined at 190 °C and 2.16 kg according to ASTM D1238 and the average MFI values reported after based on three repetitions for each sample.

3.2.3.2 Morphological observation

An Inspect F50 scanning electron microscope (SEM) (FEI, Hillsboro, OR, USA) was used at 15 kV to take micrographs of the raw materials and observe the quality of the interfacial adhesion/dispersion in the blends. For the TPO, the samples were cryogenically fractured in liquid nitrogen. All the surfaces were coated with gold/palladium to be observed at different magnifications.

3.2.3.3 Mechanical testing

Tensile tests were conducted at room temperature according to ASTM D638 using a 500 N load cell and a 10 mm/min tensile speed on an Instron (Instron, Norwood, MA, USA) universal mechanical tester model 5565. At least 5 specimens (type V) with 3 mm thickness were used for each formulation. The

averaged values of tensile strength (σ_Y), Young's modulus (E) and elongation at break (ε_b) are reported with standard deviations.

Flexural tests were done on an Instron (Instron, Norwood, MA, USA) model 5565 with a 50 N load cell according to ASTM D790 at room temperature. Rectangular specimens with dimensions of 60x12.7 mm^2 were tested with 5 repetitions for each sample in a three-point bending mode (span length of 60 mm) at a speed of 2 mm/min.

Notched Charpy impact strength was measured on a Tinius Olsen (Horsham PA, USA) model 104 at room temperature according to ASTM D256. At least 10 specimens with dimensions of 60x12.7 mm^2 were used for each compound. Before testing, all the samples were automatically V-notched on a Dynisco (Franklin, MA, USA) model ASN 120m sample notcher 24 h before testing.

3.2.3.4 Physical properties

Density measurements were performed on a gas (nitrogen) pycnometer Ultrapyc 1200e (Quantachrome Instruments, Boynton Beach, FL, USA). The test was repeated three times for each sample. Hardness (Shore A and Shore D) was determined by a 307L model durometer (PTC Instruments, Boston, MA, USA) with 10 measurements for each sample.

3.3 Results and discussion

3.3.1 Processability

The processability and flowability of GTR play an important role in melt mixing with thermoplastics and has a significant effect on the performance and properties of TPE blends. As reported above, the main difficulty in using recycled waste tires is attributed to the crosslinked structure of the vulcanized GTR, which has limited molecular chain mobility and interaction with the other components. This is why regeneration processes were developed to partially break the crosslinks and improve processability. For a simple, fast, and cost-effective quantification, MFI is used as a measure of the material's fluidity (inverse of viscosity); i.e., the ability to flow under a specific pressure which depends on the components properties (particle size and MW) and their interactions. This is of high importance, especially for injection molding (parts molding).

The results in Table 3.2 show that NRR and RR blends have decreasing MFI values from 0.45 and 0.52 g/10 min to 0.03 and 0.04 g/10 min respectively, with increasing GTR content from 20 wt.% to 90

wt.%. Decreasing trend of MFI with GTR loading can be attributed to the crosslinked network of the vulcanized rubber which has limited molecular chain mobility and interaction with the other components. It is clear that the MFI reduction trend is more important above 40 wt.%. Higher MFI values of RR blends than NRR blends indicates higher chain mobility and more particle deformability in RR particles, resulting in more fluidity of RR blends. Also, the presence of some processing oil in the RR formulation can be responsible for the higher MFI (lower viscosity) of RR blends compared to NRR blends.

To get information of the blends processability, the pressure loss in the die (2.7 mm in diameter) with a L/D ratio of 40 and motor torque values were measured during the extrusion step. This information can also be directly related to the blend viscosity under the processing conditions (screw rotational speed and flow rate) [239].

According to the MFI results, increasing the GTR content increased the blend viscosity, leading to high motor torque since higher force is required to disperse the crosslinked GTR particles into the rHDPE matrix and push materials along the screws, as reported for GTR in PP [14]. Increasing the GTR content from 20 wt.% to 90 wt.% led to 34% (38 to 51 Nm) and 33% (36 to 48 Nm) increases in torque values for NRR and RR blends, respectively. Higher melt viscosity results in higher pressure loss across the die and higher pressure drop at the die exit [240]. For NRR and RR blends, the pressure increased from 280 and 180 psi to 1050 and 880 psi respectively, by increasing the GTR loading from 20 wt.% to 90 wt.%. Similar to MFI trends, more important increases are observed above 40 wt.% which can be associated to more interaction between the GTR particles.

Finally, RR blends seem to have better flowability (1.2 times higher MFI) and processability (6% lower motor torque and 27% lower die pressure) compared to NRR blends. This behavior can be related to two main reasons: (i) higher friction between more rigid NRR particles with small size and higher surface area compared with RR particles, and (ii) higher chain mobility and more particle deformability in RR particles. Also, the presence of some processing oil in the RR formulation can be responsible for the lower viscosity (higher MFI) of RR blends compared to NRR blends.

Table 3.2 Parameters related to the processability of the compounds produced.

Sample Code	MFI (±0.02 g/10 min)	Motor torque (±2 Nm)	Die pressure (±20 psi)
rHDPE	1.31	-	-
NR20	0.45	49	280
NR30	0.34	51	410
NR40	0.20	52	470
NR50	0.13	56	650
NR60	0.09	59	750
NR70	0.07	60	800
NR80	0.05	61	870
NR90	0.03	65	1050
RR20	0.52	46	180
RR30	0.39	47	240
RR40	0.23	50	350
RR50	0.17	52	480
RR60	0.11	54	530
RR70	0.08	55	600
RR80	0.06	58	700
RR90	0.04	61	880

3.3.2 Morphology

Figure 3.2 presents SEM images of the NRR and RR particles at different magnifications to determine the effect of the regeneration process on the GTR particles size and geometry. It can be seen that both types of rubber particles show a significant number of impurities related to their recycled origin. Different shapes of rubber particles like porosity or smooth angular surfaces with different sizes can be related to different types of tires or different grinding methods. Figure 3.2 B shows that the NRR particles have a more irregular surface, with cracks on their surface, compared to RR particles (Figure 3.2 D). As shown in Figure 3.2 C, the average particle size of RR particles is larger than NRR particles (Figure 3.2 A), mainly because of the use of a processing oil leading to possible particle swelling and agglomeration. Larger particle size is known to lower the specific surface area, limiting the GTR interaction with the thermoplastic matrix during melt mixing.

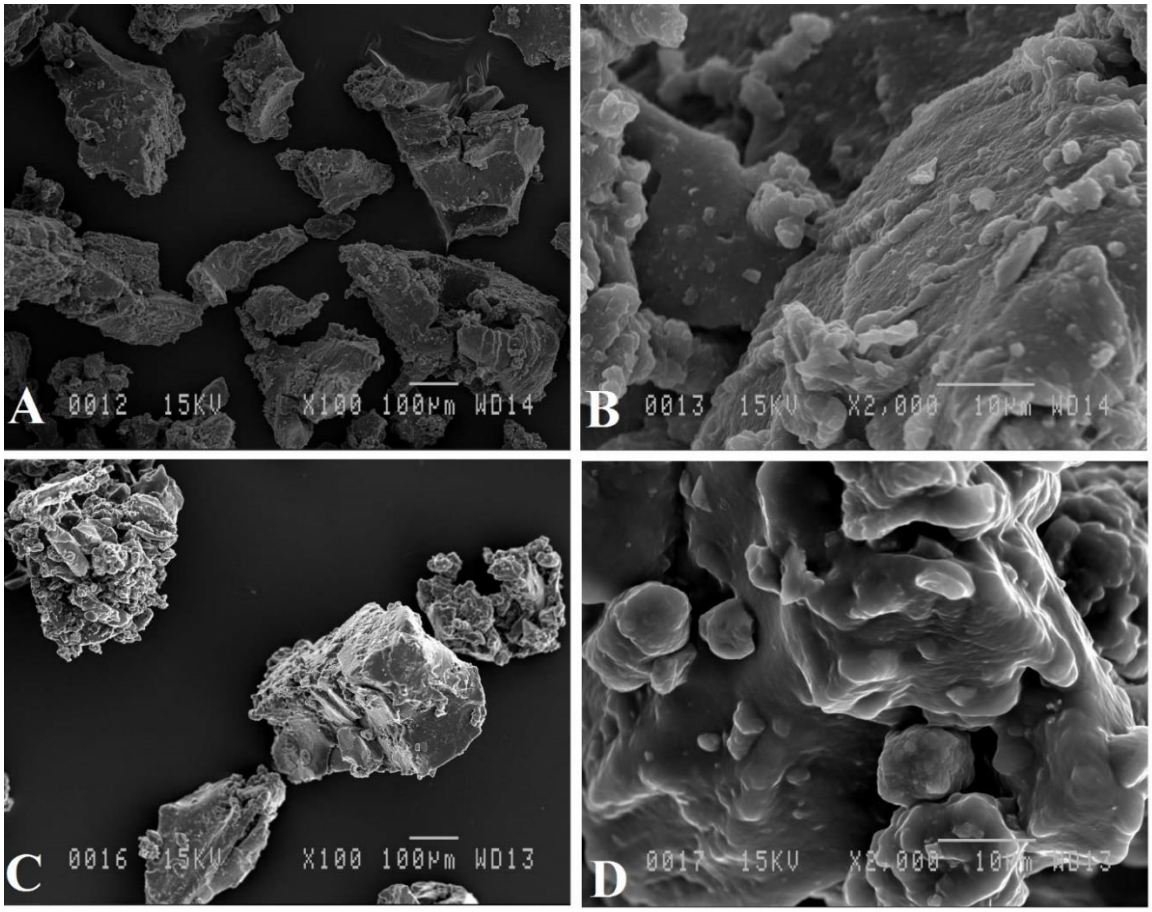

Figure 3.2 SEM images of NRR (A, B) and RR (C, D) particles at different magnification.

Also, SEM images were used to determine how the blend composition influenced the GTR dispersion state and the interfacial adhesion with the matrix. Figure 3.3 B shows a considerable increase in the domain size of the GTR dispersed phase at 40 wt.% RR, attributed to agglomerated RR particles and poor dispersion. Increasing the GTR content led to a clear distinction between both rubber particles and thermoplastic with interfacial gaps (Figure 3.3 D). In fact, clean surfaces of the particles are related to low adhesion between GTR and rHDPE due to their poor compatibility, which is more evident in RR blends. These clean interfaces also lead to limited stress transfer from rHDPE to GTR, so failure occurs

at the interface. It is known that good compatibility leads to failure initiation in the continuous phase instead of the interface, generating higher mechanical properties [12].

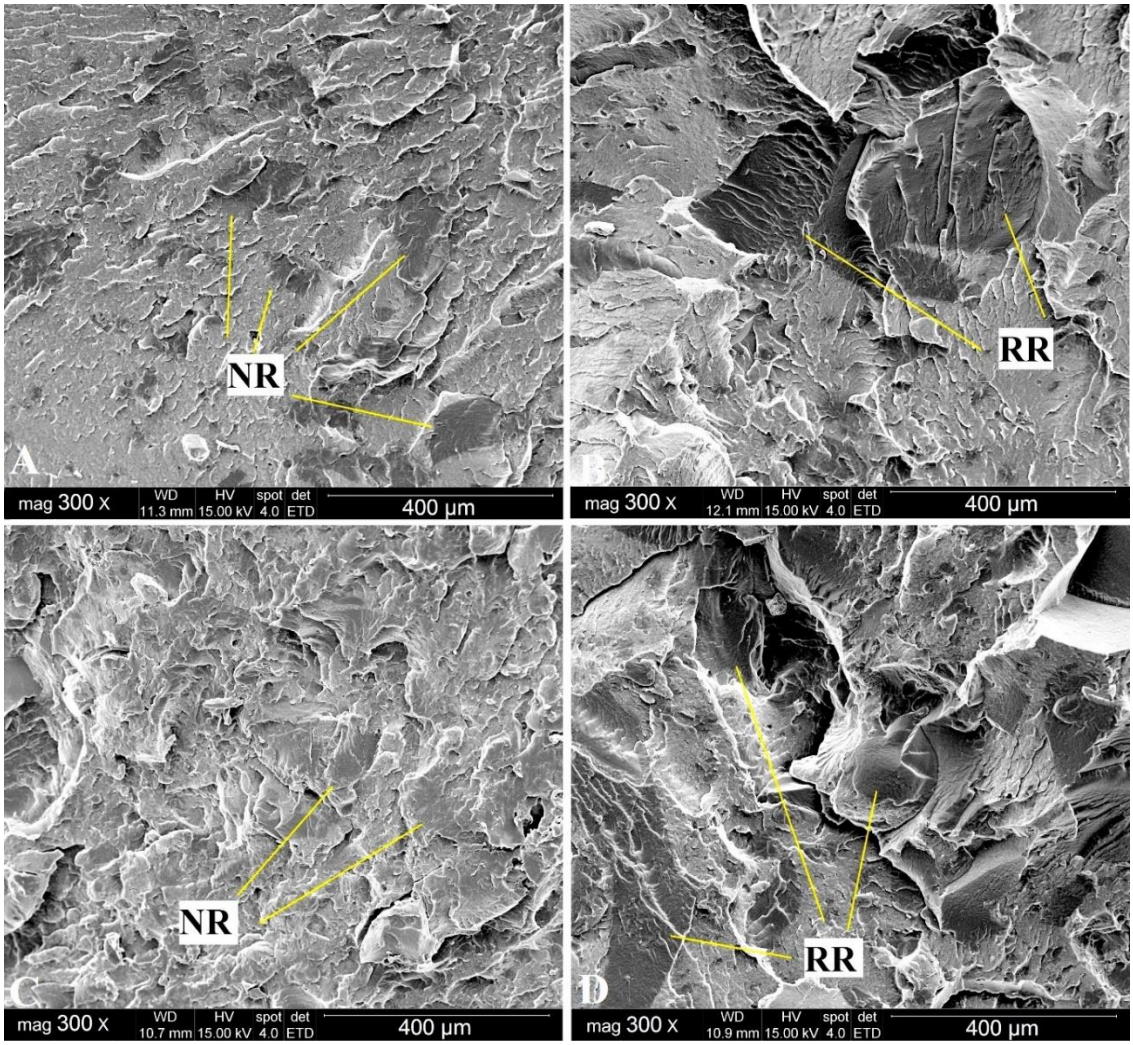

Figure 3.3 SEM images of NR40 (A), RR40 (B), NR50 (C), and RR50 (D) blends.

The effect of GTR content and regeneration on the morphology of highly filled blends is illustrated in Figure 3.4. Figure 3.4 A shows that the addition of 80 wt.% NRR produced a more homogeneous structure than samples containing RR particles (Figure 3.4 C), but the GTR particles can still be distinguished in the compounds. The addition of 80 wt.% GTR leads to poor rubber dispersion and the presence of cracks/defects on the fractured surface due to the high surface energy between the GTR and rHDPE phases. However, NR80 (Figure 3.4 B) presents a more textured fractured surface compared to RR80 (Figure 3.4 D). This indicates better interaction and bonding with the polymer matrix, so, higher energy was required to produce a failure. According to morphological observations, the large domain size of RR samples indicates an incomplete dispersion/agglomerated state, resulting in poor

stress transfer associated to the smooth surface fracture. This behavior is related to the weak interfacial adhesion of both phases, which is expected to control the mechanical properties, as described later.

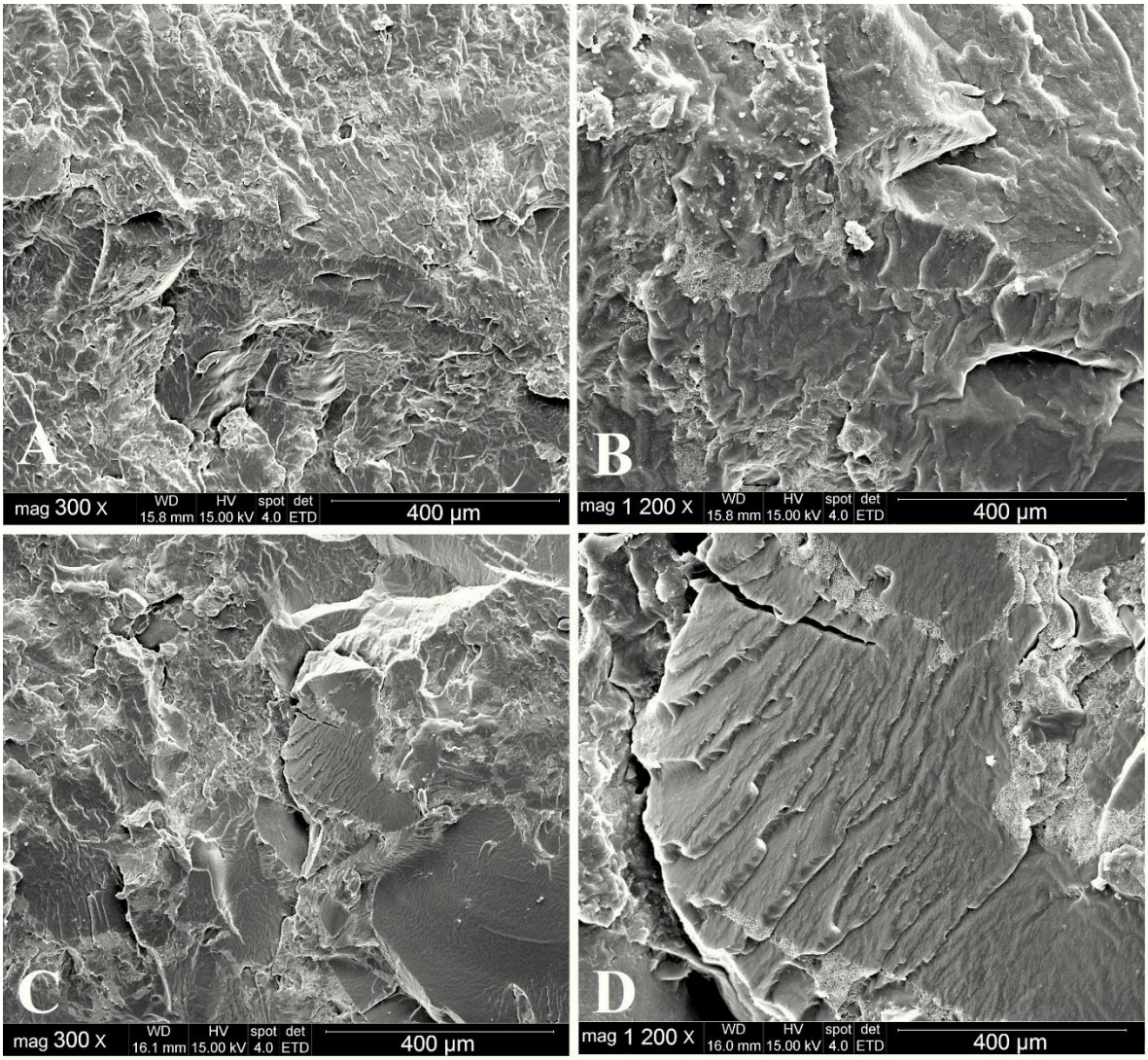

Figure 3.4 SEM images of NR80 (A, B) and RR80 (C, D) blends at different magnifications.

3.3.3 Mechanical properties

3.3.3.1 Tensile properties

The mechanical properties of the TPE are always expected to be much lower than those of the thermoplastic matrix. As shown in Figure 3.5, the tensile strength decreased from 21.3 MPa for rHDPE, to 8.5 and 8.9 MPa with 40 wt.% NRR and RR, respectively. Further increase in GTR content produced a significant drop of the tensile strength. For example, increasing the GTR content from 40 to 80 wt.% led to a tensile strength decrease from 8.5 to 3.1 MPa (64%) for NRR blends and a drop from 8.9 to

2.1 MPa (76%) in RR blends. This behavior is related to the low interfacial interaction and the low modulus of the rubber particles compared to rHDPE.

The Young's modulus is reported in Figure 3.6. As expected, similar trends as the tensile strength was obtained in which the Young's modulus decreased with increasing GTR content. There are two critical contents here: 40 wt.% and 80 wt.% GTR. For example, increasing the NRR content from 40 to 50 wt.% decreased the Young's modulus by 26% (from 122.1 to 90.7 MPa), while increasing it from 80 to 90 wt.% decreased the Young's modulus by 76% (from 14.2 to 3.4 MPa). On the other hand, increasing the RR content from 40 to 50 wt.% decreased the Young's modulus by 38% (from 120 to 74.8 MPa), while increasing it from 80 to 90 wt.% led to a 88% decrease (from 16.4 to 2.0 MPa).

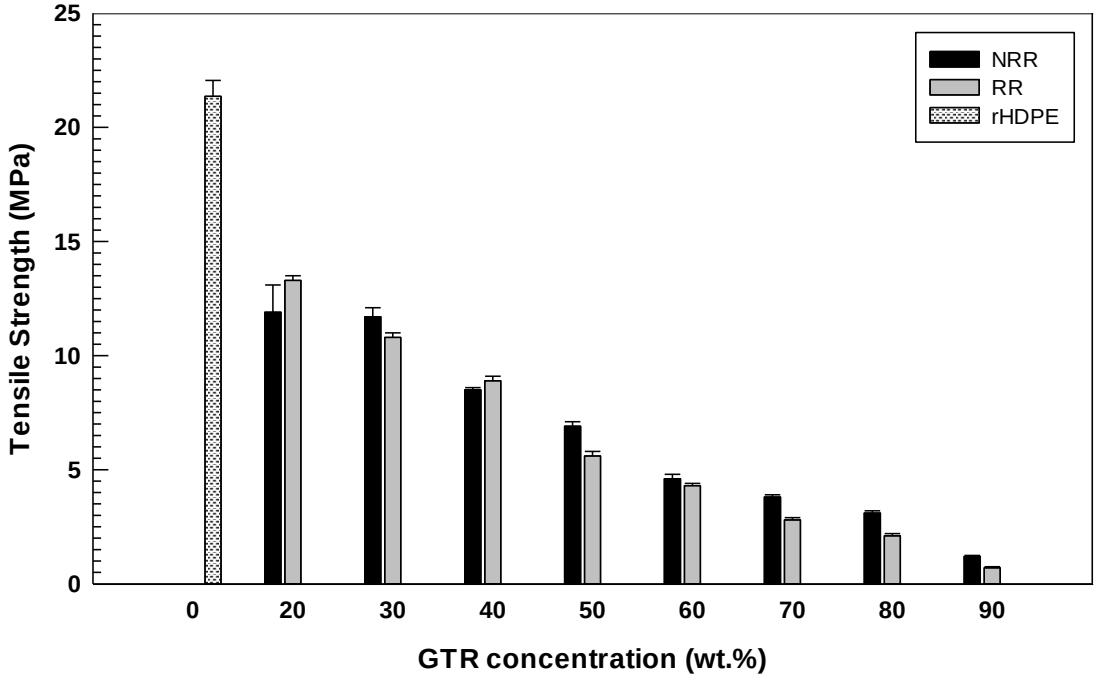

Figure 3.5 Tensile strength of NRR and RR blends.

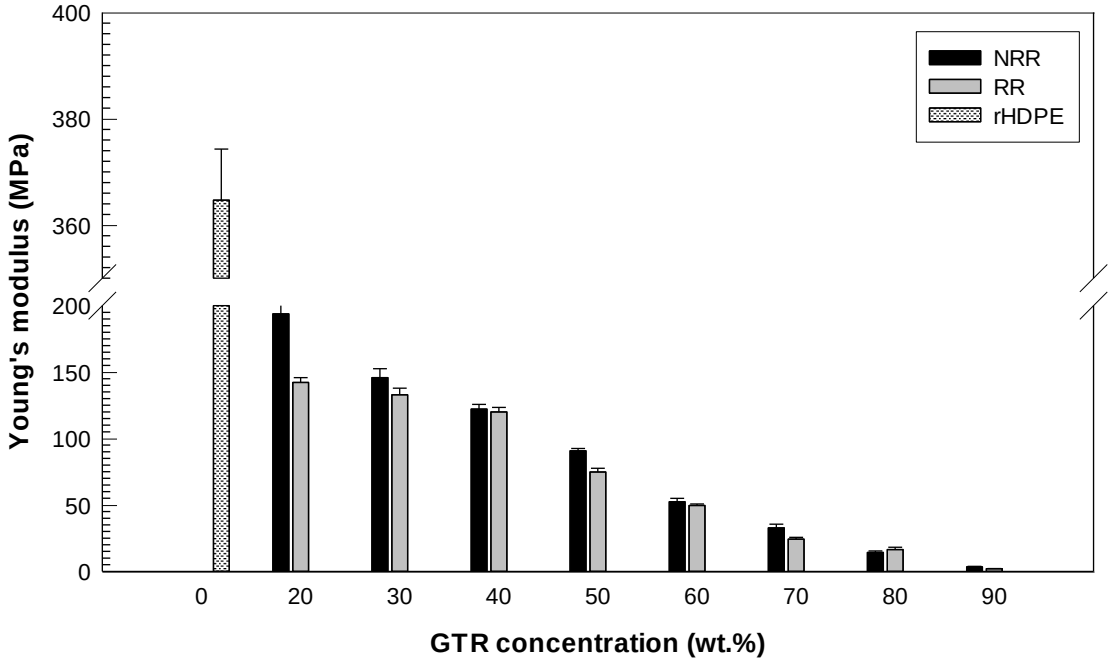

Figure 3.6 Young's modulus of NRR and RR blends.

The elongation at break is the most significant property controlled by the TPE homogeneity and phase compatibility. Figure 3.7 shows that the elongation at break of the TPE increased with NRR and RR content, but the values are much lower than that of the neat matrix (1060%). It should be mentioned that rHDPE and GTR particles, both as nonpolar materials containing a high amount of contamination, led to low compatibility (immiscible blends), as well as forming stress concentration points acting as crack initiation points. The addition of 20-40 wt.% GTR did not show significant changes in the elongation at break. However, increasing the GTR content from 40 to 80 wt.% led to higher elongation at break due to the presence of a more elastic content. But further GTR addition decreased the elongation at break from 127% (NR80) to 119% (NR90). This behavior can be related to inhomogeneity in the blends and insufficient bonding between the NRR particles and rHDPE. On the other hand, RR90 showed higher elongation at break compared with RR80 blend due to the softening effect of the regenerating oil inducing higher deformation/elasticity of the compounds. Good TPE are required to have an elongation at break of at least 100% [22]. So melt mixing of 80 wt.% NRR with 20 wt.% rHDPE was able to satisfy this criterion with 127%. Ismail et al. [14] reported the positive effect of smaller GTR particles to improve the elongation at break of TPE. The improvement observed in NRR blends can

also be related to their smaller size compared to RR particles, leading to better interaction (more surface area) with rHDPE chains.

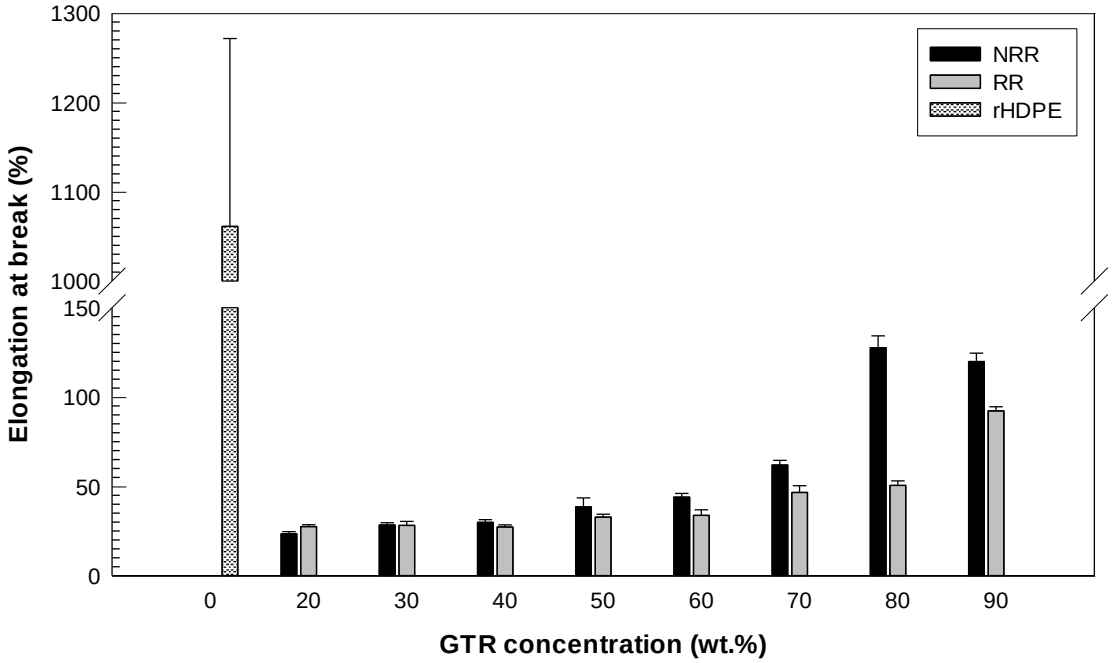

Figure 3.7 Elongation at break of NRR and RR blends.

The tensile results of Figure 3.5, Figure 3.6, and Figure 3.7, as well as the processing parameters (Table 3.2), indicate that 80 wt.% seems to be a critical GTR concentration for these compounds as a balance between homogeneity, elasticity and processability is obtained.

The results of flexural modulus are presented in Figure 3.8. As expected, a decreasing trend is observed with increasing GTR content as reported for the Young's modulus (Figure 3.6). This behavior is related to the soft nature of GTR, which is as a low modulus phase and, to the presence of interfacial voids/defects. For example, increasing the GTR content from 20 to 80 wt.% deceased the flexural modulus of both NRR and RR blends by 92% (from 221 to 19.5 MPa) and 91% (from 191.8 to 18.8 MPa), respectively. NRR blends show higher flexural modulus than RR blends up to 80 wt.% GTR attributed to restricted chain mobility caused by the three-dimensional (3D) crosslink network of NRR particles (more rigid structure).

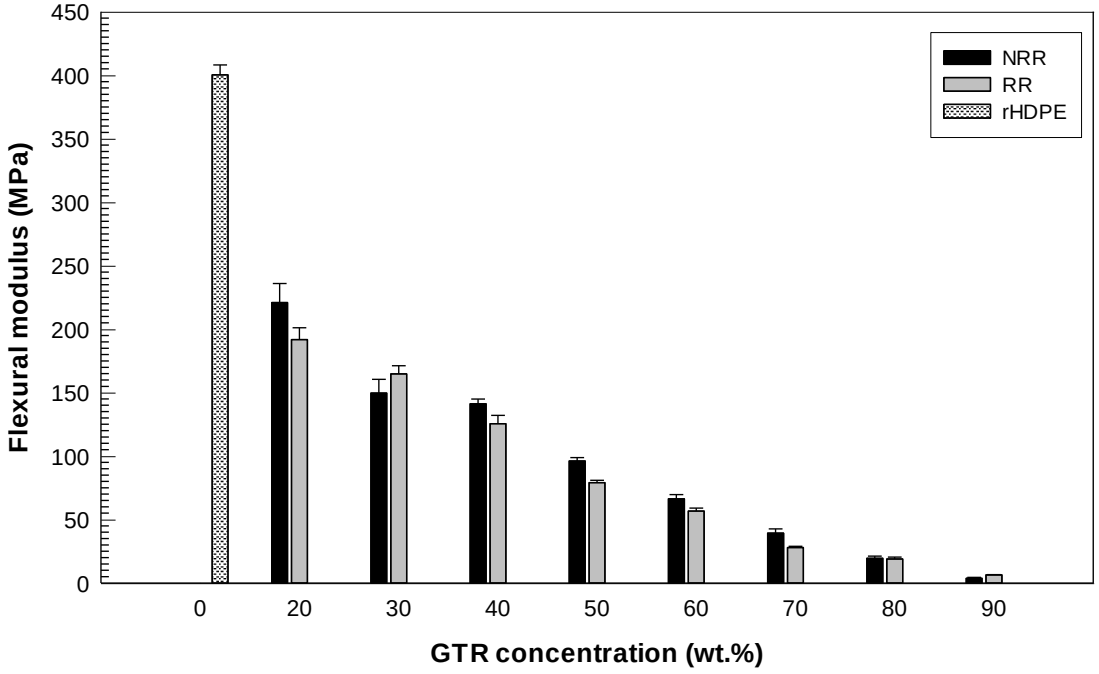

Figure 3.8 Flexural modulus of NRR and RR blends.

3.3.3.2 Impact strength

As shown in Figure 3.9, increasing the GTR content increased the impact strength of both NRR and RR blends up to 80 wt.% GTR, which implies a positive effect of GTR on the impact strength of these compounds based on rHDPE (360 J/m). At higher GTR content, the values are lower due to poor homogeneity of the sample, as reported in Figure 3.4. Also, the impact strength of NRR blends is higher than that of RR blends due to better adhesion at the interface between NRR and rHDPE (see Figure 3.3). This behavior can be related to the crosslinked structure of NRR, making the particles more deformable and able to absorb the energy before crack initiation. However, the regeneration process is expected to decrease the crosslink density of RR particles by partial break-up the 3D crosslinked structure, decreasing their ability to absorb the energy before crack initiation and propagation.

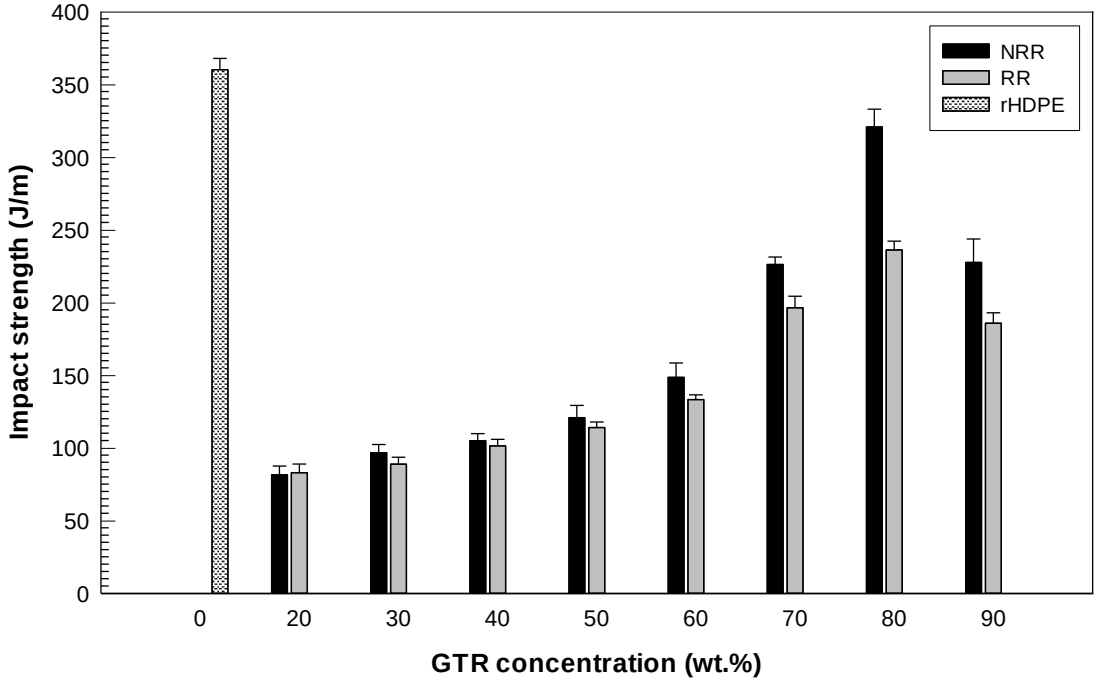

Figure 3.9 Impact strength of NRR and RR blends.

3.3.4 Physical properties

3.3.4.1 Hardness

Another important TPE property is hardness, which is affected by GTR content, as reported in Figure 3.10 for NRR and RR blends. As expected, Shore A and D values decreased with increasing GTR as an elastomeric component was added in the rigid matrix [241]. The higher hardness of NRR blends is in agreement with the tensile behavior of the blends (Figure 3.5), which might be related to better interfacial bonding between rHDPE and NRR particles with smaller size and higher surface area compared with RR particles. Also, higher crosslink density of NRR particles could induce more rigidity in NRR blends, leading to higher hardness compared to RR blends, and also could be related to the presence of processing oil, as a softening agent. For example, increasing the NRR content from 40 wt.% to 80 wt.% decreased the Shore A hardness by 6 points (from 95.5 to 89.0) and the Shore D by 16 points (55.1 to 38.7). On the other hand, increasing the RR content from 40 wt.% to 80 wt.% decreased the Shore A hardness by 9 points (from 95.7 to 87.9) and the Shore D by 21 points (56.4 to 35.2). Once again, significant drops are observed above 80 wt.% for all the systems investigated.

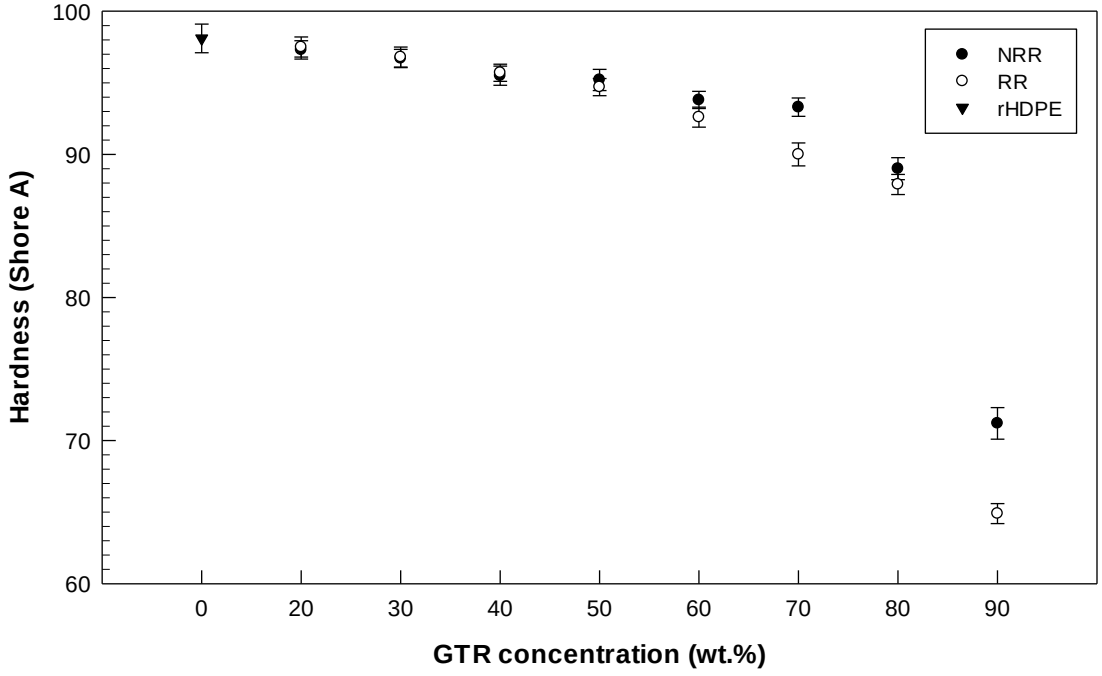

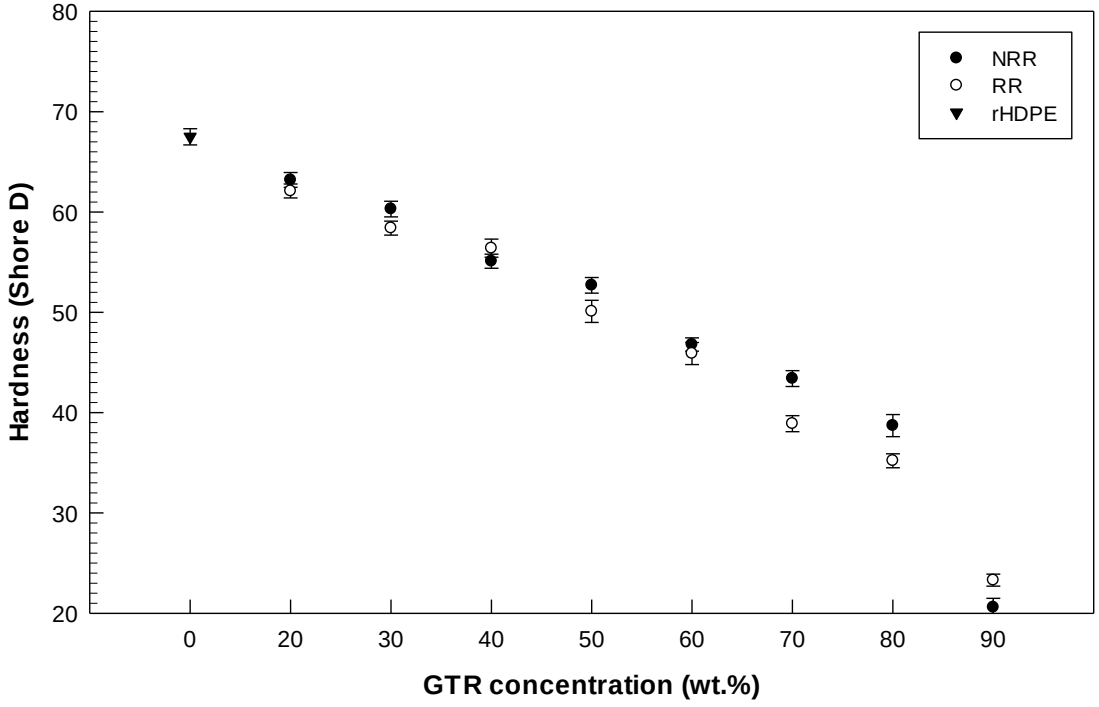

Figure 3.10 Hardness (Shore A and Shore D) of NRR and RR blends.

3.3.4.2 Density

Density is an important physical property, especially for automotive and packaging applications. Here, the density increased with GTR content due to the higher density of NRR (1.169 g/cm^3) and RR (1.246 g/cm^3) compared to rHDPE (0.967 g/cm^3). Figure 3.11 shows that the regeneration (and the presence of a processing oil) has a dominant effect on the compound density, resulting in slightly higher (about 1%) density of all RR blends compared to NRR blends.

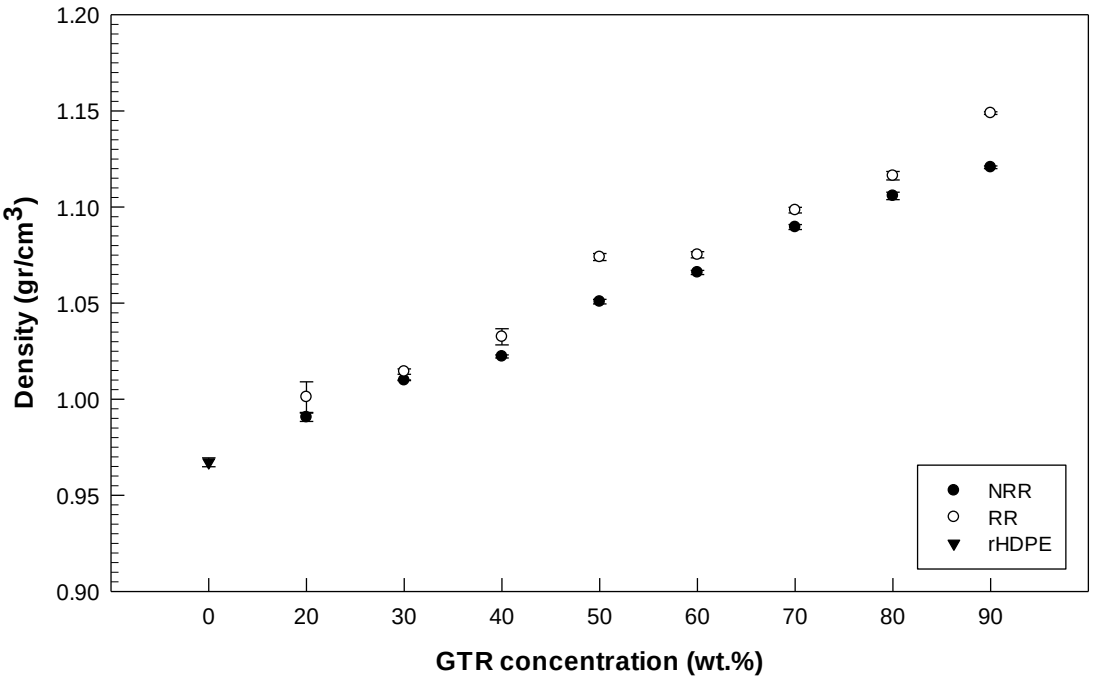

Figure 3.11 Density of NRR and RR blends.

3.4 Conclusion

Highly filled (up to 90 wt.%) TPE based on rHDPE and OTR-based GTR (NRR or RR) were prepared by melt blending (extrusion compounding followed by compression molding). The effect of rubber regeneration and concentration were investigated in terms of morphological, mechanical, and physical properties.

According to the mechanical results, the tensile strength, Young's modulus and flexural modulus decreased with increasing GTR content for both NRR and RR blends, which is related to low interfacial interaction and low modulus rubber particles compared with rHDPE. For example, increasing the GTR content from 20 to 80 wt.% decreased the tensile strength (74%), Young's modulus (93%) and flexural

modulus (92%) of NRR blends. Similarly, increasing the RR content from 20 to 80 wt.% decreased the tensile strength (84%), Young's modulus (89%) and flexural modulus (91%) of the blends. But the elongation at break was found to increase with GTR addition up to 80 wt.%, while further GTR addition decreased the elongation at break from 127% (NR80) to 119% (NR90), which was attributed to an inhomogeneous dispersion of NRR and insufficient interfacial interactions as a result of difficult processing (very high GTR concentration). On the other hand, the elongation at break of RR blends increased up to 90 wt.% from 50% (RR80) to 92% due to the softening effect of the regenerating oil, inducing higher deformation/elasticity to the compound. Also, the impact strength was found to increase with GTR content as more energy is absorbed by the elastomeric phase. The GTR regeneration also led to lower hardness due to a partial break-up of the crosslinked RR structure, leading to softer particles combined with the softening effect of the processing oil in RR formulation. Finally, the density of RR blends increased more than NRR blends due the higher density of the RR particles.

More importantly, RR compounds were easier to process as lower motor torque and die pressure drop were observed during the extrusion compounding step. This behavior can mainly be attributed to the effect of the regeneration process, leading to higher chain mobility and the presence of the processing oil. This also led to higher MFI of the final compounds.

Based on all the characterization performed, the addition of 80 wt.% GTR in rHDPE seems to be the optimum formulation for the production of low cost and eco-friendly TPE compounds based on fully recycled materials. This condition represents a good balance between processability, elasticity and low raw material costs.

Acknowledgment

The authors acknowledge the financial support of the Natural Sciences and Engineering Research Council of Canada and the technical support of the Research Center on Advanced Materials (CERMA). The rubber particles used for this work were kindly supplied by Phoenix Innovation Technologies (Montreal, Canada). Finally, the technical help of Mr. Yann Giroux was highly appreciated.

CHAPTER 4 EFFECT OF GROUND TIRE RUBBER (GTR) PARTICLE SIZE AND CONTENT ON THE MORPHOLOGICAL AND MECHANICAL PROPERTIES OF RECYCLED HIGH-DENSITY POLYETHYLENE (rHDPE)/GTR BLENDS

Résumé

Ce travail étudie l'effet de la granulométrie de la poudrette de pneu usé (GRT) et leur concentration sur les propriétés morphologiques, mécaniques, physiques et thermiques des mélanges d'élastomères thermoplastiques (TPE) à base de polyéthylène haute densité recyclé (rHDPE). Les échantillons ont été préparés par mélange à l'état fondu (extrusion bi-vis suivie d'un moulage par compression) pour préparer différentes séries de mélanges, en utilisant le GTR avec trois tailles de particules différentes (0-250 μm, 250-500 μm et 500-850 μm) pour différentes concentrations de GTR (0, 20, 35, 50 et 65% en poids). Les propriétés thermiques ont été caractérisées par calorimètre différentielle à balayage (DSC) et la morphologie des mélanges a été étudiée par microscopie électronique à balayage (MEB). Les propriétés mécaniques et physiques des mélanges ont été étudiées par des essais de traction et de flexion quasi-statiques, combinés à la résistance aux chocs et à l'analyse mécanique dynamique (DMA). Les observations MEB indiquent une certaine incompatibilité et inhomogénéité dans les mélanges en raison de la faible adhérence interfaciale entre le rHDPE et le GTR (en particulier pour le GTR > 50% en poids). L'augmentation de la teneur en GTR jusqu'à 65% en poids entraîne une mauvaise interphase (tension interfaciale élevée) et une agglomération, entraînant la formation de vides autour des particules de GTR et une augmentation des défauts/fissures dans la matrice. Mais l'introduction de fines particules GTR (0-250 μm) avec une surface spécifique plus élevée a conduit à une structure plus homogène et à une dispersion uniforme des particules en raison de l'amélioration des interactions physiques/interfaciales. Les résultats montrent également que, pour une composition fixe, des particules de GTR plus petites (0 à 250 μm) donnent un indice de fluidité à chaud (MFI) inférieur mais une résistance à la traction/un module/un allongement à la rupture et une ténacité plus élevés par rapport aux particules de GTR plus grosses (250 à 500 μm et 500 à 850 μm).

Mots-clés : Recyclage, polyéthylène haute densité recyclé, caoutchouc de pneu, élastomère thermoplastique, la taille des particules

Abstract

This work investigates the effect of ground rubber tire (GRT) particle size and their concentration on the morphological, mechanical, physical, and thermal properties of thermoplastic elastomer (TPE) blends based on recycled high-density polyethylene (rHDPE). The samples were prepared via melt blending (twin-screw extrusion followed by compression molding) to prepare different series of blends using GTR with three different particle sizes (0–250 μm, 250–500 μm and 500–850 μm) for different GTR concentrations (0, 20, 35, 50 and 65 wt.%). The thermal properties were characterized by differential scanning calorimeter (DSC) and the morphology of the blends was studied by scanning electron microscopy (SEM). The mechanical and physical properties of the blends were investigated by quasi-static tensile and flexural tests, combined with impact strength and dynamic mechanical analysis (DMA). The SEM observations indicate some incompatibility and inhomogeneity in the blends due to low interfacial adhesion between rHDPE and GTR (especially for GTR > 50 wt.%). Increasing the GTR content up to 65 wt.% leads to poor interphase (high interfacial tension) and agglomeration resulting in the formation of voids around GTR particles and increasing defects/cracks in the matrix. But introducing fine GTR particles (0–250 μm) with higher specific surface area led to a more homogenous structure and uniform particle dispersion due to improved physical/interfacial interactions. The results also show that for a fixed composition, smaller GTR particles (0–250 μm) gives lower melt flow index (MFI) but higher tensile strength/modulus/elongation at break and toughness compared to larger GTR particles (250–500 μm and 500–850 μm).

Keywords: Recycling, high-density polyethylene, ground tire rubber, thermoplastic elastomer, particle size

4.1 Introduction

Problems associated with storage and elimination of end-of-life tires lead to growing worldwide environmental concern. This is why a great deal of effort is devoted to seek profitable and eco-friendly solutions for the recovery and recycling of discarded tires [5,9]. Upcycling is an effective recycling approach aiming at incorporating shredded waste tires into polymer blends to produce added-value products for various applications such as artificial reef, playground equipment, erosion control and highway crash barrier. Ground tire rubber (GTR), produced via different downsizing (grinding) processes, contains a high amount of high quality natural and synthetic rubbers that can be used as potential sources of valuable raw materials for incorporation into polymers (thermoplastics, thermosets and rubbers) [1,242]. Polymer blends based on recycled rubbers and thermoplastic resins lead to the production of thermoplastic elastomers (TPE) exhibiting flexibility from the rubber phase and reprocessability from the thermoplastic resin. These blends can be economical alternatives for virgin TPE [8].

Recyclable compounds being processed at large scale with high level of recycled contents is a growing market. For these applications, high-density polyethylene (HDPE) is often used due to its availability, low density and low cost, combined with good rigidity and hardness, and with excellent electrical and chemical resistance [11,30]. Recently, the availability of large quantities of recycled high-density polyethylene (rHDPE) with easy processability (low melting point) have directed TPE research and industry toward the production of TPE based on rHDPE for both indoor and outdoor applications [12,243,244]. However, increasing the GTR content above 50% usually leads to substantial decreases in the tensile properties due improper homogenization (GTR distribution and high viscosity) and poor compatibility between the crosslinked rubber particles and thermoplastic matrix [12]. For example, Kakroodi and Rodrigue reported that incorporation of GTR in HDPE led to a 64% decrease in the strain at break of GTR/HDPE (70/30), while further increase in GTR content significantly decreased this value by another 44% for GTR/HDPE (90/10) [12]. In general, the mechanical properties of TPE, as a binary system, depends on the components compatibility as well as the GTR particle size. In general, decreasing the particle size gives better dispersion and higher specific surface area, promoting interfacial interactions via bonding (mechanical and physical) and co-crosslinking possibilities during mixing leading to better tensile properties [1]. Mujal-Rosas et al. [19] observed significant decrease in the tensile strength of a neat ethylene vinyl acetate (EVA) (23 MPa) upon addition of only 10 wt.% GTR (12.7 MPa) having particle sizes less than 200 μm. But increasing the particle size to 200–500 μm or

above 500 μm led to even lower values with 10.4 MPa and 8.4 MPa, respectively. This trend is associated to lower compatibility between the components when the GTR size increased. Alshukri et al. [245] also reported a gradual tensile strength decrease for styrene butadiene rubber (SBR) from 16.0 MPa to 10.8 MPa and 7.5 MPa after the introduction of 30 wt.% of recycled rubber crumbs with particle sizes of 180–250 μm and 425–600 μm, respectively. These results were similar to the ones reported by Han and Han [210]. This trend was again expected as the incorporation of larger rubber particles decreases the specific contact area between both phases, leading to lower filler-matrix bonding which are acting as stress concentration points facilitating crack initiation and growth, leading to premature failure. So, the control of the GTR particle size and blend morphology is important to promote blend compatibility.

Larger GTR particles also increases the probability of GTR agglomeration and the formation of larger voids around them, while smaller particles will develop smaller cracks [246]. Colom et al. [247] observed that adding 20 wt.% GTR (200 μm) decreased the tensile strength of HDPE by 25% (from 24 to 18 MPa), while an acid treatment (sulphonitric) of GTR showed only a decrease of 13% (from 24 to 20.8 MPa). They concluded that this chemical surface treatment (etching effect) led to increased surface roughness, modifying the interaction with the matrix, producing better blends with higher tensile properties, especially for smaller particles (<200 μm).

It should be noticed that the GTR particle size, shape and specific surface area depend on the grinding process. Comparing three methods of waste tires grinding (roller grinding, elastic-strain grinding and cryogenic grinding), the particles obtained from roller grinding are expected to show the best reinforcement properties due to higher specific surface area generated to improve interfacial bonding with the matrix [163].

Based on our previous work [248], this study aims at providing a detailed study on the effects of recycled rubber particle sizes and blend composition on the melt processability, morphological and mechanical properties of recycled TPE blends. In particular, we evaluate the possibility of melt blending different GTR particle sizes (0–250, 250–500 and 500–850 μm) with a rHDPE matrix and optimize the formulation to obtain a 100% recycled blend with good mechanical performance. The TPE were produced via melt mixing of rHDPE with different GTR content (0, 20, 35, 50 and 65 wt.%) via twin-screw extrusion followed by compression molding as a first step.

4.2 Result and Discussion

4.2.1 Processability

The processability and flowability of the TPE blends depend on the GTR particle size, content, and interaction to determine the melt flow resistance at a specific temperature and stress/strain. Melt flow index (MFI) was used here as a simple tool to determine material fluidity (inverse of viscosity). Table 4.1 reports the values for the rHDPE/GTR blends. It was found that increasing the GTR content from 35 to 50 wt.% at a fixed particle size (0–250 μm) led to a MFI reduction from 0.42 to 0.24 g/10 min. A similar observation was reported for the effect of recycled rubber loading on decreasing the TPE flowability as an indication of higher viscosity due to the crosslinked structure of GTR, which does not flow and agglomerates in the matrix, leading to higher viscosity [239]. But the variation of MFI with GTR content is not linear and more significant decreases occur for blends filled with smaller GTR (0–250 μm). For the same GTR content (35 wt.%), increasing the particle sizes from 0–250 μm to 250–500 μm and 500–850 μm increased the MFI from 0.42 to 0.46 and 0.48 g/10 min, respectively. It can be concluded that small GTR particles promote chain entanglements and particles cluster, providing less available space for the GTR particles to move around and flow [249]. Decrease in MFI (inverse relation with viscosity) translates to higher extruder motor torque, since higher force is required to disperse the crosslinked GTR particles into the rHDPE matrix. To get information on the blends processability, the motor torque and pressure loss in the die were also measured during the melt extrusion step and presented in Table 4.1. Initially, the torque rose sharply because of the mechanical resistance exerted on the rotors by the unmelted materials. While the materials melted and subjected to mechanical-induced shear force, the torque value decreased until a stabilized level, as reported in Table 4.1. It can be seen that the stabilized torque increased with increasing GTR content, related to the crosslinked rubber network restricting the flow. Ismail et al. [14] reported that polypropylene (PP)/GTR blends containing up to 60 wt.% recycled rubber with fine GTR (250–500 μm) exhibited a slightly higher equilibrium torque than that of blends with larger GTR particles (500–710 μm and 710–1000 μm), due to higher flow resistance associated with the high friction related to the higher surface area of the fine GTR. They also reported an increase in the equilibrium torque from 4 N.m to 8 N.m upon increase in the fine GTR content (from 20 to 60 wt.%) because of higher required forces to disperse the crosslinked GTR in the PP matrix. Also, in agreement with lower MIF values (higher viscosity), the pressure loss across the die increased with GTR content. For instance, increase the GTR (0–250 μm) content from

35 to 50 wt.% led to a torque variation of 6% (49 to 52 N.m) and pressure loss by 42% (350 to 500 psi), while the same increase in GTR content for larger particles (500–850 μm) led to higher torque by 4% (48 to 50 N.m) and die pressure loss by 41% (290 to 410 psi). It was found that smaller GTR particles exerted a noticeable effect on MFI, motor torque and pressure loss, which can be associated to higher friction between GTR particles with smaller size and higher surface generating higher filler-matrix interactions [11,239]. Specific mechanical energy is a measure of how much mechanical energy is required for melt extrusion, which can affect the melting and interaction between the components of blends. Increase in GTR content for all range of particle sizes increased the specific mechanical energy, and this can be attributed to the higher amount of energy needed by the motor to turn the screws for mixing crosslinked rubber particles (non-melting) with thermoplastic resins [239]. For examples, increasing the GTR (0–250 μm) content from 35 to 50 wt.% increased the consumed energy from 615 to 653 J/g because of higher extruder motor torque and higher required force to disperse the crosslinked fillers at higher mixing ratio. In agreement with torque values, the motor load, hence the specific mechanical energy, was more significantly increased by the addition of smaller GTR particles (0–250 μm) compared to larger ones (250–500 μm and 500–850 μm). For the same GTR content (35 wt.%), melt extrusion of fine GTR particles (0–250 μm) showed the highest specific mechanical energy (615 J/g), associated with the higher contact area between smaller particles (higher specific surface area) and rHDPE, which increased the friction between the components and the extruder barrel.

Table 4.1 Parameters related to the compounds processability. See Table 4.3 for definition.

Sample Code	MFI (±0.02 g/10 min)	Motor Torque (±2 N·m)	Die Pressure Loss (±20 psi)	Specific Mechanical Energy (±25 J/g)
RHD	1.31	-	-	-
G20S	0.55	46	260	577
G35S	0.42	49	350	615
G50S	0.24	52	500	653
G65S	0.10	54	550	678
G20M	0.60	45	180	565
G35M	0.46	48	300	602
G50M	0.30	50	440	628
G65M	0.16	52	490	653
G20L	0.61	45	170	565
G35L	0.48	48	290	602
G50L	0.33	50	410	628
G65L	0.19	51	480	640

4.2.2 Crystallinity

Differential scanning calorimeter (DSC) analysis was used to detect possible changes in crystallinity and microstructure of the matrix upon incorporation of a second component (GTR). Table 4.2 presents the T_m, T_c, melting enthalpy and crystallinity degree (%) of the rHDPE/GTR blends as a function the GTR content and particle size. It was found that T_m and T_c slightly decreased with increasing GTR content from 20 to 65 wt.% for all particle sizes. A decrease trend for the melting temperature can be related to lower thickness of the lamella as non-crystalline GTR particles limit the growth of lamellae on the crystalline side [11]. Also, the melting enthalpy decreased with further GTR addition since the crystallizable material (rHDPE) decreased in volume and space [11]. For example, increasing the GTR content from 35 to 50 wt.% at a fixed particle size (0–250 μm) led to lower melting enthalpy from 102.9 to 76.3 J/g. This is in agreement with Colom et al. [247] who concluded that small GTR particles (<200 μm) in HDPE/GTR (60/40) blends acted as nucleating agents, leading to the compactness of the structure in their boundaries. The promoted crystallization led to an increase of the melting enthalpy to 200 J/g, while particle sizes of 200–500 μm decreased the melting enthalpy to 160 J/g as the nucleation effect is not triggered for larger particles. To investigate the effect of GTR content and particle size on the rHDPE crystallization, the crystallinity degree was calculated by Equation (4.1). Decreasing crystallinity with increasing GTR content is a common observation in rubber-thermoplastic blends, irrespective of the rubber being virgin or recycled.

As shown in Table 4.2, the crystallinity degree for all the compositions decreased with the introduction of a flexible amorphous phase (GTR), disturbing the packing of matrix chains. Increasing the GTR content disorganized the crystalline structure of the thermoplastic resin by confining rHDPE segments (steric hinderance), resulting in the formation of a smaller crystalline phase and lower crystallinity [11]. Moreover, possible sulfur crosslinking of GTR during melt mixing can act as local defects to deteriorate the close packing and compactness of the polymer chains, leading to lower matrix crystallinity [250]. But smaller GTR particles are responsible for a higher level of compactness since the polymer chains have more freedom to organize themselves around them. This leads a structure modification at their boundaries influencing the matrix crystallinity due to better interaction with the matrix [19]. As presented in Table 4.2, the slightly higher melting temperature when small particles are used compared to larger ones is associated to a more compact crystalline structure (GTR: 0–250 μm) [247]. Increasing the GTR particles size from 0–250 μm to 250–500 μm and 500–850 μm led to lower crystallinity for GTR35 from 55.3% to 54.4% and 53.9%, respectively. The higher crystallinity obtained with small GTR particles is

associated to a more compact crystalline structure and higher melting temperature of the blends filled with small particle (0–250 μm), and correlates well with higher tensile strength and modulus as described later.

$$X_c = \frac{\Delta \mathrm{H}_m}{(1-\varphi)\,\Delta \mathrm{H}_{m0}} \times 100 \tag{4.1}$$

Table 4.2 Thermal parameters of rHDPE/GTR blends calculated from DSC. See Table 4.3 for definition.

Sample Code	T_m (°C)	T_c (°C)	ΔH_m (J/g)	X_c (%)
RHD	129.5	117.6	163.0	57.1
G20S	123.4	112.3	128.2	56.2
G35S	122.7	111.9	102.9	55.3
G50S	122.7	111.3	76.3	53.4
G65S	122.0	111.0	50.0	49.9
G20M	122.9	111.8	127.8	55.8
G35M	122.5	111.7	101.1	54.4
G50M	121.9	111.2	75.4	52.7
G65M	121.9	110.8	49.3	49.2
G20L	122.7	111.6	126.6	55.3
G35L	122.6	111.3	100.2	53.9
G50L	121.7	110.9	75.2	52.6
G65L	121.5	110.7	48.2	48.1

4.2.3 Morphology

Figure 4.1 presents SEM micrographs of the GTR particle at different magnifications. Figure 4.1 b, d, and f illustrate the presence of considerable amounts of impurities due to the recycled origin of GTR. As shown in Figure 4.2, energy dispersive spectroscopy (EDS) illustrates the presence of metals or other additives related to several materials used for the reinforcement of tire parts, resulting in some impurities in GTR. Also, several sources of waste tires and grinding methods are responsible for a variety of shapes like porous or smooth angular surfaces on the GTR particles. Due to the heterogeneous nature of recycled rubber particles, it is difficult to obtain a specific size and distribution. However, mechanical sieving is simple and cost effective to achieve a good separation of each particle size selected (60, 35 and 20 mesh). The SEM micrographs show that the sieved materials are in the range of less than 250 μm (Figure 4.1 a), up to around 500 μm (Figure 4.1 b) and up to 850 μm (Figure 4.1 c).

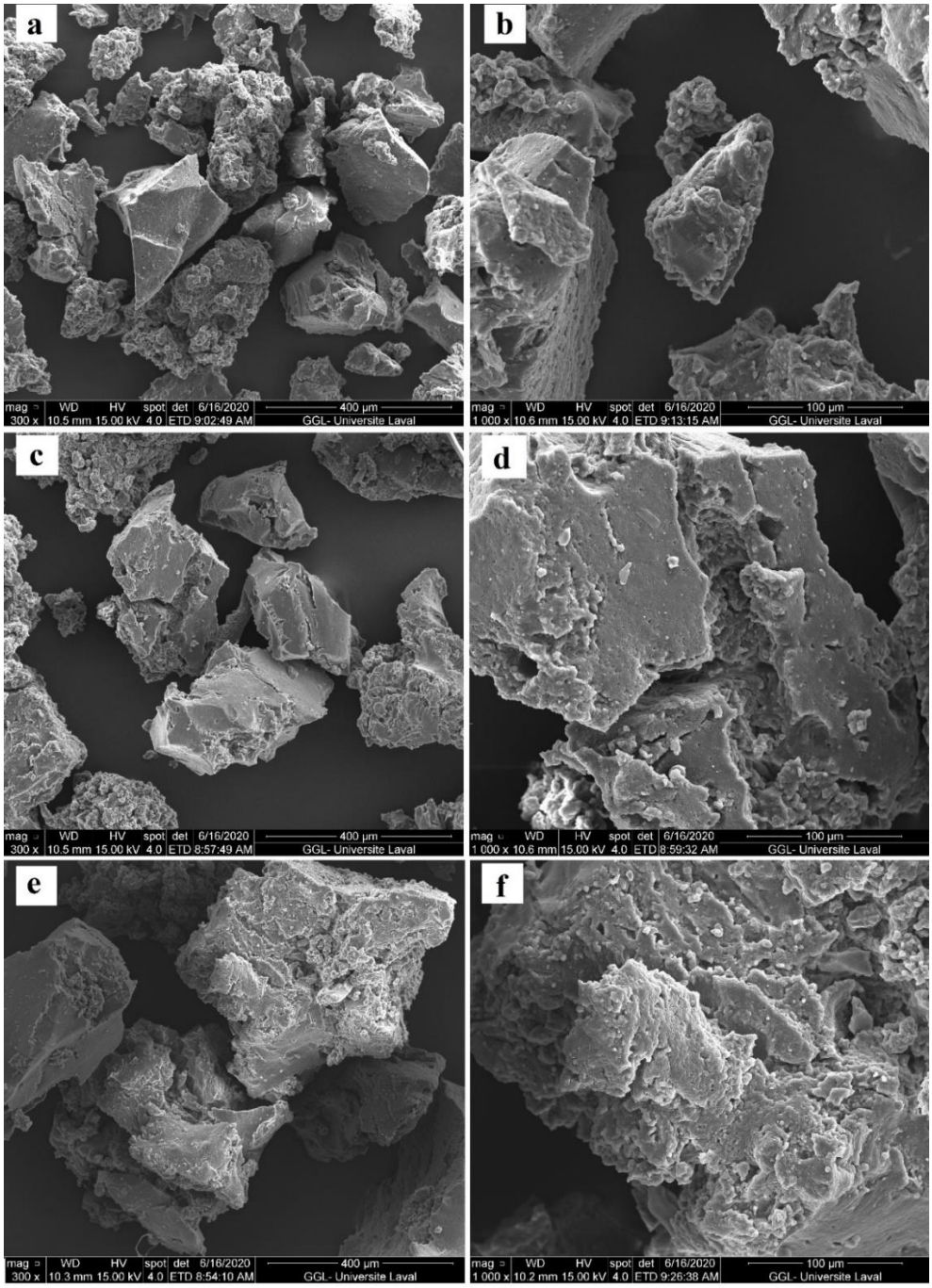

Figure 4.1 SEM images at different magnification of GTR particles: (a, b) 0–250 µm, (c, d) 250–500 µm and (e, f) 500–850 µm.

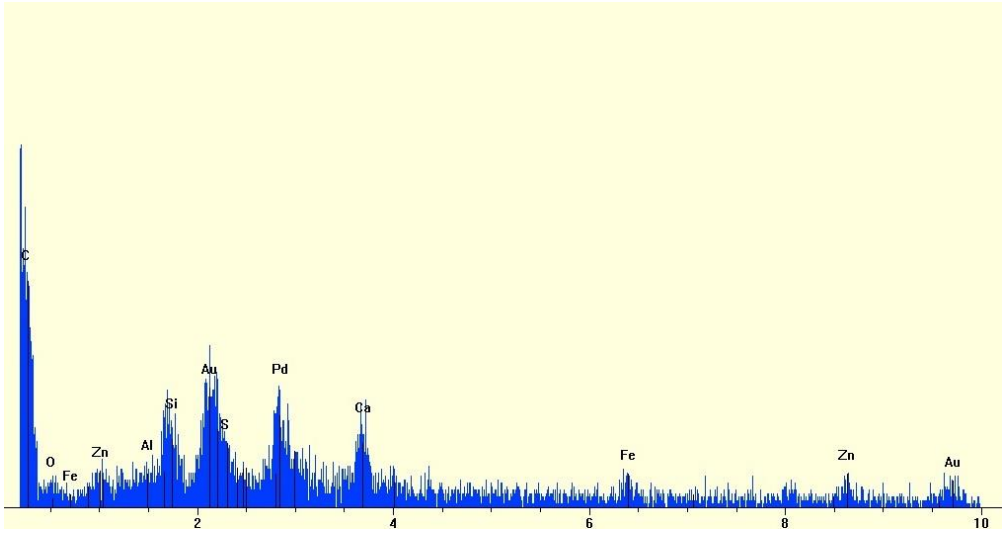

Figure 4.2 EDS spectra of the GTR particles showing some impurities.

SEM images were also used to determine how the blend composition and particle size influenced the GTR dispersion state and the interfacial adhesion with the matrix. Figure 4.3 shows for rHDPE/GTR blends containing 35 and 50 wt.% GTR, a dispersed phase (GTR) in a continuous matrix (rHDPE). As shown in Figure 4.3 a–c, the dispersed phase size in blends containing 35 wt.% filler increased with increasing GTR particles size (0–250 μm, 250–500 μm and 500–850 μm). Further increase in GTR content (50 wt.%) makes the GTR particles, especially larger ones (250–500 μm and 500–850 μm), to cluster/agglomerate, promoting the formation of voids around them (Figure 4.3 e, f). This suggests that coarser GTR particles easily agglomerate or coalesce during melt mixing, leading to a difficult distribution of filler particles and larger clusters in the matrix. The possibility of coalescence and cluster of large recycled rubber particles (over 500 μm) during compounding at high rubber concentrations (50 wt.% in Figure 4.3 f) was also reported elsewhere [242,247].

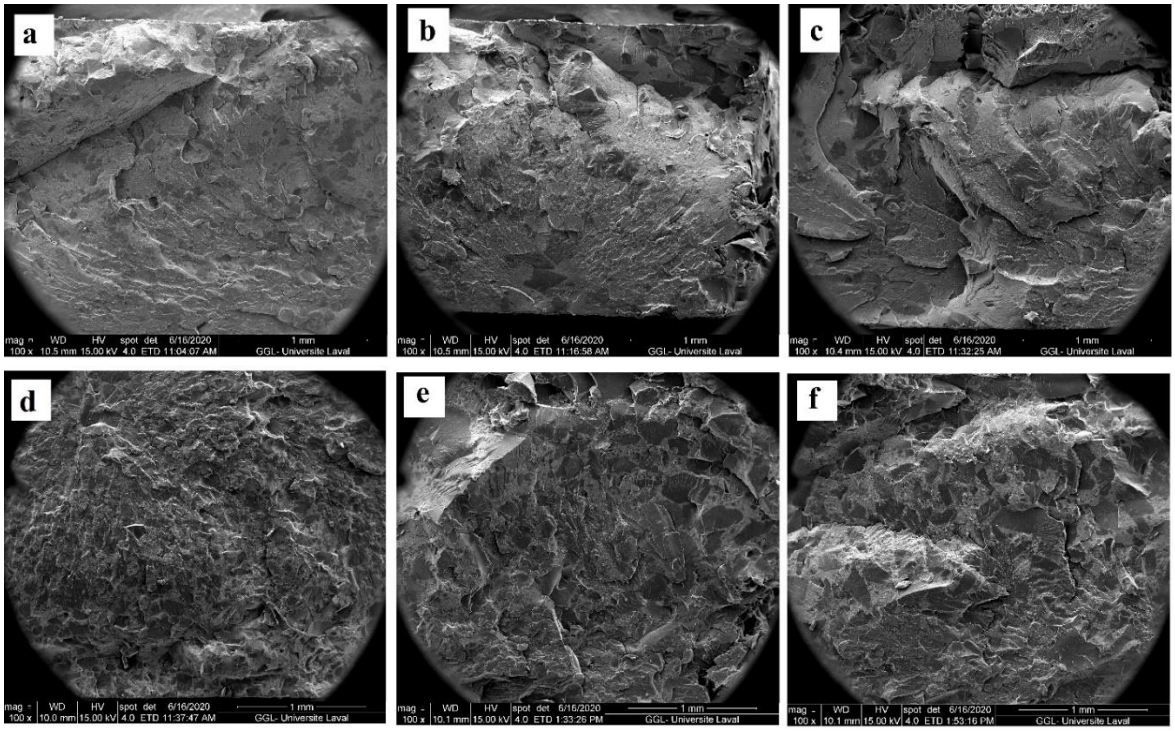

Figure 4.3 SEM micrographs of the fractured surfaces of: (a) G35S, (b) G35M, (c) G35L, (d) G50S, (e) G50M and (f) G50L. See Table 4.3 for definition.

Figure 4.4 presents the SEM micrographs of rHDPE/GTR (50/50) blends at different levels of magnification, which allows to understand the relation between the evolution of morphology with GTR particle sizes. Detection of the rubber phase is difficult in GTR50S (Figure 4.4 a) because of a more textured surface and uniform filler distribution compared to GTR50M (Figure 4.4 b) and GTR50L (Figure 4.4 c). This observation can be related to better interaction and bonding of small GTR particles (higher specific surface area) with the polymer matrix. So higher energy is required for sample failure. On the other hand, blends filled with GTR particles larger than 250 µm (250–500 µm or 500–850 µm) show some cracks and pores around them (Figure 4.4 e, f). The presence of these voids is associated with GTR particles being easily pulled out due to poor interaction with the matrix. Clean surfaces of the GTR particles also implies incomplete dispersion of agglomerated recycled rubber particles due to weak interfacial adhesion. These effects are expected to influence the mechanical properties, as described next.

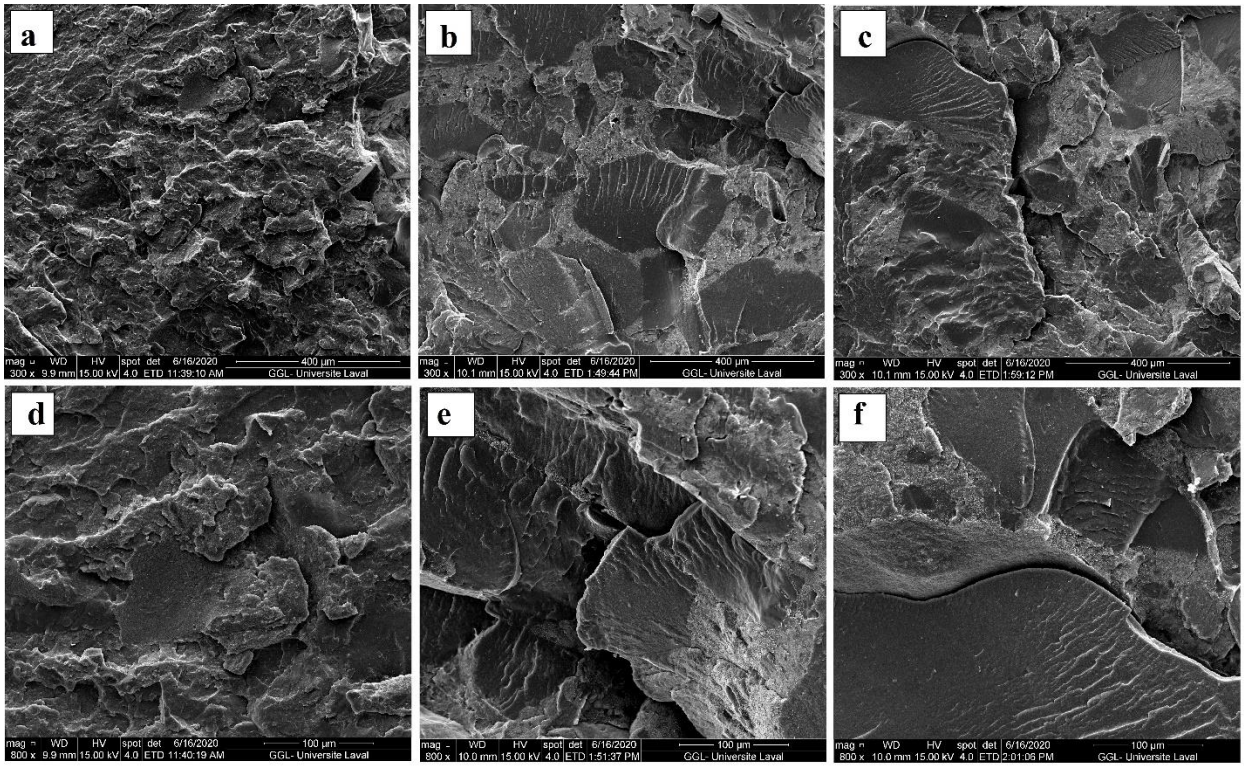

Figure 4.4 SEM micrographs of the fractured surfaces of: (a, d) GTR50S, (b, e) GTR50M and (c, f) GTR50L. See Table 4.3 for definition.

4.2.4 Mechanical Properties

4.2.4.1 Tensile Properties

It is expected to observe a decreasing trend in the rHDPE tensile properties with the introduction of recycled rubber particles (GTR) mainly associated to the rubbery (soft) nature of the rubber phase, weak interfacial adhesion between GTR and rHDPE, and limited stress transfer between the phases [5]. Figure 4.5 and Figure 4.6 respectively present the tensile strength and tensile modulus of rHDPE/GTR blends as a function of GTR content and particle sizes. The addition of GTR decreases the tensile strength (21.3 MPa) and tensile modulus (364.7 MPa) of the neat matrix. For example. increase the GTR content (0–250 µm) from 35 to 50 wt.% decreases the tensile strength by 33% (11.6 to 7.7 MPa) and the Young's modulus by 42% (156 to 89.5 MPa). This decreasing trend is not only related to low affinity between GTR and rHDPE, but also to degradation of recycled materials (plastic and rubber) by exposure to oxygen/ozone, mechanical and thermal stresses during their service life, grinding and processing [251]. The effect of GTR particle size is clearly observed when comparing the different range of particles selected. For example, changing the smaller particles (0–250 µm) for larger ones (500–850 µm) led to a decrease in tensile strength and Young's modulus of rHDPE/GTR (65/35)

by 8% (11.6 to 10.6 MPa) and 23% (156 to 119.3 MPa), respectively. Lower tensile properties for larger particles is attributed to more agglomeration and poor particle-particle/particle-matrix interaction of larger GTR particles (Figure 4.3 and Figure 4.4) resulting in stress concentrations points and weak interfacial adhesion increasing the probability of crack initiation and premature failure (easier crack propagation). It is clear that GTR contents below 50 wt.% contributed to higher tensile strength and Young's modulus in agreement with similar observations in LDPE/GTR blends [129]. The effects of GTR particle size and blending composition on the elongation at break, as the most important parameter indicating the compatibility and homogeneity of TPE blends, are shown in Figure 4.7. Although GTR introduction led to a drop of the elongation at break of the neat rHDPE (1061%), increasing the GTR content from 20 to 65 wt.% led to a slight increase in plastic deformation due to the presence of a more elastic phase inducing higher deformation/elasticity of the samples. Incorporation of small GTR particles resulted in higher elongation at break but increasing the GTR particle size from 0–250 μm to 250–500 μm and 500–850 μm for rHDPE/GTR (35/65) resulted in ε_b of 44.5% to 38.3% and 36.7%, respectively. However, the ε_b values are relatively low which can be ascribed to the incompatibility and low affinity between the crosslinked recycled rubber and rHDPE with poor interfacial stress transfer. The presence of vulcanized (crosslinked) rubber particles as stress concentration points (crack initiation points) hindered flow and mobility of rubber particles, as well as possible entanglement with thermoplastic molecules [30,252]. Wang et al. [30] reported a similar trend with an elongation at break of recycled PE/GTR (40/60) around 50% due to the low homogeneity and poor interfacial adhesion between the phases leading to easy crack initiation and their fast propagation. Also, high amount of contamination and impurities in recycled thermoplastic matrixes (also generating cracks), as well as high shear force and elevated temperature during recycling/reprocessing (main chain degradation) can be responsible for the low plastic deformation of recycled TPE [30,253].

It is found that the effect of filler particle size on tensile properties at lower GTR content (less than 50 wt.%) is more important, while poor interfacial interaction is the main factor controlling the tensile properties of TPE at higher GTR content [254]. Finally, particle sizes smaller than 500 μm produce better mechanical properties compared to larger ones, attributed to the higher specific surface area of the former, promoting better interfacial stress transfer and interaction between GTR and rHDPE [19,255].

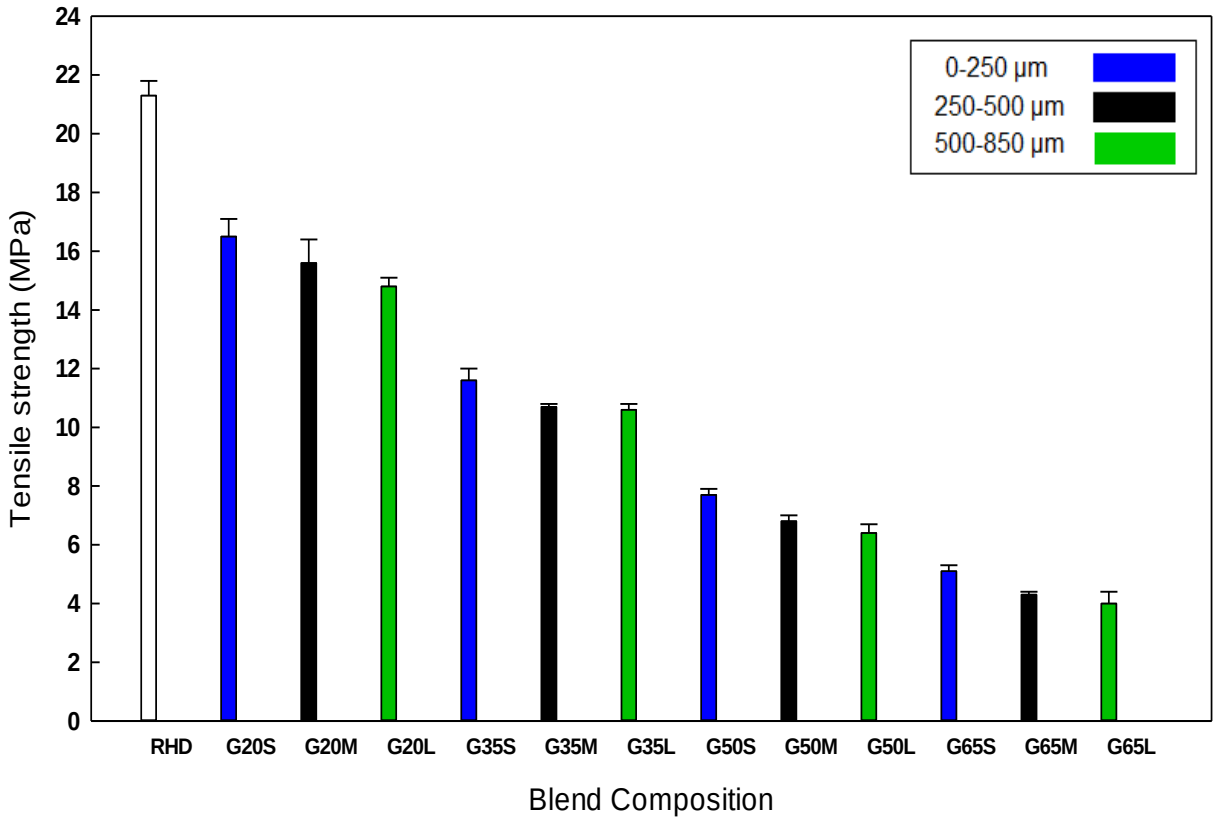

Figure 4.5 Tensile strength of rHDPE/GTR blends. See Table 4.3 for definition.

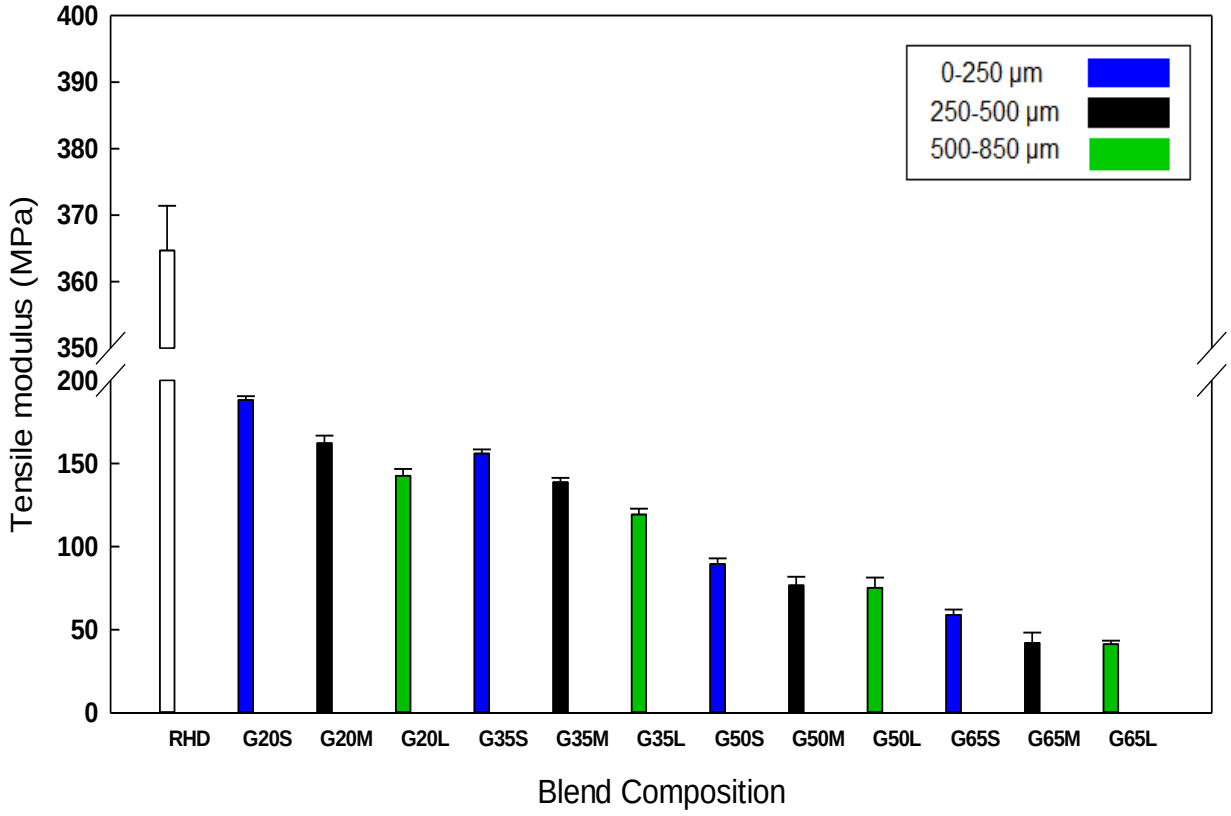

Figure 4.6 Tensile modulus of rHDPE/GTR blends. See Table 4.3 for definition.

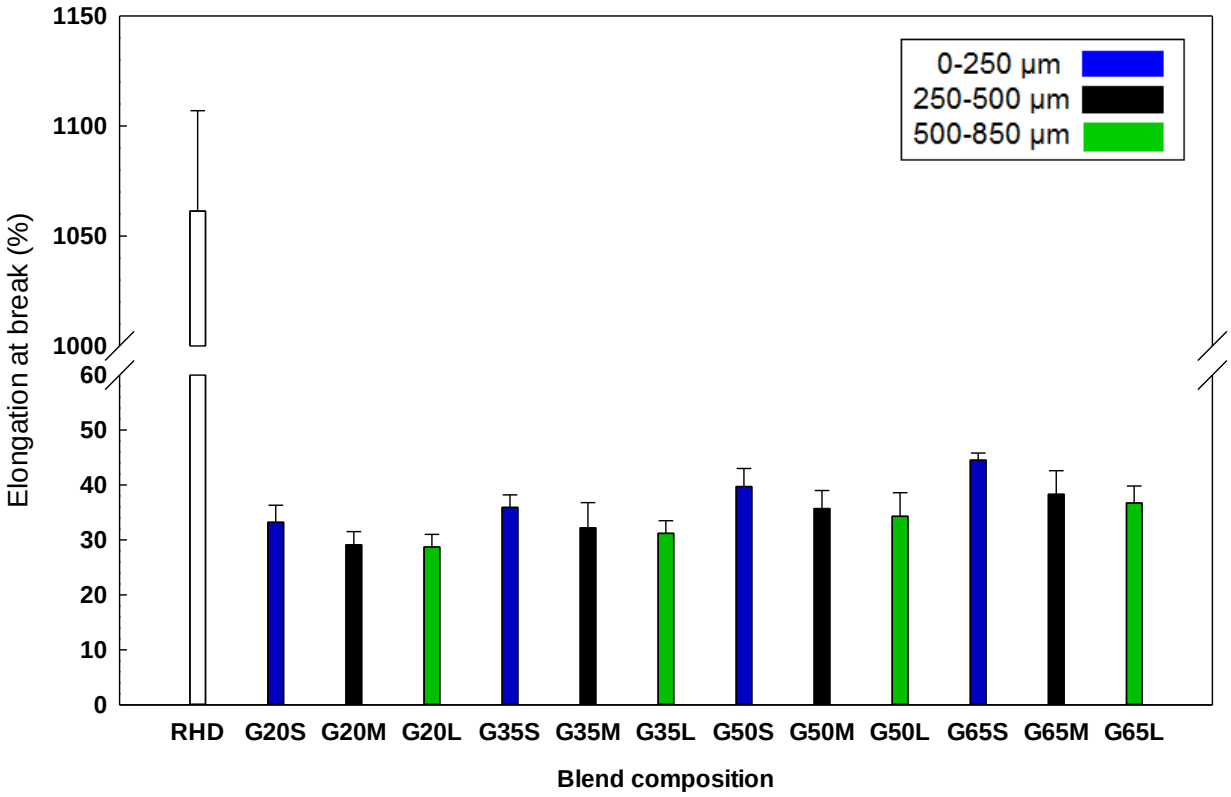

Figure 4.7 Elongation at break of rHDPE/GTR blends. See Table 4.3 for definition.

4.2.4.2 Flexural Modulus

The flexural modulus is presented in Figure 4.8. As expected, the values decrease with increasing GTR content as for the tensile modulus (Figure 4.6). For example, increasing the GTR content from 35 to 50 wt.% deceased the flexural modulus of G50S, G50M and G50L by 33% (201.8 to 133.6 MPa), 35% (175.9 to 115.1 MPa) and 40% (164.9 to 98.1 MPa), respectively. This can be related to the presence of a low modulus GTR phase (low stiffness) in rHDPE and interfacial voids/defects inside the blends (Figure 4.3 and Figure 4.4). The mechanical properties strongly depend on the filler dispersion (GTR) and interfacial interaction controlled by both the GTR content and particle size. Lower flexural modulus is also observed by using larger GTR particle (500–850 µm). For example, the flexural modulus of G35S, G35M and G35L is 201.8, 175.9 and 164.9 MPa, respectively. Again, higher flexural modulus using smaller particles is attributed to better interfacial interactions (higher specific surface area) between the small particles and the thermoplastic molecules, leading to less structural defects.

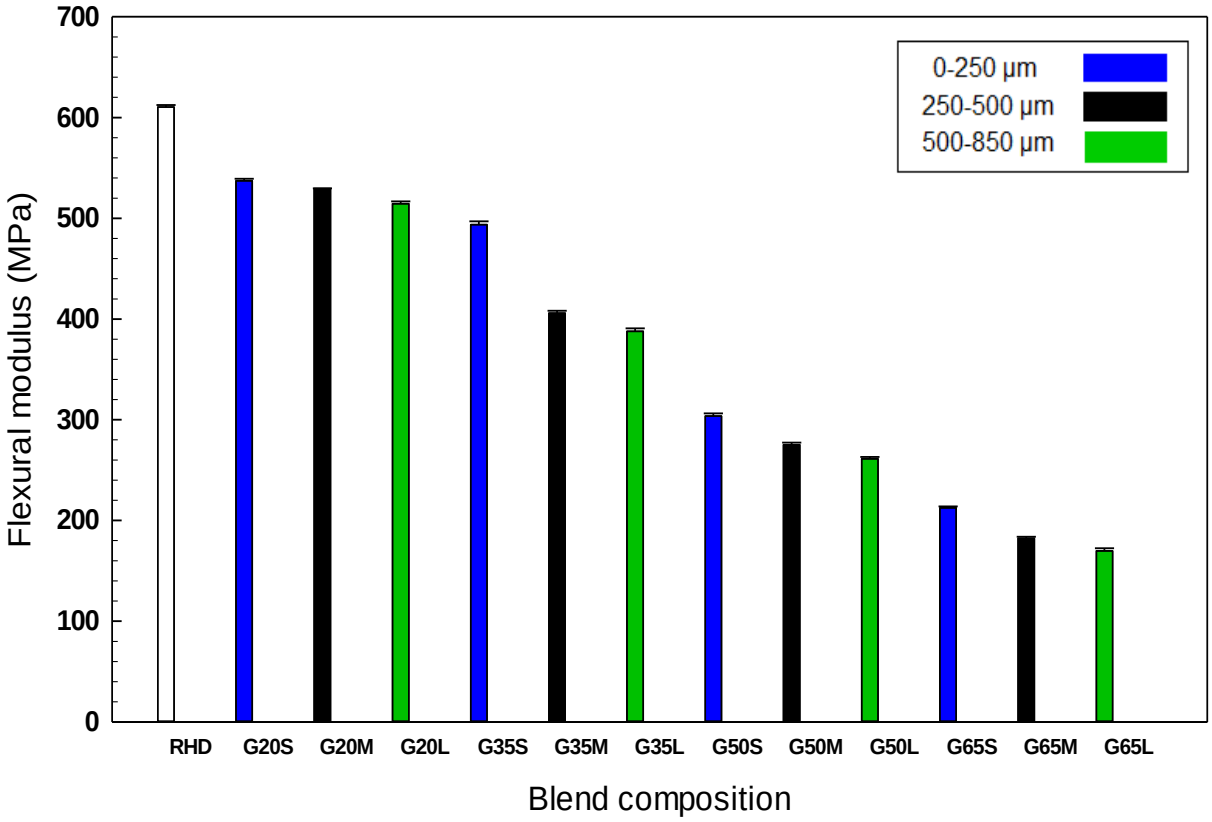

Figure 4.8 Flexural modulus of rHDPE/GTR blends. See Table 4.3 for definition.

4.2.4.3 Impact Strength

Figure 4.9 presents the impact strength, showing the effect of GTR content and particle size on toughness. The addition of GTR decreased the impact strength of the neat rHDPE (360 J/m) due to low compatibility between the recycled crosslinked rubber particles and the thermoplastic phase, since the rubber molecules do not have enough freedom to entangle with the rHDPE molecules and create strong bonding [256]. This behavior can also be related to the presence of carbon black causing defect points, inducing a split in the layer structure of the rHDPE/GTR blend and providing a shorter path for fracture propagation, producing lower impact strength [238]. Despite lower rHDPE toughness with GTR addition, increasing the recycled rubber content from 35 to 50 wt.% slightly improved by 14% (121.5 to 138.9 J/m) the toughness of blends filled with small GTR particles (0–250 µm). This can be attributed to the crosslinked structure of the GTR, making the particles more deformable to absorb more energy before crack initiation. In our case, smaller particles lead to increased toughness. For instance, G35S showed higher impact strength (121.5 J/m) compared to G35M (107.6 J/m) and G35L (105.7 J/m). This can be explained by high interfacial tension between GTR and rHDPE, leading to GTR particles

cluster/agglomeration and the formation of voids around large GTR increasing the number of defects, voids, and cracks. On the other hand, smaller GTR particles (higher specific surface area) were more easily dispersed into the matrix, and improved interaction was produced between GTR and rHDPE [250].

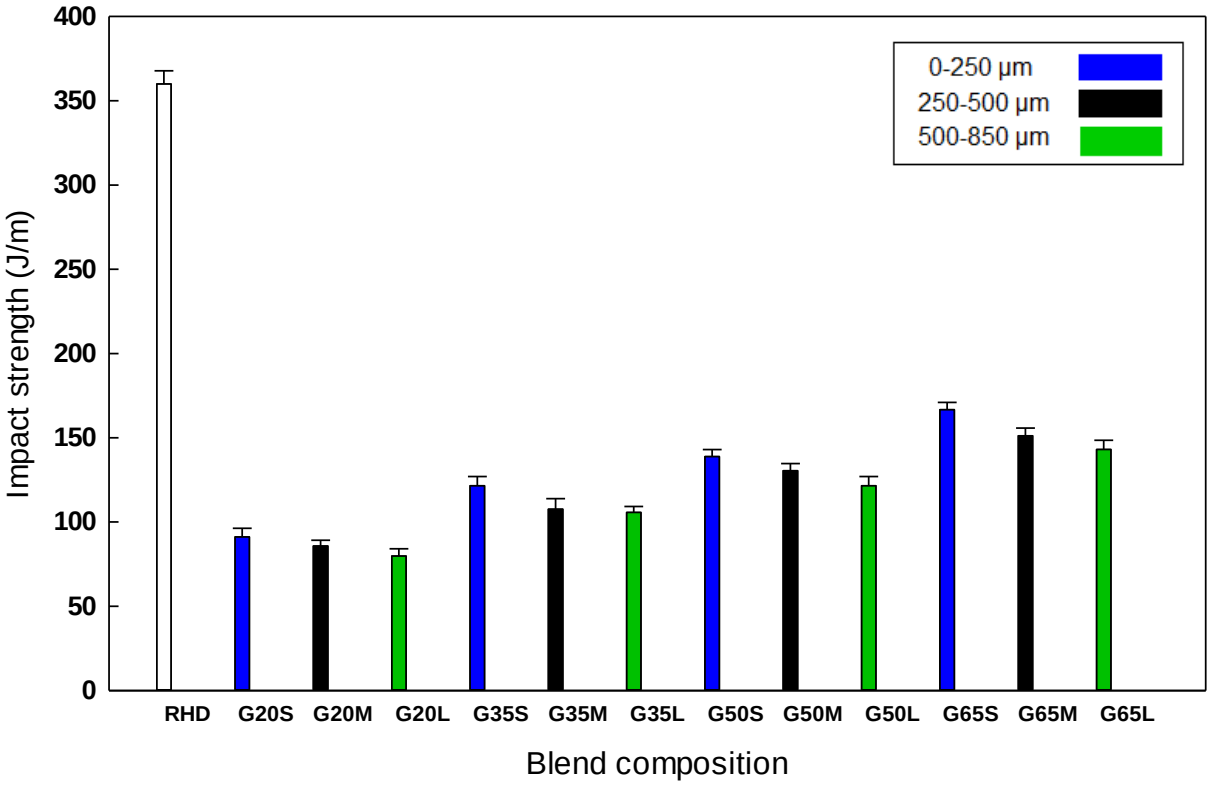

Figure 4.9 Charpy impact strength of rHDPE/GTR blends. See Table 4.3 for definition.

4.2.5 Hardness

In general, the hardness of a TPE compound is influenced by the elastic modulus and crosslink density of the rubber phase (GTR) [8]. Figure 4.10 shows that the variation of TPE hardness as a function of GTR content and particle size follows a similar trend to that of the modulus (Figure 4.6) [242,257]. A reduction in hardness (Shore A and Shore D) is observed as the rubber content increases from 20 to 65 wt.% for all GTR particle sizes attributed to the presence of a higher content of a soft elastomeric component (GTR) in the rigid matrix (rHDPE). For example, increasing the GTR content (0–250 µm) from 35 to 50 wt.% decreased the Shore A hardness by 3 points (from 98 to 95) and the Shore D by 4 points (61 to 57). The results also show that hardness increased along with the recycled rubber particle size for a fixed blend composition (50 wt.% GTR). Increasing the GTR particle size from 0–250 µm to

250–500 μm and 500–850 μm resulted in lower hardness from 57 to 56 and 54 (Shore D), respectively. In agreement with similar reports, using small GTR particles (0–250 μm) produced higher hardness due to higher chain mobility restriction and blend rigidity as a result of a more uniform filler distribution and better interfacial interaction of small particles (high surface area) with the matrix [258,259].

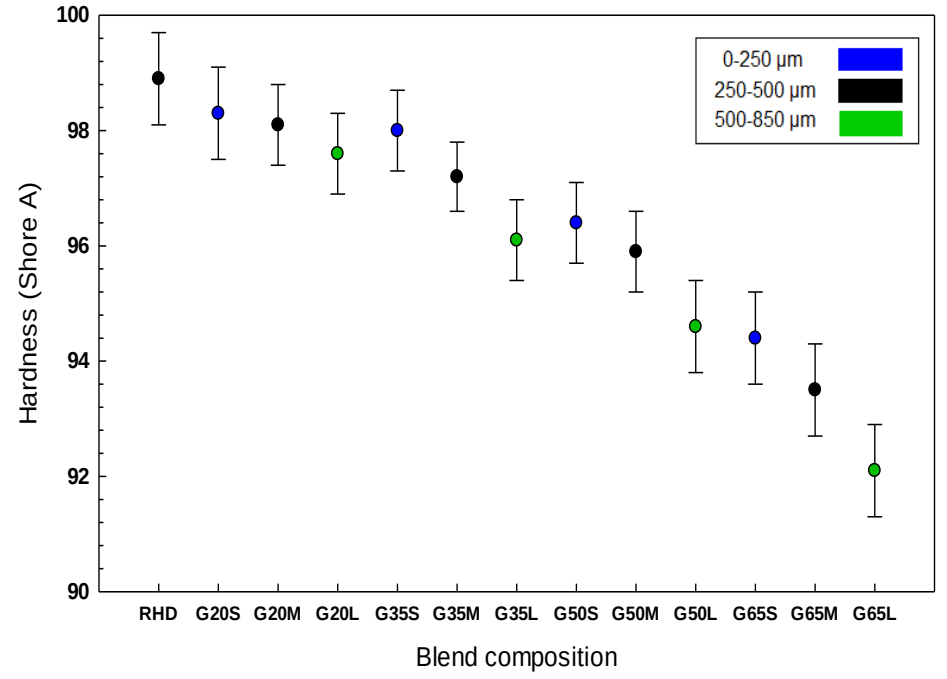

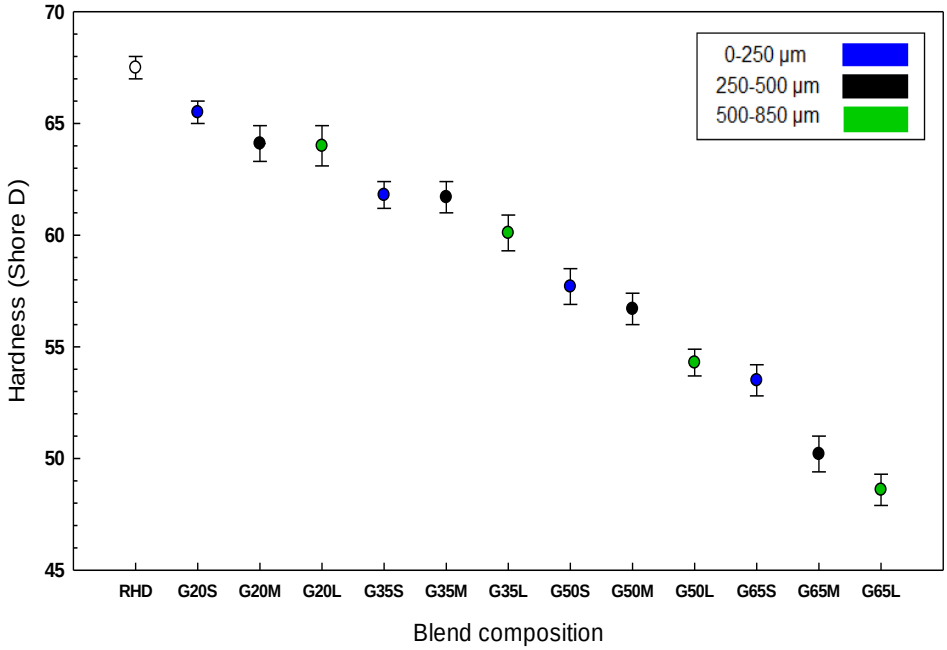

Figure 4.10 Hardness (Shore A, D) of rHDPE/GTR blends. See Table 4.3 for definition.

4.2.6 Dynamic Mechanical Analysis

The storage modulus curves as a function of temperature can help to understand the stiffness of the polymer blends with respect to phase morphology and interfacial bonding. The storage modulus indicates the maximum energy that can be stored in a period of time and reflects the rigidity of materials

[260]. Figure 4.11 shows the storage modulus (E') as a function of temperature. As expected, higher E' of the matrix compared to the blends is attributed to a semi-crystalline structure of rHDPE and the presence of crystallites offering relatively high stiffness [261]. As shown in Figure 4.11, increasing the GTR content up to 65 wt.% decreased the E', which is associated to material softening by the inclusion of soft rubber particles (low elastic modulus) in the rigid matrix inducing lower rigidity [29]. Also, incorporation of small GTR particles (0–250 μm) led to higher rigidity (E') due to a more efficient stress transfer between the phases as a result of better interaction between small GTR particles and rHDPE (Figure 4.3 and Figure 4.4). As reported before, higher specific surface area of smaller GTR particles can reduce the interfacial tension between each phase, resulting in better interfacial interaction and higher modulus [249].

The variation of the damping factor (tan δ) with temperature is shown in Figure 4.12. In general, damping is influenced by the quality of the blend interface and the friction or delamination resulting from the sliding of unbounded areas between the filler and the matrix [262]. As shown in Figure 4.12, higher GTR content (50 and 65 wt.%) led to a more viscous behavior, implying improved damping properties. This observation implies that the rubber particles dissipate energy during the stress transfer from the matrix to GTR. Figure 4.12 also shows that for the same blend composition, incorporation of small GTR particles (0–250 μm) led to lower tan δ compared to larger particles (250–500 μm and 500–850 μm). The lower damping peak corresponds to a lower degree of molecular mobility, in agreement with the tensile (Figure 4.6) and flexural (Figure 4.8) moduli, as well as hardness trends (Figure 4.10) as small GTR particles effectively restrict the rubber molecular chains motion and this reduces the elasticity of the compound generating friction between chains leading to more rigidity [263]. Such changes in dynamic mechanical properties with filler particle size are in line with tensile properties (see Figure 4.6).

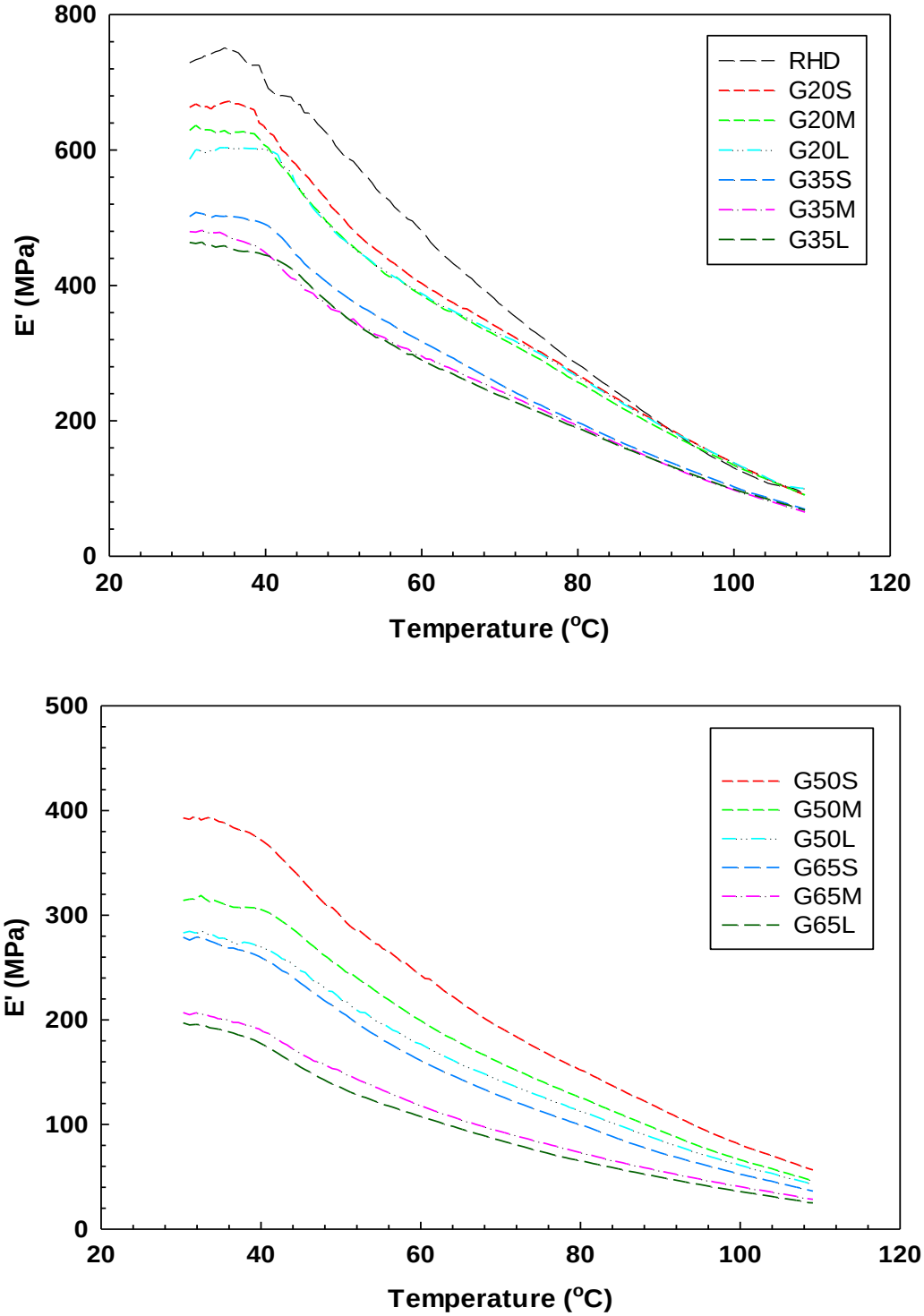

Figure 4.11 Storage modulus of rHDPE/GTR blends as a function of temperature. See Table 4.3 for definition.

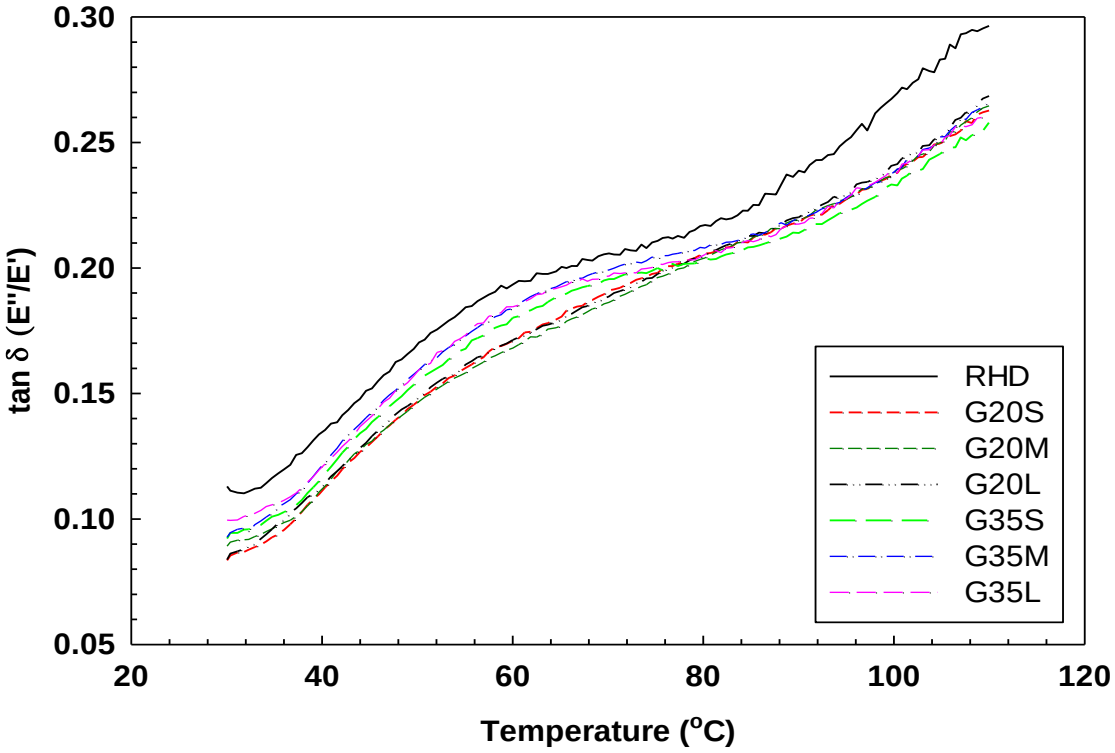

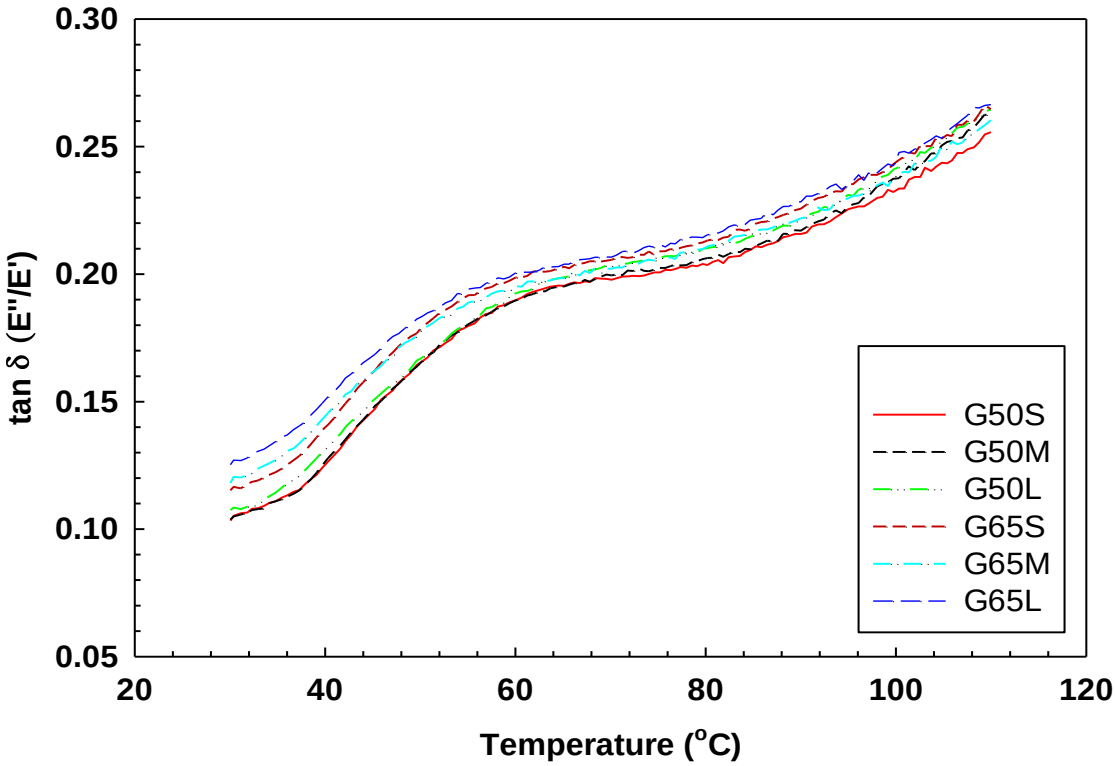

Figure 4.12 Damping factor of rHDPE/GTR blends as a function of temperature. See Table 4.3 for definition.

4.3 Materials and Methods

4.3.1 Materials

The post-consumer rHDPE was kindly provided by Gaudreau (Victoriaville, QC, Canada) and used as the matrix. This polymer has a melt flow index (MFI) of 1.3 g/10 min (at 190 °C and 2.16 kg) according to ASTM D1238. The density (ASTM D2856) and melting point (ASTM D3418) of the rHDPE are 0.967 g/cm^3 and 129.5 °C, respectively. The GTR particles (manufactured through ambient mechanical grinding of tire rubber) were obtained from Phoenix Innovation Technologies (Montreal, QC, Canada) and used as received. The recycled rubber powder has a particle size distribution between 50 and 1000 µm with a density of 1.169 g/cm^3.

4.3.2 Processing

The GTR powder was firstly separated by sieving into three categories: 0–250 µm (S: small), 250–500 µm (M: medium) and 500–850 µm (L: large). These particles were used to produce the rHDPE/GTR compounds with different GTR contents (0, 20, 35, 50 and 65 wt.%) as presented in Table 4.3. For sieving, about 300 g of GTR was placed in a series of sieves with mesh sizes of 60, 35 and 20, and shaken for 30 min to obtain the three different GTR ranges. Then, all the samples were compounded by melt blending rHDPE pellets with GTR particles using a twin-screw extruder (Leistritz ZSE-27, Nürnberg, Germany) with a L/D ratio of 40 and 10 heating zones (die diameter of 2.7 mm). The screw speed and side feeder were set at 100 rpm to get a total flow rate of 3 kg/h. The temperature profile was set at 175 °C for all zones to limit degradation since the decomposition temperature of GTR starts around 190 °C [12]. The plastic pellets (rHDPE) were fed to the extruder through the first zone (main feeder), while GTR particles were fed to the side feeder (zone 4) to limit the effect of high viscosity at higher GTR content (high motor torque and die pressure). Next, the produced blends were cooled in a water bath and pelletized using a model 304 pelletizer (Conair, CA, USA) followed by drying at 70 °C for 6 h to eliminate any residual water. The sheets were produced via compression molding at 180 °C to prepare samples for further analysis. The compounds were preheated for 3 min without pressure followed by 5 min under pressing (3 tons) using an automatic compression molding press (Carver, AutoFour/1512-PL,H, 3893, IN, USA) with a mold dimension of 115 × 115 × 3 mm^3.

Table 4.3 Sample code and formulations

Sample Code	GTR (wt.%)			rHDPE (wt.%)
	0–250 µm	250–500 µm	500–850 µm	
RHD	-	-	-	100
G20S	20	-	-	80
G35S	35	-	-	65
G50S	50	-	-	50
G65S	65	-	-	35
G20M	-	20	-	80
G35M	-	35	-	65
G50M	-	50	-	50
G65M	-	65	-	35
G20L	-	-	20	80
G35L	-	-	35	65
G50L	-	-	50	50
G65L	-	-	65	35

4.3.3 Characterization

4.3.3.1 MFI and Specific Mechanical Energy

MFI measurement was done at 190 °C and 2.16 kg according to ASTM D1238 and the average values were reported after three repetitions for each sample.

The specific mechanical energy (J/g) was calculated as:

$$\text{Specific mechanical energy} = \frac{2\pi\omega Tr}{\dot{m}} \tag{4.2}$$

where ω is the screw speed (rpm), *Tr* is the torque (N·m), and $\dot{m}$ is the mass flow rate of the material processed in g/min.

4.3.3.2 Morphological Observation

An Inspect F50 SEM (FEI, Hillsboro, OR, USA) was used at 15 kV to take micrographs of the raw materials and the blends. The samples were cryogenically fractured in liquid nitrogen and the surface were coated with gold/palladium to be observed at different magnifications. GTR was also investigated by EDS using the same device to identify impurities (contamination).

4.3.3.3 DSC Analysis

The melting and crystallization behaviors of the samples were recorded on a DSC7 (Perkin Elmer, MA, USA). About 5–10 mg was placed in an aluminum pan and measurements were performed by heating from 50 to 200 °C at 10 °C/min under a nitrogen atmosphere, then cooling back to 50 °C at 10 °C/min. The melting temperature (T_m), crystallization temperature (T_c) and enthalpy of melting (ΔH_m) of the samples were calculated from the maximum of the endothermic peak, the maximum of the exothermic peak and the area under the endothermic peak, respectively. The crystallinity degree (X_c) was calculated as:

$$X_c = \frac{\Delta \mathrm{H}_m}{(1-\varphi)\,\Delta \mathrm{H}_{m0}} \times 100 \qquad (4.3)$$

where φ is the weight fraction of recycled rubber in the blend, ΔH_m is the melting enthalpy of the sample and ΔH_{m0} is the melting enthalpy of 100% crystalline HDPE (285.8 J/g) [11].

4.3.3.4 Mechanical Testing

Tensile tests were conducted at room temperature according to ASTM D638 using a 500 N load cell and a strain rate of 10 mm/min on an Instron (Instron, Norwood, MA, USA) universal mechanical tester model 5565. At least 5 dog bone specimens (type V) with 3 mm thickness were used for each formulation. The averaged values of tensile strength (σ_Y), Young's modulus (E) and elongation at break (ε_b) are reported with their standard deviations.

Flexural tests were done on an Instron (Instron, Norwood, MA, USA) model 5565 with a 50 N load cell according to ASTM D790 at room temperature. Rectangular specimens with dimensions of 60 × 12.7 mm^2 were tested with 5 repetitions for each formulation in a three-point bending mode (span length of 60 mm) at a speed of 2 mm/min.

Notched Charpy impact strength was measured on a Tinius Olsen (Horsham, PA, USA) model 104 at room temperature according to ASTM D256. At least 10 specimens with dimensions of 60 × 12.7 mm^2 were used for each sample. Before testing, all the samples were automatically V-notched on a Dynisco (Franklin, MA, USA) model ASN 120m sample notcher 24 h before testing.

Hardness (Shore A and Shore D) was measured by using a 307L model durometer (PTC Instruments, Boston, MA, USA) with 10 measurements for each sample.

5.3.3.5. Dynamic Mechanical Analysis (DMA)

The RSA3 (TA Instruments, New Castle, DE, USA) was used with rectangular specimens having dimensions of 60 × 12.7 × 3 mm^3 in the three-point bending mode (span of 40 mm). The linear viscoelastic range of the blends was studied first via strain sweeps and then temperature ramps at a strain of 0.01% with a frequency of 1 Hz were performed between 30 and 110 °C at a heating rate of 3 °C/min. The storage modulus (E') and tan δ results are presented to determine the behavior of each sample.

4.4 Conclusions

The incorporation of recycled rubber particles (GTR) into a recycled thermoplastic matrix (rHDPE) led to a decrease of the mechanical performance because of weak interfacial adhesion and insufficient interaction between the crosslinked rubber particles with the thermoplastic chains. In this work, samples were produced via continuous melt-mixing (twin-screw extruder) of rHDPE with different GTR particle sizes (0–250 µm, 250–500 µm and 500–850 µm) over a range of concentration (0–65 wt.%). The results confirmed the effect of GTR particle size and concentration on the properties of recycled TPE blends. It was found that agglomeration of larger GTR particles (above 500 µm), especially at higher concentration (above 50 wt.%), led to poor rubber dispersion and higher defects, leading to lower mechanical properties. Due to their crosslinked network, GTR particles do not flow and agglomerate in the matrix, increasing the blend viscosity (lower MFI), leading to higher motor torque and die pressure loss in extrusion, especially for smaller particles (0–250 µm). Increasing the GTR content disorganized the crystalline structure of the thermoplastic resin, while using smaller GTR particles (0–250 µm) led to higher melting temperature of the blends associated to close packing of the polymer chains and higher crystallinity of the blends, correlating well with the higher tensile properties of rHDPE/GTR blends filled with smaller GTR. Scanning electron micrographs of the blends showed that smaller GTR (0–250 µm) had better interaction with the matrix (less voids/defects) due to their higher specific surface area. However, the introduction of larger GTR (250–500 µm and 500–850 µm) showed more defaults/cracks in the matrix, hence lower interfacial adhesion compared to similar blends filled with small GTR particles. The results indicated that all blends containing small GTR particles (0–250 µm) had higher tensile strength, Young's modulus, flexural modulus and elongation at break compared to samples produced based on larger GTR particles (250–500 µm and 500–850 µm). As the introduction of larger

GTR particles induced higher defects (stress concentration points), the probability for crack initiation and propagation also led to lower toughness.

Based on our results, it is suggested that GTR particle size below 250 μm is the most suitable range to be used in melt mixing for producing TPE based on with recycled GTR/rHDPE blends. This observation is related to the higher specific surface area (higher value and better contact) between the small rubber particles and the matrix. Also, agglomeration of large particles inhibited their uniform dispersion which was the origin of TPE performance degradation. However, the smaller particle size showed marginal improvement of mechanical strength at high GTR content (above 50 wt.%) since incompatibility and poor interphase quality played a more significant role.

Acknowledgments

The authors acknowledge the financial support of the Natural Sciences and Engineering Research Council of Canada (NSERC) and the technical support of the Research Center on Advanced Materials (CERMA). Finally, the technical help of Yann Giroux was highly appreciated.

CHAPTER 5 THERMOPLASTIC ELASTOMERS BASED ON RECYCLED HDPE/GTR/EVA: EFFECT OF GTR REGENERATION ON MORPHOLOGICAL AND MECHANICAL PROPERTIES

Résumé

Ce travail étudie les propriétés de différents types de caoutchoucs recyclés régénérés (RR_1 et RR_2) pour produire des élastomères thermoplastiques (TPE) à base de polyéthylène haute densité recyclé (rHDPE) comme matrice. Le degré de régénération plus élevé de RR_2 (24%) par rapport à RR_1 (15%) a permis de mieux restaurer l'élasticité et la capacité de traitement de la poudrette de pneu usé (GTR). Ainsi, un meilleur enchevêtrement entre les chaînes libres de RR_2 et les macromolécules thermoplastiques a été obtenu, induisant une interaction interfaciale plus forte conduisant à un allongement à la rupture (159%) et une résistance aux chocs (342 J/m) plus élevés des mélanges avec 80% en poids de RR_2. Pour améliorer encore l'adhérence et obtenir des propriétés similaires à celles du caoutchouc, de l'éthylène-acétate de vinyle recyclé (rEVA) a été utilisé comme agent de compatibilité. L'analyse de la microstructure a montré que la dispersion uniforme des particules et l'encapsulation du GTR par rEVA augmentaient la résistance à la propagation des fissures et à la défaillance des mélanges compatibles. Le gonflement, les propriétés mécaniques et physiques des mélanges ternaires (rHDPE/GTR/rEVA) ont montré que le rEVA améliorait les interactions interfaciales entre le GTR et le rHDPE qui ont été confirmées par un allongement à la rupture (203%) et une résistance aux chocs (379 J/m) améliorés par l'ajout de 10% en poids de rEVA.

Mots-clés: Recyclage, régénération du caoutchouc, polyéthylène haute densité recyclé, caoutchouc de pneu rectifié, compatibilisation

Abstract

This work investigates the properties of different types of regenerated recycled rubbers (RR_1 and RR_2) to produce thermoplastic elastomers (TPE) based on recycled high-density polyethylene (rHDPE) as the matrix. The higher regeneration degree of RR_2 (24%) compared to RR_1 (15%) was able to better restore the elasticity and processability of the ground tire rubber (GTR). So better entanglement between RR_2 free chains and the thermoplastic macromolecules was obtained, inducing stronger interfacial interaction, leading to higher elongation at break (159%) and impact strength (342 J/m) of the blends filled with 80 wt.% RR_2. To further improve the adhesion and achieve rubber-like properties, recycled ethylene vinyl acetate (rEVA) was used as a compatibilizer. The microstructure analysis showed that uniform dispersion of the particles and GTR encapsulation by rEVA increased the resistance to crack propagation and failure of the compatibilized blends. The swelling, mechanical and physical properties of the ternary blends (rHDPE/GTR/rEVA) showed that rEVA improved the interfacial interactions between GTR and rHDPE which were confirmed by enhanced elongation at break (203%) and impact strength (379 J/m) by the addition of 10 wt.% rEVA.

Keywords: Recycling, rubber regeneration, high density polyethylene, ground tire rubber, compatibilization

5.1 Introduction

The reuse, recycling, and recovery of waste tires, as one of the largest and most problematic waste materials, is an intensively studied topic to find new applications for ground tire rubber (GTR). Tires are mainly composed of vulcanized rubbers (crosslinked thermoset structure) and different additives (stabilizers, anti-oxidants, antiozonants, etc.), making such waste not degradable (very slow) and not reprocessable by direct melting like thermoplastic [1,2]. Recently, the development and growth of thermoplastic elastomers (TPE) has gained significant attraction for using waste tires by producing polymer blends, combining the elastomer properties of rubbers with the easy processability of thermoplastics [5,9]. Several efforts have been made regarding the preparation and characterization of TPE containing GTR and thermoplastics such as low density polyethylene (LDPE) [106,129,264,265], high density polyethylene (HDPE) [266,267], or polypropylene (PP) [257,268-270]. But most of the research focused on melt blending GTR with virgin thermoplastics, while TPE production based on recycled resins is more sustainable and environmentally friendly to produce green and inexpensive TPE materials.

HDPE is one of the most common polyolefins with applications in several markets (packaging, automotive, electrical, pipes and fittings) because of its good mechanical properties, excellent processability and low cost. Therefore, using HDPE from recycled sources could produce a great advantage for GTR recycling [11,12,30]. But TPE materials, based on a physical mixture of thermoplastic and GTR (thermoset material), are generally incompatible blends with low mechanical properties [12]. It is well established that adding rubber with a crosslinked network leads to low tensile properties of the resulting thermoplastic blends, which is attributed to incompatibility and poor interfacial interaction between the phases [28]. Crosslinked rubber molecules, with restricted chain mobility, do not entangle with the matrix macromolecules to create suitable interaction, leading to GTR particles agglomeration and voids formation around the rubber particles (poor interfacial adhesion and compatibility) resulting in low mechanical properties [5]. But the addition of GTR with a vulcanized structure into a thermoplastic matrix increases the blend viscosity (processing torque) which results in difficult processing, especially as GTR content increases [11,14]. In general, increasing the GTR concentration with a three dimensional (3D) crosslinked structure and restricted chain mobility decreases the tensile properties of the resulting blends, especially the elongation at break due to poor compatibility between the components. For example, Kakroodi and Rodrigue [12] reported that the incorporation of GTR inside HDPE led to very low homogeneity as the elongation at break of GTR/HDPE (70/30) was only 64%,

while further GTR addition significantly decreased this value down to 44% at a GTR/HDPE (90/10) ratio.

But TPE compatibility can be improved via different approaches: decreasing interfacial tension, morphology stabilization, size reduction of the dispersed phase and increasing the interfacial adhesion for better stress transfer. Several methods, such as partial regeneration [197,222] and coupling agent addition [11,12,28], have been proposed to improve the compatibility between GTR and thermoplastics. Rubber crosslinked network breakdown through GTR regeneration can improve the rubber chain mobility (molecular freedom) and plasticity of recycled rubbers to promote molecular interactions and chains bonding through partially soluble fraction of regenerated rubber (RR) [218]. Also, GTR regeneration is able to induce lower friction between RR particles and lower viscosity of the blend, leading to better processability [204]. A comparison between the tensile properties of natural rubber (NR) compounds filled with 10 wt.% GTR or RR showed that blends filled with RR particles had higher tensile strength (23.2 MPa) and elongation at break (612%) compared to the tensile strength (13.7 MPa) and elongation at break (417%) of GTR based blends attributed to the presence of less carbon black and lower gel fraction (acting as stress concentration points) in RR blends [215]. Shaker and Rodrigue [129] reported that RR have smaller particle size and smoother surface compared to GTR due to particle break-up by shear/elongational forces associated with the thermomechanical regeneration process. It is expected that smaller RR particle size have higher specific surface areas compared to GTR particles, resulting in improved filler distribution, stronger interfacial bonding and better stress transfer between the components [129].

It is important to determine the relationships between the phase morphology and the mechanical properties of TPE. In general, a minimum of 100% elongation at break is required [22]. This can be easily achieved with polyolefins (mainly polyethylene (PE)). But these resins are non-polar and have low affinity for blending with GTR or RR. Nevertheless, the addition of copolymers, such as ethylene vinyl acetate (EVA) [252,271] or ethylene-octene copolymer (POE) [57], can act as a bridge (coupling agent) to improve the interactions between the matrix and the rubber particles. These copolymers are practical compatibilizers to improve the interfacial adhesion and uniform distribution through the encapsulation of filler particles during melt mixing [57,252]. EVA copolymers having rubber-like properties with excellent ozone, weather and stress-crack resistance are good compatibilizers for TPE [19]. Mészáros et al. [252] reported that EVA (20 wt.%) produced strong adhesion between LDPE and GTR as the elongation at break of LDPE/GTR blends increased by 60% (from 100% to 160%), while

the rubber-like nature of EVA decreased the tensile modulus by 25% (from 80 MPa to 60 MPa). In a similar study, the addition of EVA as a polar compatibilizer into recycled low-density polyethylene (rLDPE)/LDPE/GTR (40/30/30) blends increased the elongation at break from 125% to 225% due to GTR encapsulation by EVA reducing the surface energy of the components to form a strong interphase [20].

In our previous work, recycled high-density polyethylene (rHDPE)/GTR blends (RR and non-regenerated rubber; NRR) recycled rubber contents between 0 to 90 wt.%) showed clear incompatibility and low interfacial adhesion between rHDPE and GTR (RR and NRR) for all formulations. The results showed that melt blending of rHDPE with 80 wt.% of GTR yielded elongation at break of 129% and 50% for NRR and RR blends, respectively. In this work, the main objective is to study the effect of GTR regeneration (evaluation of the regeneration degree and crosslink density) and blend composition on the swelling, morphological, mechanical, and physical properties of highly filled TPE blends (above 70 wt.% GTR) by comparing different regenerated rubbers. NRR and two types of RR particles (RR_1 and RR_2) in the range of 70, 80 and 90 wt.% were introduced into rHDPE via continuous melt-mixing in a twin-screw extruder and the specimens were compression molded for further analysis. Also, the effect of recycled ethylene vinyl acetate (rEVA) content (5-15 wt.%) as a compatibility/interfacial adhesion promoter is investigated to produce ternary blends of rHDPE/GTR/rEVA.

5.2 Experimental

5.2.1 Materials

The rHDPE was kindly provided by Gaudreau (Victoriaville, QC, Canada) and used as the matrix. This polymer has a melt flow index (MFI) of 1.3 g/10 min (190 °C and 2.16 kg) according to ASTM D1238. The density (ASTM D2856) and melting point (ASTM D3418) of the rHDPE are 0.967 g/cm^3 and 129.5 °C, respectively. The GTR particles were provided by Phoenix Innovation Technology (Montreal, QC, Canada) from the same source of off-the-road (OTR) waste tires composed of NR as the main component. Such GTR particles were exposed to two different regeneration process by Phoenix Innovation Technology and were used as received in three forms: regenerated rubber (RR_1) with an average particle size of ~600 µm and a density of 1.246 g/cm^3; regenerated rubber (RR_2) with an average particle size of ~500 µm and a density of 1.193 g/cm^3; and a NRR with an average particle size of ~300 µm and a density of 1.169 g/cm^3. The rEVA, as a copolymer of ethylene and vinyl acetate, was kindly provided by Ecofib (Drummondville, QC, Canada) and was used as received. This

copolymer has a density of 0.946 g/cm^3 and a MFI of 1.81 g/10 min (190 °C and 2.16 kg) according to ASTM D1238.

5.2.2 Processing

The rHDPE thermoplastic matrix, GTR (NRR, RR_1 and RR_2) particles, and rEVA were compounded using a Leistritz ZSE-27 twin-screw extruder with a L/D ratio of 40 and 10 heating zones coupled to a circular die (2.7 mm in diameter). Different amounts of GTR particles (70, 80 and 90 wt.%) were used to produce the compounds according to the formulation presented in Table 5.1. The temperature of the extruder was set at 175 °C for all zones to prevent degradation, while the screw speed was set at 100 rpm. As shown in Figure 5.1, the rHDPE/rEVA was dry-blended and fed to the extruder through the first zone (main feeder), while the GTR particles were fed through a side feeder (zone 4). The overall flow rate was 3 kg/h for all the blends to prevent high motor torque and die pressure associated to the high viscosity of GTR containing compounds. Then, the compounds were cooled in a water bath and pelletized using a model 304 pelletizer (Conair, Stanford, USA). Next, the pellets were dried in a convection oven for 6 h at 75 °C to eliminate any residual water before compression molding. The molding was performed at 180 °C using 3 min of preheating without pressure and 5 min of pressing under a load of 3 tons using an automatic compression molding press (Carver, AutoFour/1512-PL,H, 3893, USA) with mold dimensions of 115 x 115 x 3 mm^3.

Table 5.1 Coding and formulation of the samples produced

Sample code	rHDPE (wt.%)	NRR (wt.%)	RR_1 (wt.%)	RR_2 (wt.%)	rEVA (wt.%)
rHDPE	100	-	-	-	-
N70	30	70	-	-	-
R70	30	-	70	-	-
RR70	30	-	-	70	-
N80	20	80	-	-	-
R80	20	-	80	-	-
RR80	20	-	-	80	-
N90	10	90	-	-	-
R90	10	-	90	-	-
RR90	10	-	-	90	-
N70(5)	25	70	-	-	5
N70(10)	20	70	-	-	10
N70(15)	15	70	-	-	15
N80(5)	15	80	-	-	5
N80(10)	10	80	-	-	10
N80(15)	5	80	-	-	15
R70(5)	25	-	70	-	5
R70(10)	20	-	70	-	10
R70(15)	15	-	70	-	15
R80(5)	15	-	80	-	5
R80(10)	10	-	80	-	10
R80(15)	5	-	80	-	15
RR70(5)	25	-	-	70	5
RR70(10)	20	-	-	70	10
RR70(15)	15	-	-	70	15
RR80(5)	15	-	-	80	5
RR80(10)	10	-	-	80	10
RR80(15)	5	-	-	80	15

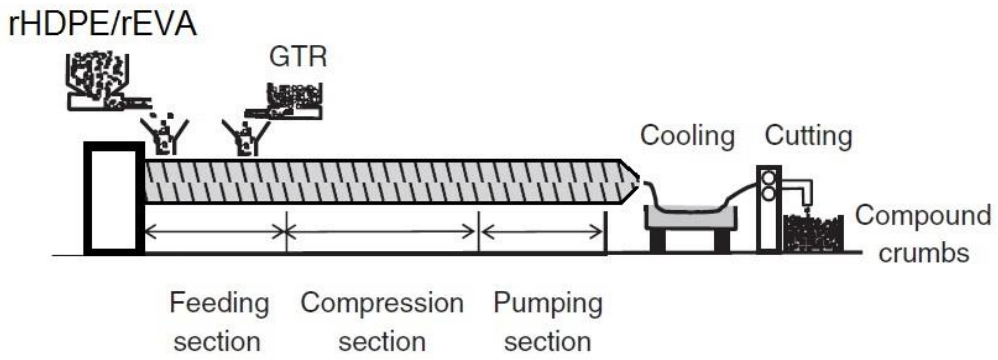

Figure 5.1 Schematic representation of the melt blending process for rHDPE/GTR/rEVA compounds

5.2.3 Characterization

5.2.3.1 Thermogravimetric analysis (TGA)

Thermal stability of the raw materials was investigated via TGA on a Q5000 IR (TA Instruments, New Castle, USA) at a heating rate of 10 °C min^{-1} from 50 to 850 °C. The tests were performed in nitrogen and air to evaluate both the thermal and oxidative resistance of the materials.

5.2.3.2 Morphological observation

An Inspect F50 scanning electron microscope (SEM) (FEI, Hillsboro, USA) was used at 15 kV to take micrographs of the GTR particles and observe the interfacial adhesion quality inside the blends. The samples were cryogenically fractured in liquid nitrogen and the surface coated with gold/palladium to be observed at different magnifications.

5.2.3.3 Swelling degree and regeneration degree

The crosslink density was determined according to ASTM D6814 via equilibrium swelling in toluene at room temperature. Firstly, acetone was used to remove the low molecular weight (MW) substances of GTR such as processing oils for 16 h. Then, constant weight (0.5 or 1 g) specimens were immersed in toluene at room temperature for 72 h and the swollen samples were weighted. Then samples were dried overnight in an oven at 70 °C and the dried samples were weighted. After three repetition for each specimen, the crosslink density was calculated according to the Flory-Rehner equation as [184]:

$$\eta_{swell} = \frac{-[\ln(1 - v_r) + v_r + \chi v_r^2]}{\left[v_s \left(v_r^{1/3} - V_r\right)/2\right]} \quad (5.1)$$

where η_{swell} is the crosslink density (mol/cm^3), V_r is the rubber volume fraction in the swollen sample, V_s is the solvent molar volume (106.2 cm^3/mol for toluene) and χ is the polymer-solvent interaction parameter (0.391 for toluene) [195].

The rubber volume in the swollen sample was calculated according to:

$$V_r = \frac{W_r/d_r}{W_r/d_r + W_s/d_s} \quad (5.2)$$

where W_r and W_s are the weight fraction of the dry rubber sample and weight fraction of the solvent absorbed by the sample (g) respectively, while d_r and d_s are the density of the dry rubber sample and density of the solvent (g/cm^3), respectively.

The regeneration degree of RR_1 and RR_2 were evaluated as a function of the crosslink density as:

$$\% \text{ Regeneration} = \left(1 - \frac{\xi}{\xi_0}\right) \times 100 \quad (5.3)$$

where ξ and ξ_0 are the crosslink densities of RR (RR_1 or RR_2) and NRR, respectively.

The sol fraction was determined according to:

$$\text{Sol fraction}(\%) = \frac{W_0 - W_r}{W_0} \times 100\% \quad (5.4)$$

$$\text{Gel fraction } (\%) = 100 - \text{Sol fraction } (\%) \quad (5.5)$$

where W_0 and W_r are the initial weight of the sample (g) and the weight of the dried sample (g), respectively.

In order to analyze the crosslink structure, the swelling degree (swelling ratio) of the blend samples was determined by equilibrium swelling of the specimens in a solvent according to ASTM D471-16a. Around 0.5 g of sample was immersed in 100 ml toluene at room temperature for 72 h to achieve an

equilibrium state of swelling. The swollen samples were taken out periodically and excess liquid on the specimen surface was removed with filter paper and the swollen sample was weighed. The swelling degree (Q) was calculated as:

$$Q = \frac{m_t - m_0}{m_0} \times 100\% \quad (5.6)$$

where m_t and m_0 are the mass of the swollen sample (g) and the mass of the sample (g), respectively.

5.2.3.4 Mechanical testing

Tensile tests were performed at room temperature according to ASTM D638 using a 500 N load cell and a tensile speed of 10 mm/min on an Instron (Instron, Norwood, USA) universal mechanical tester model 5565. At least 5 dog bone specimens (type V) were used for each blend composition. The average values of the tensile strength (σ_Y), Young's modulus (E) and elongation at break (ε_b) were reported with their standard deviations.

Flexural tests were done on an Instron (Instron, Norwood, USA) model 5565 with a 50 N load cell according to ASTM D790 at room temperature. Rectangular specimens with dimensions of 60 mm x 12.7 mm^2 were tested with 5 repetitions for each sample in a three-point bending mode (span length of 60 mm) at a speed of 2 mm/min.

Notched Charpy impact strength was measured on a Tinius Olsen (Horsham, USA) model 104 at room temperature according to ASTM D256. At least 10 specimens with dimensions of 60 mm x 12.7 mm^2 were used for each sample. Before testing, all the samples were automatically V-notched on a Dynisco (Franklin, USA) model ASN 120m sample notcher 24 h before testing.

5.2.3.5 Physical properties

Hardness values (Shore A and Shore D) were measured by using a 307L model durometer (PTC Instruments, Boston, USA) with 10 measurements for each sample.

Density measurements were performed on a gas (nitrogen) pycnometer Ultrapyc 1200e (Quantachrome Instruments, Boynton Beach, USA). The test was repeated three times for each sample.

5.3 Result and Discussion

5.3.1 TGA analysis

Figure 5.2 presents the weight curves (TGA) and their derivative (derivative thermogravimetry; DTG) for the raw materials used: rHDPE, rEVA and GTR (NRR, RR_1 and RR_2). The curves under nitrogen show that the initial degradation of rHDPE is around 400 °C, while the maximum decomposition rate is around 490 °C. The decomposition of rEVA occurs in two steps. The initial weight loss between 250 and 350 °C is related to the deacetylation process in which acetic acid is released and C=C bonds form along the polymer backbone. The second degradation step (between 350 and 500 °C) is attributed to the oxidation and volatilization of hydrocarbons resulting from the decomposition of the backbone [272]. The thermal decomposition of all GTR (NRR, RR_1 and RR_2) obtained from same source of OTR recycled rubber begins around the same temperature (200 °C), so the processing temperature for all TPE blends should not exceed 200 °C to avoid negative effects on the final TPE properties. The first decomposition step between 200 and 350 °C can be related to the evaporation or decomposition of processing oils, additives and other compounds with low molar mass and/or low boiling temperature in the GTR formulation [273]. The second decomposition step between 350 and 430 °C can be related to the decomposition of the polymeric material present in the tire rubber such as NR. The last stage of decomposition (430 to 800 °C) is ascribed to the residual materials. The char residues in an inert atmosphere (nitrogen) are about 32.2, 33.6 and 33.9% for NRR, RR_1 and RR_2 respectively, indicating the presence of inorganic particles in GTR. The breakup of crosslinks during regeneration can thermally destabilize the rubber and promote its degradation at lower temperatures. However, the higher char residue of RR (RR_1 and RR_2) particles than NRR particles can be attributed to the presence of higher amounts of carbon black which act as a physical barrier and adsorb low MW volatile products formed during thermal degradation, thus improving their apparent thermal stability, as reported elsewhere [132]. The DTG curve of NRR, RR_1 and RR_2 in nitrogen shows a wide bump between 350 and 430 °C which is composed of two peaks. This two-stage decomposition of GTR under an inert atmosphere might be attributed to the different decomposition temperature of natural and synthetic rubbers [274]. The small peak or shoulder close to the main peaks around 220 °C is representative of other additives degradation [222].

It was expected that exposure to oxygen under air decreases the thermal stability of all recycled materials. The rHDPE has almost no branches in its molecular structure (HDPE), leading to high

thermal stability. As expected, the thermal stability of rHDPE decreased due to the presence of oxygen in air, while the initial weight loss of rHDPE started earlier at around 300 °C (Figure 5.2 c) and the DTG curve of rHDPE shows a single peak at 430 °C [275]. The TGA curves of rEVA under air shows that the thermal degradation included similar stages as the TGA curves in N_2. The loss of acetic acid, because of the decomposition of vinyl acetate groups and the decomposition of polyethylene chains, is responsible for this degradation stage under air, while almost no residue was left [276]. Figure 5.2 c shows that the initial weight loss of GTR (NRR, RR_1 and RR_2) starts around 200 °C and all GTR particles degraded almost completely around 570 °C. Also, the DTG curves of GTR present several peaks between 250 and 530 °C related to the GTR decomposition and its complex structure as a mixture of various components. The highest decomposition temperature of GTR might be attributed to the oxidation of carbon residues generated at lower temperatures, leading to the formation of carbon dioxide [277].

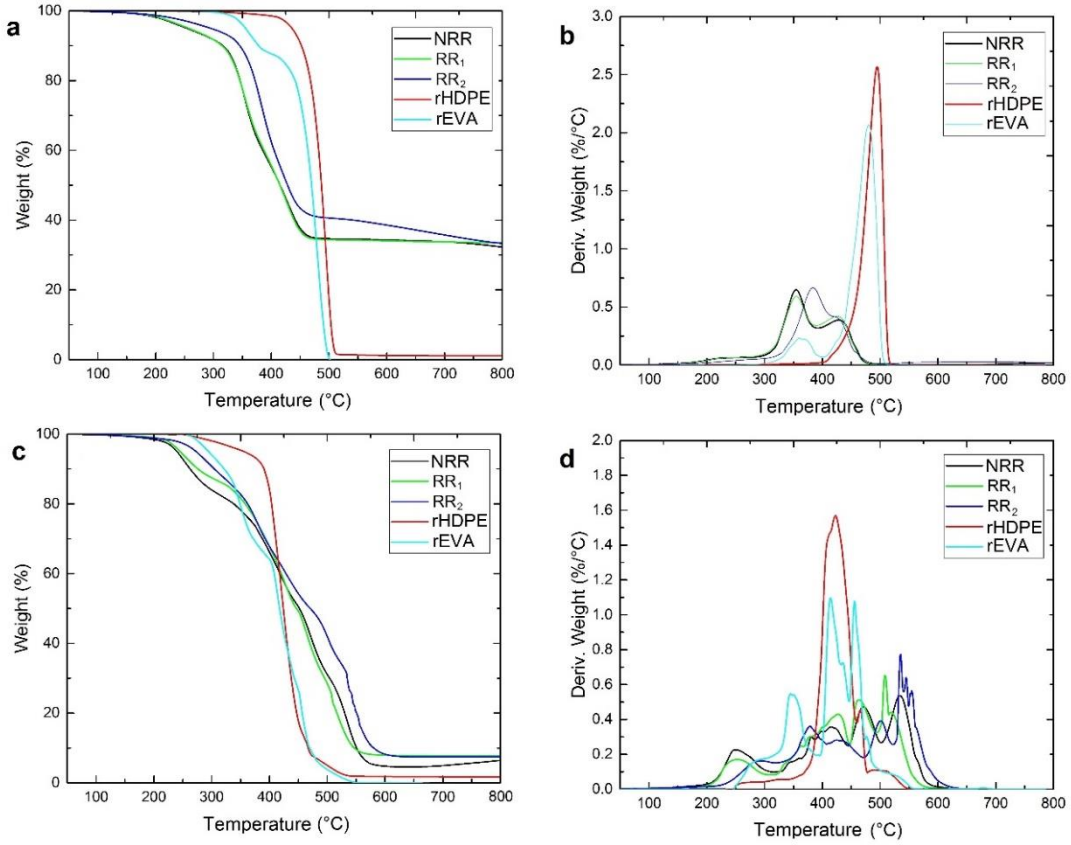

Figure 5.2 TGA and DTG curves of the raw materials in: (a, b) nitrogen and (c, d) air.

5.3.2 Swelling properties

Table 5.2 presents the sol fraction, gel fraction, crosslink density and regeneration degree of the GTR particles before (NRR) and after regeneration (RR_1 and RR_2). This information is a direct quantification of the extent of rubber network breakup during regeneration. Upon GTR regeneration, the sol fraction increased from 2.6% for NRR, to 6.5% and 11.6% for RR_1 and RR_2, respectively. Higher sol fraction of RR particles compared to NRR particles is related to random crosslink (polysulfidic, disulfidic and monosulfidic) and polymer chain scission by mechanical shearing and heat during the thermo-mechano-chemical regeneration of GTR (NRR). The shear forces might cause unselective scission of the rubber main chains and the reduction of the performance of RR particles [278]. The crosslink density of NRR particles decreased from 7.2×10^{-4} mol/cm^3 to 6.1×10^{-4} mol/cm^3 (RR_1) and 5.5×10^{-4} mol/cm^3 (RR_2) after rubber regeneration. The immobilized fraction of rubber chains decreased with decreasing crosslink density of RR because the vulcanized network is partially broken-up which increased the chain mobility and flexibility of the polymer, while lower chain restriction leads to low rigidity and modulus after regeneration. It is clear that both the gel fraction and crosslink density of NRR decreased after regeneration, so the breakdown of the rubber crosslinked structure led to restore GTR plasticity and reprocessability. The regeneration degree of RR_1 and RR_2 are 15.2% and 24.1%, respectively. Lower regeneration degree of RR_1 means that a higher crosslink density remains in the particles compared to RR_2. But more crosslinked molecular chains will result in a more uneven stress distribution and lower tensile strength, as described later [25]. Another reason for the higher regeneration degree of RR_2 might be related to a more selective cleavage of the sulfur crosslinks with less molecular main chains scission compared to the RR_1 regeneration in which main chain scission is dominant, resulting in a drop of MW and a loss of mechanical strength for RR_1 blends [279]. The regeneration degree is the main parameter controlling the processing and mechanical performance of TPE blends filled with RR particles, as described later.

Table 5.2 Sol and gel fraction, crosslink density and regeneration degree of the GTR particles.

Sample	Sol fraction (%)	Gel fraction (%)	Crosslink density (10^{-4} mol/cm^3)	Regeneration degree (%)
NRR	2.6 (0.1) *	97.4 (0.1)	7.2	-
RR_1	6.5 (0.1)	93.5 (0.1)	6.1	15.2 (0.6)
RR_2	11.6 (0.2)	88.4 (0.2)	5.5	24.1 (0.9)

**(Standard deviation)*

The swelling degree of rubber compounds represents the sorption behavior of a solvent, such as toluene, to determine the crosslink density of TPE. An inverse relation between the swelling degree and the crosslink density exists as lower swelling degree, imply a higher crosslink density [8]. The swelling test was performed to evaluate the swelling degree of the TPE blends to determine the effect of GTR regeneration and toluene uptake on the mechanical properties as discussed later. The swelling degree of compatibilized (rHDPE/GTR/rEVA) and uncompatibilized (rHDPE/GTR) blends are presented in Table 5.3. Increasing the GTR content leads to higher swelling degrees due to a higher elastomer content, which in turn results in the absorption of more toluene. This observation is in agreement with other reports showing that GTR particles contain some soluble molecules which can absorb the solvent and swell [280]. Increasing the GTR content by 10% (from 70 to 80 wt.%) in rHDPE/GTR blends increased the swelling degree of N80 from 138 to 145%, while the swelling degree of RR_1 and RR_2 blends increased from 160% to 169% and from 172% to 180%, respectively. This difference is attributed to the lower resistance to non-polar solvents of partially destroyed crosslinked structure of RR particles which promotes swelling [281]. The higher swelling degree of RR blends compared to NRR blends is associated to the lower crosslink density of RR_1 (6.1×10^{-4} mol/cm^3) and RR_2 (5.5×10^{-4} mol/cm^3) compared to NRR (7.2×10^{-4} mol/cm^3) particles [14]. Also, the presence of fillers and other non-crosslinkable products in the blends can affect the swelling degree, as the rHDPE/GTR/rEVA blends show lower toluene uptake compared to rHDPE/GTR blends. For example, by adding 10 wt.% rEVA, the swelling degree of rHDPE/GTR (20/80) blends decreased by 1.4% (from 145 to 143%), 3.9% (from 169 to 163%) and 2.9% (from 180 to 175%) for NRR, RR_1 and RR_2 blends, respectively. This observation might be related to good filler/matrix interaction, favorable for interfacial interaction, resulting in lower voids in the blends, leading to more difficult solvent penetration [282].

Table 5.3 Swelling degree of the rHDPE/GTR and rHDPE/GTR/rEVA blends. See Table 5.1 for sample composition.

Sample	Swelling degree (%)	Sample	Swelling degree (%)	Sample	Swelling degree (%)
N70	138 (0.7)	**R70**	160 (0.8)	**RR70**	172 (0.9)
N80	145 (0.6)	**R80**	169 (0.8)	**RR80**	180 (0.8)
N90	154 (0.8)	**R90**	187 (0.8)	**RR90**	192 (0.7)
N70(5)	135 (0.4)	**R70(5)**	159 (0.6)	**RR70(5)**	168 (0.5)
N70(10)	131 (0.3)	**R70(10)**	157 (0.4)	**RR70(10)**	164 (0.5)
N70(15)	132 (0.8)	**R70(15)**	143 (0.7)	**RR70(15)**	154 (0.7)
N80(5)	144 (0.5)	**R80(5)**	168 (0.4)	**RR80(5)**	178 (0.6)
N80(10)	143 (0.6)	**R80(10)**	163 (0.8)	**RR80(10)**	175 (0.9)
N80(15)	140 (0.3)	**R80(15)**	162 (0.4)	**RR80(15)**	171(0.4)

5.3.3 Morphological observation

Figure 5.3 presents SEM micrographs of the rHDPE/GTR blends at two different GTR content (80 and 90 wt.%) to show the effect of the blend composition and regeneration process on the GTR distribution and the interfacial adhesion between the components. Increasing the GTR concentration is expected to create a less homogeneous structure due to the difficult dispersion of highly crosslinked rubber particles in a highly viscous thermoplastic matrix [12]. As shown in Figure 5.3, a clear distinction between the rubber particles (NRR, RR_1 and RR_2) and rHDPE with interfacial gaps implies a weak interface, which is getting worse with increasing the GTR content from 80 to 90 wt.% (Figure 5.3 d, e and f). In fact, the clean fractured surface of the blends indicates an easy removal of weekly connected GTR particles from the rHDPE thermoplastic related to a lack of strong interfacial bonding, which is more evident in RR_1 blends (Figure 5.3 b and e) and higher GTR loading (90 wt.%). The high surface energy between the GTR and rHDPE leads to limited interfacial stress transfer, so failure occurs at the interface, as crack initiation and propagation are easy [20]. Melt mixing of rHDPE with 80 wt.% RR_2 led to the production of more homogeneous blends (Figure 5.3 c) compared to the blends containing the same concentration of NRR (Figure 5.3 a) or RR_1 (Figure 5.3 b). The higher sol fraction of RR_2 11.6%)

results in better bonding with the polymer matrix to improve interfacial adhesion between the phases [54].

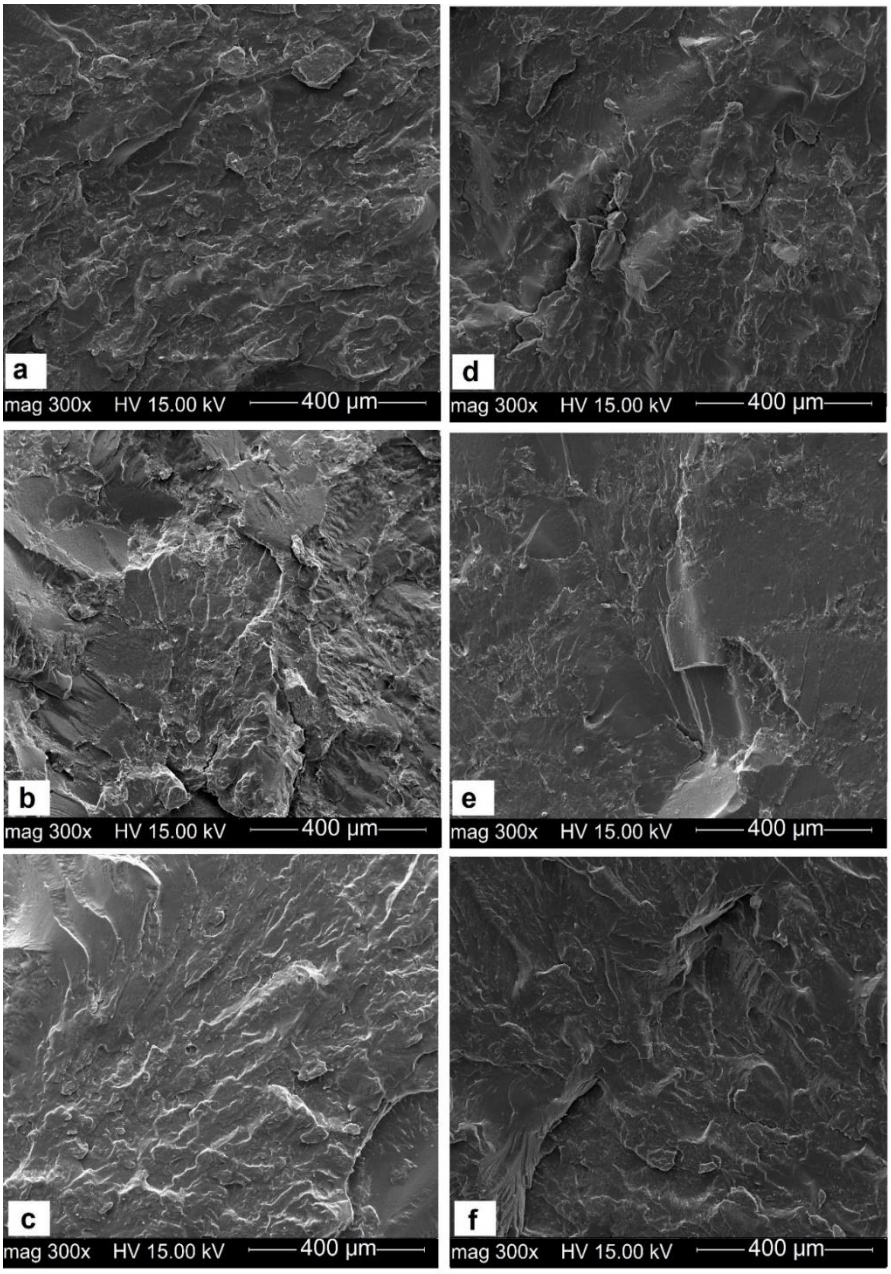

Figure 5.3 SEM micrograph of: (a) N80, (b) R80, (c) RR80, (d) N90, (e) R(90) and (f) RR(90). See Table 5.1 for sample composition.

Figure 5.4 shows typical SEM micrographs of the fractured surface of rHDPE/GTR/rEVA blends containing 10 wt.% rEVA to determine the effect of a compatibilizer on the state of interfacial adhesion and compatibility in the blends. It is known that in multicomponent blends, the fracture behavior strongly depends on the interfacial bonding between the components [20]. So good compatibility in the blends

leads to failure starting in the continuous phase instead of the interface generating higher mechanical properties [12].

The clean and smooth fractured surface of R80(10) (Figure 5.4 a) implies an easy detachment and pull-out of RR_1 particles from the rHDPE matrix under tensile stress. On the other hand, the rough fracture surface of RR80(10) (Figure 5.4 c) indicates that RR_2 particles are strongly embedded in the rHDPE matrix and higher energy is required for their detachment. This observation is related to the incomplete dispersion and agglomeration of RR_1 particles due to the low compatibility between the recycled rubber (RR_1) and rHDPE and low stress transfer [57]. In RR80(10), the rubber particles are more uniformly dispersed in rHDPE (Figure 5.4 c), and detection of the rubber phase is difficult even at high magnification (Figure 5.4 d). Li et al. [57] calculated the interfacial tension between polymer pairs in HDPE/GTR/elastomer composites and predicted that the lower interfacial tension of GTR/elastomer compared to HDPE/GTR can lead to GTR encapsulation by the elastomer (rEVA). Also, Lima et al. [257] observed that EPDM was able to encapsulate GTR particles to create an interphase between a thermoplastic PP matrix and crosslinked GTR particles, thus improving the blends compatibility. As shown in Figure 5.4 d, no gap between each phase is observed, so it can be concluded that some rubber particles are covered by the elastomer, leading to a lower surface energy between the RR_2 and rHDPE phases, improving the fine dispersion of RR_2 particles. Similar observations have been reported for PP/filler/elastomer composites with the addition of rEVA as a polar elastomer covering filler particles (calcium carbonate) and resulting in PP/filler composites with an encapsulated structure [283]. Figure 5.5 presents a schematic representation of the compatibilization mechanism for a thermoplastic/GTR/elastomer system in which the GTR particles are encapsulated by rEVA. Decreasing the rubber particles size results in higher probability of GTR particles encapsulation by the elastomer leading to the formation of a strong interphase between the components [106]. The presence of processing oil in RR_1 might lead to particle swelling and agglomeration, so large rubber particles with

lower specific surface area limit the possibility of RR_1 encapsulation by rEVA to form a strong interphase.

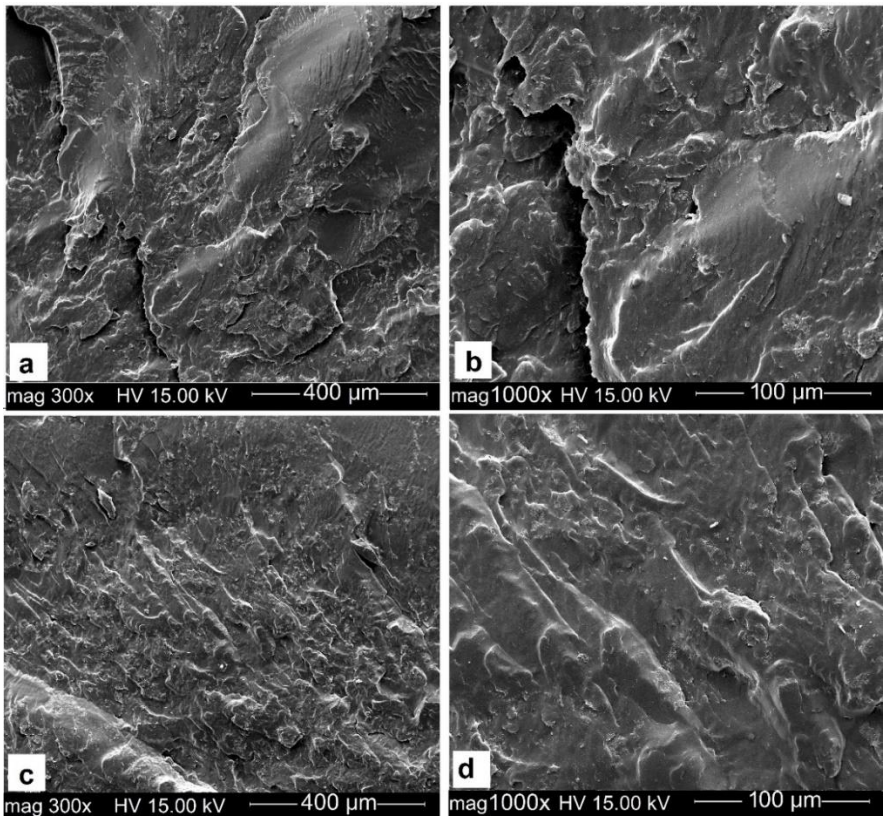

Figure 5.4 SEM micrographs of: (a, b) R80(10) and (c, d) RR80(10).

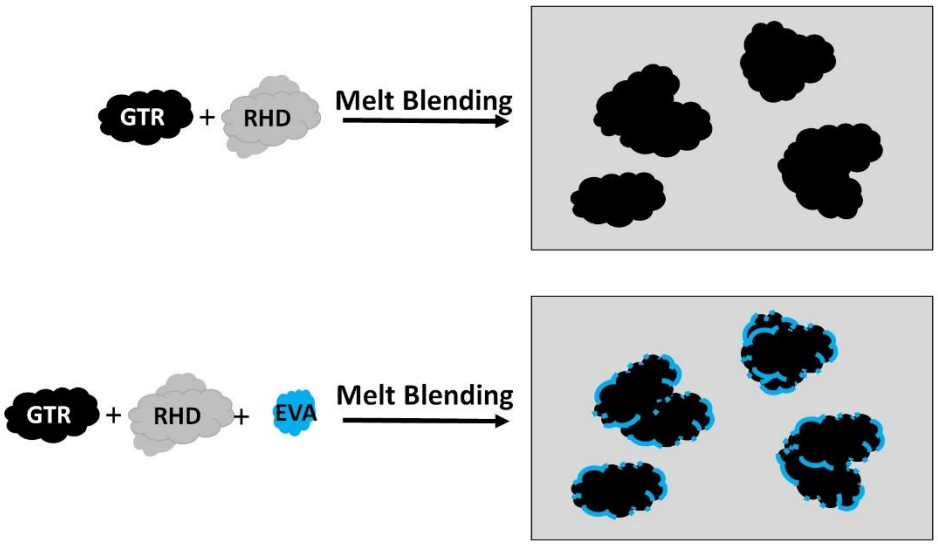

Figure 5.5 Proposed compatibilization mechanism of a thermoplastic (rHDPE)/GTR/elastomer (rEVA).

5.3.4 Mechanical properties

5.3.4.1 Tensile properties

As shown in Figure 5.6, the tensile strength of rHDPE decreased from 21.3 MPa to 3.1, 2.1 and 3.4 MPa after melt blending with 80 wt.% of NRR, RR_1 and RR_2, respectively. This can be attributed to the presence of GTR particles acting as stress concentration points (crack initiation points) [30] and lack of entanglement between the crosslinked GTR and thermoplastic matrix resulting in low affinity (incompatibility) and weak interfacial adhesion [252]. Other reasons for the lower tensile properties after rubber incorporation originates from GTR exposure to ozone, mechanical and thermal degradation during its service life and also during the grinding process [251]. The tensile strength of RR_2 blends is higher than for RR_1 blends because of the lower gel fraction (88.4%) and crosslink density (5.5×10^{-4} mol/cm^3) of RR_2 compared to the gel fraction (93.5%) and crosslink density (6.1×10^{-4} mol/cm^3) of RR_1. Higher crosslink density and limited mobility of the RR_1 molecular chains caused uneven stress distribution and the lower tensile strength of RR_1 blends [57]. Addition of rEVA (10 wt.%) showed slight tensile strength increase from 3.4 MPa for RR80 to 3.6 MPa for RR80(10) because of enhanced dispersion of recycled rubber particles in the thermoplastic resin (compatibilizing effect of rEVA) and enhanced interaction between rHDPE and the soluble fraction of RR_2 (11.6%). However, incorporation of 15 wt.% rEVA led to a tensile strength drop since an excessive amount of compatibilizer partially destroys the continuity of the rHDPE matrix, leading to lower mechanical strength [284].

As shown in Figure 5.7, the Young's modulus of the rHDPE/GTR composites decreased from 364.7 MPa (rHDPE) to 16.4, 14.2 and 14.8 MPa after melt blending with 80 wt.% NRR, RR_1 and RR_2, respectively. Significant decrease in Young's modulus with GTR content was expected due to the inherent soft nature of the rubber phase [129]. Incorporation of a compatibilizer (rEVA) led to better compatibility between rHDPE and GTR, improving the stress transfer from the matrix to the rubber particles leading to lower rigidity of the compounds [29]. Addition of 10 wt.% EVA into rHDPE/GTR (20/80) decreased the Young's modulus of NRR, RR_1 and RR_2 blends by 65% (from 16.4 to 5.7 MPa), 66% (from 14.2 to 4.8 MPa) and 63% (from 14.8 to 5.4 MPa), respectively. Also, a decreasing trend in Young's modulus with increasing rEVA content is ascribed to the low modulus of rEVA (26 MPa) compared to rHDPE (364.7 MPa). Mészáros et al. [20] also concluded that increasing the rEVA content (from 10 to 30 wt.%) substantially decreased the Young's modulus of rLDPE/LDPE/GTR/rEVA (40/20/30/10) from 310 MPa to 180 MPa (40/0/30/30).

The elongation at break is the most important property to determine the compatibility and homogeneity of TPE blends [12]. Although the elongation at break of NRR blends increased from 61.9 to 127.6% with increasing NRR content from 70 to 80 wt.% due to the presence of a more elastic content, the values are much less than for the rHDPE matrix (1060%) (Figure 5.8). Similarly, Li et al. [57] reported decreasing elongation at break of HDPE from 800 to 33% after the addition of 40 wt.% GTR. The poor GTR distribution in the polymer matrix promoted particle-particle interactions and contributed to weak sites upon stress-transfer between the rubber and matrix interface which are failure points [215]. In general, the regeneration process leads to more free chains via partial breakdown of the rubber network improving possible interactions between GTR and the corresponding polymer matrix. However, melt blending rHDPE with 80 wt.% regenerated rubber show different elongation at break of 50% and 159% for R80 and RR80, respectively. This observation can be attributed to the higher sol fraction of RR_2 (11.6%) compared to RR_1 (6.5%) which promoted interfacial adhesion between the soluble content of RR_2 and rHDPE and hence higher plastic deformation of RR80 [285]. Also, it can be proposed that a more efficient regeneration of RR_2 (24.1%) to break-up the vulcanized structure with less scission of the main chains contributes to the higher plastic deformation of RR_2 blends [286]. The regeneration process is not a 100% selective rupture of sulfur bonds alone, and might also produce degradation of the main chains of the recycled rubber during regeneration (extensive shear and high temperature), lowering the MW and degrading the tensile properties [25].

Figure 5.8 shows that the addition of 10 wt.% rEVA increased the elongation at break of N80(10), R80(10) and RR80(10) to 144% (from 128%), 58% (from 51%) and 203% (from 159%), respectively. In agreement with other observations, this behavior shows the effect of rEVA on improving the mechanical properties by reducing the stress concentration around the particles (GTR encapsulation) and inhibiting fracture phenomena [20,57,106]. It must be pointed out that increasing the rEVA content also decreased the rHDPE content in our case.

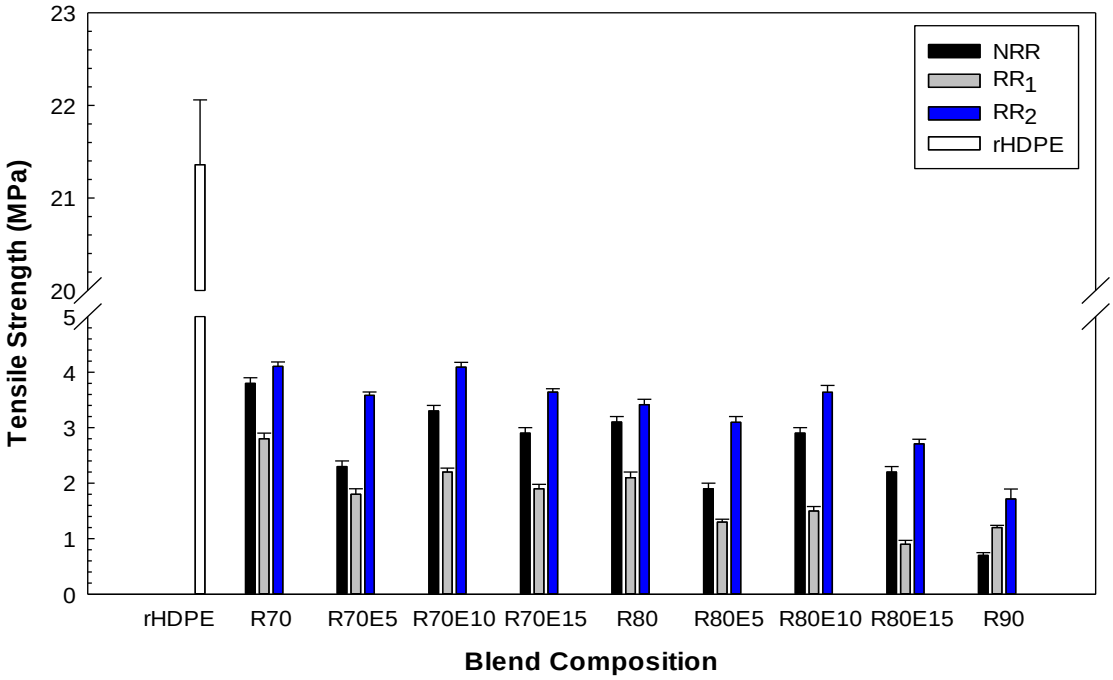

Figure 5.6 Tensile strength of the rHDPE/GTR and rHDPE/GTR/rEVA blends. See Table 5.1 for sample composition.

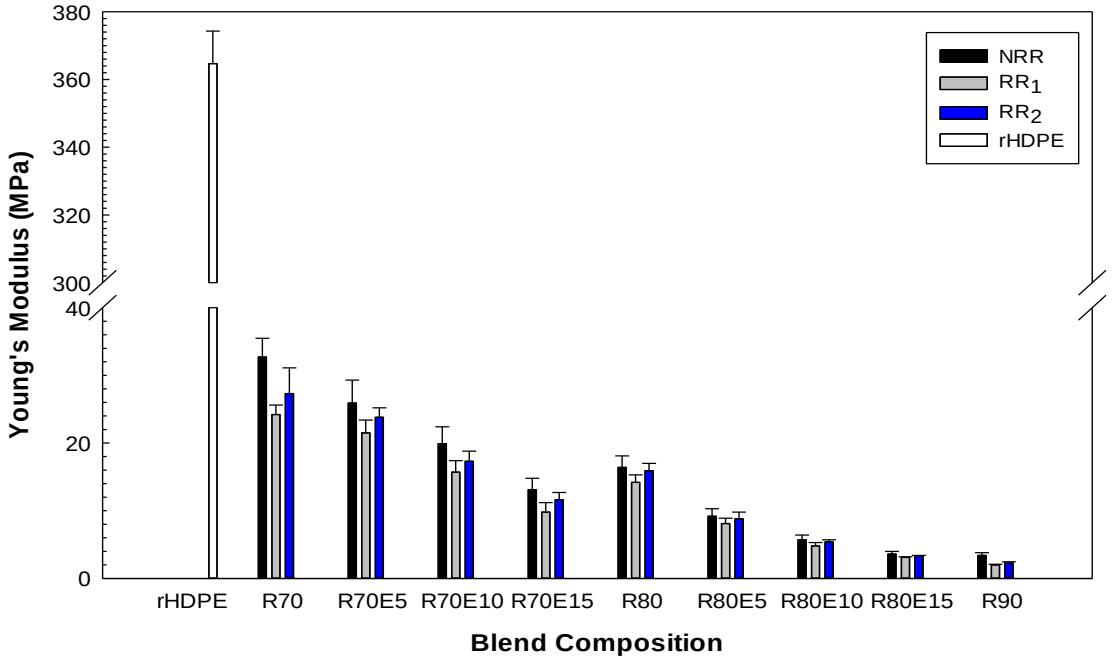

Figure 5.7 Young's modulus of the rHDPE/GTR and rHDPE/GTR/rEVA blends. See Table 5.1 for sample composition.

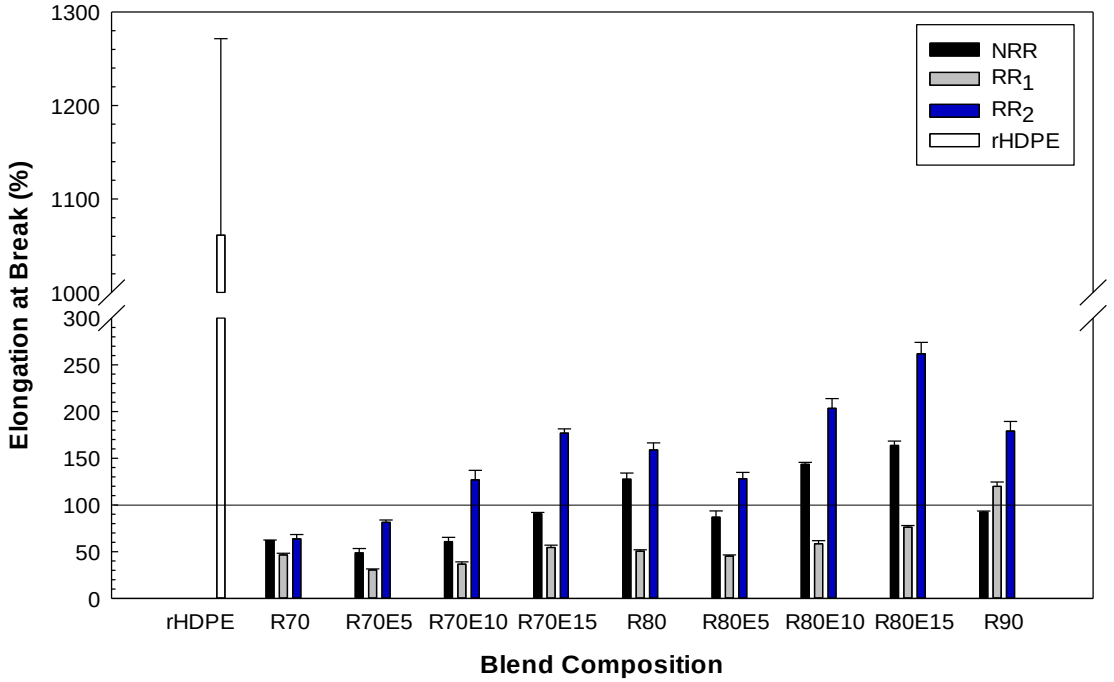

Figure 5.8 Elongation at break of the rHDPE/GTR and rHDPE/GTR/rEVA blends. See Table 5.1 for sample composition.

The results of flexural modulus are presented in Figure 5.9. Increasing the GTR content from 70 to 80 wt.% decreased the flexural modulus of NRR, RR_1 and RR_2 blends by 50% (from 39.3 to 19.5 MPa), 32% (from 27.9 to 18.8 MPa) and 47% (from 36.5 to 19.2 MPa), respectively. The soft nature of GTR as a low modulus phase and the presence of interfacial voids/defects are responsible for the decreasing flexural modulus trend with increasing GTR content similar to the Young's modulus (Figure 5.7). Incorporation of NRR with a vulcanized structure and higher crosslink density than RR_1 and RR_2 particles (Table 5.2), as well as further chain mobility restriction, led to more rigidity and higher flexural modulus of the NRR blends. It should be noticed that GTR regeneration leads to smaller fragments and shorter chains of RR which can act as plasticizers, as well as the presence of a processing oil used in regeneration, so the flexural modulus of blends with RR_1 and RR_2 are lower than that of NRR blends. The flexural modulus also substantially decreased with the presence of a with low modulus rEVA. For example, adding 10 wt.% of rEVA into blends with 80 wt.% GTR decreased the flexural modulus by 42% (from 19.5 to 11.3 MPa), 50% (from 18.8 to 9.3) and 43% (from 19.2 to 10.8 MPa), for NRR, RR_1 and RR_2 blends, respectively.

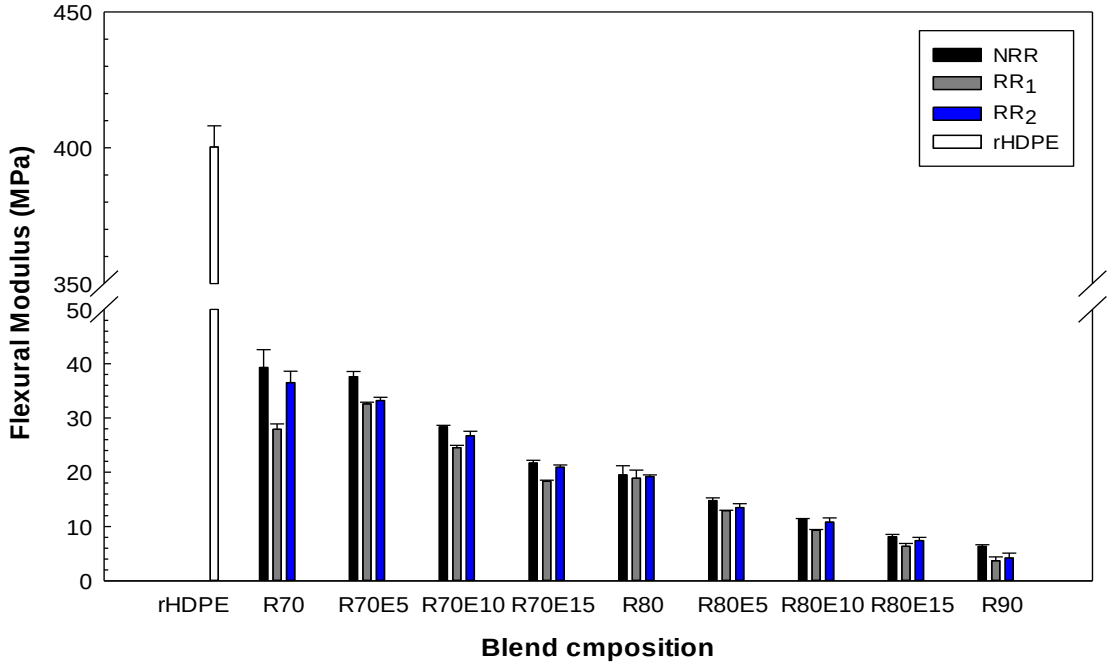

Figure 5.9 Flexural modulus of the rHDPE/GTR and rHDPE/GTR/rEVA blends. See Table 5.1 for sample composition.

5.3.4.2 Impact strength

As shown in Figure 5.10, increasing the GTR content from 70 to 80 wt.% increased the impact strength for all the formulations. The higher impact strength of RR80 (342 J/m) compared to that of N80 (321 J/m) and R80 (236 J/m) can be attributed to better interfacial adhesion between RR_2 and rHDPE (Figure 5.3 and Figure 5.4) inhibiting crack propagation. However, further GTR increase (up to 90 wt.%) led to a drop in impact strength because of poor sample homogeneity (Figure 5.3) [57]. This indicates that a GTR concentration between 80 and 90 wt.% seems to be a critical point for these compounds. The addition of 10 wt.% rEVA into the blends containing 80 wt.% GTR increased the impact strength of NRR, RR_1 and RR_2 blends by 9% (from 321 to 348 J/m), 7% (from 236 to 254 J/m) and 11% (from 342 to 379 J/m), respectively. The presence of rEVA improves the toughness and increases the absorbed energy before crack initiation and propagation by inducing interfacial bonding in rHDPE/GTR/elastomer blends. The rEVA can promote a more uniform GTR dispersion in the matrix by encapsulating the GTR particles and decreasing the surface energy leading to better rHDPE deformability around the GTR particles [57,106].

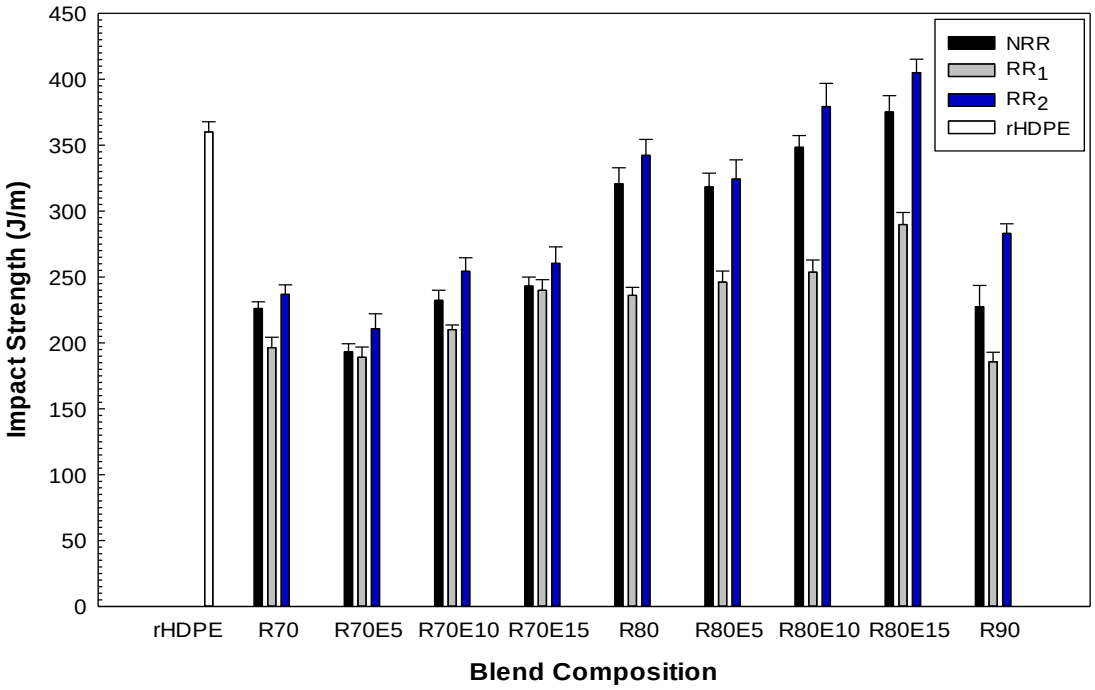

Figure 5.10 Impact strength of the rHDPE/GTR and rHDPE/GTR/rEVA blends. See Table 5.1 for sample composition.

5.3.5 Physical properties

5.3.5.1 Hardness

Figure 5.11 presents the hardness (Shore A and Shore D) of the blends as a function of different GTR types (NRR, RR_1 and RR_2) for compatibilized and uncompatibilized samples. In general, the hardness of TPE is influenced by the elastic modulus and crosslink density. Despite the presence of carbon black in GTR, adding recycled rubber particles as an elastomeric component into a rigid (thermoplastic) phase results in lower hardness values [12]. For instance, melt blending of 80 wt.% GTR with rHDPE decreased the Shore A hardness of rHDPE from 98 to 89 for NRR blends, while the value are 87 and 88 for R80 and RR80, respectively. Also, the Shore D values decreased from 67 for rHDPE to 38, 35 and 36 after melt blending with 80 wt.% NRR, RR_1 and RR_2, respectively. The hardness results can also be used as a rough approximation of the crosslink level of the blends. The regeneration process led to lower rigidity of the blends due to improved chain mobility (lower crosslink density) and the presence of processing oil in the recycled rubber, as reported by Shaker and Rodrigue [129]. The hardness of R80(10) decreased by 16 points Shore A (87 to 71) and 11 points Shore D (35 to 24), while the hardness of RR80(10) decreased by 15 points Shore A (88 to 73) and 10 points Shore D (36

to 26). Significant decrease in hardness for the compatibilized blends is related to the presence of a soft compatibilizer (10 wt.% rEVA), which promoted elasticity and softness [29].

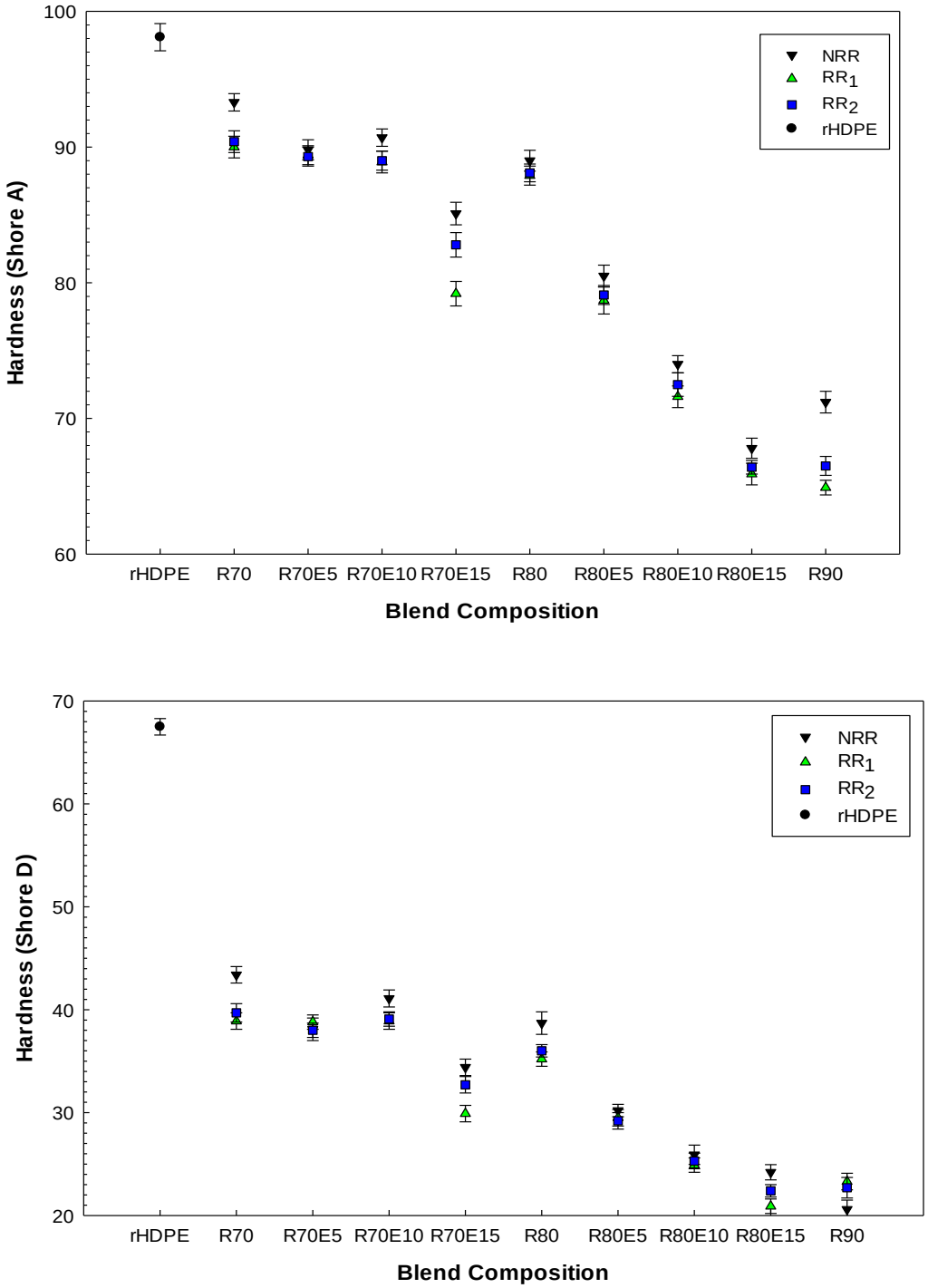

Figure 5.11 Hardness (Shore A and Shore D) of the rHDPE/GTR and rHDPE/GTR/rEVA blends. See Table 5.1 for sample composition.

5.3.5.2 Density

Figure 5.12 presents the density of the blends as a function of GTR content for compatibilized and uncompatibilized blends. In general, the density increased with GTR content due to its higher density (NRR = 1.169 g/cm^3, RR_1 = 1.246 g/cm^3 and RR_2 = 1.193 g/cm^3) compared to rHDPE (0.967 g/cm^3). Higher density of the blends containing RR_1 can be related to the presence of a processing oil in RR_1 particles resulting in slightly higher (about 1%) density of all RR_1 blends. The density of the compatibilized samples is slightly lower (1%) than the uncompatibilized compounds since rEVA has the lowest density (0.946 g/cm^3). Once again, increasing the rEVA content decreases the rHDPE content.

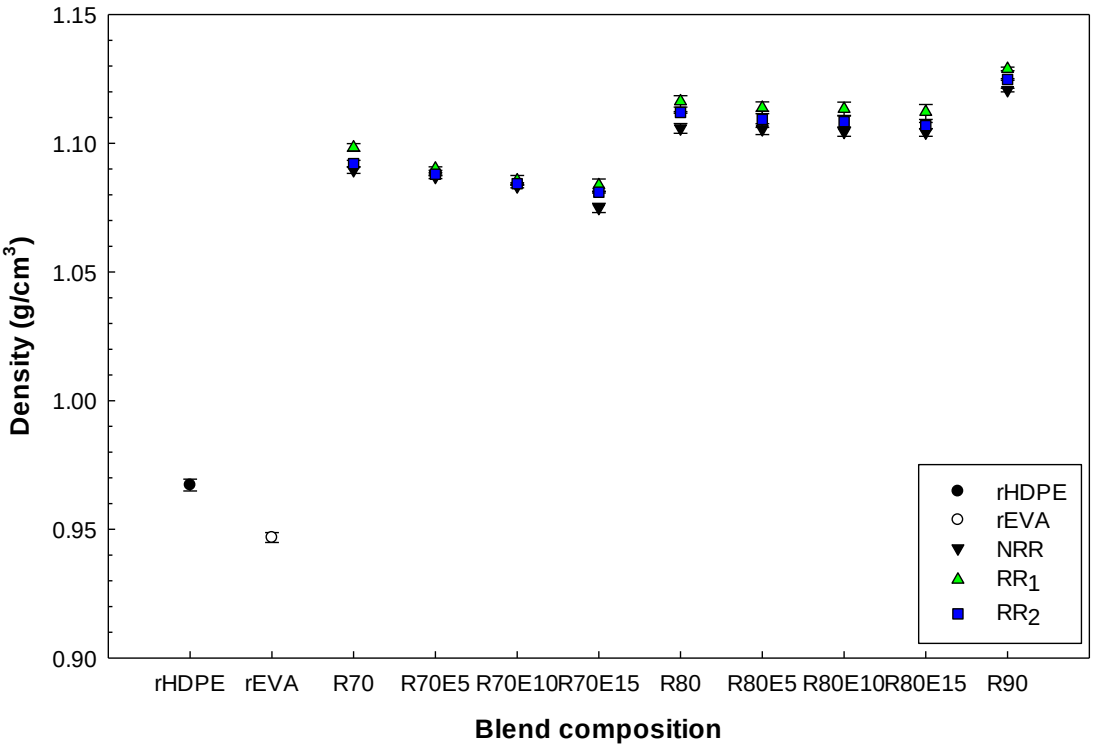

Figure 5.12 Density of rHDPE/GTR and rHDPE/GTR/rEVA blends. See Table 5.1 for sample composition.

5.4 Conclusion

GTR regeneration was proposed as a promising approach to improve the interfacial interaction between the soluble fraction of recycled rubber (RR) and a recycled thermoplastic matrix (rHDPE). The samples were produced via continuous melt-mixing of rHDPE with different types of ground tire rubber GTR (NRR, RR_1 and RR_2) in the range of 70 to 90 wt.% using a twin-screw extruder. Also, recycled

rEVA was used as a polar compatibility/interfacial adhesion promoter to produce ternary blends of rHDPE/GTR/rEVA with different rEVA content (5-15 wt.%).

The results confirmed the influence of the GTR regeneration and concentration on the mechanical and morphological properties of the resulting TPE. The morphological and mechanical results revealed that an efficient breakdown of the crosslinked network of RR_2 (regeneration degree of 24.1%) with a low gel fraction (88.4%) and crosslink density (5.5×10^{-4} mol/cm^3) would contribute to sufficient chain entanglement between RR_2 and rHDPE to create a strong interphase, leading to higher plastic deformation and toughness. But partial substitution of rHDPE by rEVA (5, 10 and 15 wt.%) gave rise to higher TPE homogeneity and compatibility. For example, rHDPE/GTR/rEVA (10/80/10) blends showed lower toluene uptake compared to rHDPE/GTR (80/20) blends since the addition of 10 wt.% rEVA slightly decreased the swelling ratio of N80(10), R80(10) and RR80(10) between 1.4% and 3.9%. It can be concluded that good filler/matrix interaction resulted in lower voids and less solvent penetration into the compatibilized blends. For the mechanical properties, the presence of 10 wt.% rEVA increased the elongation at break of RR80(10) to 203% (from 159% without rEVA), while the elongation at break of N80(10) and R80(10) increased to 144% (from 128%) and to 75% (from 51%), respectively. Lower plastic deformation of RR_1 blends compared to that of RR_2 and even NRR blends might be attributed to the regeneration process (extensive shear and high temperature) which caused partial degradation of the main rubber chain instead of a selective rupture of the sulfur crosslinks. Also, rEVA addition in N80(10), R80(10) and RR80(10) increased the impact strength between 9% and 11%.

It can be concluded that rEVA addition can promote a more uniform GTR dispersion (especially RR_2) by particles encapsulation to create a strong interphase and increase the deformation ability of the rHDPE matrix around these particles to improve plastic deformation and toughness.

Acknowledgement

The authors acknowledge the financial support of the Natural Sciences and Engineering Research Council of Canada (NSERC) and the technical support of the Research Center on Advanced Materials (CERMA).

CHAPTER 6 PHASE MORPHOLOGY, MECHANICAL, AND THERMAL PROPERTIES OF FIBER REINFORCED THERMOPLASTIC ELASTOMER: EFFECTS OF BLEND COMPOSITION AND COMPATIBILIZATION

Résumé

Dans ce travail, du polyéthylène haute densité recyclé (rHDPE) a été mélangé avec du caoutchouc de pneu régénéré (RR) (35-80% en poids) et renforcé avec des fibres de pneu recyclées (RTF) (20% en poids) dans un premier temps. Les matériaux ont été mélangés par extrusion à l'état fondu, moulés par injection et caractérisés en termes de propriétés morphologiques, mécaniques, physiques et thermiques. Bien que le remplacement de la phase de caoutchouc par du RTF ait compensé les pertes de modules de traction/flexion des mélanges rHDPE/RR/RTF en raison de la nature plus rigide des fibres, augmentant la rigidité des composites, la résistance aux chocs a remarquablement diminué. Ainsi, une nouvelle approche est proposée pour la modification de l'impact en ajoutant un mélange de polyéthylène greffé à l'anhydride maléique (MAPE)/RR (70/30) dans un composite caoutchouté renforcé de fibres. Dans ce cas, une répartition plus homogène des charges a été observée grâce à une meilleure compatibilité entre MAPE, rHDPE et RR. Les propriétés de traction ont été améliorées lorsque l'allongement à la rupture a augmenté jusqu'à 173% en raison d'une meilleure adhérence interfaciale. La modification de l'impact des composites élastomères thermoplastiques (TPE) résultants à base de rHDPE/(RR/MAPE)/RTF a été réalisée avec succès (résistance améliorée de 60%) via l'encapsulation de la phase de caoutchouc par le MAPE formant une interphase épaisse/flexible, diminuant la concentration de contrainte interfaciale ralentissant la fracture. Enfin, la stabilité thermique du TPE renforcé de fibres caoutchoutées a également révélé l'effet positif de l'ajout de MAPE sur les enchevêtrements moléculaires et une forte liaison entraînant une perte de poids inférieure, tandis que la microstructure et le degré de cristallinité n'ont pas changé de manière significative jusqu'à 60% en poids de RR/MAPE (70 /30).

Mots-clés : Recyclage, caoutchouc de pneu, fibre textile, composite TPE, compatibilisation

Abstract

In this work, recycled high density polyethylene (rHDPE) was compounded with regenerated tire rubber (RR) (35-80 wt.%) and reinforced with recycled tire textile fiber (RTF) (20 wt.%) as a first step. The materials were compounded by melt extrusion, injection molded and characterized in terms of morphological, mechanical, physical, and thermal properties. Although the replacement of the rubber phase with RTF compensated the tensile/flexural moduli losses of rHDPE/RR/RTF blends because of the more rigid nature of fibers increasing the composites stiffness, the impact strength significantly decreased. So, a new approach is proposed for impact modification by adding a blend of maleic anhydride grafted polyethylene (MAPE)/RR (70/30) into a fiber reinforced rubberized composite. In this case, a more homogeneous distribution of the fillers was observed due to better compatibility between MAPE, rHDPE and RR. The tensile properties were improved as the elongation at break increased up to 173% because of better interfacial adhesion. Impact modification of the resulting thermoplastic elastomer (TPE) composites based on rHDPE/(RR/MAPE)/RTF was successful (toughness improvement by 60%) via encapsulation of the rubber phase by MAPE forming a thick/soft interphase, decreasing interfacial stress concentration and slowing down fracture. Finally, the thermal stability of rubberized fiber reinforced TPE also revealed the positive effect of MAPE addition on molecular entanglements and strong bonding, yielding lower weight loss, while the microstructure and crystallinity degree did not significantly change up to 60 wt.% RR/MAPE (70/30).

Keywords: Recycling, tire rubber, textile fiber, TPE composite, compatibilization

6.1 Introduction

Recycling the increasing amount of waste tires across the globe as hazardous materials accumulating in landfills is a worldwide environmental concern since their natural decomposition is estimated to be over 600 years [287]. Presently, end-of-life (EOF) tire rubber and tire textile fibers are buried or burned as tire-derived fuels releasing toxic gases [1]. Therefore, alternative environmentally friendly and added-value uses for these large amounts of wastes are required to be developed. Compared to virgin rubbers, using recycled rubber (mainly obtained from waste tires) benefits from lower cost (less use of raw materials), environmental friendliness and simpler processing conditions (there is no need for dynamic vulcanization of the elastomer phase) [288]. The most common option in terms of rubber recycling is to combine waste tire rubber with thermoplastic resins to develop fully recycled compounds called thermoplastic elastomers (TPE) with reduced materials costs and enhanced performance/processability of plastics and rubbers [5]. However, the crosslinked network of ground tire rubber (GTR) does not have enough molecular freedom to entangle with the matrix macromolecules, resulting in low compatibility and weak interfacial adhesion which is the origin of poor mechanical properties and low durability of these compounds [8,12]. In general, introduction of GTR serving as stress concentration points around the rubber clusters might result in multiple micro-void formations at the interface facilitating fracture by lowering the absorbed energy before break-up [289].
But waste tire rubber can be subjected to a regeneration process by partially breaking down the crosslinked structure via C-S and/or S-S bonds break-up with limited hydrocarbon backbone chains rupture. Therefore, the soluble fraction of regenerated rubber (RR) can generate stronger interactions between the TPE phases [8,286]. However, it is difficult to obtain a high sol fraction with acceptable molecular weight (MW) without scission of the main rubber chains, resulting in a MW drop coupled with a loss of mechanical strength [5,290].

One way of overcoming this problem is the use of short fibers, inducing good strength and stiffness [288,289,291]. Fiber-reinforced TPE have been shown to have good mechanical properties, leading to a growing interest due to the lower density of these reinforcements combined with lower cost, renewability and environmentally friendly source of several fibers [256,288,292]. The efficiency of short fiber reinforcements depends on the fiber type, aspect ratio, concentration, orientation and distribution after mixing, as well as the level of adhesion between the fiber and the matrix [293,294]. But the low affinity of short fiber and crosslinked rubber particles towards several polymer matrixes contributes to high surface energy and phase incompatibility, leading to poor plastic deformation and impact strength

due to insufficient interfacial bonding [295,296]. Once good adhesion is obtained, the incorporation of fibers can lead to increased tensile and flexural properties of the composites [289]. For example, Kakroodi et al. [297] observed that the tensile modulus of recycled polypropylene (rPP)/GTR (80/20) blends was improved by 25% (from 320 to 400 MPa) after the incorporation of 20 wt.% birch wood flour. However, introducing high amounts of fibers led to interfacial voids, creating structural defects due to fiber-fiber interactions and poor dispersion, thus decreasing impact resistance (toughness) [298]. To solve this problem, the addition of elastomers is the most common method to increase the impact strength (toughness) increasing the amount of energy absorbed before rupture [28]. To this end, several copolymers, such as ethylene-propylene-diene monomer (EPDM) [299], styrene-butadiene-styrene (SBS) [106], and styrene-ethylene-butylene-styrene (SEBS) [300], have been proposed for impact modification. Lima et al. [257] claimed that EPDM tends to coat the recycle tire particles surface, providing a soft interface and improving compatibility with PP. The results showed that the impact strength of PP/EPDM/GTR (70/15/15) increased by 65% (from 2.9 to 4.8 kJ/m^2) compared to PP/GTR (70/30).

The addition of maleated polyolefins (interfacial modifiers) was also shown to be very effective by forming a strong interface between the rubber particles and thermoplastic matrixes via selective localization at the interfacial area between immiscible polymer blends, leading to improved physical compatibility (higher interfacial adhesion), resulting in higher tensile properties [11,28,301]. For example, the addition of 10 wt.% of maleic anhydride grafted polyethylene (MAPE) into high density polyethylene (HDPE) filled with 30 wt.% of reclaimed rubber increased the plastic deformation by 10% (from 125 to 138%). This improvement was associated to chemical bonds being created between the maleic anhydride group of MAPE and unsaturated C=C bonds on the rubber surface [11]. Tensile elongation at break helps to determine the compatibility and homogeneity of TPE blends, while elongation at break of recycled TPE are lower than virgin compounds because of contamination and impurities (crazing points), as well as degradation of recycled materials (mechanical and thermal stresses) during their service life, grinding and regeneration [30,248].

Although a large body of literature is available on recycled tire rubber, very few studies investigated the potential of recycled tire fibers (RTF) for TPE reinforcement [29,32]. Hence, this work investigates the effect of both recycled tire rubber and fiber contents on the properties of TPE composites with a focus on the structure–property relationships. The effect of reinforcement type and content on the phase morphology, as well as mechanical and thermal properties, especially blend toughening, was

thoroughly investigated. In particular, a new approach is proposed for impact modification by using a RR/MAPE masterbatch into a fiber reinforced rubberized composite. The results also show how the encapsulation of the rubber phase by MAPE can further improve the physical compatibility (higher interfacial adhesion) and the fracture resistance of a fiber-reinforced system combined with improved stiffness.

6.2 Experimental

6.2.1 Materials

Post-consumer rHDPE in flakes coming from recycled solid HDPE bottles was used as thermoplastic matrix (Figure 6.1 A). Recycled rubbed particles (RR) from regenerated car tire as rubber phase and RTF as reinforcement fibers were used without modification (Figure 6.1 B and C). The MAPE was used as coupling agent to compatibilize fiber reinforced rubberized composites. Table 6.1 presents an overview of the materials used for this study.

Table 6.1 Specification and properties of the materials used.

Material	rHDPE	RR	RTF	MAPE
Commercial name	-	PI3.1.C	-	Epolene C-26
Producer/supplier	Service de Consultation Sinclair (Drummondville, Canada)	Phoenix Innovation Technologies (Montreal, Canada)	Quebec Transloc (Lévis, Canada)	Westlake Chemical Corp (TX, USA)
Density (ASTM D2856 [302])	0.986 g/cm^3	1.184 g/cm^3	1.268 g/cm^3	0.920 g/cm^3
MFI (190 °C and 2.16 kg; ASTM D1238 [303])	6.7 g/10 min	-	-	8 g/10 min
Form (appearance)	flakes	Powders	Fibers/Fluffy	Pellets
Remarks	Melting point of 127.5 °C (ASTM D3418 [304])	Average particle size of 500 µm	-	MW of 65 kg/mol, and acid number of 8 mg KOH/g

Figure 6.1 General view of the (A) rHDPE flakes, (B) RR particles and (C) RTF as received.

6.2.2 Processing

A co-rotating twin-screw extruder Leistritz ZSE-27 with a L/D ratio of 40 and 10 heating zones (die diameter of 2.7 mm) was used for melt blending of samples. The melt extrusion temperature was set at 175 °C for all zones to limit RR degradation, while the screw speed was set at 120 rpm. The overall flow rate was 4 kg/h for all the blends to prevent high motor torque and die pressure associated with the high viscosity of RR compounds. The materials were cooled in a water bath and then pelletized using a model 304 pelletizer (Conair, Stanford, USA), followed by drying for 6 h in an oven at 70 °C to eliminate any residual water for further processing (injection molding).

6.2.2.1 Composites without compatibilizer

Different rHDPE-based composites with fillers (RR or RR/RTF) were produced with various compositions as presented in Table 6.2. As shown in Figure 6.2 A, the rHDPE pellets were introduced through the main feeder (zone 1), while the RR particles (35, 50, 65 and 80 wt.%) were introduced via a side-stuffer located in zone 4 of the extruder to limit thermal degradation. Then, different concentrations of RR particles (15, 30, 45, and 60 wt.%) were dry-blended with RTF (20 wt.%) after being oven-dried at 70 °C for 12 h. Again, the rHDPE was fed to the extruder in the first zone (main feed), while the RR/RTF mixtures were fed via the side feeder (zone 4). The processing temperature was fixed at 175 °C with a screw speed of 120 rpm and a flow rate of 4 kg/h. All the extrudates were cooled in a water bath before pelletizing (Figure 6.2 B).

6.2.2.2 Composites with compatibilizer

As illustrated in Figure 6.3, RR/MAPE masterbatches were produced by melt blending of RR particles (70 wt.%) with MAPE pellets (30 wt.%) to get good surface coverage. In this case, the MAPE pellets

were fed to the extruder in the first zone (main feed), while RR particles were fed via the side feeder (zone 4). The processing conditions were fixed at a temperature of 175 °C, a screw speed of 120 rpm and a flow rate of 4 kg/h. Again, the materials were cooled in a water bath and pelletized. Then, these pellets (RR/MAPE masterbatch) were introduced in the main feeder at different concentrations (15, 30, 45 and 60 wt.%) along with rHDPE (65, 50, 35 and 20 wt.%) in a second extrusion step, while the RTF (20 wt.%) was introduced via the side-stuffer located at zone 4. All the formulations with codes are presented in Table 6.2. After drying, the final samples were produced on a PN60 (Nissei, Japan) injection molding machine. The temperature profile was set as 180-170-170-160 °C (nozzle, front, middle and rear). The mold had four cavities to directly produce the standard geometries for characterization. The injection pressure was adjusted (45 to 55 MPa) depending on the compound viscosity, while the mold temperature was fixed at 30 °C.

Table 6.2 List of the compositions investigated (% wt.).

Sample	rHDPE	RR	RTF	Masterbatch RR/MAPE (70/30)
RHD	100	-	-	-
R35	65	35	-	-
R50	50	50	-	-
R65	35	65	-	-
R80	20	80	-	-
R15F	65	15	20	-
R30F	50	30	20	-
R45F	35	45	20	-
R60F	20	60	20	-
R15F*	65	-	20	15
R30F*	50	-	20	30
R45F*	35	-	20	45
R60F*	20	-	20	60

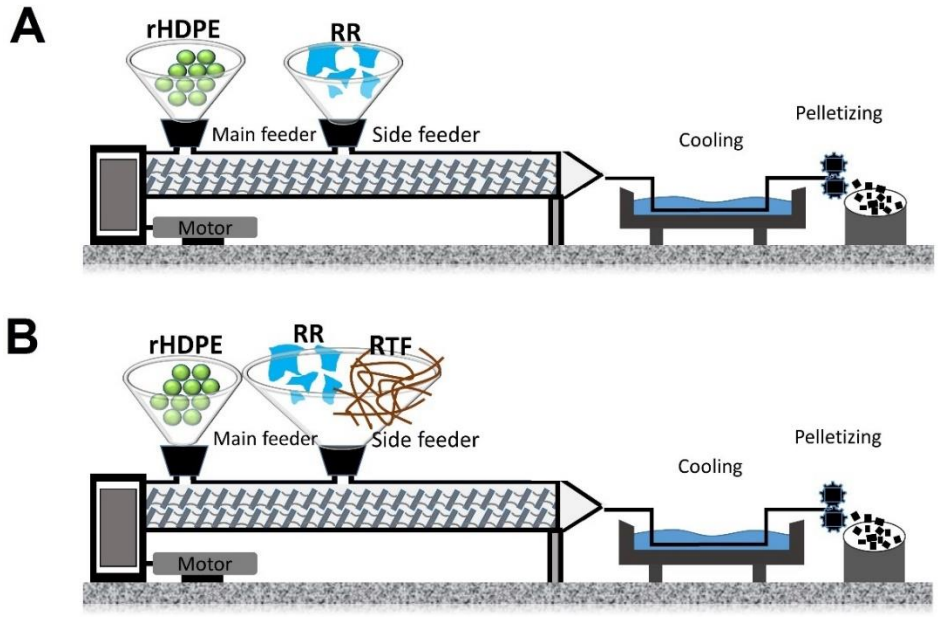

Figure 6.2 Melt extrusion of (A) rHDPE/RR and (B) rHDPE/RR/RTF samples.

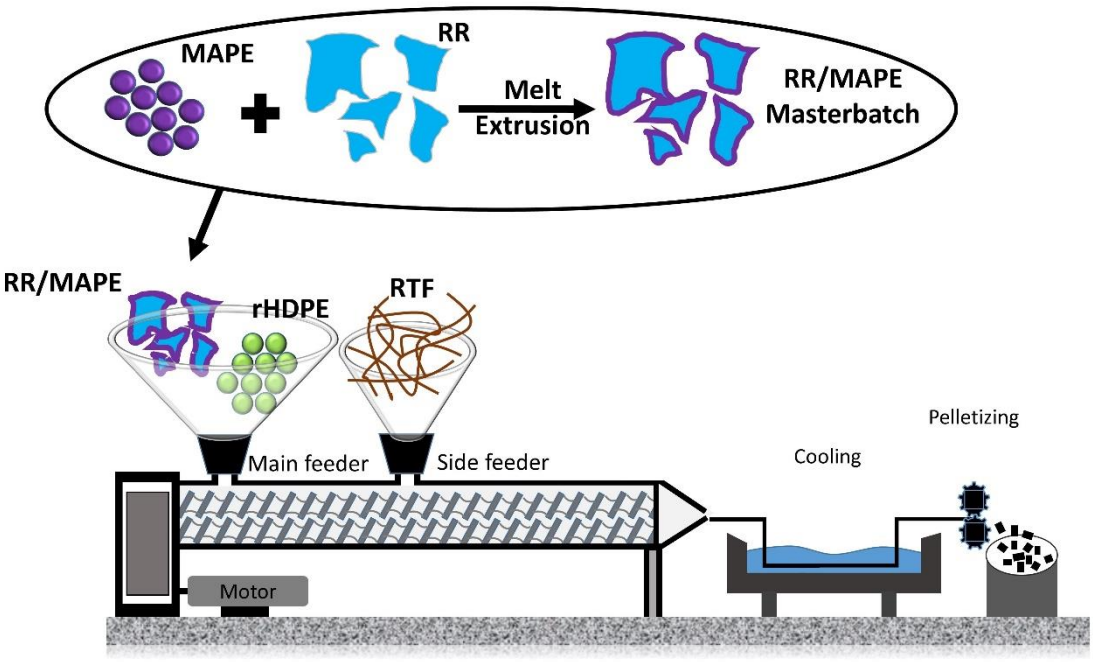

Figure 6.3 Melt extrusion steps for the different rHDPE/(RR/MAPE)/RTF samples.

6.2.3 Characterization

6.2.3.1 Morphology

An Inspect F50 scanning electron microscope (SEM) (FEI, Hillsboro, OR, USA) was used at 15 kV to take micrographs of the raw materials and observe the quality of the interfacial adhesion/dispersion in the blends. The samples were cryogenically fractured in liquid nitrogen and the surfaces were coated with gold/palladium to be observed at different magnifications. RR and RTF were also investigated by energy dispersive spectroscopy (EDS) using the same device to identify impurities (contamination).

6.2.3.2. Mechanical testing

Tensile tests were conducted at room temperature according to ASTM D638-14 [305] using a 500 N load cell and a 10 mm/min crosshead speed on an Instron (Instron, Norwood, MA, USA) universal mechanical tester model 5565. At least 5 specimens (type IV) with 3 mm thickness were used for each formulation. The averaged values of tensile strength (σ_Y), Young's modulus (E) and elongation at break (ε_b) are reported with standard deviations.

Flexural tests were done on an Instron (Instron, Norwood, MA, USA) model 5565 with a 50 N load cell according to ASTM D790-10 [306] at room temperature. Rectangular specimens with dimensions of 60x12.7 mm^2 were tested with 5 repetitions for each sample in a three-point bending mode (span length of 60 mm) at a crosshead speed of 2 mm/min.

Notched Charpy impact strength was measured on a Tinius Olsen (Horsham PA, USA) model 104 at room temperature according to ASTM D256-10 [307]. At least 10 specimens with dimensions of 60x12.7 mm^2 were used for each compound. Before testing, all the samples were automatically V-notched on a Dynisco (Franklin, MA, USA) model ASN 120m sample notcher 24 h before testing.

6.2.3.3 Physical properties

Hardness (Shore D) was determined by a model 307L durometer (PTC Instruments, Boston, MA, USA) with 10 measurements for each sample. Density was determined by a gas (nitrogen) pycnometer Ultrapyc 1200e (Quantachrome Instruments, Boynton Beach, FL, USA). Each measure was repeated three times for each sample.

6.2.3.4 Thermogravimetric Analysis (TGA)

Thermal stability of the raw materials and the compounds were investigated via TGA on a Q5000 IR (TA Instruments, New Castle, DE, USA) with a heating rate of 10 °C/min from 50 to 850 °C. The tests were performed in nitrogen and air atmospheres to evaluate both thermal and oxidative resistance of the materials.

6.2.3.5 Differential scanning calorimetry (DSC)

The melting and crystallization behaviors of the samples were examined on a DSC7 (Perkin Elmer, USA). About 5-10 mg of sample was placed in an aluminum pan and the test was performed by heating from 50 to 200 °C at 10 °C/min under a nitrogen atmosphere, followed by cooling back to 50 °C at 10 °C/min. The maximum of the endothermic peak, the maximum of the exothermic peak and the area under the endothermic peak were used for evaluation of the melting temperature (T_m), crystallization temperature (T_c) and enthalpy of fusion (ΔH_m) of the samples, respectively. Also, the matrix crystallinity degree (X_c) was calculated as:

$$X_c = \frac{\Delta \mathrm{H}_m}{(1-\varphi)\,\Delta \mathrm{H}_{m0}} \times 100 \qquad (6.1)$$

where φ is the total weight fraction of filler (RR+RTF) in the blend and ΔH_{m0} is the melting enthalpy of 100% crystalline HDPE (285.8 J/g) [11].

6.3 Results and Discussion

6.3.1 Morphological Characterization

SEM micrographs of RR particles and RTF are presented in Figure 6.4 at different magnifications. Several steps of waste tires grinding lead to a size reduction of both rubber/fibers and the heterogeneous nature of recycled materials making it difficult to obtain a specific size and distribution. Nevertheless, the SEM images show that for the material received, the RR particle size distribution is about 500 µm (Figure 6.4 A and B), while the recycled fibers have a length and diameter of 1000-3000 µm and 20-30 µm (Figure 6.4 C and D), respectively. The RR particles show irregular surfaces with cracks and different shapes of porous/smooth surfaces because of different types of tires and/or different grinding processes used for their production coupled with thermomechanical degradation during the regeneration step.

SEM micrographs also show that the recycled rubber particles and fibers contain some impurities because of a wide variety of materials used in tires formulation. EDS analysis of RR (Figure 6.5 A) and RTF (Figure 6.5 B) indicates that typical impurities are mostly metal alloys and other additives (processing/vulcanization package) or polymeric materials [308]. To get qualitative and quantitative analysis about these materials, the elemental compositions of RR and RTF are presented in Table 6.3 and Table 6.4 respectively, in terms of weight and atomic percentage. The chemical analysis reveals the predominance of carbon and oxygen, while small amounts of S, Al, Si, Cu and Zn are also detected. For example, sulfur and zinc oxide (ZnO) are part of the curing system used to crosslink the rubber, while aluminum silicates are reinforcing fillers leading to harder vulcanizates compared to calcium silicates. The presence of oxygen is associated to the additives and metal oxides [309].

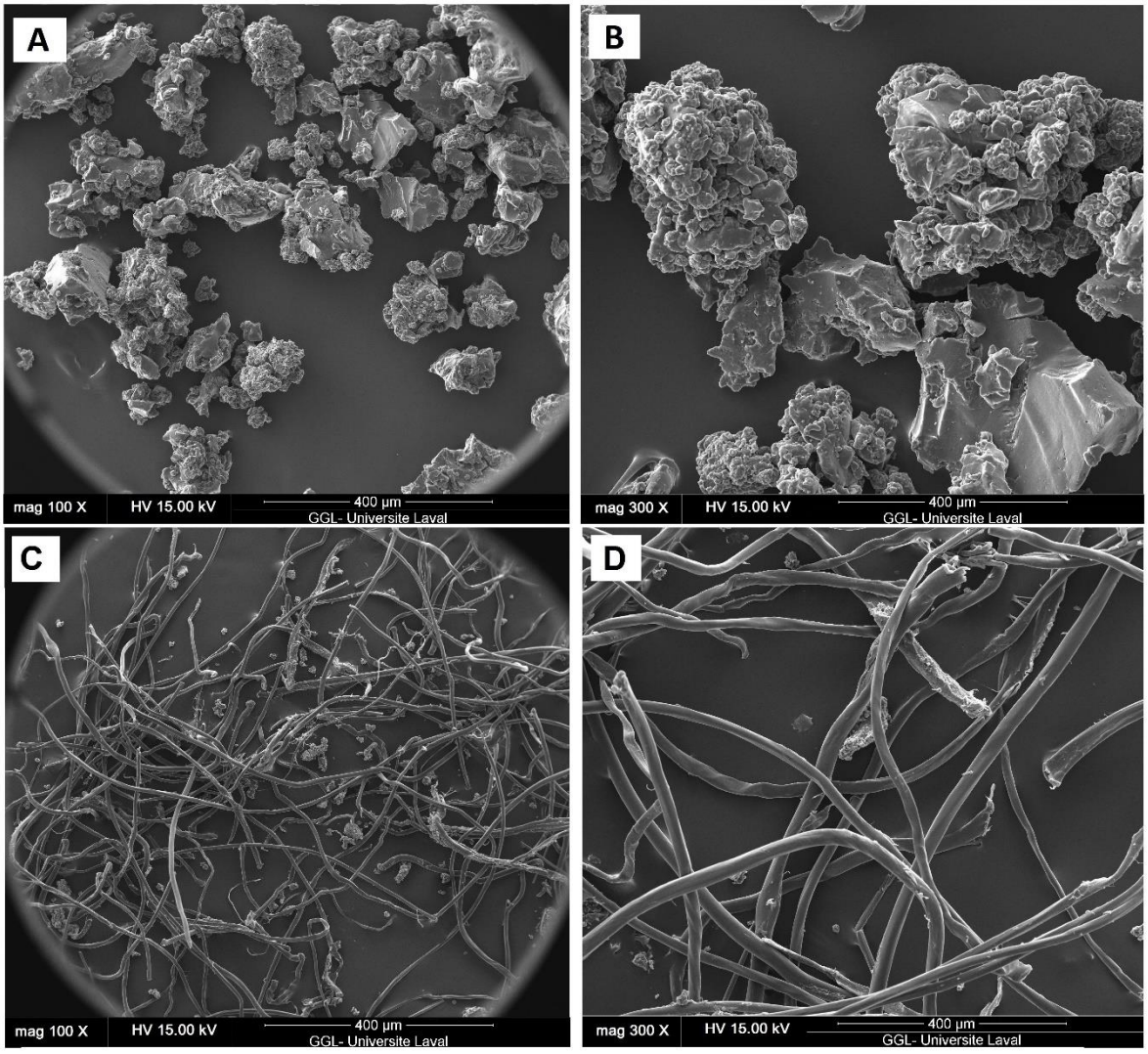

Figure 6.4 SEM micrographs of: (A, B) RR and (C, D) RTF at different magnifications.

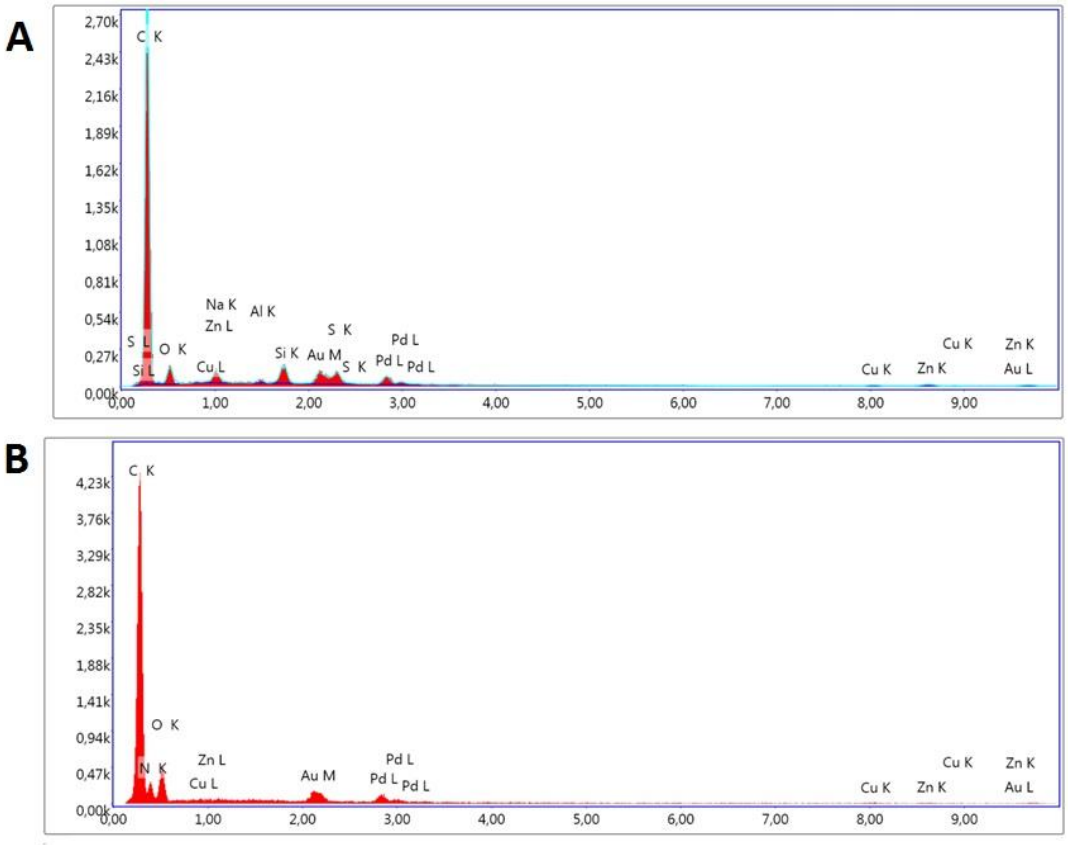

Figure 6.5 EDS spectra of: (A) RR and (B) RTF to show impurities.

Table 6.3 Chemical analysis compositions of RR (EDS quantitative results).

Element	Weight (%)	Atomic (%)
C	83.1	92.3
O	5.1	4.2
Al	0.4	0.2
Si	2.0	1.0
S	1.9	0.8
Cu	2.1	0.5
Zn	5.3	1.1

Table 6.4 Chemical analysis compositions of RTF (EDS quantitative results).

Element	Weight (%)	Atomic (%)
C	66.9	72.7
N	16.5	15.5
O	14.0	11.4
Cu	1.4	0.3
Zn	1.7	0.2

Figure 6.6 presents typical SEM micrographs of cryogenically fractured cross-section surfaces of blends containing 60 and 80 wt.% of RR (Figure 6.6 A and B) or RR/RTF mixture (Figure 6.6 C and D).

Micrographs of the compatibilized samples are also presented to compare the fracture behavior at the interface and general morphologies. As shown in Figure 6.6, large domains and protrusions of the dispersed phase indicate that the fillers have low affinity towards the rHDPE matrix due to incompatibility. In general, immiscible TPE blends present typical matrix/dispersed droplet-type morphology where large particle size of the dispersed domains (rubber phase), and sharp interface region between the crosslinked rubber and matrix indicate high interfacial tension between the components [310]. Fillers poorly bonded to the matrix led to clean and smooth surface of R60 and R80 with voids around the fibers from debonding and/or rupture of the rubber particles, as well as easy pull-out of the dispersed rubber particles [12,311]. This implies that the weak interface could not transfer the load from the matrix to the reinforcements, and failure occurred at the interface [12]. As shown in Figure 6.6 (C and D), poor surface interaction between RTF and rHDPE (easy debonding and fiber pull-out from the matrix) in R45F and R60F leads to the formation of large voids/cracks around the fibers. This non-homogeneous morphology with poor adhesion between the phases (high interfacial tension) leads to low mechanical properties, especially as the number of defects increased with filler content [29,32].

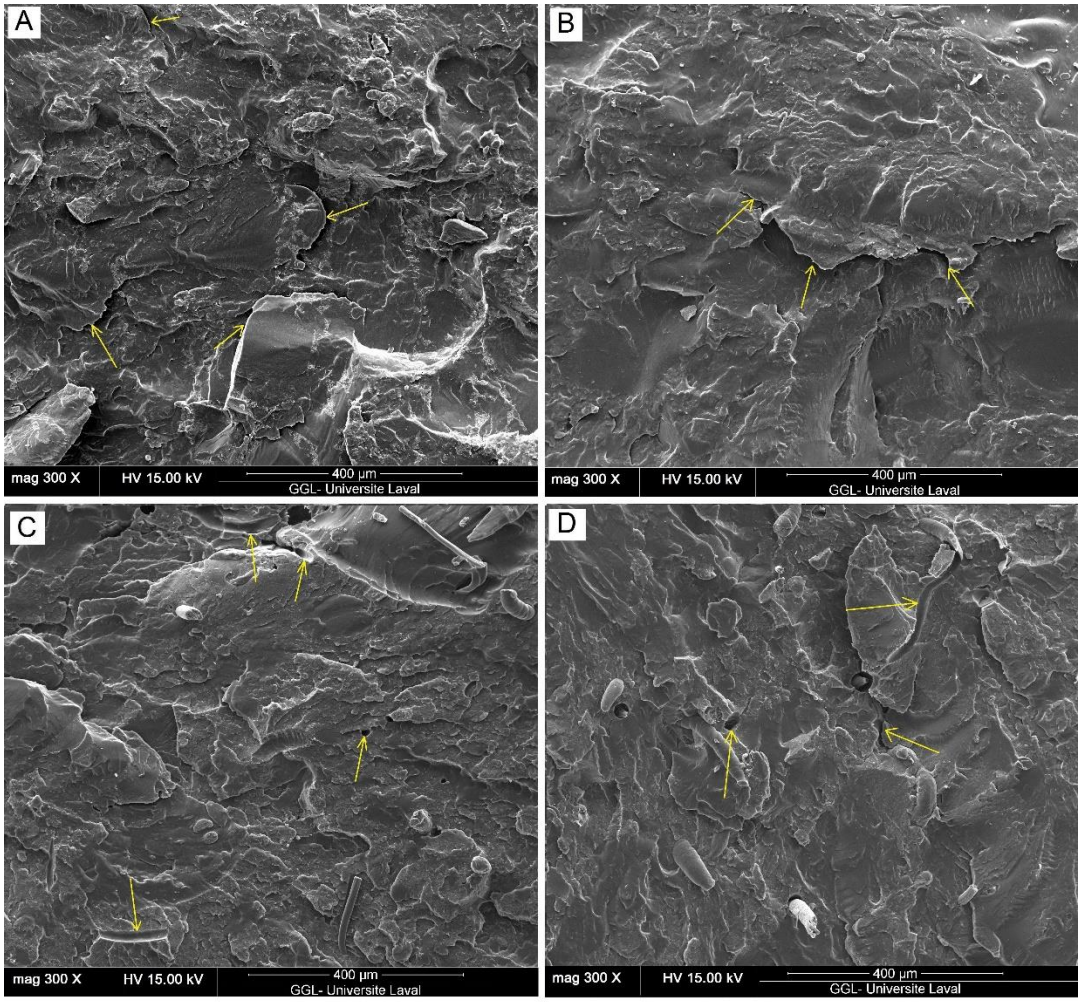

Figure 6.6 SEM micrographs of: (A) R60, (B) R80, (C) R45F and (D) R60F composites (Arrows are used for ease identification of the failure phenomena).

SEM micrographs are presented at different magnifications to get an idea of the interface quality of compatibilized composites (Figure 6.7). Phase morphology of multicomponent blends is determined by the interfacial interactions and compatibility between the phases which are known to control the compound properties [310,311]. As shown in Figure 6.7, R45F* and R60F* show coarser fractured surface compared to their uncompatibilized counterparts (Figure 6.6 C and D), as fewer gaps/voids at the filler/matrix interfaces can be seen (Figure 6.7 B and D). This behavior is attributed to the improved interface quality and better fracture resistance. The presence of MAPE changed the morphology from a heterogeneous structure for uncompatibilized systems (Figure 6.6 C and D) to a more homogeneous morphology for compatibilized ones (Figure 6.7 A and C). Interactions between the compatibilizer and both RR and rHDPE result in stronger interfacial interaction (reduced interfacial tension), producing a good dispersion of the rubber phase in the matrix and a more homogeneous structure [310]. Figure 6.7

B and D also show that RR particles are completely embedded within the matrix, as it is very difficult to distinguish them from the matrix on the fractured surfaces. Furthermore, much less gaps and defects are present, which is ascribed to good rubber particles coverage (due to the masterbatch step used) by the compatibilizer to form molecular entanglement at the interface layer, leading to better interfacial interaction [29]. Improved compatibility between RR and compatibilizer is related to chemical bonds formed between the unsaturated C=C bonds on the rubber surface and the maleic anhydride group of MAPE [312,313]. Contrary to R45F and R60F, no fiber pull-out is detected in R45F* and R60F*, so RTF are also well embedded in the matrix, suggesting more affinity between the components (reduced surface energy), thereby increased failure resistance through effective load transfer can be expected [257,314]. This special morphology is also expected to improve all the mechanical properties, especially the elongation at break and impact strength, as described next.

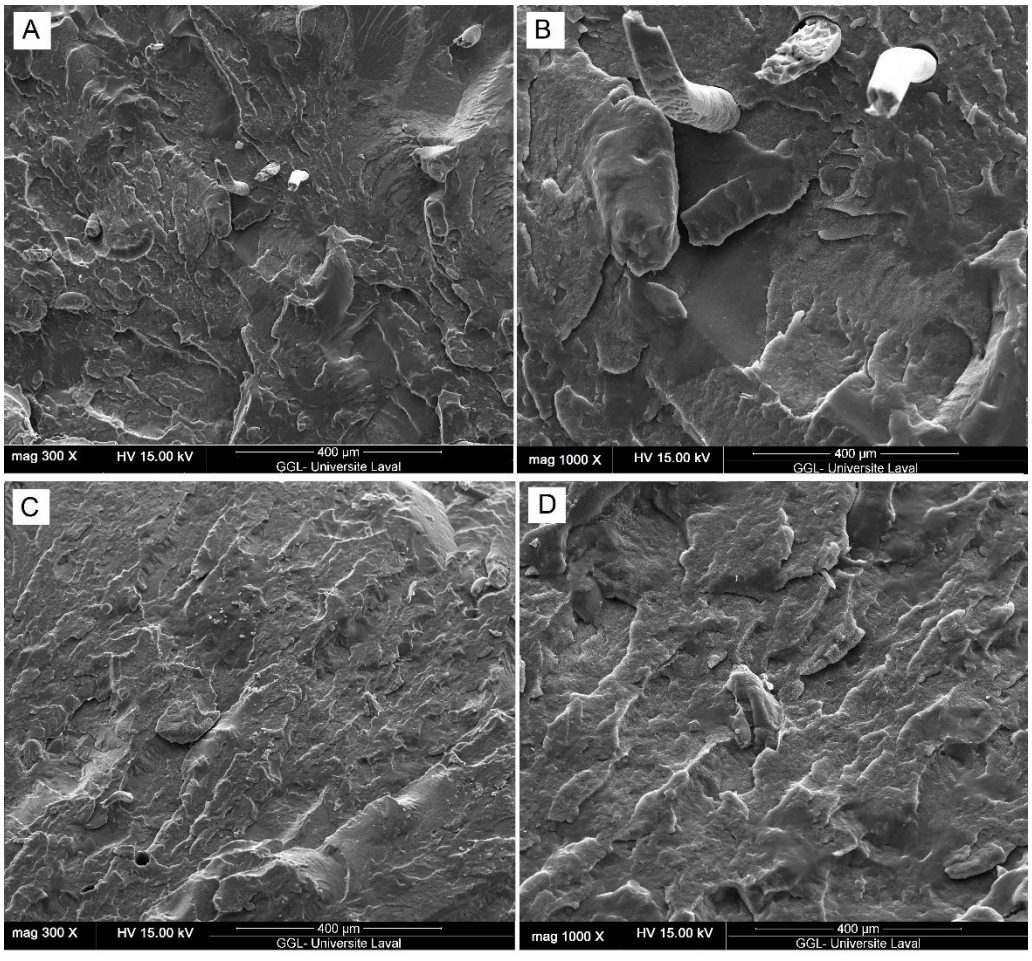

Figure 6.7 SEM micrographs of: (A, B) R45F* and (C, D) R60F* composites at different magnifications.

6.3.2 Mechanical (tension and flexion) Properties

The effect of blend composition and compatibilizer addition on the mechanical and physical properties of the composites are presented in Table 6.5. Almost all the binary blends of thermoplastic resins filled with recycled rubbers (vulcanized structure) have very poor mechanical properties, especially low tensile strain at break and impact strength [248]. This is attributed to very low entanglement between the crosslinked rubber particles and matrix (low compatibility), leading to the formation of voids around rubber particles (stress concentration points), facilitating crazing and interfacial debonding [20]. Increasing the RR content decreases the tensile strength of all samples. For example, the tensile strength of R65 and R80 are 60% and 76% lower than neat rHDPE (19.0 MPa). Higher filler ratio (RR = soft phase) transformed into larger rubber agglomerates with high gel content (crosslinked) acting as stress concentration point at the interface of binary blends (polar and non-polar materials) [29]. Adding RTF to the rHDPE/RR compounds did not modify the tensile strength values, showing poor fiber-matrix interaction. This can be related to the effect of reinforcing fibers (organic and inorganic) interfering the continuity of the matrix, which indicates the prominent role of incompatibility between filler and rHDPE on the tensile properties [297]. However, using the RR/MAPE masterbatch had a substantial effect on the tensile strength of compatibilized samples compared to their uncompatibilized counterparts. As shown in Table 6.5, the tensile strength of R60F* (8.8 MPa) is respectively 79% and 87% higher than that of R60F (4.9 MPa) and R80 (4.7 MPa). The introduction of MAPE is shown to create remarkable blend compatibility and improved interfacial bonding, promoting smooth stress transfer and hence improved tensile strength of the compatibilized samples. The interaction of the maleic anhydride group (MAPE) with the hydroxyl group on carbon black surface or carboxyl groups of the RR may be responsible for interfacial interaction between rubber and compatibilizer [315,316]. It is also reported that possible reaction between ZnO as a component of RR (Table 6.3) with maleic anhydride (MA) during melt mixing can be responsible for the tensile strength improvement of compatibilized TPE blends [317].

The increase in RR content from 35 wt.% to 80 wt.% showed a significant decreasing trend of Young's modulus from 191.2 MPa to 32.5 MPa attributed to the substitution of the rigid thermoplastic resin with a soft rubber phase of low rigidity. It is well established that adding RR to thermoplastic resins decreases their tensile modulus because of the lower glass transition temperature of rubber compared to that of semi-crystalline plastic, so RR is in the rubbery state and has much lower modulus at room temperature [310]. The introduction of RTF somewhat increased Young's modulus because of the stiff nature of these short fibers and limited stress transfer from the matrix [32]. For example, adding 20 wt.%

RTF into the binary blends (rHDPE/RR) increased Young's modulus of R35 and R80 from 191.2 MPa and 32.5 MPa to 246.5 MPa (22 %) and 45.8 MPa (40 %) for R15F and R60F samples, respectively.

Flexural modulus results present a similar decreasing trend as tensile modulus by adding RR particles as R80 (103.6 MPa) show the lowest value compared to R60F (134.7 MPa) and R60F* (182.7 MPa) being 83% lower than rHDPE (594.4 MPa). But conversely, adding recycled fibers slightly increased the flexural modulus of all fiber reinforced composites, attributed to the replacement of rubber particle (RR) by stiffer reinforcements (RTF) in RR/RTF. This increasing trend is more noticeable at low RR content (R15F) since lower rubber concentration in TPE blends requires more stress for deformation [28]. As shown in Table 6.5, the introduction of RTF (20 wt.%) increased the flexural modulus of R35 from 384.1 MPa to 405.6 MPa for R15F. Higher flexural modulus of R15F* (437.9 MPa) compared to R15F (405.6 MPa) and R35 (384.1 MPa) is obtained because the addition of a compatibilizer improved the interfacial adhesion between each phase similar to tensile properties. Also, it is claimed that maleated compatibilizers can promote surface crystallization to form a trans-crystalline layer around short fibers with higher rigidity and lower deformability contributing to much higher modulus [318].

The introduction of RR particles into the matrix led to lower tensile elongation at break and the values are much less than that of rHDPE (949.2%). However, increasing the rubber content from 35 to 80 wt.% led to higher elongation at break of R80 by 104% (from 38.1 to 77.9%) due to the presence of a more elastic phase, inducing higher deformation/elasticity [248]. Also, the addition of a fixed concentration of rigid fibers (20 wt.% RTF) resulted in a further drop because of the lower volume fraction of the soft rubber phase replaced by rigid fibers (solid phase) with low elasticity and poor affinity with the matrix (Figure 6.6). Similarly, Moghaddamzadeh and Rodrigue [29] observed a very low tensile strain at break (25%) of linear low density polyethylene (LLDPE) composites reinforced with recycled tire fibers (50 wt.%). A mixture of thermoplastic/rubber is considered as a TPE compound if it shows at least 100% deformation [22], so R45F* and R60F* are interesting compounds with elongation at break of 138.2% and 172.3%, respectively. The compatibilized samples exhibit the highest elongation at break among the samples studied in this work, which is related to the rubber-toughening effect and enhanced interfacial adhesion due to MAPE, which is in agreement with the morphological findings [311]. It is well-documented that the compatibilizing effect of MAPE in TPE blends is attributed to the interaction between the MA group of maleated copolymers as a polar component with the natural rubber (NR) (the main component of RR) as a nonpolar material [310].

Table 6.5 Mechanical properties of the samples produced (see Table 6.2 for definition).

Sample	Tensile Strength (MPa)	Young's Modulus (MPa)	Tensile Strain at Break (%)	Flexural Modulus (MPa)
rHDPE	19.0 (0.3)	427.1 (14.9)	949.2 (26.4)	594.4 (11.3)
R35	13.0 (0.3)	191.2 (4.3)	38.1 (4.8)	384.1 (3.5)
R50	9.2 (0.3)	152.3 (3.2)	44.2 (7.2)	281.8 (5.4)
R65	7.7 (0.1)	99.3 (4.2)	56.7 (5.3)	189.4 (3.8)
R80	4.7 (0.4)	32.5 (5.4)	77.9 (8.6)	103.6 (4.7)
R15F	9.5 (0.1)	246.5 (6.1)	30.2 (6.1)	405.6 (2.1)
R30F	9.2 (0.3)	170.5 (6.6)	36.4 (4.9)	308.5 (3.8)
R45F	7.4 (0.2)	109.3 (4.7)	45.3 (6.4)	202.7 (3.5)
R60F	4.9 (0.1)	45.8 (5.2)	65.2 (5.7)	134.7 (2.9)
R15F*	13.2 (0.2)	277.3 (4.9)	64.5 (8.2)	437.9 (3.4)
R30F*	12.1 (0.2)	212.2 (5.3)	87.6 (7.9)	384.6 (4.5)
R45F*	9.8 (0.1)	126.5 (3.6)	138.2 (7.6)	262.5 (4.2)
R60F*	8.8 (0.4)	80.9 (4.5)	172.3 (8.3)	182.7 (5.1)

6.3.3 Fracture Analysis

Using recycled instead of virgin materials benefits from lower cost (less use of raw materials), environmental friendliness and simpler processing conditions (there is no need for dynamic vulcanization of the elastomer phase), as well as increased tensile and flexural modulus of TPE [288].

The low impact strength (toughness) of short fiber reinforced TPE, especially at low temperatures, limits the industrial application of such composites [28,289]. Therefore, toughness improvement of these composites is of high importance. As shown in Figure 6.8, the toughness of R35 and R15F filled with only 35 wt.% of reinforcements (RR and RR/RTF (15/20)) are 48% and 68% lower than the impact strength of neat rHDPE (360 J/m).

The introduction of a small amount of rubber and fiber increased the stress concentration around the rubber clusters and multiple micro-void formations at the interface, facilitating fracture by lowering the absorbed energy before break-up [289].

In a similar report, poor interfacial adhesion between filler and matrix decreased the impact strength of ethylene vinyl acetate (EVA) from 72.3 J/m to 29.2 J/m (59%) upon the addition of 10 wt.% waste rubber crumbs (<200 μm) [19]. Despite the negative effect of filler content on toughness loss, further increase in recycled rubber content from 35 to 65 and 80 wt.% increased the toughness of R65 (272.5 J/m) and R80 (324.4 J/m) because of higher energy absorption through deformation of the rubbery particles, retarding fracture phenomena [319]. In agreement with Figure 6.8, Luna et al. [320] reported toughness improvement in polystyrene (PS) composites by up to 77% with increasing recycled styrene butadiene rubber (SBR) content from 20 wt.% (37.5 J/m) to 50 wt.% (66.5 J/m). For rHDPE/RR/RTF blends, replacing the rubber phase with constant RTF content (20 wt.%) decreased the toughness of fiber reinforced specimens as the impact strength of R45F and R60F are respectively 9% and 11% lower than R65 and R80, both having 65 and 80 wt.% of fillers. As discussed above, for fiber-reinforced TPE composites with low crack resistance, small microcracks and sharp crack could easily propagate along with weak interfacial voids around rigid fibers, resulting in reduced absorbed energy before sample failure [321]. It should be noticed that the higher toughness of R60F (275.6 J/m) compared to R45F (246.5 J/m) is attributed to the higher content of regenerated rubber particles (lower crosslinked density) in R60F, making the particles more deformable to absorb more energy and delay failure phenomena [238].

The improved toughness upon increasing recycled filler content is at a cost of lower tensile strength and Young's modulus (Table 6.5). Therefore, different attempts were made to produce a multiphase material with balanced toughness and tensile properties, which can be obtained by the inclusion of an interfacial modifier to improve the compatibility of the blends [28,106]. Surface coating of rubber crumbs (waste or virgin), using suitable block copolymer/compatibilizers which is compatible with the polyolefin matrix, forms a thick/soft interphase to improve bonding and promote smooth stress transfer between the RR and the matrix [257]. Formela et al. [106] observed that SBS, having partial miscibility with polyethylene and GTR, improved interfacial adhesion of LDPE/GTR blends by creating a strong interface between the matrix and rubber particles. As shown in Figure 6.8, a substantial increase in composites toughness is obtained by adding MAPE. The effect is more pronounced on the impact strength of R45F* (368.2 J/m) and R60F* (398.7 J/m) compared to R45F (246.5 J/m) and R60F (275.6 J/m). It can be assumed that MAPE surface coated RR seems to slow down crazing propagation through uniform filler dispersion in the matrix via thick interphase around RR particles, reducing the stress concentration, leading to more energy dissipated during crack growth (propagation) [57,322]. In

a similar work, Kakroodi and Rodrigue [28] reported about 81% higher toughness of PP–glass fiber composites (from 23.1 to 41.9 J/m) by adding 15% MAPP/EPDM compound because of improved interfacial adhesion as a result of the chemical similarity between EPDM and PP (propylene blocks) and strong bonding between C=C bonds in EPDM with MAPP. Also, impact modification of natural fiber reinforced PP composites by the direct addition of MAPP coupling agent led to partially located MAPP at the interface of TPE blend with slightly improved toughness [28]. It is well documented that the efficiency of direct incorporation of compatibilizer depends on its localization at the interfacial zone, which subsequently would influence the homogeneity (filler dispersion) and interfacial strength, which are controlled by the mixing strategy (component addition order) [311]. Based on tensile and impact properties, the strength of interfacial interactions increases with MAPE content, increasing the possibility of rubber encapsulation by more coupling agents contributing to better compatibility between the rubber and thermoplastic phases [28].

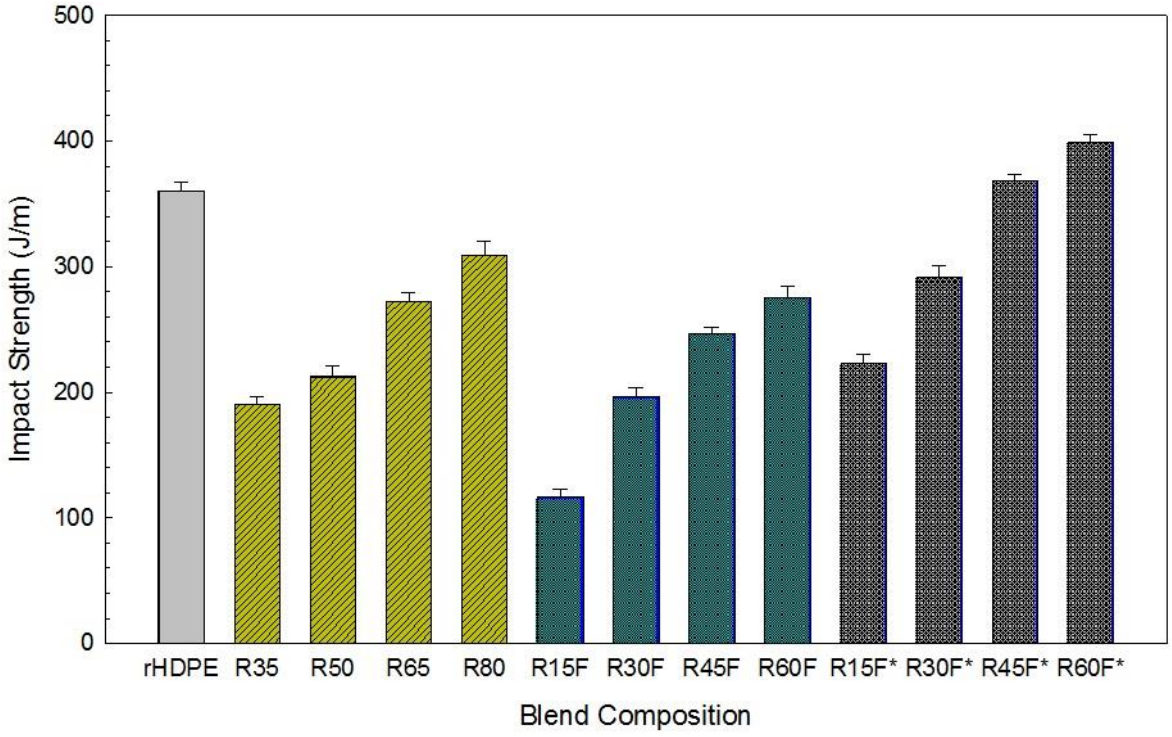

Figure 6.8 Impact strength of the samples produced (see Table 6.2 for definition).

6.3.3 Physical (hardness and density) Properties

In general, the hardness of a TPE compound is determined by the elastic modulus and crosslink density of the rubber phase (GTR) [8]. Table 6.6 shows that in spite of the presence of carbon black in recycled

tire rubber, the hardness of the composites decreased with increasing RR content, which is attributed to the soft nature of rubber particles with low rigidity [12]. Also, the regeneration process results in a less crosslinked network (lower crosslink density), contributing to lower rigidity of the blends filled with RR [248]. The variation of hardness with RTF addition follows a similar trend as the variation of tensile modulus (Table 6.5) and the addition of surface coated RR with MAPE did not modify this trend. For example, the introduction of 80 wt.% RR decreased the hardness (Shore D) of rHDPE from 66 to 39, while the hardness values are respectively 41.2 and 43.7 (Shore D) for R60F and R60F* filled with RR/RTF (60/20) and 60 wt.% RR/MAPE (70/30) masterbatch.

Table 6.6 shows that the density increased due to the higher filler densities (RTF = 1.268 g/cm^3 and RR = 1.184 g/cm^3) compared to rHDPE (0.986 g/cm^3) and MAPE (0.920 g/cm^3). It should be noticed that fiber reinforced rubberized composites filled with RR/RTF contain lower rubber content compared with RR filled composites. So the density of R60F (1.129 g/cm^3) is higher than R80 (1.093 g/cm^3), while R60F* has the lowest density (1.084 g/cm^3), leading to superior specific mechanical properties (mechanical properties per unit of mass) [28].

Table 6.6 Physical properties of the samples produced (see Table 6.2 for definition).

Sample	Hardness (Shore D)	Density (g/cm^3)
rHDPE	66.0 (0.6)	0.986 (0.002)
R35	61.2 (0.4)	1.022 (0.001)
R50	54.3 (0.3)	1.039 (0.002)
R65	43.2 (0.7)	1.064 (0.003)
R80	39.0 (0.4)	1.093 (0.002)
R15F	63.4 (0.6)	1.052 (0.002)
R30F	55.1 (0.3)	1.095 (0.003)
R45F	47.1 (0.4)	1.112 (0.002)
R60F	41.2 (0.8)	1.129 (0.003)
R15F*	63.7 (0.5)	1.025 (0.003)
R30F*	56.8 (0.4)	1.069 (0.002)
R45F*	48.9 (0.4)	1.063 (0.003)
R60F*	43.7 (0.3)	1.084 (0.003)

6.3.4 Thermal stability

Thermogravimetric analysis is an important characterization technique to determine the thermal stability of TPE since these materials are degraded during service life, as well as recycling (grinding) and regeneration processes which influence their long term properties [12]. Table 6.7 presents an overview of the TGA results to compare the thermal and oxidative stabilities of the samples in terms of

T_{max}, which represents the temperature at which the rate of thermal degradation is at its peak evaluated from the derivative thermogravimetry (DTG) curves, as well as T_{10} and T_{50} which represent the temperatures at which 10% and 50% of the initial mass disappeared, respectively. As shown in Table 6.7, the thermal stability of the neat materials can be classified in the order of (from the highest to the lowest thermal stability): MAPE > rHDPE > GTR > RTF. T_{10} for rHDPE and MAPE in air are 390 °C and 394 °C respectively, compared to 303 °C and 281 °C for RR and RTF, respectively. So the introduction of both recycled rubber particles and tire fibers decreased the thermal stability of the thermoplastic resin, as reported elsewhere [289,300]. Table 6.7 also shows that T_{10} of R80 (341 °C) and R60F (329 °C) are lower than T_{10} of rHDPE (390 °C) in air and T_{10} of these composites are also lower than that of rHDPE in nitrogen. Such low thermal stability can be ascribed to the presence of volatile material in the fillers such as processing oils, additives and other compounds with low molar mass and/or low boiling temperature [273]. Thermal decomposition temperatures are much higher in nitrogen compared to air (lower thermal stability in oxygen atmosphere), showing the effect of oxidation on the thermal decomposition of these compounds [28]. In the case of compatibilized composites, R60F* shows 10% and 50% of initial mass loss at 352 °C and 451 °C in air, while T_{10} and T_{50} are at 371 °C and 463°C in nitrogen. Higher T_{10} and T_{50} values suggest good compatibility of MAPE with rHDPE and RR associated with the good thermal stability of MAPE [225]. The higher amount of residues can inhibit the degradation process of the undecomposed polymer as the out-diffusion of the volatile decomposition products is hindered by char content as a direct result of reduced permeability [289]. For example, the residues of R60F* are 7.9% and 24.8% in air and nitrogen respectively, which are higher than that of R80 and R0F composites. It is worth mentioning that Formela et al. [106] reported higher thermal stability of LDPE/GTR (50/50) blends with the addition of SBS (compatibilizer), creating a soft interface around GTR particles, improving interfacial adhesion and yielding higher residues for the compatibilized sample at 550 °C by 39% (from 18.3 to 25.5 wt.%). For better comparison, the TGA and DTG curves of rHDPE, R80, R60F and R60F* in air and nitrogen are shown in Figure 6.9. It is clear that the thermal decomposition of the TPE starts earlier than rHDPE, attributed to the degradation of processing oils and additives at low temperature, as well as lower crosslink density of the generated rubber, promoting its degradation at lower temperatures [132]. Regardless of filler loading (RR or RR/RTF), the presence of recycled rubber particles increased the residues at 850 °C compared to rHDPE. This observation can be related to the presence of minerals (such as carbon black and SiO_2 usually around 30–35 wt.%) in the recycled tire formulation [300]. The presence of the compatibilizer

influenced the ultimate weight loss as R60F* compatibilized with 18 wt.% MAPE with strong molecular entanglements and interfacial adhesion between the phases showed the highest residues. Also, the carbon black content of tire rubber can adsorb low MW volatile products formed during thermal degradation, creating a barrier effect by producing a more tortuous path for these gases decreasing the ultimate weight loss [132]. DTG curves show that the thermal degradation of TPE under air occurs as a multistep process related to rHDPE and MAPE degradation [12], decomposition of NR and synthetic rubber (SBR and/or polybutadiene rubber; BR) [132], and carbon black leading to the formation of carbon dioxide [277]. The difference between the residuals in air and nitrogen is related to an additional oxidation step of carbon black to carbon dioxide around 540 °C leading to lower value of residuals in air [323].

Table 6.7 Decomposition temperatures (T_{10}, T_{50} and T_{max}) and residues of the samples produced (see Table 6.2 for definition).

Sample	**T_{max} (°C)**		**T_{10} (°C)**		**T_{50} (°C)**		**Residues (wt.%)**	
	Air	N_2	Air	N_2	Air	N_2	Air	N_2
rHDPE	423	491	390	425	423	479	1.1	1.6
MAPE	452	486	394	418	442	463	0.3	0.8
RR	341	417	303	342	466	435	7.4	32.7
RTF	338	394	281	305	391	423	4.5	11.4
R35	439	467	378	392	460	475	4.8	4.5
R50	440	475	364	378	457	470	4.2	8.8
R65	451	480	352	359	458	466	5.7	13.3
R80	459	489	341	343	450	466	6.6	15.9
R15F	437	464	365	379	458	472	3.4	5.6
R30F	443	473	355	368	456	469	4.5	7.9
R45F	450	478	341	356	455	465	6.1	12.6
R60F	456	486	329	347	450	461	6.4	15.5
R15F*	440	468	394	410	462	476	5.1	13.1
R30F*	445	477	375	400	460	471	5.8	16.8
R45F*	453	482	364	387	457	465	7.3	17.2
R60F*	466	489	352	371	451	463	7.9	24.8

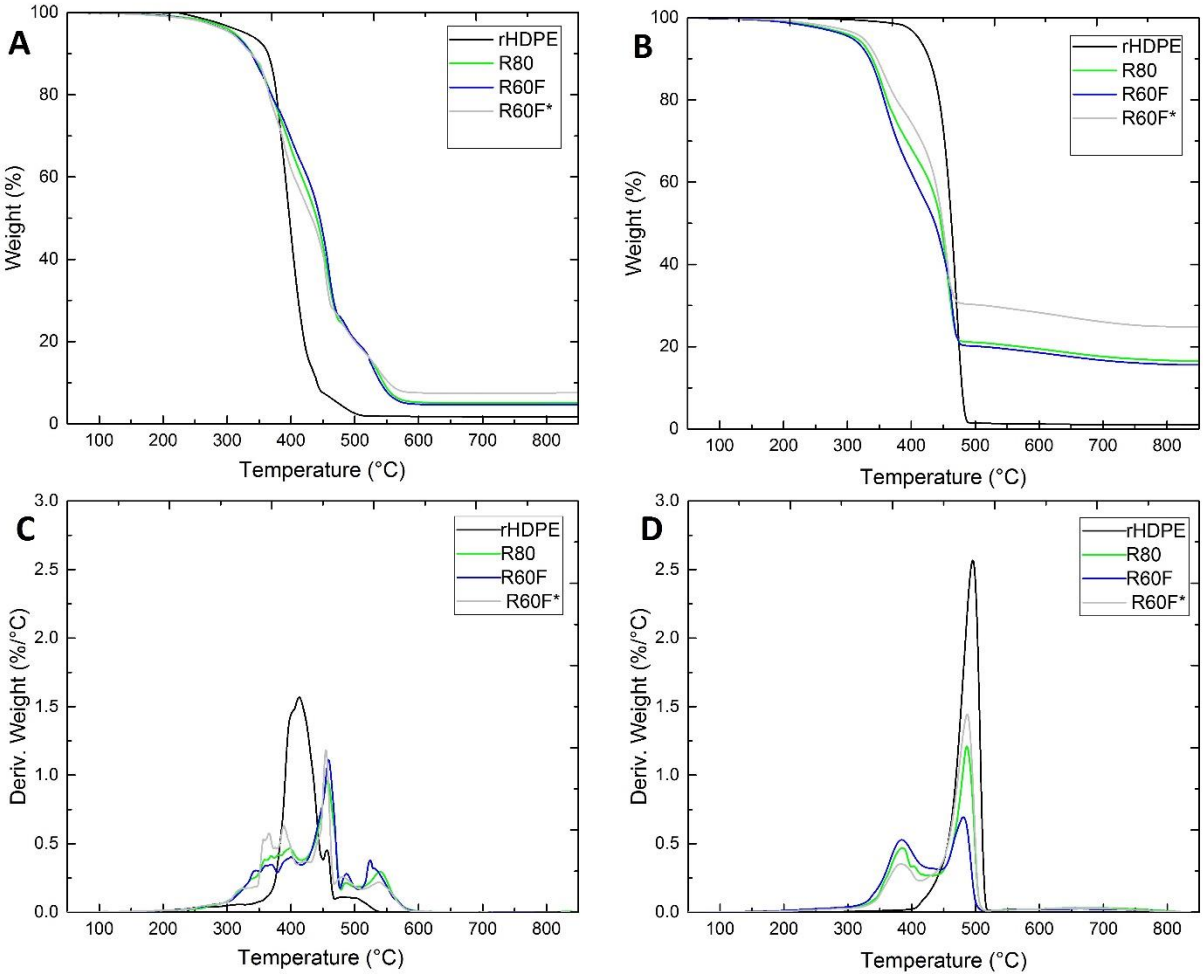

Figure 6.9 Weight and derivative curves as a function of temperature for rHDPE, R80, R60F and R60F* in: (A,C) air and (B,D) nitrogen (see Table 6.2 for definition).

6.3.4 Differential scanning calorimetry

The crystalline structure in TPE blends is of high importance, as their mechanical properties are influenced by the matrix crystallinity, especially the impact strength of composites. DSC analysis was used to determine possible crystallinity changes of the matrix upon filler and compatibilizer addition. The melting (T_m) and crystallization (T_c) temperatures, melting enthalpy (ΔH_m) and crystallinity degree (X_c) are summarized in Table 6.8. Earlier studies reported that the presence of crosslinked rubber only had a slight effect on the matrix microstructure because of the poor compatibility in binary blends [10]. According to Table 6.8, the addition of RR and RTF resulted in small changes in T_m and T_c compared to rHDPE, and a slight increase in Tc of the compatibilized composites compared to the neat matrix. These results are attributed to the solid fillers dispersed in the semi-crystalline matrix improving heterogeneous nucleation. The lowest crystallization temperature of R60F* (117.9 °C) among the

compatibilized samples reflects a better filler encapsulation by MAPE, since well covered and finely dispersed particles did not effectively improved heterogeneous nucleation [311]. But increasing the filler (RR or RR/RTF) content led to a drop in ΔH_m, which implies a crystallization perturbed by the presence of amorphous fillers. For example, R80 (26.1 J/g) and R60F (25.7 J/g) showed the lowest enthalpy of melting due to the lower content of crystallizable material (plastic phase) [11,300]. Variation in the crystallinity degree might influence the impact strength, since a higher level of crystallinity is known to reduce toughness [324]. Restricted flowability of rubber particles (amorphous nature) increases the blend viscosity, slowing down the diffusion of PE segments to crystallization sites (limited mobility of crystallizable chain segment), limiting the growth of lamellae on the crystalline side, resulting in smaller crystalline phase and lower crystallinity [11,106]. It is well documented that addition of virgin or recycled rubber into TPE contributes to a drop in chain regularity (restriction in mobility of the rHDPE chains) resulting in smaller crystallinity and limiting the growth of thick lamellas which causes a decrease in blend crystallinity, in agreement with the fall in tensile strength and modulus [78,242]. It is also claimed that melt extrusion can lead to some crosslinking of the regenerated rubber particles (partially destroyed crosslinked network), which can serve as local defects to interfere with the compact structure of the polymer chains, thus decreasing the crystallinity degree [242]. Also, a small amount of short fibers (less than 10 wt.%) is reported to provide nucleation points to speed up the crystallization rate, but higher fiber loading (above 10 wt.%) prevents the spherulites from expanding in all direction, thus reducing crystallinity, in agreement with our results (Table 6.8) [325]. The low crystallinity level of R80 (45.6%) suggests a decrease in the overall crystallinity with decreasing rHDPE content and supports the decreasing trend of tensile strength and tensile modulus (Table 6.5) with increasing filler content (softer nature) [299]. Overall, the different blend compositions had negligible differences in their temperatures of melting and crystallization, as well as crystallinity degree which, is in agreement with previous reports [106]. According to the crystallinity and impact strength results, it can be concluded that the higher toughness (Figure 6.8) is mainly the result of the developed phase morphologies and interfacial interactions.

Table 6.8 Melting and crystallization temperatures with their corresponding enthalpy and crystallinity degree for the samples produced (see Table 6.2 for definition).

Sample Code	T_m (°C)	T_c (°C)	ΔH_m (J/g)	X (%)
rHDPE	127.5	118.1	148.5	51.9
R35	126.6	118.1	94.1	50.6
R50	126.5	118.3	71.2	49.8
R65	127.0	117.8	46.3	46.2
R80	126.7	117.5	26.1	45.6
R15F	127.2	118.0	92.3	49.6
R30F	127.0	117.4	68.6	48.1
R45F	126.0	117.5	47.2	47.2
R60F	126.0	116.8	25.7	44.9
R15F*	127.1	118.6	103.4	52.2
R30F*	126.4	118.5	85.3	50.5
R45F*	127.0	118.3	69.4	49.1
R60F*	126.1	117.8	53.2	48.9

6.4 Conclusion

This work proposed a simple approach to improve the impact strength of fiber reinforced rubberized composites via surface coating of waste rubber particles with MAPE. TPE composites based on rHDPE/(RR/MAPE)/RTF reinforced with RR (35-80 wt.%) and RTF (20 wt.%) were investigated in terms of phase morphology, tensile/flexion properties, impact toughness and thermal behavior. Despite a drop in tensile strength and Young's modulus, the presence of RR particles improved the elongation at break of rHDPE/RR blends by up to 78% (R80) which was attributed to a higher rubber content (elastic phase) inducing higher deformation/elasticity. But substitution of the RR fraction by a RR/RTF mixture compensated these tensile/flexural losses because of the more rigid nature of RTF increasing the composites stiffness, while the impact strength decreased for the binary TPE compounds. A morphological characterization was used to confirm the level of blend interaction as surface coverage of RR particles with MAPE highly enhanced the interfacial adhesion between the fillers and rHDPE, resulting in improved homogeneity (more uniform RR and RTF distribution). The presence of MAPE compatibilized the filler and matrix, leading to improved tensile properties. The tensile strength of R80 was improved by 79% (from 4.7 MPa to 8.8 MPa), and the tensile strain at break was doubled (from 65.2% to 172.3%) for R60F*. Furthermore, significant impact strength improvement (up to 60%) was obtained after RR/MAPE masterbatch addition. This increased strength was more significant (up to 398.7 J/m) as the MAPE content increased up to 18 wt.% and also for samples with higher RR contents.

It is concluded that improved compatibility between rHDPE and RR via MAPE formed stronger interface leads to reduced stress concentration around the fillers, slowing down the fracture. Finally, the proposed processing step for encapsulation of the rubber phase by MAPE provided an efficient method for waste tire recycling (rubber and fibers) by producing toughened TPE composites with acceptable mechanical properties. The fiber reinforced rubberized TPE composites studied in this paper with acceptable elasticity and toughness have protentional industrial application such as artificial sports equipment, automotive sector (e.g. bumper fascia, wiper blades, fender liners, sight shields, and stone deflectors) and construction industries (e.g. retrofit slabs, beams, signboards, and guardrails).

Acknowledgments

The authors acknowledge the technical support of the Research Center on Advanced Materials (CERMA). Also, the technical help of Yann Giroux was highly appreciated.

CONCLUSIONS AND RECOMMENDATIONS

General conclusions

Currently, the disposal of waste polymers (plastics and tires) is a serious environmental issue since their large quantity and complex structure/composition can pollute the environment. The majority of post-consumer/post-industrial tires are still being burnt or buried, which represents a very serious threat to the ecology due to the enormous space in landfills and emission of hazardous gases. In recent decades, several studies focused on the development of cost-effective and environmentally friendly methods for recycling waste tires through blend compounding, with a focus on TPE. Although various strategies have been used to improve the performance and durability of TPE, main drawback of low mechanical properties and toughness remained unsettled, especially focusing on the melt blending of recycled polyolefins with GTR and/or RTF.

This project focused on waste polymer recycling and the possibility to reuse recycled tire rubber (impact strength modifier) and fiber (good tensile strength and modulus) as reinforcing fillers to produce high quality TPE compounds based on a recycled thermoplastic matrix. The selection of recycled HDPE with good mechanical properties, excellent processability and high availability as the matrix for blending with GTR not only benefits from the potential for further reprocessing and recycling of the compounds, but also results in economic and eco-friendly advantages, such as decreasing use of virgin materials (less generation of polymer wastes) and reduction of the final cost (raw materials). This section presents an overview of the most significant conclusions and highlights of this research and provides some recommendations for future works.

According to the results, poor GTR distribution in the polymer matrix promoted particle-particle interactions and contributed to weak sites upon stress-transfer, leading to lower tensile strength with increasing GTR content from 20 to 90 wt.% (both NRR and RR). This decreasing trend in modulus (tension and flexion) with GTR loading (more significant decreases occurred for blends filled RR particles) was related to the GTR regeneration, leading to partial break-up of the vulcanized rubber crosslinked structure, combined with the softening effect of the processing oil in RR formulation, leading to lower rigidity and hardness. As expected, the addition of GTR particles produced higher elongation at break and impact strength due to the presence of a more elastic content, inducing high deformation/elasticity and more energy absorption by the elastomeric phase before failure.

The second part of the work presented a complete series of studies to determine the influence of the rubber particle size and rubber content on the processability, structure and overall properties of TPE. The particle size was varied by mechanical sieving and ranged from 0–250 μm to 250–500 μm and 500–850 μm. The results showed that GTR particles with their crosslinked network did not flow, and agglomerated in the rHDPE matrix, increasing the blend viscosity (lower MFI), leading to higher motor torque and die pressure loss in extrusion, especially for smaller particles (0–250 μm). According to DSC results, the crystallinity degree for all the compositions decreased with the introduction of a flexible amorphous phase (GTR) disturbing the packing of matrix chains. However, smaller particles induced higher level of compactness, since the polymer chains had more freedom to organize themselves, leading to a structure modification at their boundaries, influencing on the matrix crystallinity. SEM micrographs showed that smaller GTR (0–250 μm) had better interaction with the matrix (less voids/defects) due to their higher specific surface area. Lower tensile and impact properties for large particles can be ascribed to particle agglomeration and poor particle-particle/particle-matrix interaction, resulting in stress concentration points and weak interfacial adhesion, increasing the probability of crack initiation/propagation and premature failure (easier break-up). It can be concluded that smaller GTR below 50 wt.% contributed to better mechanical properties, attributed to the higher specific surface area of the particles, promoting better interfacial stress transfer and interaction between GTR and rHDPE.

The next step investigated the effect of GTR regeneration, blend composition and compatibility/interfacial adhesion promoter on the performance of ternary blends of rHDPE/GTR/rEVA from 100% recycled sources. The results revealed that an efficient breakdown of the crosslinked network of RR_2 (regeneration degree of 24%) with a low gel fraction (88%) and crosslink density (5.5×10^{-4} mol/cm^3) would contribute to sufficient chain entanglement between RR_2 and rHDPE to create a strong interphase, leading to higher tensile strain at break and toughness. It should be noticed that rubber regeneration is not a 100% selective rupture of sulfur bonds alone, and might also produce degradation of the main chains (backbones) of the recycled rubber during regeneration (extensive shear/elongation and high temperature), lowering the MW and degrading the tensile properties (RR_1 filled blends). Partial substitution of rHDPE by rEVA gave rise to higher blend homogeneity and compatibility. It can be concluded that good filler/matrix interaction resulted in lower voids and less solvent penetration into the compatibilized blends, because of lower toluene uptake of ternary blends compared to that of rHDPE/GTR blends. Inclusion of rEVA (10 wt.%) contributed to higher elongation

at break (203%) and toughness improvement (11%). It can be claimed that adding a recycled elastomer copolymer promoted a more uniform GTR dispersion (especially RR_2) via filler encapsulation creating a strong interphase (decreasing the surface energy) and increasing the deformation ability of the rHDPE around these particles to improve the impact resistance.

As the last step of this work, a new approach was proposed for impact modification by using a RR/MAPE masterbatch into a fiber reinforced rubberized composite. Although RR replacement by a RR/RTF mixture compensated for the tensile/flexural moduli losses because of the more rigid nature of RTF increasing the composites stiffness, the impact strength of the blends decreased. Bur after RR/MAPE addition, a morphological characterization showed that RR particles were completely embedded within the matrix (very difficult to distinguish them from the matrix) and much less gaps/voids/defects were detected due to rubber particles coverage by MAPE generating molecular entanglement at the interface, leading to better interfacial interaction. It can be assumed that MAPE surface coated RR seemed to slow down crazing propagation through uniform filler dispersion in the matrix via thick interphase around RR particles, reducing the stress concentration, leading to significant impact strength improvement (up to 60%). Finally, TGA results showed that the presence of a suitable compatibilizer influenced the ultimate weight loss, as compatibilized samples with strong molecular entanglements and interfacial adhesion between the phases showed the highest weight retention. Blend composition and compatibilizer addition also showed negligible effect on crystallinity. It can thus be concluded that the impact modification of TPE was mainly influenced by the developed phase morphologies and interfacial interactions.

Based on the findings of this thesis, the production of recycled TPE compounds reinforced with GTR/RTF and compatibilized with rEVA and RR/MAPE not only contributed to improve the elasticity and toughness of the blends, but can also result in use of a high volume of waste materials after their end of life to help solving an environmental issue.

Recommendations for future work

Based on the results obtained in this study, the following recommendations are proposed for future works:

1. This thesis investigated the reinforcement role of GTR obtained from NR (OTR) and SBR (PI3.1.C) for their incorporation into rHDPE. For the next step, it is recommended to investigate recycled rubbers with different sources, such as EPDM or NBR into other thermoplastics (PP for example).
2. In this work, thermoplastic elastomers based on rHDPE, rEVA and GTR were produced. It is suggested to prepare blends with similar formulations and processing conditions using virgin HDPE and EVA to compare and determine the effect of using recycled materials (contamination, etc.).
3. This work focused on the preparation and characterization of recycled TPE by the addition of a recycled polar elastomer. It would be interesting to study the effect of the type and grade of different EVA elastomers acting as interfacial modifier to improve TPE toughness.
4. In order to decrease the costs, replacing virgin MAPE with maleated recycled thermoplastics can be interesting to improve the compatibility of all recycled TPE reinforced with GTR/RTF.
5. Despite several attempts devoted to the preparation and characterization of TPE foams based on GTR filled compounds, there is a lack of literature about RTF-filled TPE foams. It could also be of interest to investigate the combined effects of GTR and RTF on the final properties of polyolefins based foamed composites with balanced mechanical properties.
6. It is well documented that melt blending GTR with thermoplastics (recycled or virgin) benefits the potential for further reprocessing and recycling of the compounds. Nevertheless, it is difficult to find information about the stability for these compounds to withstand different degradations (during service life and reprocessing). It would be of interest to investigate the effect of different degradation mechanisms (thermal ageing, weathering and re-processing) on TPE compounds.
7. Although rHDPE was selected as the matrix for this study, the incorporation of GTR as an impact modifier into a bio-based/bio-degradable matrix, like PLA (brittle) with very low elongation at break and toughness, could also be of interest for the production toughened PLA blends.

8. A recycled copolymer (rEVA) was proposed as an appropriate interfacial modifier for the preparation of ternary TPE blends with balanced mechanical properties. We believe there is strong potential to use this idea at an industrial scale for the development of recyclable TPE compounds offering high resistance to fracture/deformation and excellent flexibility for specific applications like floor mats, dampers and containers (recycling bins). A feasibility study for industrial implementation of this idea is of high interest, including more advanced economics/life cycle/mechanical analyses.

REFERENCES

1. Ramarad, S.; Khalid, M.; Ratnam, C.; Chuah, A.L.; Rashmi, W. Waste tire rubber in polymer blends: A review on the evolution, properties and future. *Progress in Materials Science* **2015**, *72*, 100-140.
2. Sienkiewicz, M.; Kucinska-Lipka, J.; Janik, H.; Balas, A. Progress in used tyres management in the European Union: A review. *Waste Management* **2012**, *32*, 1742-1751.
3. Agencies, C.A.o.T.R. *CATRA 2018 Annual Report*; 2018.
4. Sienkiewicz, M.; Janik, H.; Borzędowska-Labuda, K.; Kucińska-Lipka, J. Environmentally friendly polymer-rubber composites obtained from waste tyres: A review. *Journal of Cleaner Production* **2017**, *147*, 560-571.
5. Fazli, A.; Rodrigue, D. Waste Rubber Recycling: A Review on the Evolution and Properties of Thermoplastic Elastomers. *Materials* **2020**, *13*, 782.
6. Medina, N.F.; Garcia, R.; Hajirasouliha, I.; Pilakoutas, K.; Guadagnini, M.; Raffoul, S. Composites with recycled rubber aggregates: Properties and opportunities in construction. *Construction and Building Materials* **2018**, *188*, 884-897.
7. Massey, L.K. *The Effect of UV Light and Weather: On Plastics and Elastomers*; William Andrew: 2006.
8. Fazli, A.; Rodrigue, D. Recycling Waste Tires into Ground Tire Rubber (GTR)/Rubber Compounds: A Review. *Journal of Composites Science* **2020**, *4*, 103.
9. Karger-Kocsis, J.; Mészáros, L.; Bárány, T. Ground tyre rubber (GTR) in thermoplastics, thermosets, and rubbers. *Journal of Materials Science* **2013**, *48*, 1-38.
10. Sonnier, R.; Leroy, E.; Clerc, L.; Bergeret, A.; Lopez-Cuesta, J. Polyethylene/ground tyre rubber blends: Influence of particle morphology and oxidation on mechanical properties. *Polymer Testing* **2007**, *26*, 274-281.
11. Esmizadeh, E.; Naderi, G.; Bakhshandeh, G.R.; Fasaie, M.R.; Ahmadi, S. Reactively compatibilized and dynamically vulcanized thermoplastic elastomers based on high-density polyethylene and reclaimed rubber. *Polymer Science, Series B* **2017**, *59*, 362-371.
12. Kakroodi, A.R.; Rodrigue, D. Highly filled thermoplastic elastomers from ground tire rubber, maleated polyethylene and high density polyethylene. *Plastics, rubber and composites* **2013**, *42*, 115-122.
13. Shanmugharaj, A.; Kim, J.K.; Ryu, S.H. UV surface modification of waste tire powder: characterization and its influence on the properties of polypropylene/waste powder composites. *Polymer Testing* **2005**, *24*, 739-745.
14. Ismail, H.; Awang, M.; Hazizan, M. Effect of waste tire dust (WTD) size on the mechanical and morphological properties of polypropylene/waste tire dust (PP/WTD) blends. *Polymer-Plastics Technology and Engineering* **2006**, *45*, 463-468.
15. Zhang, S.L.; Zhang, Z.X.; Pal, K.; Xin, Z.X.; Suh, J.; Kim, J.K. Prediction of mechanical properties of waste polypropylene/waste ground rubber tire powder blends using artificial neural networks. *Materials & Design* **2010**, *31*, 3624-3629.
16. Macsiniuc, A.; Rochette, A.; Brisson, J.; Rodrigue, D. Polystyrene/recycled SBR powder compounds produced in an internal batch mixer. *Progress in Rubber Plastics and Recycling Technology* **2014**, *30*, 185-210.
17. Veilleux, J.; Rodrigue, D. Properties of recycled PS/SBR blends: effect of SBR pretreatment. *Progress in Rubber Plastics and Recycling Technology* **2016**, *32*, 111-128.
18. Hassan, M.M.; Badway, N.A.; Gamal, A.M.; Elnaggar, M.Y.; Hegazy, E.-S.A. Studies on mechanical, thermal and morphological properties of irradiated recycled polyamide and waste rubber powder blends. *Nuclear Instruments and Methods in Physics Research Section B: Beam Interactions with Materials and Atoms* **2010**, *268*, 1427-1434.
19. Mujal-Rosas, R.; Orrit-Prat, J.; Ramis-Juan, X.; Marin-Genesca, M.; Rahhali, A. Study on dielectric, thermal, and mechanical properties of the ethylene vinyl acetate reinforced with ground tire rubber. *Journal of Reinforced Plastics and Composites* **2011**, *30*, 581-592.

20. Mészáros, L.; Fejős, M.; Bárány, T. Mechanical properties of recycled LDPE/EVA/ground tyre rubber blends: Effects of EVA content and postirradiation. *Journal of Applied Polymer Science* **2012**, *125*, 512-519.
21. Fernández, A.; Barriocanal, C.; Alvarez, R. Pyrolysis of a waste from the grinding of scrap tyres. *Journal of Hazardous Material* **2012**, *203*, 236-243.
22. Lievana, E.; Karger-Kocsis, J. Use of ground tyre rubber (GTR) in thermoplastic polyolefin elastomer compositions. *Progress in Rubber Plastics and Recycling Technology* **2004**, *20*, 1-10.
23. Hejna, A.; Olszewski, A.; Zedler, Ł.; Kosmela, P.; Formela, K. The Impact of Ground Tire Rubber Oxidation with H2O2 and KMnO4 on the structure and performance of flexible polyurethane/ground tire rubber composite foams. *Materials* **2021**, *14*, 499.
24. Sonnier, R.; Leroy, E.; Clerc, L.; Bergeret, A.; Lopez-Cuesta, J. Polyethylene/ground tyre rubber blends: Influence of particle morphology and oxidation on mechanical properties. *Polymer Testing* **2007**, *26*, 274-281.
25. Tao, G.; He, Q.; Xia, Y.; Jia, G.; Yang, H.; Ma, W. The effect of devulcanization level on mechanical properties of reclaimed rubber by thermal-mechanical shearing devulcanization. *Journal of Applied Polymer Science* **2013**, *129*, 2598-2605.
26. Meysami, M.; Tzoganakis, C.; Mutyala, P.; Zhu, S.; Bulsari, M. Devulcanization of scrap tire rubber with supercritical CO2: A study of the effects of process parameters on the properties of devulcanized rubber. *International Polymer Processing* **2017**, *32*, 183-193.
27. Sripornsawat, B.; Saiwari, S.; Nakason, C. Thermoplastic vulcanizates based on waste truck tire rubber and copolyester blends reinforced with carbon black. *Waste Management* **2018**, *79*, 638-646.
28. Kakroodi, A.R.; Rodrigue, D. Impact modification of polypropylene-based composites using surface-coated waste rubber crumbs. *Polymer Composites* **2014**, *35*, 2280-2289.
29. Moghaddamzadeh, S.; Rodrigue, D. The effect of polyester recycled tire fibers mixed with ground tire rubber on polyethylene composites. Part II: Physico-mechanical analysis. *Progress in Rubber, Plastics and Recycling Technology* **2018**, *34*, 128-142.
30. Wang, Y.-H.; Chen, Y.-K.; Rodrigue, D. Production of Thermoplastic Elastomers Based on Recycled PE and Ground Tire Rubber: Morphology, Mechanical Properties and Effect of Compatibilizer Addition. *International Polymer Processing* **2018**, *33*, 525-534.
31. Shojaei, A.; Yousefian, H.; Saharkhiz, S. Performance characterization of composite materials based on recycled high-density polyethylene and ground tire rubber reinforced with short glass fibers for structural applications. *Journal of Applied Polymer Science* **2007**, *104*, 1-8.
32. Zhang, X.X.; Lu, C.H.; Liang, M. Preparation of rubber composites from ground tire rubber reinforced with waste-tire fiber through mechanical milling. *Journal of Applied Polymer Science* **2007**, *103*, 4087-4094.
33. Ikeda, Y.; Kato, A.; Kohjiya, S.; Nakajima, Y. *Rubber Science*; Springer: 2018.
34. Fukumori, K.; Matsushita, M.; Okamoto, H.; Sato, N.; Suzuki, Y.; Takeuchi, K. Recycling technology of tire rubber. *JSAE review* **2002**, *23*, 259-264.
35. Nakajima, N. *Science and practice of rubber mixing*; iSmithers Rapra Publishing: 2000.
36. Liu, Q.; Zhang, Y.; Xu, H. Properties of vulcanized rubber nanocomposites filled with nanokaolin and precipitated silica. *Applied Clay Science* **2008**, *42*, 232-237.
37. Heinrich, G.; Vilgis, T.A. Contribution of entanglements to the mechanical properties of carbon black-filled polymer networks. *Macromolecules* **1993**, *26*, 1109-1119.
38. Okada, A.; Usuki, A. The chemistry of polymer-clay hybrids. *Materials Science and Engineering: C* **1995**, *3*, 109-115.
39. Niyogi, U.K. *Introduction to Fibre Science and Rubber Technology B. Rubber Technology* Shri Ram Institute for Industrial Research, 2007.
40. Mente, P.; Motaung, T.; Hlangothi, S. Natural rubber and reclaimed Rubber composites–A Systematic Review. *Polymer Sciences* **2016**, *2*, 1-19.
41. Wypych, G. Handbook of polymers. 2nd ed.; Elsevier: 2016.
42. Morton, M. *Rubber technology*; Springer Science & Business Media: 2013.

43. Mitra, S.; Jørgensen, M.; Pedersen, W.B.; Almdal, K.; Banerjee, D. Structural determination of ethylene-propylene-diene rubber (EPDM) containing high degree of controlled long-chain branching. *Journal of Applied Polymer Science* **2009**, *113*, 2962-2972.
44. Milani, G.; Milani, F. EPDM accelerated sulfur vulcanization: a kinetic model based on a genetic algorithm. *Journal of Mathematical Chemistry* **2011**, *49*, 1357-1383.
45. Milani, G.; Milani, F. Simple kinetic numerical model based on rheometer data for Ethylene–Propylene–Diene Monomer accelerated sulfur crosslinking. *Journal of Applied Polymer Science* **2012**, *124*, 311-324.
46. Akindoyo, J.O.; Beg, M.; Ghazali, S.; Islam, M.; Jeyaratnam, N.; Yuvaraj, A. Polyurethane types, synthesis and applications–a review. *RSC Advances* **2016**, *6*, 114453-114482.
47. Percec, V.; Pugh, C. Comprehensive Polymer Science and Supplements. **1989**.
48. Lievana, E.J. Recycling of ground tyre rubber and polyolefin wastes by producing thermoplastic elastomers. Doctor of Philosophy, Technical University of Kaiserslautern, Germany, 2005.
49. Fang, Y.; Zhan, M.; Wang, Y. The status of recycling of waste rubber. *Materials & Design* **2001**, *22*, 123-128.
50. Amari, T.; Themelis, N.J.; Wernick, I.K. Resource recovery from used rubber tires. *Resources Policy* **1999**, *25*, 179-188.
51. Shah, J.; Jan, M.R.; Mabood, F. Catalytic conversion of waste tyres into valuable hydrocarbons. *Journal of Polymers and the Environment* **2007**, *15*, 207-211.
52. Van Beukering, P.J.; Janssen, M.A. Trade and recycling of used tyres in Western and Eastern Europe. *Resources, Conservation and Recycling* **2001**, *33*, 235-265.
53. İlkılıç, C.; Aydın, H. Fuel production from waste vehicle tires by catalytic pyrolysis and its application in a diesel engine. *Fuel Processing Technology* **2011**, *92*, 1129-1135.
54. Adhikari, B.; De, D.; Maiti, S. Reclamation and recycling of waste rubber. *Progress in Polymer Science* **2000**, *25*, 909-948.
55. Singh, N.; Hui, D.; Singh, R.; Ahuja, I.; Feo, L.; Fraternali, F. Recycling of plastic solid waste: A state of art review and future applications. *Composites Part B: Engineering* **2017**, *115*, 409-422.
56. Sunthonpagasit, N.; Duffey, M.R. Scrap tires to crumb rubber: feasibility analysis for processing facilities. *Resources, Conservation and Recycling* **2004**, *40*, 281-299.
57. Li, Y.; Zhang, Y.; Zhang, Y. Morphology and mechanical properties of HDPE/SRP/elastomer composites: effect of elastomer polarity. *Polymer Testing* **2004**, *23*, 83-90.
58. Kear, K.E. *Developments in Thermoplastic Elastomers*; 2003; Volume 14.
59. Holden, G. Thermoplastic Elastomers. In *Applied Plastics Engineering Handbook*, Kutz, M., Ed.; 2011; pp. 77-91.
60. Drobny, J.G. *Handbook of thermoplastic elastomers*; Elsevier: 2014.
61. Asaletha, R.; Kumaran, M.; Thomas, S. Thermoplastic elastomers from blends of polystyrene and natural rubber: morphology and mechanical properties. *European Polymer Journal* **1999**, *35*, 253-271.
62. Carone Jr, E.; Kopcak, U.; Goncalves, M.; Nunes, S. In situ compatibilization of polyamide 6/natural rubber blends with maleic anhydride. *Polymer* **2000**, *41*, 5929-5935.
63. Ghazali, Z.; Johnson, A.; Dahlan, K. Radiation crosslinked thermoplastics natural rubber (TPNR) foams. *Radiation Physics and Chemistry* **1999**, *55*, 73-79.
64. Mina, M.; Ania, F.; Balta Calleja, F.; Asano, T. Microhardness studies of PMMA/natural rubber blends. *Journal of Applied Polymer Science* **2004**, *91*, 205-210.
65. Nakason, C.; Nuansomsri, K.; Kaesaman, A.; Kiatkamjornwong, S. Dynamic vulcanization of natural rubber/high-density polyethylene blends: effect of compatibilization, blend ratio and curing system. *Polymer Testing* **2006**, *25*, 782-796.
66. Nakason, C.; Jarnthong, M.; Kaesaman, A.; Kiatkamjornwong, S. Thermoplastic elastomers based on epoxidized natural rubber and high-density polyethylene blends: Effect of blend compatibilizers on the mechanical and morphological properties. *Journal of Applied Polymer Science* **2008**, *109*, 2694-2702.
67. Grohens, Y.; Kumar, S.K.; Boudenne, A.; Weimin, Y. *Recycling and Reuse of Materials and Their Products*; CRC Press: 2013.

68. Pichaiyut, S.; Nakason, C.; Kaesaman, A.; Kiatkamjornwong, S. Influences of blend compatibilizers on dynamic, mechanical, and morphological properties of dynamically cured maleated natural rubber and high-density polyethylene blends. *Polymer Testing* **2008**, *27*, 566-580.
69. Ning, N.; Li, S.; Wu, H.; Tian, H.; Yao, P.; Guo-Hua, H.; Tian, M.; Zhang, L. Preparation, microstructure, and microstructure-properties relationship of thermoplastic vulcanizates (TPVs): A review. *Progress in Polymer Science* **2018**, *79*, 61-97.
70. Koning, C.; Van Duin, M.; Pagnoulle, C.; Jerome, R. Strategies for compatibilization of polymer blends. *Progress in Polymer Science* **1998**, *23*, 707-757.
71. Flory, P.J. *Principles of polymer chemistry*; Cornell University Press: 1953.
72. Maris, J.; Bourdon, S.; Brossard, J.-M.; Cauret, L.; Fontaine, L.; Montembault, V. Mechanical recycling: Compatibilization of mixed thermoplastic wastes. *Polymer Degradation and Stability* **2018**, *147*, 245-266.
73. Iyer, S.; Schiraldi, D.A. Role of ionic interactions in the compatibility of polyester ionomers with poly (ethylene terephthalate) and nylon 6. *Journal of Polymer Science Part B: Polymer Physics* **2006**, *44*, 2091-2103.
74. Ramezani Kakroodi, A. Production and characterization of thermoplastic elastomers based on recycled rubber. Doctor of Philosophy, Laval University, Canada, 2013.
75. Kumar, C.R.; Fuhrmann, I.; Karger-Kocsis, J. LDPE-based thermoplastic elastomers containing ground tire rubber with and without dynamic curing. *Polymer Degradation and Stability* **2002**, *76*, 137-144.
76. Kim, J.; Ryu, S.; Chang, Y. Mechanical and dynamic mechanical properties of waste rubber powder/HDPE composite. *Journal of Applied Polymer Science* **2000**, *77*, 2595-2602.
77. Rocha, M.C.G.; Leyva, M.E.; Oliveira, M.G.d. Thermoplastic elastomers blends based on linear low density polyethylene, ethylene-1-octene copolymers and ground rubber tire. *Polímeros* **2014**, *24*, 23-29.
78. Magioli, M.; Sirqueira, A.S.; Soares, B.G. The effect of dynamic vulcanization on the mechanical, dynamic mechanical and fatigue properties of TPV based on polypropylene and ground tire rubber. *Polymer Testing* **2010**, *29*, 840-848.
79. Canavate, J.; Carrillo, F.; Casas, P.; Colom, X.; Sunol, J. The use of waxes and wetting additives to improve compatibility between hdpe and ground tyre rubber. *Journal of Composite Materials* **2010**, *44*, 1233-1245.
80. He, M.; Li, Y.; Qiao, B.; Ma, X.; Song, J.; Wang, M. Effect of dicumyl peroxide and phenolic resin as a mixed curing system on the mechanical properties and morphology of TPVs based on HDPE/ground tire rubber. *Polymer Composites* **2015**, *36*, 1907-1916.
81. Fazli, A.; Moosaei, R.; Sharif, M.; Ashtiani, S.J. Developments of graphene-based polymer composites processing based on novel methods for innovative applications in newborn technologies. *Indian Journal of Science and Technology* **2015**, *8*, 38-44.
82. Peigney, A.; Laurent, C.; Flahaut, E.; Bacsa, R.; Rousset, A. Specific surface area of carbon nanotubes and bundles of carbon nanotubes. *Carbon* **2001**, *39*, 507-514.
83. Yu, Q. Application of nanomaterials in alkali-activated materials. In *Nanotechnology in Eco-efficient Construction*; Elsevier: 2019; pp. 97-121.
84. Taguet, A.; Cassagnau, P.; Lopez-Cuesta, J.-M. Structuration, selective dispersion and compatibilizing effect of (nano) fillers in polymer blends. *Progress in Polymer Science* **2014**, *39*, 1526-1563.
85. de Luna, M.S.; Filippone, G. Effects of nanoparticles on the morphology of immiscible polymer blends–challenges and opportunities. *European Polymer Journal* **2016**, *79*, 198-218.
86. Amani, M.; Sharif, M.; Kashkooli, A.; Rahnama, N.; Fazli, A. Effect of mixing conditions on the selective localization of graphite oxide and the properties of polyethylene/high-impact polystyrene/graphite oxide nanocomposite blends. *RSC Advances* **2015**, *5*, 77723-77733.
87. Bai, L.; Sharma, R.; Cheng, X.; Macosko, C.W. Kinetic control of graphene localization in co-continuous polymer blends via melt compounding. *Langmuir* **2017**, *34*, 1073-1083.

88. Favis, B.D.; Chalifoux, J.-P. The effect of viscosity ratio on the morphology of polypropylene/polycarbonate blends during processing. *Polymer Engineering & Science* **1987**, *27*, 1591-1600.
89. Favis, B.D. Polymer alloys and blends: Recent advances. *the Canadian journal of chemical Engineering* **1991**, *69*, 619-625.
90. Li, L.; Miesch, C.; Sudeep, P.; Balazs, A.C.; Emrick, T.; Russell, T.P.; Hayward, R.C. Kinetically trapped co-continuous polymer morphologies through intraphase gelation of nanoparticles. *Nano Letters* **2011**, *11*, 1997-2003.
91. Huang, S.; Bai, L.; Trifkovic, M.; Cheng, X.; Macosko, C.W. Controlling the morphology of immiscible cocontinuous polymer blends via silica nanoparticles jammed at the interface. *Macromolecules* **2016**, *49*, 3911-3918.
92. Owens, D.K.; Wendt, R. Estimation of the surface free energy of polymers. *Journal of Applied Polymer Science* **1969**, *13*, 1741-1747.
93. Yehia, A.; Mull, M.; Ismail, M.; Hefny, Y.; Abdel-Bary, E. Effect of chemically modified waste rubber powder as a filler in natural rubber vulcanizates. *Journal of Applied Polymer Science* **2004**, *93*, 30-36.
94. Colom, X.; Cañavate, J.; Carrillo, F.; Velasco, J.; Pages, P.; Mujal, R.; Nogues, F. Structural and mechanical studies on modified reused tyres composites. *European Polymer Journal* **2006**, *42*, 2369-2378.
95. Sonnier, R.; Leroy, E.; Clerc, L.; Bergeret, A.; Lopez-Cuesta, J.-M.; Bretelle, A.-S.; Ienny, P. Compatibilizing thermoplastic/ground tyre rubber powder blends: efficiency and limits. *Polymer Testing* **2008**, *27*, 901-907.
96. Diao, B.; Isayev, A.; Levin, V.Y. Basic study of continuous ultrasonic devulcanization of unfilled silicone rubber. *Rubber Chemistry and Technology* **1999**, *72*, 152-164.
97. Oliphant, K.; Baker, W. The use of cryogenically ground rubber tires as a filler in polyolefin blends. *Polymer Engineering & Science* **1993**, *33*, 166-174.
98. Oliphant, K.; Baker, W.J.P.E.; Science. The use of cryogenically ground rubber tires as a filler in polyolefin blends. **1993**, *33*, 166-174.
99. Choudhury, N.R.; Bhowmick, A.K. Adhesion between individual components and mechanical properties of natural rubber-polypropylene thermoplastic elastomeric blends. *Journal of Adhesion Science and Technology* **1988**, *2*, 167-177.
100. Choudhury, N.R.; Bhowmick, A.K.J.J.o.a.s.; technology. Adhesion between individual components and mechanical properties of natural rubber-polypropylene thermoplastic elastomeric blends. **1988**, *2*, 167-177.
101. Esmizadeh, E.; Naderi, G.; Bakhshandeh, G.R.; Fasaie, M.R.; Ahmadi, S. Reactively compatibilized and dynamically vulcanized thermoplastic elastomers based on high-density polyethylene and reclaimed rubber. 59, 2017.
102. Rajalingam, P.; Sharpe, J.; Baker, W. Ground rubber tire/thermoplastic composites: effect of different ground rubber tires. *Rubber Chemistry and Technology* **1993**, *66*, 664-677.
103. Rajalingam, P.; Sharpe, J.; Baker, W.J.R.C.; Technology. Ground rubber tire/thermoplastic composites: effect of different ground rubber tires. **1993**, *66*, 664-677.
104. Noriman, N.; Ismail, H.; Rashid, A. Characterization of styrene butadiene rubber/recycled acrylonitrile-butadiene rubber (SBR/NBRr) blends: The effects of epoxidized natural rubber (ENR-50) as a compatibilizer. *Polymer Testing* **2010**, *29*, 200-208.
105. Noriman, N.; Ismail, H.; Rashid, A.J.P.t. Characterization of styrene butadiene rubber/recycled acrylonitrile-butadiene rubber (SBR/NBRr) blends: The effects of epoxidized natural rubber (ENR-50) as a compatibilizer. **2010**, *29*, 200-208.
106. Formela, K.; Korol, J.; Saeb, M.R. Interfacially modified LDPE/GTR composites with non-polar elastomers: From microstructure to macro-behavior. *Polymer Testing* **2015**, *42*, 89-98.
107. Song, P.; Li, S.; Wang, S. Interfacial interaction between degraded ground tire rubber and polyethylene. *Polymer Degradation and Stability* **2017**, *143*, 85-94.

108. Sae-Oui, P.; Sirisinha, C.; Sa-nguanthammarong, P.; Thaptong, P. Properties and recyclability of thermoplastic elastomer prepared from natural rubber powder (NRP) and high density polyethylene (HDPE). *Polymer Testing* **2010**, *29*, 346-351.
109. Patel, G.; Patel, H.; Sharma, P.; Patel, H.; John, N. A study on grafting of natural rubber and nitrile rubber on thermoplastic low density polyethylene using maleic anhydride and acrylic acid. *International Journal of Polymeric Materials* **2006**, *55*, 413-424.
110. Mehta, S.; Mirabella, F.M.; Rufener, K.; Bafna, A. Thermoplastic olefin/clay nanocomposites: morphology and mechanical properties. *Journal of Applied Polymer Science* **2004**, *92*, 928-936.
111. Naderi, G.; Lafleur, P.G.; Dubois, C. The influence of matrix viscosity and composition on the morphology, rheology, and mechanical properties of thermoplastic elastomer nanocomposites based on EPDM/PP. *Polymer Composites* **2008**, *29*, 1301-1309.
112. Lopattananon, N.; Tanglakwaraskul, S.; Kaesaman, A.; Seadan, M.; Sakai, T. Effect of nanoclay addition on morphology and elastomeric properties of dynamically vulcanized natural rubber/polypropylene nanocomposites. *International Polymer Processing* **2014**, *29*, 332-341.
113. Colom, X.; Carrillo, F.; Canavate, J. Composites reinforced with reused tyres: surface oxidant treatment to improve the interfacial compatibility. *Composites Part A: Applied Science and Manufacturing* **2007**, *38*, 44-50.
114. Liu, H.; Mead, J.; Stacer, R. Process development of scrap rubber/thermoplastic blends. *Chelsea Center for Recycling and Economic Development, Chelsea, MA* **2001**.
115. Sripornsawat, B.; Saiwari, S.; Pichaiyut, S.; Nakason, C. Influence of ground tire rubber devulcanization conditions on properties of its thermoplastic vulcanizate blends with copolyester. *European Polymer Journal* **2016**, *85*, 279-297.
116. D, V.J.a.R. Optimization of a polymer blend based on recycled polystyrene and styrene-butadien rubber In Proceedings of the Third US-Mexico Meeting "Advances in Polymer Science" and XXVII SPM National Congress Nueva Vallarta, Mexico, 2014.
117. McKeen, L.W. *The effect of long term thermal exposure on plastics and elastomers*; William Andrew: 2013.
118. Nuzaimah, M.; Sapuan, S.; Nadlene, R.; Jawaid, M. Recycling of waste rubber as fillers: A review. In Proceedings of the IOP Conference Series: Materials Science and Engineering, 2018; p. 012016.
119. Rubber, S.N. Natural rubber and reclaimed Rubber composites–A Systematic Review. *Polymer* **2016**, *2*, 7.
120. Fiksel, J.; Bakshi, B.R.; Baral, A.; Guerra, E.; DeQuervain, B. Comparative life cycle assessment of beneficial applications for scrap tires. *Clean Technologies and Environmental Policy* **2011**, *13*, 19-35.
121. De, S.K.; Isayev, A.; Khait, K. *Rubber Recycling*; CRC Press: 2005.
122. Khan, S.R.; Zeeshan, M.; Masood, A. Enhancement of hydrocarbons production through co-pyrolysis of acid-treated biomass and waste tire in a fixed bed reactor. *Waste Management* **2020**, *106*, 21-31.
123. Banar, M.; Akyıldız, V.; Özkan, A.; Çokaygil, Z.; Onay, Ö. Characterization of pyrolytic oil obtained from pyrolysis of TDF (Tire Derived Fuel). *Energy Conversion and Management* **2012**, *62*, 22-30.
124. Shu, X.; Huang, B. Recycling of waste tire rubber in asphalt and portland cement concrete: An overview. *Construction and Building Materials* **2014**, *67*, 217-224.
125. Ge, D.; Yan, K.; You, Z.; Xu, H. Modification mechanism of asphalt binder with waste tire rubber and recycled polyethylene. *Construction and Building Materials* **2016**, *126*, 66-76.
126. Yung, W.H.; Yung, L.C.; Hua, L.H. A study of the durability properties of waste tire rubber applied to self-compacting concrete. *Construction and Building Materials* **2013**, *41*, 665-672.
127. Aiello, M.A.; Leuzzi, F. Waste tyre rubberized concrete: Properties at fresh and hardened state. *Waste Management* **2010**, *30*, 1696-1704.
128. Araujo-Morera, J.; Hernández Santana, M.; Verdejo, R.; López-Manchado, M.A. Giving a Second Opportunity to Tire Waste: An Alternative Path for the Development of Sustainable Self-Healing Styrene–Butadiene Rubber Compounds Overcoming the Magic Triangle of Tires. *Polymers* **2019**, *11*, 2122.

129. Shaker, R.; Rodrigue, D. Rotomolding of Thermoplastic Elastomers Based on Low-Density Polyethylene and Recycled Natural Rubber. *Applied Sciences* **2019**, *9*, 5430.
130. Zhang, X.; Zhu, X.; Liang, M.; Lu, C. Improvement of the properties of ground tire rubber (GTR)-filled nitrile rubber vulcanizates through plasma surface modification of GTR powder. *Journal of Applied Polymer Science* **2009**, *114*, 1118-1125.
131. Aggour, Y.A.; Al-Shihri, A.S.; Bazzt, M.R. Surface Modification of Waste Tire by Grafting with Styrene and Maleic Anhydride. *Open Journal of Polymer Chemistry* **2012**, *2*, 70-76.
132. Garcia, P.; De Sousa, F.; De Lima, J.; Cruz, S.; Scuracchio, C. Devulcanization of ground tire rubber: Physical and chemical changes after different microwave exposure times. *Express Polymer Letters* **2015**, *9*.
133. Wang, L.; Lang, F.; Li, S.; Du, F.; Wang, Z. Thermoplastic elastomers based on high-density polyethylene and waste ground rubber tire composites compatibilized by styrene–butadiene block copolymer. *Journal of Thermoplastic Composite Materials* **2014**, *27*, 1479-1492.
134. Thomas, B.S.; Gupta, R.C. A comprehensive review on the applications of waste tire rubber in cement concrete. *Renewable and Sustainable Energy Reviews* **2016**, *54*, 1323-1333.
135. Mohajerani, A.; Burnett, L.; Smith, J.V.; Markovski, S.; Rodwell, G.; Rahman, M.T.; Kurmus, H.; Mirzababaei, M.; Arulrajah, A.; Horpibulsuk, S. Recycling waste rubber tyres in construction materials and associated environmental considerations: A review. *Resources, Conservation and Recycling* **2020**, *155*, 104679.
136. Sathiskumar, C.; Karthikeyan, S. Recycling of waste tires and its energy storage application of by-products–a review. *Sustainable Materials and Technologies* **2019**, e00125.
137. Bockstal, L.; Berchem, T.; Schmetz, Q.; Richel, A. Devulcanisation and reclaiming of tires and rubber by physical and chemical processes: A review. *Journal of Cleaner Production* **2019**.
138. Shulman, V.L. Tyre Recycling. In *Waste, Academic Press, Boston*; 2011; pp. 297-320.
139. Evans, A.; Evans, R. The composition of a tyre: typical components. *The Waste & Resources Action Programme* **2006**, *5*.
140. Shulman, V.L. Tire recycling. In *Waste*, Trevor M. Letcher, Vallero, D.A., Eds.; Elsevier: 2019; pp. 489-515.
141. Akiba, M.a.; Hashim, A. Vulcanization and crosslinking in elastomers. *Progress in Polymer Science* **1997**, *22*, 475-521.
142. Vergnaud, J.-M.; Rosca, I.-D. *Rubber curing and properties*; CRC Press: 2016.
143. Morin, J.E.; Farris, R.J. Recycling of 100% Cross Linked Rubber Powder by High Temperature High Pressure Sintering. *Encyclopedia of Polymer & Engineering* **2000**, *37*, 95-101.
144. Association, U.S.T.M. *U.S. Scrap Tire Management Summary*; The U.S. Tire Manufacturers Association: Washington, DC, 2017.
145. Imbernon, L.; Norvez, S. From landfilling to vitrimer chemistry in rubber life cycle. *European Polymer Journal* **2016**, *82*, 347-376.
146. Czajczyńska, D.; Krzyżyńska, R.; Jouhara, H.; Spencer, N. Use of pyrolytic gas from waste tire as a fuel: A review. *Energy* **2017**, *134*, 1121-1131.
147. Zebala, J.; Ciepka, P.; Reza, A.; Janczur, R. Influence of rubber compound and tread pattern of retreaded tyres on vehicle active safety. *Forensic Science International* **2007**, *167*, 173-180.
148. Lebreton, B.; Tuma, A. A quantitative approach to assessing the profitability of car and truck tire remanufacturing. *International Journal of Production Economics* **2006**, *104*, 639-652.
149. Gieré, R.; Smith, K.; Blackford, M. Chemical composition of fuels and emissions from a coal+ tire combustion experiment in a power station. *Fuel* **2006**, *85*, 2278-2285.
150. Tsang, H.-H. Uses of scrap rubber tires. *Rubber: Types, Properties and Uses* **2013**, 477-491.
151. Saha, P.; Colom, X.; Haponiuk, J.T.; John, M.; Naskar, K.; Thomas, S.; Noordermeer, J.W.; Azura, R.; Rathanasamy, R.; Sadasivuni, K. *Rubber Recycling: Challenges and Developments*; Royal Society of Chemistry: 2018.

152. Oriaku, E.; Agulanna, C.; Odenigbo, J.; Nnoruka, N. Waste to wealth through the incineration of waste tyres and recovery of carbon black. *International Journal of Multidisciplinary Sciences and Engineering* **2013**, *4*, 30-36.
153. Singh, S.; Nimmo, W.; Gibbs, B.; Williams, P. Waste tyre rubber as a secondary fuel for power plants. *Fuel* **2009**, *88*, 2473-2480.
154. Gnanaraj, J.S.; Lee, R.J.; Levine, A.M.; Wistrom, J.L.; Wistrom, S.L.; Li, Y.; Li, J.; Akato, K.; Naskar, A.K.; Paranthaman, M.P. Sustainable waste tire derived carbon material as a potential anode for lithium-ion batteries. *Sustainability* **2018**, *10*, 2840.
155. Navarro, F.; Partal, P.; Martınez-Boza, F.; Gallegos, C. Thermo-rheological behaviour and storage stability of ground tire rubber-modified bitumens. *Fuel* **2004**, *83*, 2041-2049.
156. Benazzouk, A.; Douzane, O.; Langlet, T.; Mezreb, K.; Roucoult, J.; Quéneudec, M. Physico-mechanical properties and water absorption of cement composite containing shredded rubber wastes. *Cement and Concrete Composites* **2007**, *29*, 732-740.
157. Oikonomou, N.; Mavridou, S. Improvement of chloride ion penetration resistance in cement mortars modified with rubber from worn automobile tires. *Cement and Concrete Composites* **2009**, *31*, 403-407.
158. Hejna, A.; Korol, J.; Przybysz-Romatowska, M.; Zedler, Ł.; Chmielnicki, B.; Formela, K. Waste tire rubber as low-cost and environmentally-friendly modifier in thermoset polymers–A review. *Waste Management* **2020**, *108*, 106-118.
159. Hassan, M.M.; Mahmoud, G.A.; El-Nahas, H.H.; Hegazy, E.S.A. Reinforced material from reclaimed rubber/natural rubber, using electron beam and thermal treatment. *Journal of Applied Polymer Science* **2007**, *104*, 2569-2578.
160. Dierkes, W. Untreated and treated rubber powder. In *Rubber recycling*; CRC Press: 2005; pp. 151-175.
161. Rutherford Sr, D. Process for recycling vehicle tires. 5115983, 1992 US Patent.
162. Dufton, P. *End-of-life tyres: Exploiting their value*; iSmithers Rapra Publishing: 2001.
163. Adhikari, J.; Das, A.; Sinha, T.; Saha, P.; Kim, J.K. Grinding of Waste Rubber. **2018**.
164. Colom, X.; Canavate, J.; Carrillo, F.; Velasco, J.; Pages, P.; Mujal, R.; Nogues, F. Structural and mechanical studies on modified reused tyres composites. *European Polymer Journal* **2006**, *42*, 2369-2378.
165. Martínez-Barrera, G.; del Coz-Díaz, J.J.; Álvarez-Rabanal, F.P.; Gayarre, F.L.; Martínez-López, M.; Cruz-Olivares, J. Waste tire rubber particles modified by gamma radiation and their use as modifiers of concrete. *Case Studies in Construction Materials* **2020**, *12*, e00321.
166. Feng, W.; Isayev, A. Recycling of tire-curing bladder by ultrasonic devulcanization. *Polymer Engineering & Science* **2006**, *46*, 8-18.
167. Seghar, S.; Asaro, L.; Rolland-Monnet, M.; Hocine, N.A. Thermo-mechanical devulcanization and recycling of rubber industry waste. *Resources, Conservation and Recycling* **2019**, *144*, 180-186.
168. Fan, P.; Lu, C. A study on functionalization of waste tire rubber powder through ozonization. *Journal of Polymers and the Environment* **2011**, *19*, 943-949.
169. Cañavate, J.; Colom, X.; Saeb, M.; Przybysz, M.; Zedler, L.; Formela, K. Influence of microwave treatment conditions of GTR on physico-mechanical and structural properties of NBR/NR/GTR composites. *Afinidad* **2019**, *76*.
170. Romero-Sánchez, M.a.D.; Pastor-Blas, M.M.; Martín-Martínez, J.M. Treatment of a styrene-butadiene-styrene rubber with corona discharge to improve the adhesion to polyurethane adhesive. *International Journal of Adhesion and Adhesives* **2003**, *23*, 49-57.
171. Satyanarayana, M.; Bhowmick, A.K.; Kumar, K.D. Preferentially fixing nanoclays in the phases of incompatible carboxylated nitrile rubber (XNBR)-natural rubber (NR) blend using thermodynamic approach and its effect on physico mechanical properties. *Polymer* **2016**, *99*, 21-43.
172. Akca, E.; Gursel, A.; Sen, N. A review on devulcanization of waste tire rubber. *Periodicals of Engineering and Natural Sciences* **2018**, *6*, 154-160.
173. Cheng, X.; Long, D.; Huang, S.; Li, Z.; Guo, X. Time effectiveness of the low-temperature plasma surface modification of ground tire rubber powder. *Journal of Adhesion Science and Technology* **2015**, *29*, 1330-1340.

174. Yoshida, S.; Hagiwara, K.; Hasebe, T.; Hotta, A. Surface modification of polymers by plasma treatments for the enhancement of biocompatibility and controlled drug release. *Surface and Coatings Technology* **2013**, *233*, 99-107.
175. Xiaowei, C.; Sheng, H.; Xiaoyang, G.; Wenhui, D. Crumb waste tire rubber surface modification by plasma polymerization of ethanol and its application on oil-well cement. *Applied Surface Science* **2017**, *409*, 325-342.
176. Park, H.B.; Han, D.W.; Lee, Y.M. Effect of a UV/ozone treatment on siloxane-containing copolyimides: surface modification and gas transport characteristics. *Chemistry of Materials* **2003**, *15*, 2346-2353.
177. Diaz-Quijada, G.A.; Wayner, D.D. A simple approach to micropatterning and surface modification of poly (dimethylsiloxane). *Langmuir* **2004**, *20*, 9607-9611.
178. Cataldo, F.; Ursini, O.; Angelini, G. Surface oxidation of rubber crumb with ozone. *Polymer Degradation and Stability* **2010**, *95*, 803-810.
179. Sahakaro, K. Mechanism of reinforcement using nanofillers in rubber nanocomposites. In *Progress in Rubber Nanocomposites*; Elsevier: 2017; pp. 81-113.
180. Shan, C.; Gu, Z.; Wang, L.; Li, P.; Song, G.; Gao, Z.; Yang, X. Preparation, characterization, and application of NR/SBR/Organoclay nanocomposites in the tire industry. *Journal of Applied Polymer Science* **2011**, *119*, 1185-1194.
181. Zhang, C.-L.; Feng, L.-F.; Gu, X.-P.; Hoppe, S.; Hu, G.-H. Efficiency of graft copolymers as compatibilizers for immiscible polymer blends. *Polymer* **2007**, *48*, 5940-5949.
182. Botros, S. Preparation and characteristics of NR/EPDM rubber blends. *Polymer-Plastics Technology and Engineering* **2002**, *41*, 341-359.
183. Abou-Helal, M.; El-Sabbagh, S. A study on the compatibility of NR-EPDM blends using electrical and mechanical techniques. *Journal of Elastomers & Plastics* **2005**, *37*, 319-346.
184. Flory, P.J.; Rehner Jr, J. Statistical mechanics of cross-linked polymer networks I. Rubberlike elasticity. *The Journal of Chemical Physics* **1943**, *11*, 512-520.
185. Markl, E.; Lackner, M. Devulcanization Technologies for Recycling of Tire-Derived Rubber: A Review. *Materials* **2020**, *13*, 1246.
186. Formela, K.; Cysewska, M. Efficiency of thermomechanical reclaiming of ground tire rubber conducted in counter-rotating and co-rotating twin screw extruder. *Polimery* **2014**, *59*.
187. Zanchet, A.; Carli, L.N.; Giovanela, M.; Crespo, J.S.; Scuracchio, C.H.; Nunes, R.C. Characterization of microwave-devulcanized composites of ground SBR scraps. *Journal of Elastomers & Plastics* **2009**, *41*, 497-507.
188. Yun, J.; Yashin, V.; Isayev, A. Ultrasonic devulcanization of carbon black–filled ethylene propylene diene monomer rubber. *Journal of Applied Polymer Science* **2004**, *91*, 1646-1656.
189. Isayev, A.I.; Liang, T.; Lewis, T.M. Effect of particle size on ultrasonic devulcanization of tire rubber in twin-screw extruder. *Rubber Chemistry and Technology* **2014**, *87*, 86-102.
190. Zhang, X.; Saha, P.; Cao, L.; Li, H.; Kim, J. Devulcanization of waste rubber powder using thiobisphenols as novel reclaiming agent. *Waste Management* **2018**, *78*, 980-991.
191. Wang, X.; Shi, C.; Zhang, L.; Zhang, Y. Effects of shear stress and subcritical water on devulcanization of styrene–butadiene rubber based ground tire rubber in a twin-screw extruder. *Journal of Applied Polymer Science* **2013**, *130*, 1845-1854.
192. Yazdani, H.; Karrabi, M.; Ghasmi, I.; Azizi, H.; Bakhshandeh, G.R. Devulcanization of waste tires using a twin-screw extruder: The effects of processing conditions. *Journal of Vinyl and Additive Technology* **2011**, *17*, 64-69.
193. Horikx, M. Chain scissions in a polymer network. *Journal of Polymer Science* **1956**, *19*, 445-454.
194. Seghar, S.; Asaro, L.; Hocine, N.A. Experimental Validation of the Horikx Theory to be Used in the Rubber Devulcanization Analysis. *Journal of Polymers and the Environment* **2019**, *27*, 2318-2323.
195. Shi, J.; Jiang, K.; Ren, D.; Zou, H.; Wang, Y.; Lv, X.; Zhang, L. Structure and performance of reclaimed rubber obtained by different methods. *Journal of Applied Polymer Science* **2013**, *129*, 999-1007.

196. Zanchet, A.; Carli, L.; Giovanela, M.; Brandalise, R.; Crespo, J. Use of styrene butadiene rubber industrial waste devulcanized by microwave in rubber composites for automotive application. *Materials & Design* **2012**, *39*, 437-443.
197. Rooj, S.; Basak, G.C.; Maji, P.K.; Bhowmick, A.K. New route for devulcanization of natural rubber and the properties of devulcanized rubber. *Journal of Polymers and the Environment* **2011**, *19*, 382-390.
198. Mandal, S.K.; Alam, N.; Debnath, S.C. Reclaiming of ground rubber tire by safe multifunctional rubber additives: I. Tetra benzyl thiuram disulfide. *Rubber Chemistry and Technology* **2012**, *85*, 629-644.
199. Kojima, M.; Tosaka, M.; Ikeda, Y. Chemical recycling of sulfur-cured natural rubber using supercritical carbon dioxide. *Green Chemistry* **2004**, *6*, 84-89.
200. Thaicharoen, P.; Thamyongkit, P.; Poompradub, S. Thiosalicylic acid as a devulcanizing agent for mechano-chemical devulcanization. *Korean Journal of Chemical Engineering* **2010**, *27*, 1177-1183.
201. Diaz, R.; Colomines, G.; Peuvrel-Disdier, E.; Deterre, R. Thermo-mechanical recycling of rubber: Relationship between material properties and specific mechanical energy. *Journal of Materials Processing Technology* **2018**, *252*, 454-468.
202. Li, X.; Deng, X.-Q.; Dong, C. Effect of Temperature on Devulcanization of Waste Sidewall Rubber by Supercritical Ethanol. *Journal of the Brazilian Chemical Society* **2018**, *29*, 2169-2179.
203. Sreeja, T.; Kutty, S. Cure characteristics and mechanical properties of natural rubber/reclaimed rubber blends. *Polymer-Plastics Technology and Engineering* **2000**, *39*, 501-512.
204. Li, S.; Lamminmäki, J.; Hanhi, K. Effect of ground rubber powder and devulcanizates on the properties of natural rubber compounds. *Journal of Applied Polymer Science* **2005**, *97*, 208-217.
205. Yehia, A.; Ismail, M.; Hefny, Y.; Abdel-Bary, E.; Mull, M. Mechano-Chemical Reclamationof Waste Rubber Powder andIts Effect on the performanceof NR and SBR Vulcanizates. *Journal of Elastomers & Plastics* **2004**, *36*, 109-123.
206. Nelson, P.; Kutty, S. Studies on Maleic anhydride grafted reclaimed rubber/acrylonitrile butadiene rubber blends. *Progress in Rubber Plastics and Recycling Technology* **2003**, *19*, 171-188.
207. Sreeja, T.; Kutty, S. Studies on acrylonitrile butadiene rubber. *Journal of Elastomers and Plastics* **2002**, *34*, 145-155.
208. Sreeja, T.; Kutty, S. Styrene butadiene rubber/reclaimed rubber blends. *International Journal of Polymeric Materials* **2003**, *52*, 599-609.
209. Lamminmäki, J.; Li, S.; Hanhi, K. Feasible incorporation of devulcanized rubber waste in virgin natural rubber. *Journal of Materials Science* **2006**, *41*, 8301-8307.
210. Han, S.C.; Han, M.H. Fracture behavior of NR and SBR vulcanizates filled with ground rubber having uniform particle size. *Journal of Applied Polymer Science* **2002**, *85*, 2491-2500.
211. De, D.; Maiti, S.; Adhikari, B. Reclaiming of rubber by a renewable resource material (RRM). III. Evaluation of properties of NR reclaim. *Journal of Applied Polymer Science* **2000**, *75*, 1493-1502.
212. De, D.; Panda, P.K.; Roy, M.; Bhunia, S. Reinforcing effect of reclaim rubber on natural rubber/polybutadiene rubber blends. *Materials & Design* **2013**, *46*, 142-150.
213. Sombatsompop, N.; Kumnuantip, C. Rheology, cure characteristics, physical and mechanical properties of tire tread reclaimed rubber/natural rubber compounds. *Journal of Applied Polymer Science* **2003**, *87*, 1723-1731.
214. Vlachopoulos, J. Die Swell and Normal Stresses: An Explanation. *Rubber Chemistry and Technology* **1978**, *51*, 133-138.
215. Zhang, X.; Lu, C.; Liang, M. Properties of natural rubber vulcanizates containing mechanochemically devulcanized ground tire rubber. *Journal of Polymer Research* **2009**, *16*, 411-419.
216. Rattanasom, N.; Poonsuk, A.; Makmoon, T. Effect of curing system on the mechanical properties and heat aging resistance of natural rubber/tire tread reclaimed rubber blends. *Polymer Testing* **2005**, *24*, 728-732.
217. Li, Y.; Zhao, S.; Wang, Y. Microbial desulfurization of ground tire rubber by Sphingomonas sp.: a novel technology for crumb rubber composites. *Journal of Polymers and the Environment* **2012**, *20*, 372-380.
218. Li, Y.; Zhao, S.; Wang, Y. Improvement of the properties of natural rubber/ground tire rubber composites through biological desulfurization of GTR. *Journal of Polymer Research* **2012**, *19*, 9864.

219. De, D.; De, D. Processing and material characteristics of a reclaimed ground rubber tire reinforced styrene butadiene rubber. *Materials Sciences and Applications* **2011**, *2*, 486.
220. Fernández-Berridi, M.J.; González, N.; Mugica, A.; Bernicot, C. Pyrolysis-FTIR and TGA techniques as tools in the characterization of blends of natural rubber and SBR. *Thermochimica Acta* **2006**, *444*, 65-70.
221. Formela, K.; Formela, M.; Thomas, S.; Haponiuk, J. Styrene-Butadiene Rubber/Modified Ground Tire Rubber Blends Co-Vulcanization: Effect of Accelerator Type. In Proceedings of the Macromolecular Symposia, 2016; pp. 64-72.
222. Colom, X.; Marín-Genescà, M.; Mujal, R.; Formela, K.; Cañavate, J. Structural and physico-mechanical properties of natural rubber/GTR composites devulcanized by microwaves: Influence of GTR source and irradiation time. *Journal of Composite Materials* **2018**, *52*, 3099-3108.
223. De, D.; De, D.; Singharoy, G. Reclaiming of ground rubber tire by a novel reclaiming agent. I. Virgin natural rubber/reclaimed GRT vulcanizates. *Polymer Engineering & Science* **2007**, *47*, 1091-1100.
224. Kumnuantip, C.; Sombatsompop, N. Dynamic mechanical properties and swelling behaviour of NR/reclaimed rubber blends. *Materials Letters* **2003**, *57*, 3167-3174.
225. Balasubramanian, M. Cure modeling and mechanical properties of counter rotating twin screw extruder devulcanized ground rubber tire—natural rubber blends. *Journal of Polymer Research* **2009**, *16*, 133-141.
226. Kraus, G. Modification of asphalt by block polymers of butadiene and styrene. *Rubber Chemistry and Technology* **1982**, *55*, 1389-1402.
227. Igwe, I.O.; Ezeani, O.E. Studies on the transport of aromatic solvents through filled natural rubber. *International journal of polymer science* **2012**, *2012*.
228. De, D.; Das, A.; De, D.; Dey, B.; Debnath, S.C.; Roy, B.C. Reclaiming of ground rubber tire (GRT) by a novel reclaiming agent. *European Polymer Journal* **2006**, *42*, 917-927.
229. Dubkov, K.; Semikolenov, S.; Ivanov, D.; Babushkin, D.; Panov, G.; Parmon, V. Reclamation of waste tyre rubber with nitrous oxide. *Polymer Degradation and Stability* **2012**, *97*, 1123-1130.
230. Jana, G.; Das, C. Devulcanization of natural rubber vulcanizates by mechanochemical process. *Polymer-Plastics Technology and Engineering* **2005**, *44*, 1399-1412.
231. Hong, C.K.; Isayev, A.I. Plastic/rubber blends of ultrasonically devulcanized GRT with HDPE. *Journal of Elastomers & Plastics* **2001**, *33*, 47-71.
232. Sharma, V.; Mincarini, M.; Fortuna, F.; Cognini, F.; Cornacchia, G. Disposal of waste tyres for energy recovery and safe environment. *Energy Conversion and Management* **1998**, *39*, 511-528.
233. Mui, E.L.; Ko, D.C.; McKay, G. Production of active carbons from waste tyres—a review. *Carbon* **2004**, *42*, 2789-2805.
234. Nakason, C.; Wannavilai, P.; Kaesaman, A. Effect of vulcanization system on properties of thermoplastic vulcanizates based on epoxidized natural rubber/polypropylene blends. *Polymer Testing* **2006**, *25*, 34-41.
235. Nakason, C.; Saiwari, S.; Kaesaman, A. Rheological properties of maleated natural rubber/polypropylene blends with phenolic modified polypropylene and polypropylene-g-maleic anhydride compatibilizers. *Polymer Testing* **2006**, *25*, 413-423.
236. Bhowmick, A.K.; Heslop, J.; White, J. Effect of stabilizers in photodegradation of thermoplastic elastomeric rubber–polyethylene blends—a preliminary study. *Polymer Degradation and Stability* **2001**, *74*, 513-521.
237. Dahlan, H.; Zaman, M.K.; Ibrahim, A. The morphology and thermal properties of liquid natural rubber (LNR)-compatibilized 60/40 NR/LLDPE blends. *Polymer Testing* **2002**, *21*, 905-911.
238. Punnarak, P.; Tantayanon, S.; Tangpasuthadol, V. Dynamic vulcanization of reclaimed tire rubber and high density polyethylene blends. *Polymer Degradation and Stability* **2006**, *91*, 3456-3462.
239. Egodage, S.M.; Harper, J.F.; Walpalage, S. Ground tyre rubber/waste polypropylene blends–Effect of composition on mechanical properties. *Progress in Rubber Plastics and Recycling Technology* **2009**, *25*, 213-231.

240. Rabinovitch, E.B.; Isner, J.D.; Sidor, J.A.; Wiedl, D.J. Effect of extrusion conditions on rigid PVC foam. *Journal of Vinyl and Additive Technology* **1997**, *3*, 210-215.
241. Arroyo, M.; Zitzumbo, R.; Avalos, F. Composites based on PP/EPDM blends and aramid short fibres. Morphology/behaviour relationship. *Polymer* **2000**, *41*, 6351-6359.
242. Egodage, S.M.; Harper, J.; Walpalage, S. The development of rubber-thermoplastic blends from ground tyre rubber and waste polypropylene. *Journal of the National Science Foundation of Sri Lanka* **2009**, *37*.
243. Zhang, X.; Chen, C.; Lu, C. High-Density Polyethylene/Ground Tyre Rubber Blends: Effective Dispersion and Mechanical Property Enhancement through Solid-State Mechanochemical Milling. *Progress in Rubber Plastics and Recycling Technology* **2012**, *28*, 81-94.
244. Mujal-Rosas, R.; Marin-Genesca, M.; Orrit-Prat, J.; Rahhali, A.; Colom-Fajula, X. Dielectric, mechanical, and thermal characterization of high-density polyethylene composites with ground tire rubber. *Journal of Thermoplastic Composite Materials* **2012**, *25*, 537-559.
245. Alshukri, A.A.; Faieza, A.A.; Sapuan, S.M.; Nuraini, A.A.; Al-Maamori, M.; Zageer, D.S. Effect of Crumb Rubber Content and Particle Size on the Mechanical and Rheological Properties of Passenger Tyre Tread Composite. *Journal of Engineering and Applied Sciences* **2017**, *12*, 232 - 238.
246. Ratnam, C.T.; Ramarad, S.; Khalid, M.; Noraini, N. Effect of Pre-Irradiation of Waste Tire Dust on the Properties of Ethylene Vinyl Acetate/Waste Tire Dust Blend (EVA/WTD) Blends. *Journal of Composite and Biodegradable Polymers* **2013**, *1*, 16-22.
247. Colom, X.; Canavate, J.; Carrillo, F.; Suñol, J. Effect of the particle size and acid pretreatments on compatibility and properties of recycled HDPE plastic bottles filled with ground tyre powder. *Journal of Applied Polymer Science* **2009**, *112*, 1882-1890.
248. Fazli, A.; Rodrigue, D. Morphological and Mechanical Properties of Thermoplastic Elastomers Based on Recycled High Density Polyethylene and Recycled Natural Rubber. *International Polymer Processing* **2021**, *36*, 156-164.
249. Abbas-Abadi, M.S.; Haghighi, M.N.; Yeganeh, H.; Bozorgi, B. The effect of melt flow index, melt flow rate, and particle size on the thermal degradation of commercial high density polyethylene powder. *Journal of Thermal Analysis and Calorimetry* **2013**, *114*, 1333-1339.
250. Tantayanon, S.; Juikham, S. Enhanced toughening of poly (propylene) with reclaimed-tire rubber. *Journal of Applied Polymer Science* **2004**, *91*, 510-515.
251. Meysami, M. A Study of Scrap Rubber Devulcanization and Incorporation of Devulcanized Rubber into Virgin Rubber Compound. **2012**.
252. Mészáros, L.; Tábi, T.; Kovács, J.; Bárány, T. The effect of EVA content on the processing parameters and the mechanical properties of LDPE/ground tire rubber blends. *Polymer Engineering & Science* **2008**, *48*, 868-874.
253. Grigoryeva, O.; Fainleb, A.; Shumskii, V.; Vilenskii, V.; Kozak, N.; Babkina, N. The Effect of multi-reprocessing on the structure and characteristics of thermoplastic elastomers based on recycled polymers. *Polymer Science Series A* **2009**, *51*, 216-225.
254. Hassan, M.M.; Aly, R.O.; Aal, S.A.; El-Masry, A.M.; Fathy, E. Mechanochemical devulcanization and gamma irradiation of devulcanized waste rubber/high density polyethylene thermoplastic elastomer. *Journal of Industrial and Engineering Chemistry* **2013**, *19*, 1722-1729.
255. Karaağaç, B.; Turan, H.O.; Oral, D.D. Use of ground EPDM wastes in EPDM-based rubber compounds: With and without compatibilization. *Journal of Elastomers & Plastics* **2015**, *47*, 117-135.
256. Kakroodi, A.R.; Kazemi, Y.; Rodrigue, D. Mechanical, rheological, morphological and water absorption properties of maleated polyethylene/hemp composites: Effect of ground tire rubber addition. *Composites Part B: Engineering* **2013**, *51*, 337-344.
257. Lima, P.; Oliveira, J.; Costa, V. Partial replacement of EPDM by GTR in thermoplastic elastomers based on PP/EPDM: effects on morphology and mechanical properties. *Journal of Applied Polymer Science* **2014**, *131*.
258. Sanjay, O.S. Effect of Crumb-rubber Particle Size on the Mechanical Response of Polyurethane Foam Composites. Master of Science, Oklahoma State University, United States, 2014.

259. Herrero, S.; Mayor, P.; Hernández-Olivares, F. Influence of proportion and particle size gradation of rubber from end-of-life tires on mechanical, thermal and acoustic properties of plaster–rubber mortars. *Materials & Design* **2013**, *47*, 633-642.
260. Moghaddamzadeh, S.; Rodrigue, D. Rheological characterization of polyethylene/polyester recycled tire fibers/ground tire rubber composites. *Journal of Applied Polymer Science* **2018**, *135*, 46563.
261. Saleesung, T.; Saeoui, P.; Sirisinha, C. Mechanical and thermal properties of thermoplastic elastomer based on low density polyethylene and ultra-fine fully-vulcanized acrylonitrile butadiene rubber powder (UFNBRP). *Polymer Testing* **2010**, *29*, 977-983.
262. Zhao, X.; Hu, H.; Zhang, D.; Zhang, Z.; Peng, S.; Sun, Y. Curing behaviors, mechanical properties, dynamic mechanical analysis and morphologies of natural rubber vulcanizates containing reclaimed rubber. *e-Polymers* **2019**, *19*, 482-488.
263. Pal, K.; Pal, S.; Das, C.; Kim, J.K. Relationship between normal load and dynamic co-efficient of friction on rock-rubber wear mechanism. *Materials & Design* **2010**, *31*, 4792-4799.
264. Formela, K.; Sulkowski, M.; Saeb, M.R.; Colom, X.; Haponiuk, J.T. Assessment of microstructure, physical and thermal properties of bitumen modified with LDPE/GTR/elastomer ternary blends. *Construction and Building Materials* **2016**, *106*, 160-167.
265. Soriano-Corral, F.; Hernández-Gámez, J.F.; Durón-Sánchez, L.H.; Ramos de Valle, L.F.; Lozano-Estrada, M.; Soto-Lara, Y.A. Polymer Foams Based on Low Density Polyethylene/Ethylene Vinyl Acetate/Ground Tire Rubber (LDPE/EVA/GTR): Influence of the GTR Particle Size and Content on the Cellular Morphology and Density of the Final Foamed Compounds. In Proceedings of the Key Engineering Materials, 2018; pp. 64-70.
266. Başboğa, İ.H.; Atar, İ.; Karakuş, K.; Mengeloğlu, F. Determination of Some Technological Properties of Injection Molded Pulverized-HDPE Based Composites Reinforced with Micronized Waste Tire Powder and Red Pine Wood Wastes. *Journal of Polymers and the Environment* **2020**, *28*, 1-19.
267. Jiang, C.; Zhang, Y.; Ma, L.; Zhou, L.; He, H. Tailoring the properties of ground tire rubber/high-density polyethylene blends by combining surface devulcanization and in-situ grafting technology. *Materials Chemistry and Physics* **2018**, *220*, 161-170.
268. Jose, J.; Nag, A.; Nando, G. Processing and characterization of recycled polypropylene and acrylonitrile butadiene rubber blends. *Journal of Polymers and the Environment* **2010**, *18*, 155-166.
269. Mahallati, P.; Hassanabadi, H.M.; Wilhelm, M.; Rodrigue, D. Rheological characterization of thermoplastic elastomers (TPE) based on PP and recycled EPDM. *Applied Rheology* **2016**, *26*, 32-38.
270. Ismail, H.; Awang, M. Natural weathering of polypropylene and waste tire dust (PP/WTD) blends. *Journal of Polymers and the Environment* **2008**, *16*, 147-153.
271. Mészáros, L.; Bárány, T.; Czvikovszky, T. EB-promoted recycling of waste tire rubber with polyolefins. *Radiation Physics and Chemistry* **2012**, *81*, 1357-1360.
272. Wilson, R.; Plivelic, T.S.; Aprem, A.S.; Ranganathaiagh, C.; Kumar, S.A.; Thomas, S. Preparation and characterization of EVA/clay nanocomposites with improved barrier performance. *Journal of Applied Polymer Science* **2012**, *123*, 3806-3818.
273. Scuracchio, C.; Waki, D.; Da Silva, M. Thermal analysis of ground tire rubber devulcanized by microwaves. *Journal of Thermal Analysis and Calorimetry* **2007**, *87*, 893-897.
274. Kleps, T.; Piaskiewicz, M.; Parasiewicz, W. The use of thermogravimetry in the study of rubber devulcanization. *Journal of Thermal Analysis and Calorimetry* **2000**, *60*, 271-277.
275. Kumar, S.; Singh, R. Recovery of hydrocarbon liquid from waste high density polyethylene by thermal pyrolysis. *Brazilian Journal of Chemical Engineering* **2011**, *28*, 659-667.
276. Lou, F.; Wu, K.; Wang, Q.; Qian, Z.; Li, S.; Guo, W. Improved flame-retardant and ceramifiable properties of EVA composites by combination of ammonium polyphosphate and aluminum hydroxide. *Polymers* **2019**, *11*, 125.
277. Liang, H.; Hardy, J.-M.; Rodrigue, D.; Brisson, J. EPDM recycled rubber powder characterization: thermal and thermogravimetric analysis. *Rubber Chemistry and Technology* **2014**, *87*, 538-556.

278. Ghorai, S.; Mondal, D.; Dhanania, S.; Chattopadhyay, S.; Roy, M.; De, D. Reclaiming of waste guayule natural rubber vulcanizate—reclaim rubber for green tire applications: An approach for sustainable development. *Journal of Elastomers & Plastics* **2019**, *51*, 193-210.
279. Joseph, A.M.; George, B.; KN, M.; Alex, R. Effect of devulcanization on crosslink density and crosslink distribution of carbon black filled natural rubber vulcanizates. *Rubber Chemistry and Technology* **2016**, *89*, 653-670.
280. Egodage, S.; Harper, J.; Walpalage, S. Effect of maleimide curing on mechanical properties of ground tyre rubber/waste polypropylene blends. *Plastics, Rubber and Composites* **2012**, *41*, 332-340.
281. Cañavate Ávila, F.J.; Colom Fajula, X.; Saeb, M.R.; Przybysz, M.; Zedler, L.; Formela, K. Influence of microwave treatment conditions of GTR on physico-mechanical and structural properties of NBR/NR/GTR composites. *AFINIDAD* **2019**, *76*, 171-179.
282. Fatimah, A.; Abdul Aziz, I.H.; Supri, A.G. Effect of PEgMAH on Tensile Properties and Swelling Behaviour of Recycled High Density Polyethylene/Ethylene Vinyl Acetate/Waste Tyre Dust (r-HDPE/EVA/WTD) Composites. In Proceedings of the Applied Mechanics and Materials, 2014; pp. 137-140.
283. Premphet, K.; Horanont, P. Phase structure of ternary polypropylene/elastomer/filler composites: effect of elastomer polarity. *Polymer* **2000**, *41*, 9283-9290.
284. Wang, Z.; Zhang, Y.; Du, F.; Wang, X. Thermoplastic elastomer based on high impact polystyrene/ethylene-vinyl acetate copolymer/waste ground rubber tire powder composites compatibilized by styrene-butadiene-styrene block copolymer. *Materials Chemistry and Physics* **2012**, *136*, 1124-1129.
285. Awang, M.; Ismail, H. Preparation and characterization of polypropylene/waste tyre dust blends with addition of DCP and HVA-2 (PP/WTDP-HVA2). *Polymer Testing* **2008**, *27*, 321-329.
286. Bockstal, L.; Berchem, T.; Schmetz, Q.; Richel, A. Devulcanisation and reclaiming of tires and rubber by physical and chemical processes: A review. *Journal of Cleaner Production* **2019**, *236*, 117574.
287. Narani, S.; Abbaspour, M.; Hosseini, S.M.M.; Aflaki, E.; Nejad, F.M. Sustainable reuse of Waste Tire Textile Fibers (WTTFs) as reinforcement materials for expansive soils: With a special focus on landfill liners/covers. *Journal of Cleaner Production* **2020**, *247*, 119151.
288. Anuar, H.; Hassan, N.; Mohd Fauzey, F. Compatibilized PP/EPDM-kenaf fibre composite using melt blending method. In Proceedings of the Advanced Materials Research, 2011; pp. 743-747.
289. Zainal, Z.; Ismail, H. The effects of short glass fibre (SGF) loading and a silane coupling agent on properties of polypropylene/waste tyre dust/short Glass Fibre (PP/WTD/SGF) composites. *Polymer-Plastics Technology and Engineering* **2011**, *50*, 297-305.
290. Fazli, A.; Rodrigue, D. Effect of Ground Tire Rubber (GTR) Particle Size and Content on the Morphological and Mechanical Properties of Recycled High-Density Polyethylene (rHDPE)/GTR Blends. *Recycling* **2021**, *6*, 44.
291. Anuar, H.; Zuraida, A. Improvement in mechanical properties of reinforced thermoplastic elastomer composite with kenaf bast fibre. *Composites Part B: Engineering* **2011**, *42*, 462-465.
292. Nikpour, N.; Rodrigue, D. Effect of coupling agent and ground tire rubber content on the properties of natural fiber polymer composites. *International Polymer Processing* **2016**, *31*, 463-471.
293. Bongarde, U.; Shinde, V. Review on natural fiber reinforcement polymer composites. *International Journal of Engineering Science and Innovative Technology* **2014**, *3*, 431-436.
294. Rajak, D.K.; Pagar, D.D.; Menezes, P.L.; Linul, E. Fiber-reinforced polymer composites: Manufacturing, properties, and applications. *Polymers* **2019**, *11*, 1667.
295. Ramezani Kakroodi, A.; Rodrigue, D. Reinforcement of maleated polyethylene/ground tire rubber thermoplastic elastomers using talc and wood flour. *Journal of Applied Polymer Science* **2014**, *131*.
296. Subramaniyan, S.K.; Mahzan, S.; bin Ghazali, M.I.; Ismon, M.B.; Zaidi, A.M.A. Mechanical behavior of polyurethane composite foams from kenaf fiber and recycled tire rubber particles. In Proceedings of the Applied Mechanics and Materials, 2013; pp. 861-866.

297. Kakroodi, A.R.; Leduc, S.; González-Núñez, R.; Rodrigue, D. Mechanical properties of recycled polypropylene/SBR rubber crumbs blends reinforced by birch Wood flour. *Polymers and Polymer Composites* **2012**, *20*, 439-444.
298. Graupner, N.; Ziegmann, G.; Wilde, F.; Beckmann, F.; Müssig, J. Procedural influences on compression and injection moulded cellulose fibre-reinforced polylactide (PLA) composites: Influence of fibre loading, fibre length, fibre orientation and voids. *Composites Part A: Applied Science and Manufacturing* **2016**, *81*, 158-171.
299. Lima, P.S.; Oliveira, J.M.; Costa, V.A.F. Partial replacement of EPR by GTR in highly flowable PP/EPR blends: Effects on morphology and mechanical properties. *Journal of Applied Polymer Science* **2015**, *132*.
300. Zhang, Z.X.; Zhang, S.L.; Kim, J.K. Evaluation of mechanical, morphological and thermal properties of waste rubber tire powder/LLDPE blends. *e-Polymers* **2008**, *8*.
301. Panigrahi, H.; Sreenath, P.; Bhowmick, A.K.; Kumar, K.D. Unique compatibilized thermoplastic elastomer from polypropylene and epichlorohydrin rubber. *Polymer* **2019**, *183*, 121866.
302. ASTM D2856. *Standard Test Method for Open-Cell Content of Rigid Cellular Plastics by the Air Pycnometer* **1998**.
303. ASTM D1238. *Standard Test Method for Melt Flow Rates of Thermoplastics by Extrusion Plastometer* **2013**.
304. ASTM D3418. *Standard Test Method for Transition Temperatures and Enthalpies of Fusion and Crystallization of Polymers by Differential Scanning Calorimetry* **2015**.
305. ASTM D638. *Standard Test Method for Tensile Properties of Plastics* **2014**.
306. ASTM D790. *Standard Test Methods for Flexural Properties of Unreinforced and Reinforced Plastics and Electrical Insulating Materials* **2010**.
307. ASTM D256. *Standard Test Methods for Determining the Izod Pendulum Impact Resistance of Plastics* **2010**.
308. Janca, J.; Stahel, P.; Buchta, J.; Subedi, D.; Krcma, F.; Pryckova, J. A plasma surface treatment of polyester textile fabrics used for reinforcement of car tires. *Plasmas and Polymers* **2001**, *6*, 15-26.
309. Hakrama, K.; Guxho, G.; Liço, E. Morphological and chemical study of recycled synthetic rubber tire crumbs by using scanning electron microscopy and energy dispersive analysis. *Zastita Materijala* **2017**, *58*, 222-227.
310. Lu, Y.; Yang, Y.; Xiao, P.; Feng, Y.; Liu, L.; Tian, M.; Li, X.; Zhang, L. Effect of interfacial enhancing on morphology, mechanical, and rheological properties of polypropylene-ground tire rubber powder blends. *Journal of Applied Polymer Science* **2017**, *134*, 45354.
311. Mazidi, M.M.; Aghjeh, M.K.R.; Khonakdar, H.A.; Reuter, U. Structure–property relationships in super-toughened polypropylene-based ternary blends of core–shell morphology. *RSC Advances* **2016**, *6*, 1508-1526.
312. Rezaei Abadchi, M.; Jalali Arani, A.; Nazockdast, H. Partial replacement of NR by GTR in thermoplastic elastomer based on LLDPE/NR through using reactive blending: Its effects on morphology, rheological, and mechanical properties. *Journal of Applied Polymer Science* **2010**, *115*, 2416-2422.
313. Tripathy, A.R.; Morin, J.E.; Williams, D.E.; Eyles, S.J.; Farris, R.J. A novel approach to improving the mechanical properties in recycled vulcanized natural rubber and its mechanism. *Macromolecules* **2002**, *35*, 4616-4627.
314. Zabihzadeh, M.; Dastoorian, F.; Ebrahimi, G. Effect of MAPE on mechanical and morphological properties of wheat straw/HDPE injection molded composites. *Journal of Reinforced Plastics and Composites* **2010**, *29*, 123-131.
315. Formela, M.; Haponiuk, J.; Jasinska-Walc, L.; Formela, K. Compatibilization of polymeric composition filled with ground tire rubber–short review. *Chemistry & Chemical Technology* **2014**, 445-450.
316. Simon-Stőger, L.; Varga, C. PE-contaminated industrial waste ground tire rubber: How to transform a handicapped resource to a valuable one. *Waste Management* **2021**, *119*, 111-121.
317. Naskar, A.K.; De, S.; Bhowmick, A.K. Thermoplastic elastomeric composition based on maleic anhydride–grafted ground rubber tire. *Journal of Applied Polymer Science* **2002**, *84*, 370-378.

318. Karmarkar, A.; Chauhan, S.; Modak, J.M.; Chanda, M. Mechanical properties of wood–fiber reinforced polypropylene composites: Effect of a novel compatibilizer with isocyanate functional group. *Composites Part A: Applied Science and Manufacturing* **2007**, *38*, 227-233.
319. Mahallati, P.; Rodrigue, D. Effect of feeding strategy on the mechanical properties of PP/recycled EPDM/PP-g-MA blends. *International Polymer Processing* **2014**, *29*, 280-286.
320. Luna, C.B.B.; Siqueira, D.D.; Araújo, E.M.; Morais, D.D.d.S.; Bezerra, E.B. Toughening of polystyrene using styrene-butadiene rubber (SBRr) waste from the shoe industry. *REM-International Engineering Journal* **2018**, *71*, 253-260.
321. Clemons, C. Elastomer modified polypropylene–polyethylene blends as matrices for wood flour–plastic composites. *Composites Part A: Applied Science and Manufacturing* **2010**, *41*, 1559-1569.
322. Yang, H.; Cho, K. Surface modification effects of core–shell rubber particles on the toughening of poly (butylene terephthalate). *Journal of Applied Polymer Science* **2010**, *116*, 1948-1957.
323. Liang, H.; Gagné, J.D.; Faye, A.; Rodrigue, D.; Brisson, J. Ground tire rubber (GTR) surface modification using thiol-ene click reaction: Polystyrene grafting to modify a GTR/polystyrene (PS) blend. *Progress in Rubber, Plastics and Recycling Technology* **2020**, *36*, 81-101.
324. Odrobina, M.; Deák, T.; Székely, L.; Mankovits, T.; Keresztes, R.Z.; Kalácska, G. The Effect of Crystallinity on the Toughness of Cast Polyamide 6 Rods with Different Diameters. *Polymers* **2020**, *12*, 293.
325. Wang, Y.; Cheng, L.; Cui, X.; Guo, W. Crystallization behavior and properties of glass fiber reinforced polypropylene composites. *Polymers* **2019**, *11*, 1198.